

**UCLA**

**UCLA Electronic Theses and Dissertations**

**Title**

Nonreciprocal Parametric Amplification of Elastic Waves Applications in RF Front Ends

**Permalink**

<https://escholarship.org/uc/item/5ch0f03p>

**Author**

zakeri, mahsa

**Publication Date**

2022

Peer reviewed|Thesis/dissertation

UNIVERSITY OF CALIFORNIA

Los Angeles

Nonreciprocal Parametric Amplification of Elastic Waves  
Applications in Radio Frequency Front Ends

A dissertation submitted in partial satisfaction of the  
requirements for the degree Doctor of Philosophy  
in Mechanical Engineering

by

Mahsa Zakeri

2022

© Copyright by

Mahsa Zakeri

2022

## ABSTRACT OF THE DISSERTATION

Nonreciprocal Parametric Amplification of Elastic Waves Applications in Radio Frequency Front Ends

by

Mahsa Zakeri

Doctor of Philosophy in Mechanical Engineering

University of California, Los Angeles, 2022

Professor Christopher S. Lynch, Chair

Parametric amplification of bulk and surface elastic waves, along with a framework for using elastic waves that could enable a new generation of high performance, low noise acoustic amplifiers, mixers and circulators are presented. Nonlinear electromechanical materials are studied for the application. Using a novel approach with nonlinear materials produces highly desirable non-reciprocal characteristics. Parametric amplification of a weak elastic signal wave is achieved by an elastic pump wave of higher intensity. By careful selection of material orientation together with precise excitation of signal and pump waves, ‘up frequency conversion’ is suppressed and selective amplification of the elastic signal wave occurs at its original frequency. In addition, a general mathematical framework is developed and used for analytical studies of coupled wave equations in nonlinear anisotropic materials. The results obtained from the analytical studies are verified using a finite element implementation. Further, Lamb wave properties are analyzed and potential advantages of using Lamb waves for parametric amplification are demonstrated and discussed.

The dissertation of Mahsa Zakeri is approved.

Ajit K. Mal

Yuanxun Wang

Gregory P. Carman

Christopher S. Lynch, Committee Chair

University of California, Los Angeles

2022

This dissertation is dedicated to every consciousness in our Universe.

# Table of Contents

INTRODUCTION.....	1
<i>Motivation</i> .....	1
<i>Objective</i> .....	3
<i>Literature review</i> .....	4
<i>Scope</i> .....	7
CHAPTER 1 CRYSTALS PROPERTIES IN A ROTATED COORDINATE SYSTEM.....	8
CHAPTER 2 PROPAGATION OF LINEAR ELASTIC WAVES IN ANISOTROPIC MATERIALS .....	11
2.1. <i>Plane Elastic Waves with General Anisotropy</i> .....	11
2.1. 1. <i>Elastic Materials</i> .....	11
2.1. 2. <i>Piezoelectric Material</i> .....	15
CHAPTER 3 PROPAGATION OF NONLINEAR ELASTIC WAVES.....	28
3.1. <i>Coupled Wave Equations for Plane Elastic Waves</i> .....	28
3.2. <i>Coupled Wave Equations for Piezoelectric Surface Elastic Waves</i> .....	34
CHAPTER 4 PARAMETRIC AMPLIFICATION OF BULK ELASTIC WAVES .....	42
4.1. <i>Phase Matching Condition and Intensity of the Involving Waves</i> .....	42
4.2. <i>Parametric Amplification</i> .....	45
4.3. <i>Breaking Reciprocity</i> .....	57
CHAPTER 5 FREQUENCY MIXING IN PIEZOELECTRIC SURFACE ELASTIC WAVES.....	60
CHAPTER 6 PARAMETRIC AMPLIFICATION USING LAMB WAVES .....	64
CONCLUSIONS .....	67
APPENDIX A MATHEMATICA CODE USED FOR SOLUTION OF WAVE PROBLEMS.....	68
APPENDIX B COUPLING OF THE MODES OF AN OSCILLATOR .....	110
APPENDIX C CALCULATION OF THE INTENSITY OF AN ACOUSTIC WAVE .....	112
APPENDIX D .....	116
LINEAR AND NONLINEAR ELASTIC CONSTANTS OF $\text{LiNbO}_3$ AND ALUMINUM.....	116
REFERENCES .....	117

# List of Figures

*Figure 1. Schematics of a transceiver in RF applications .....1*

*Figure 1. 1. The crystal and local coordinate axes, represented by upper-case and lower-case letters, respectively..... 8*

*Figure 1. 2. a) rotating the local coordinate system, b) rotating the material..... 9*

*Figure 2. 1. Propagation of plane waves ..... 11*

*Figure 2. 2. Definition of the propagation vector with respect to the crystal axes in LiNbO<sub>3</sub>. ..14*

*Figure 2. 3. Phase velocity of the first (a), second(b) and third(c) mode as function of propagation direction. (d) Plot of the three phase velocities, the faster quasi-longitudinal mode and the two quasi-shear modes .....15*

*Figure 2. 4. Phase velocity for different direction of propagation in Y-Z plane -LiNbO<sub>3</sub> .....17*

*Figure 2. 5. Surface Elastic wave propagating in x direction and decay in x<sub>3</sub>.....18*

*Figure 2. 6. The flowchart to solve for the surface wave velocity iteratively..... 20*

*Figure 2. 7. The stress value son the top surface verses the direction of propagation. The values for T<sub>i3</sub> are zero, which shows the boundary conditions are satisfied..... 23*

*Figure 2. 8. Displacement field in the z direction ..... 24*

*Figure 2. 9. Voltage in the z direction ..... 24*

*Figure 2. 10. Surface elastic wave generated on 128 Y-Cut LiNbO<sub>3</sub> ..... 25*

*Figure 2. 11. One element in the y direction with continuity condition on the sides. .... 25*

*Figure 2. 12. The electric potential, u<sub>4</sub> in eq. 2.2.10, propagating in the x direction and decaying in the z direction ..... 26*

*Figure 2. 13. Displacement in the x direction, u<sub>1</sub> in eq. 2.2.10, propagating in propagating on the x direction and decaying in the z direction..... 27*



<i>Figure 3. 1. Bulk wave propagation of linear elastic wave.....</i>	<i>40</i>
<i>Figure 3. 2. Linear and nonlinear stress terms.....</i>	<i>40</i>
<i>Figure 3. 3. linear and nonlinear stress terms at frequency 3.5 [GHz].....</i>	<i>41</i>
<i>Figure 3. 4. T13 calculated at two frequencies .....</i>	<i>41</i>
<i>Figure 4. 1. Definition of the propagation vector with respect to the crystal axes in LiNbO<sub>3</sub>...</i>	<i>49</i>
<i>Figure 4. 2. (a) Value of <math>r = \Delta k_{DFG} \Delta k_{SFG} = l_{coh}(SFG) l_{coh}(DFG)</math> for different directions of propagation in the X-Y plane. (b) The gain values where <math>r &lt; 0.2</math>, overlaid with <math>r</math>, as a function of propagation direction. (c) Gain for directions that satisfy the condition <math>r &lt; 0.2</math> in three-dimension space .....</i>	<i>51</i>
<i>Figure 4. 3. a) The schematic display of the FE model. In this simulation, signal and pump waves are shown in l1 and l3 modes, respectively. (b) The amplitude of the signal, idler and SFG waves in the direction of propagation. In this case, with pump wave having the 3<sup>rd</sup> mode, the ratio <math>r = \Delta k_{DFG} / \Delta k_{SFG}</math> is large. As expected, since the proper phase matching condition is not satisfied for the process of DFG, the amplitude of the signal wave is dropped instead of being amplified.....</i>	<i>53</i>
<i>Figure 4. 4. (a) The schematic display of the FE model. In this simulation, signal and pump waves are shown in l1 and l2 modes, respectively. (b) Demonstration of the parametric amplification of the signal wave. The amplitude of the signal waves increases as it travels in the media, receiving the energy from the pump wave in the DFG process. (c) The total intensity of the combined waves is conserved in the parametric processes. (d) and (e) comparison between the plot of the signal and idler waves obtained analytically and numerically.....</i>	<i>56</i>
<i>Figure 4. 5. propagation of two elastic waves (a) in the same direction, (b) in the opposite direction. Non-reciprocal propagation of the elastic wave can be realized through the phase matching condition. ....</i>	<i>57</i>

*Figure 4. 6. (a) the schematic of the third simulations, in this setup the signal wave travels in the opposite direction of the pump wave. Amplitude (b) and intensity (c) of the signal, pump, and idler waves. This shows the amplitude of pump and signal waves are constant and idler wave is not generated. Plot of the intensity of the waves at each frequency shows no energy transfer to the signal wave. Comparing this result with the one plotted in Fig. 4(e) shows the non-reciprocal behavior of the system for the signal wave ..... 59*

*Figure 5. 1. Decaying Pump and Signal wave in the material's depth ..... 61*

*Figure 5. 2. Propagation of the Pump wave generated by sets of IDTs ..... 61*

*Figure 5. 3. The nonlinear stress terms that are input as external stress for a) Idler and b) Signal ..... 62*

*Figure 5. 4. The Strain Energy for each frequency shows the transfer of energy from the pump wave to signal and idler waves..... 62*

*Figure 5. 5. The x component of the displacement field. It shows that Signal and Idler waves are amplified, and the direction of the energy flow changes..... 63*

*Figure 6. 1. Direction of propagation and geometry of Lamb wave ..... 64*

*Figure 6. 2. Dispersion curve of the Lamb wave and selected frequencies ..... 65*

*Figure 6. 3. Excitation of the so mode of Lamb wave ..... 66*

*Figure 6. 4. Parametric Amplification of the signal wave ..... 66*

# List of Tables

*Table 1- The properties used in COMSOL simulation ..... 26*

*Table 2 - Direction of propagation with maximum gain..... 50*

*Table 3-The external stress terms for the FEM simulations are given by the following where,  
 $Cijklmn(e) = 12Cijklmn + 12Cijnl\delta km + Cnjkl\delta im + Cinkl\delta jm - Cijkl\delta mn$  and  $Cijkl$ ,  $Cijklmn$   
are the second- and third-order elastic constants..... 52*

*Table 4- Nonlinear Material Properties for Lithium Niobate (LiNbO<sub>3</sub>), ( $\times 10^9 Pa$ ) and  $C_{155} =$   
 $C_{166} = C_{125} = C_{135} = C_{145} = C_{146} = C_{225} = C_{226} = C_{235} = C_{236} = C_{136} = C_{245} = C_{246} =$   
 $C_{334} = C_{335} = C_{336} = C_{345} = C_{346} = C_{445} = C_{446} = C_{555} = C_{556} = C_{566} = C_{666} = C$  ..... 116*

*Table 5- Linear Material Properties for Lithium Niobate (LiNbO<sub>3</sub>) ( $\times 10^9 Pa$ ), density=4700  
Kg/m<sup>3</sup> and  $C_{15} = C_{16} = C_{25} = C_{26} = C_{34} = C_{35} = C_{36} = C_{45} = C_{46} = 0$  ..... 117*

*Table 6- Linear and Nonlinear Material Properties for Aluminum ( $\times 10^9 Pa$ ), density=2680  
Kg/m<sup>3</sup>..... 117*

# Vita

## Education

2015 B.S. -Mechanical Engineering

Sharif University of Technology, Tehran, Iran

## Publication

[1]- M. Zakeri, S. M. Keller, Y. E. Wang, and C. S. Lynch, “Nonreciprocal wave propagation and parametric amplification of bulk elastic waves in nonlinear anisotropic materials,” *New J. Phys.*, vol. 22, no. 2, p. 023009, Feb. 2020, doi: 10.1088/1367-2630/ab61d9

# Introduction

## Motivation

Communicating information is a key part of human life. As new technologies have advanced, almost every aspect of our life has been affected. Radio Frequency (RF) devices and wireless technology are the basis of these developments. The need for reliable and accessible communication with low cost and fast speed is increasing over time. This rapid increase mandates further developments of such systems. Information in the form of analogue voice, digital data or some type of control signal can be carried from one point to another using an RF signal. Radio frequency ranges from 3 KHz, the lowest part of the electromagnetic wave spectrum, to 300 GHz. In RF communication, a transmitter antenna using an AC current creates an Electromagnetic wave that can be detected by the receiver's antenna. The size of an antenna is proportional to the wavelength. Propagating in the same medium, lower frequencies have longer wavelength and therefore they need a larger size antenna to be transmitted. The information to be transferred, which is at lower frequency, is transmitted via a signal at much higher frequency, in the RF range. This high frequency wave is called the carrier signal. This carrier signal builds the connection between the two ends. This process is called modulation. Some property of the carrier signal is changed based on the information signal. If the amplitude of the carrier signal changes based on the data signal, it is called Amplitude Modulation or AM.

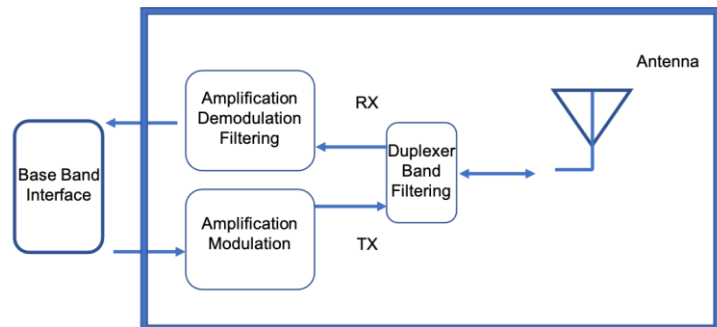


Figure 1. Schematics of a transceiver in RF applications

If the change is on the frequency of the carrier signal, it is called Frequency Modulation or FM. For example, when the data signal has its maximum magnitude, the carrier frequency gets higher and when the data signal is at its minimum value the carrier frequency gets lower.

Transceivers, transmitters (TX) and receivers (RX), are the interfaces between the wireless system and the propagation media. As shown in figure 1, filtering, amplification, modulation, and demodulation are the main functions in a transceiver. One significant problem with amplification is that an amplifier not only amplifies the signal but also any noise that is present. Therefore, a high Q, low passband loss and small bandwidth filter is required to be placed in front of the amplifier. The amplifier at this stage needs to exhibit very low noise and hence it should work in the linear region as much as possible. However, increasing the input power pushes the functionality into the nonlinear region. Based on these design issues, a high-gain amplifier cannot be used in the first stage and a Low Noise Amplifier (LNA) is required. The quality factor required for a filter to be effective is proportional to the center frequency. Lower frequency requires a lower Q. Therefore, in many applications, the signal is passed through a downconverter to an Intermediate Frequency, (IF), typically in the MHz range.

Significant improvements in lithography techniques have resulted in the feature size of silicon-based transistors being reduced dramatically. With smaller transistors, their number on a same size silicon wafer increases, thus higher performance and lower cost has been achieved. Metal Oxide Semiconductor Field Effect Transducers (MOSFET) are used extensively in amplifier applications. Despite their significant improvements in the last couple decades, further reducing their size without sacrificing their functionality has been challenging.

Parametric Amplifiers, (PAMP) provide good alternatives to field effect amplifiers. In MOSFET amplifiers the gain is transferred to the output terminal from a DC power supply. The applied voltage controls the amount of current by changing the conductance of the medium that the current is traveling in. This approach intrinsically generates thermal noise. In contrast, in a parametric process AC power is transferred to the signal through temporal modulation of the capacitance of the system. For instance, a nonlinear variable capacitor, varactor, is used to produce a time-varying signal without significant effect on the noise floor.

Surface and bulk acoustic wave (SAW, BAW) filters, delay lines and oscillators are used extensively in RF transceivers. These provide the advantage of small size due to slower wave velocity at RF frequencies relative to electromagnetic waves, and high efficiency due to reduction of resistive losses compared with similar purely electronic devices. Despite their extensive use for filtering applications, these types of devices have not yet been used as active components, such as low noise amplifiers or mixers. With parametric amplification, SAW and BAW can be utilized for these applications, especially in the IF region where the range of frequency is on the order of MHz.

## Objective

Parametric amplification of a weak signal can be achieved using the nonlinear properties of elastic materials, such as their stiffness. The objective of this research has been to investigate nonlinear elastic waves as a tool to achieve parametric amplification. Here, the framework to enable the investigation of such devices is derived. A general derivation of the coupled-wave formalism for both bulk and surface elastic waves of different frequencies is presented. This is used to identify the requirements for parametric amplification and the associated phase matching conditions. No restrictions are made on material anisotropy or direction of wave propagation. The methodologies used to derive the coupled wave equations are adopted from the field of nonlinear photonics[2]. The coupled wave equations are simplified to provide an analytical solution for collinear propagation of pump and signal waves to investigate the process of parametric difference (down) frequency conversion. The theory predicts parametric amplification of an elastic signal wave through difference frequency conversion. The numerical results and conclusions arrived at in the analytical theory are further investigated using a Finite Element Method (FEM) model to simulate the propagation and interaction of bulk and surface elastic waves in a nonlinear anisotropic medium. The analytical solutions and numerical simulations are in good agreement and provide validation of the approaches used.

## Literature review

Parametric amplification was studied during 1947 to 1970. The interest in this topic, however, diminished with the development of Metal Oxide semiconductors (MOS). Hitting the limits to further reducing the size of MOS based devices and the need for reducing the noise generated by devices has created renewed interest in parametric amplification. An important step was made by Suhl who proposed that a ferrite could be used as a variable reactance[3]. In 1958, Suhl and Tien published a paper on a traveling-wave ferromagnetic amplifier showing that the motion of the magnetization provides the nonlinearities needed for wave mixing[4]. In 1987, Hanna and Murphy[5], showed a positive gain associated with surface acoustic wave (SAW) propagation in magnetic garnet films experimentally. In more recent studies, the topic of investigating parametric systems has been applied to nonreciprocal wave propagation. Creation of non-reciprocity has been achieved with three approaches[6]. Spatiotemporal modulation of some elements of the system, applying an external symmetry breaking field such as an applied magnetic field, and utilizing non-linear behavior of the system. Time and space modulation can be applied to material properties or boundary conditions of the system to break reciprocity. In 2015, Swintek et al.[7] applied a light source with time and space variant intensity to a material with a large photo-elastic coupling to modulate its elastic properties. Spatiotemporal modulation of the elastic constants of the material produced a time dependent superlattice which demonstrated nonreciprocal propagation of a bulk elastic wave. Non-reciprocal propagation of an elastic wave in a beam with spatiotemporal modulation of its Young's modulus and density was investigated by Trainiti et al.[8] It was shown with both time and space modulation, that the dispersion diagrams for this system were no longer symmetric with respect to the frequency axis and directional band gaps were created. Croenne et al.[9] used spatiotemporal modulation of the electrical boundary conditions applied to a periodically repeated assembly of piezoelectric material sandwiched between thin metallic electrode layers. They showed nonreciprocal transmission of an input longitudinal acoustic wave. Their results showed scattering effects such



as frequency conversion and generation of harmonics. Several recent works have also reported experimental realization of reciprocity breaking in a time modulated system[9],[10]. Another approach to produce non-reciprocal behavior is to apply an external symmetry breaking bias field. External magnetic bias fields are commonly used for symmetry breaking[12]–[15], although similar methods have been demonstrated in a linear acoustic device with a circulating fluid that creates an angular-momentum bias[16] and by using magneto-elastic coupling to create a gyrotator[17]. Wang et al. [18] demonstrated breaking time reversal symmetry using gyroscopic inertial effects that creates an apparent external force. Adding a spinning gyroscope to each lattice site, they showed additional topological bands are created that enables multimode propagation of an elastic wave on the edge of the material. While external field biasing has been theoretically and experimentally shown to be effective in some applications, it may not be desirable in terms of physical packaging, fabrication, and increased dimensionality of the system.

Another prolific area, seen frequently in Phononics and metamaterials research, uses material nonlinearity and asymmetry to break reciprocity[19]–[23]. Liang et al. [19], [20]demonstrated acoustic rectification by asymmetrically coupling a super lattice to a nonlinear medium. The nonlinear mechanism, however, did not break reciprocity at the fundamental frequency. Non-reciprocity is realized in the total acoustic flux at the boundaries. Non-reciprocal acoustic propagation in which the frequency of the incident wave was preserved has been demonstrated experimentally in a system composed of a granular chain and a conical rod at low frequencies [24]. Other works have investigated nonlinear material with hierarchal asymmetry[25]–[27]. Moore et al.[26] showed breaking reciprocity within a unit cell featuring a hierarchical internal nonlinearity imposing directional transfer of energy from larger to smaller scale. Fronk et al. [27]extended this asymmetry in a lattice of non-reciprocal unit cells and showed the non-reciprocity at global scale. The general concept of using nonlinearity and asymmetry to break reciprocity is a common theme in the cited references; however, the source of nonlinearity and the asymmetry elements vary.

Each of the methods used to produce non-reciprocity has various strengths and weakness and therefore tend to be applied to specific application areas. For example, much of the work to date has focused on photonic devices or macroscale acoustic devices but has not addressed RF range applications. Other approaches rely on coupled resonators or construction techniques that are not compatible with current IC fabrication techniques. While many works have reported on the study of wave propagation in isotropic or anisotropic nonlinear elastic materials[28]–[30], to the author’s knowledge, none have shown potential for parametric amplification in a nonreciprocal RF application. Due to the high-quality factor possible with mechanical resonance, development of non-reciprocal amplification devices operating at RF frequencies based on elastic materials may prove to be a revolutionary concept and represents the focus of this dissertation. Here the framework to enable the investigation of such devices is developed.

Surface Acoustic Wave devices have been present in wireless communications for more than 4 decades. An important step in utilizing SAW in small devices was taken by White and Voltmer in 1965 by introducing the interdigital transducer as a means to launch and detect SAW[31]. The first mass production of SAW filters was for bandpass filters in TVs in the Intermediate Frequency (IF) range in early 1980[32]. They have been extensively used in digital mobile phones since the 1990’s as filters, duplexers and delay lines[33]–[36]. The application of the acoustic waves in RF devices is in the linear region. To extend their use to active elements, their nonlinear properties must be considered.

Early observation of nonlinear elastic surface waves dates back to late 1960’s. Second harmonic generation was first reported on  $\alpha$ - Quartz by Lopen[37]. Lean et al. reported on first observation of sum and difference frequency generation on  $\alpha$ - Quartz[38] Theoretical studies of nonlinear surface acoustic waves were mainly influenced by two methodologies developed by Kalyanasundram in 1981[39] and Zabolotskaya in 1991[40]. Multiple scale analysis introduced by Kalyanasundram was utilized and extended by many others including Planat[41] who developed the theoretical analysis of nonlinear surface acoustic waves in anisotropic crystals. The method

introduced by Zabolotskaya and followed by many authors applies a Hamiltonian formalism where the stress-free boundary conditions are included in the formalism. This enables one to avoid dealing with nonlinear boundary conditions. Zabolotskaya's derivations was extended for anisotropic crystals by Hamilton et al.[42]. More recent focus on the applications of nonlinear wave propagation has been attributed to nonlinear ultrasonic measurements for detection of fatigue and plastic deformation in early stages that is more sensitive than the conventional linear nondestructive testing techniques[43]. In this method measurements of third order material constants are used as an indication of the level of plastic strain or fatigue damage. Most of the studies have been conducted by sending a monochromatic wave into the nonlinear material and measuring the amplitude of the second harmonic generation[44]. These studies have been extended to investigation of noncolinear wave mixing[45]. W. Li et al.[46], showed mixing of two Lamb waves in Aluminum. The up and down frequency conversion and generation of the second harmonics were studied numerically and demonstrated experimentally.

The problem of wave mixing in nonlinear elastic media, especially for materials with general anisotropy and electromechanical coupling, requires numerical studies. This is done primarily in the time domain, which can be extremely computer time and memory consuming. In our work, the analytical and numerical frameworks are developed to solve the nonlinear wave mixing problem in the frequency domain, which can reduce the computational cost and time, dramatically.

## Scope

Chapter 1 covers transformation of coordinate systems, chapter 2 and 3 discusses propagation of elastic waves in linear and nonlinear materials, respectively to provide a foundation for the later chapters. Chapter 4 shows parametric amplification of bulk elastic waves and discusses the requirements to achieve it. Chapter 5 discusses frequency mixing for surface waves in nonlinear electromechanical material and chapter 6 looks at the use of guided Lamb waves for potential improvements in parametric amplification devices.

## Chapter 1 Crystals Properties in a Rotated Coordinate System

Unlike electromagnetic waves that can propagate through vacuum, propagation of elastic waves is the result of forces between atoms in a solid material. Energy of a propagating wave decays rapidly in an amorphous material because in this material, the atomic interactions are not purely elastic. This can be avoided by choosing single crystal media for propagation. The lattice symmetry of a crystal indicates the geometrical arrangement of the atoms or groups of atoms within the crystal. The characteristics of the propagating waves, their bulk modes and phase velocities, are functions of the direction in which the wave is propagating. Elastic waves propagating in different directions in a crystal have different physical characteristic unless the two directions align with certain crystal lattice symmetry directions. In an isotropic material for instance all the directions show the same macroscopic behavior. In this case, rotating the coordinate system or the material in any direction does not impact the propagating wave; however, in a crystal with less lattice symmetry, rotating the coordinate system and the corresponding wave propagation direction, without adjusting the materials constants, results in a different final solution and must be taken into consideration.

The coordinate system in which the axes are aligned along the edge of a cell of the crystal lattice, defines crystal axes that are represented by capital letters in figure 1.1 (for cubic symmetry for instance)[47]. In many cases, it is easier to solve the problem in a local coordinate system, which can have an arbitrary orientation with respect to the crystal axes. In this chapter, the local (spatial) coordinate system is represented by lower case letters.

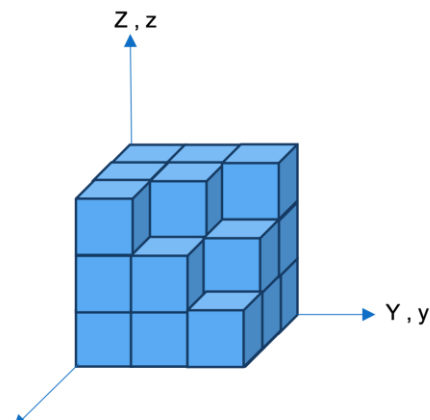


Figure 1. 1. The crystal and local coordinate axes, represented by upper-case and lower-case letters, respectively.

As an example, consider the coordinate system transformation for Y-Cut LiNbO<sub>3</sub>.

In this terminology, Y-cut means that the normal to the top free surface is the Y axis. Assume the wave is propagating in the X direction. There are two ways of looking at the problem. Either keep the material orientation constant and rotate the local coordinate system, Figure 1.2(a) or keep the local coordinate constant and rotate the material, Figure 1.2.(b).

To transform material constants of the crystal the transformation matrix must be defined between the crystal and local coordinates. Depending on the rank of each material property tensor, the transformation matrix is applied to the tensor to obtain the coefficients in the new coordinate

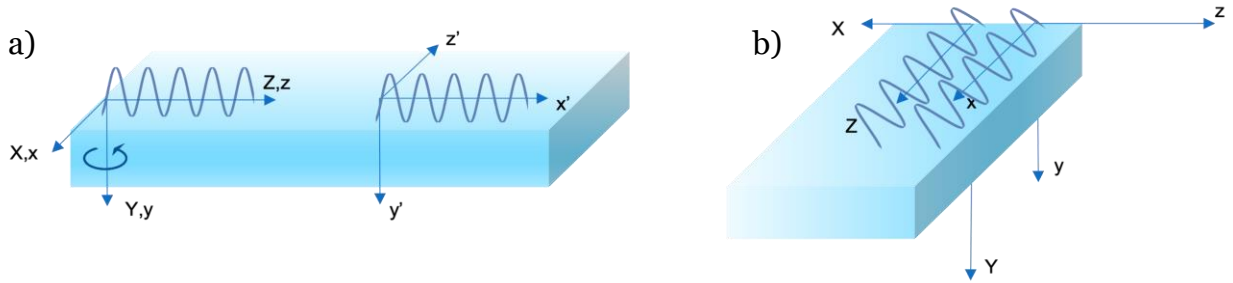


Figure 1. 2. a) rotating the local coordinate system, b) rotating the material

system. A rigorous derivation can be found in Ref. [47], and for the most general forms of transformation of any of the material constants a numerical code in mathematic was implemented as represented in Appendix A.

In this code, the material is assumed to be nonlinear electromechanical, and the material constants are defined using the volume energy expanded approximately as in eq. 1.1.

$$\Phi = \frac{1}{2} C_{ijkl} S_{ij} S_{kl} + \frac{1}{6} C_{ijklmn} S_{ij} S_{kl} S_{mn} - e_{mij} E_m S_{ij} - \frac{1}{2} e_{mijkl} E_m S_{ij} S_{kl} - \frac{1}{2} \varepsilon_{mn} E_m E_n - \frac{1}{6} \varepsilon_{mnp} E_m E_n E_p - \frac{1}{2} l_{mnij} E_m E_n S_{ij} + h. o. t . \quad (1.1)$$

In this expansion,  $C_{ijkl}$  and  $C_{ijklmn}$  are the elasticity, i.e. stiffness constants,  $S_{ij}$  is strain,  $e_{mij}$  is the piezoelectricity tensor,  $E_m$  is the electric field,  $e_{mijkl}$  is the electro elasticity constants,  $\varepsilon_{mn}$

and  $\varepsilon_{mnp}$  are the tensors of dielectric constants,  $l_{mnij}$  is the tensor of electrostriction constants, and h.o.t. is higher order terms. Each are defined in the equations below[30].

$$C_{ijkl} = \frac{\partial^2 \Phi}{\partial S_{ij} \partial S_{kl}} \quad (1.2)$$

$$C_{ijklmn} = \frac{\partial^3 \Phi}{\partial S_{ij} \partial S_{kl} \partial S_{mn}} = \frac{\partial C_{ijkl}}{\partial S_{mn}} \quad (1.3)$$

$$e_{mij} = -\frac{\partial^2 \Phi}{\partial S_{ij} \partial E_m} \quad (1.4)$$

$$e_{mijkl} = \frac{\partial e_{mij}}{\partial S_{kl}} \quad (1.5)$$

$$l_{mnij} = \frac{\partial e_{mij}}{\partial E_n} \quad (1.6)$$

$$\varepsilon_{mn} = \frac{\partial^2 \Phi}{\partial E_m \partial E_n} \quad (1.7)$$

$$\varepsilon_{mnp} = \frac{\partial \varepsilon_{mn}}{\partial E_p} \quad (1.8)$$

# Chapter 2 Propagation of Linear Elastic Waves in Anisotropic Materials

In this chapter propagation of elastic waves in a linear medium is discussed. The medium is assumed to be crystals with general anisotropy. The equations of motion and constitutive equations are used in deriving the wave formulations. The material properties of the crystals define the phase velocity of the wave and its bulk modes. In a bounded medium, such as is the case with surface waves, in addition to material properties the necessary boundary conditions determine the type of the wave and its final solution. In this chapter propagation of an elastic wave is studied for plane waves and expanded for surface elastic waves.

## 2.1. Plane Elastic Waves with General Anisotropy

This section begins with a review of the linear theory of elastic plane waves propagating in a bulk anisotropic material. The modal expansion of plane wave solutions derived in this section are utilized in development of the nonlinear theory. The term “plane waves” indicates that the properties of the wave are the same everywhere on planes perpendicular to the direction of propagation, figure 2.1.

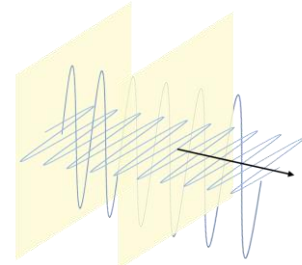


*Figure 2. 1. Propagation of plane waves*

### 2.1. 1. Elastic Materials

In the absence of body forces, the equations of motion and small strain-displacement relations for a mechanical system are represented by eqs. (2.1.1) and (2.1.2), respectively.

$$\mathbb{T}_{ij,j} = \rho \frac{\partial^2 \mathbb{u}_i}{\partial t^2} \tag{2.1.1}$$

$$\mathbb{S}_{ij} = \frac{1}{2} (\mathbb{u}_{i,j} + \mathbb{u}_{j,i}) \tag{2.1.2}$$

The mechanical fields defined in the above relations are real quantities.  $\bar{\mathbb{T}}$  is the symmetric Cauchy stress tensor,  $\rho$  is the material density,  $\bar{\mathbf{u}}$  is the displacement vector and  $\bar{\mathbb{S}}$  is the small strain tensor. They are represented in complex form, eq. (2.1.3).

$$\mathbb{Z}(\bar{\mathbf{x}}, t) = \frac{1}{2} (\mathbb{Z}(\bar{\mathbf{x}}, t) + \mathbb{Z}^*(\bar{\mathbf{x}}, t)) \quad (2.1.3)$$

Here  $\mathbb{Z}(\bar{\mathbf{x}}, t)$  represents any of the stress, strain, or displacement fields. Substituting Eq. (2.1.3) into eqs. (2.1.1) and (2.1.2) leads to eqs. (2.1.4), (2.1.5), and a similar pair of conjugate equations, respectively.

$$\mathbb{T}_{ij,j} = \rho \frac{\partial^2 u_i}{\partial t^2} \quad (2.1.4)$$

$$\mathbb{S}_{ij} = \frac{1}{2} (u_{i,j} + u_{j,i}) \quad (2.1.5)$$

Assuming material properties are instantaneous in time and local in space, the stiffness tensor  $C_{ijkl}$  can be written as eq. (2.1.6),

$$C_{ijkl}(\bar{\mathbf{r}} - \bar{\mathbf{r}}', t - t') = C_{ijkl} \delta(\bar{\mathbf{r}} - \bar{\mathbf{r}}') \delta(t - t') \quad (2.1.6)$$

where  $\delta$  is the Dirac delta function. This allows the linear stress-strain constitutive relations to be expressed in time domain as eq. (2.1.7),

$$\mathbb{T}_{ij}(\bar{\mathbf{x}}, t) = C_{ijkl} \mathbb{S}_{kl}(\bar{\mathbf{x}}, t). \quad (2.1.7)$$

Substituting the complex representation of stress and strain tensors, eq. (2.1.3), in eq. (2.1.7) results in eq. (2.1.8)

$$\mathbb{T}_{ij}(\bar{\mathbf{x}}, t) = C_{ijkl} \mathbb{S}_{kl}(\bar{\mathbf{x}}, t). \quad (2.1.8)$$

Using the definition of small strain, eq. (2.1.5), in eq. (2.1.8) together with use of the symmetry of the stiffness tensor, where  $C_{ijkl} = C_{ijlk}$ , eq. (2.1.9) is obtained.

$$\mathbb{T}_{ij}(\bar{\mathbf{x}}, t) = C_{ijkl} u_{k,l} \quad (2.1.9)$$

Substituting for  $\mathbb{T}_{ij}(\bar{\mathbf{x}}, t)$  from eq. (2.1.9) into eq. (2.1.4) results in the wave equation for elastic waves as in eq. (2.1.10)

$$C_{ijkl} u_{k,lj} = \rho \frac{\partial^2 u_i}{\partial t^2} \quad (2.1.10)$$



Following the methodology described in Ref.[30] solutions of the above equation are expressed as eq. (2.1.11).

$$u_k(\bar{x}, t) = U_k e^{I\omega(\frac{\bar{p}\cdot\bar{x}}{c}-t)} \quad (2.1.11)$$

where,  $I = \sqrt{-1}$ ,  $U_k$  is the amplitude,  $\bar{p} = (p_1, p_2, p_3)$  is a unit vector in the direction of propagation and  $c$  is the wave speed. Substituting eq. (2.1.11) into eq. (2.1.10) results in eq. (2.1.12).

$$(\Gamma_{ik} - \rho c^2 \delta_{ki})U_k = 0 \quad (2.1.12)$$

where

$$\Gamma_{ik} = C_{ijkl}p_j p_l \quad (2.1.13)$$

is a symmetric tensor called the Christoffel acoustic tensor. Eq. (2.1.12) is an eigenvalue problem in  $\bar{U}$  and for non-trivial solutions the determinant of the multiplying matrix must be zero

$$\det|\Gamma_{ik} - \rho c^2 \delta_{ki}| = 0. \quad (2.1.14)$$

This gives a cubic polynomial in terms of  $\rho c^2$ . For each eigenvalue  $c^\alpha$ , determined from the solution of eq. (2.1.14), the corresponding eigenvectors  $\bar{U}^\alpha$  are found from eq. (2.1.12). Unit vectors  $\bar{l}^\alpha$  are defined by normalizing  $\bar{U}^\alpha$  in eq. (2.1.15) and are called eigen modes.

$$l_j^\alpha = \frac{U_j^\alpha}{\sqrt{U_m^{(\alpha)} U_m^{(\alpha)}}} \quad (2.1.15)$$

*Parentheses on repeated indices, e.g.  $(\alpha)$ , are used to indicate no Einstein summation.*

Unlike in isotropic materials, anisotropic materials generally have three distinct eigenvalues or phase velocities associated with three eigenvectors. This means waves propagating in the same direction with different eigenvectors, have different wave velocities. This phenomenon is called “Birefringence” or “Trefringence” [47], depending on number of different wave velocities present in the system. Additionally, the modes  $\bar{l}^\alpha$  are not necessarily purely longitudinal or purely transverse with respect to the propagation direction. However, one of the modes has particle velocity predominately in the direction of propagation and is called the quasi-longitudinal mode and the two others have particle velocities predominately transverse to the direction of

propagation and are called the quasi-shear modes. Any wave with polarization, (particle displacement vector) other than the orthonormal eigenvectors does not have a single value for its propagation velocity and its displacement vector can be expanded in its modal form, eq. (2.1.16), with each of its components having the velocity of the corresponding modal displacement.

$$u_j(\bar{x}, t) = (U^1 e^{(ik^1 \xi)} l_j^1 + U^2 e^{(ik^2 \xi)} l_j^2 + U^3 e^{(ik^3 \xi)} l_j^3) e^{-i\omega t} \quad (2.1.16)$$

As an example, the elastic constants of a common crystal, LiNbO<sub>3</sub>, are used to find and discuss the phase velocities for different propagation directions. In this section, piezoelectric properties of LiNbO<sub>3</sub>, are neglected since only non-piezo constitutive relations are presented up to this point. Figure 2.2 refers the direction of the wave propagation vector  $\bar{p}$  relative to the crystal axes in LiNbO<sub>3</sub>, with each propagation direction determined by two angles  $\theta$  and  $\phi$  with respect to the positive Z and X axes, respectively. Figure 2.3 (a-c) shows the phase velocity for the quasi-longitudinal and the two quasi-shear modes, associated with the propagation direction in 3D

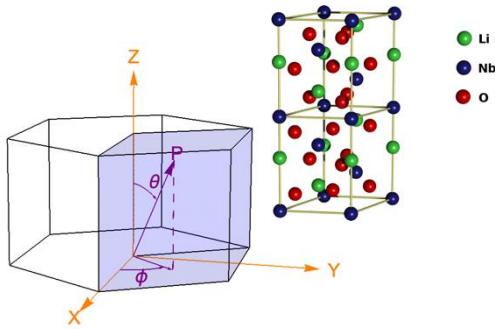


Figure 2. 2. Definition of the propagation vector with respect to the crystal axes in LiNbO<sub>3</sub>.

space. Every point on the surface corresponds to a  $(\theta, \phi)$  pair that defines the propagation direction and the distance from the origin is the magnitude of the modes' wave speed. In addition, the speed values are color coded as indicated in the bar-legend attached. Figure 2.3(d) shows the wave speed of all three modes overlaid. In LiNbO<sub>3</sub>, for  $\theta = 0^\circ$ , that is propagation in the Z direction, the

two shear velocities are equal. This indicates the isotropic behavior of shear modes oriented in the X-Y plane. Figure 2.3(d) shows that the two quasi-shear modes have approximately half the longitudinal wave speed.

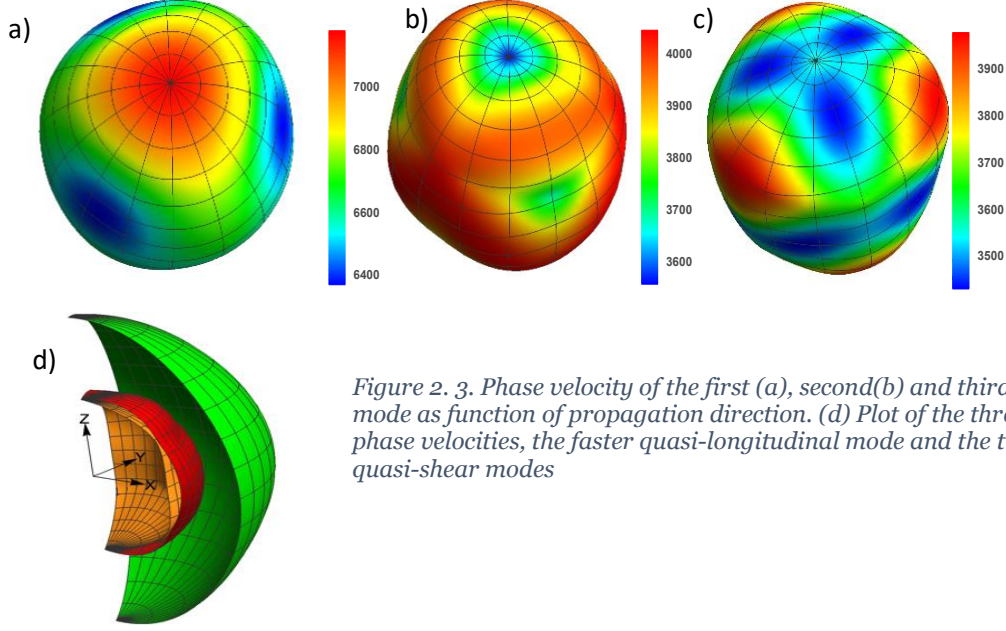


Figure 2. 3. Phase velocity of the first (a), second(b) and third(c) mode as function of propagation direction. (d) Plot of the three phase velocities, the faster quasi-longitudinal mode and the two quasi-shear modes

The above figures were plotted using a code in Mathematica, Appendix A. To find the solutions, eq. (2.1.14) is solved with different propagating vector defined as eq. (2.1.17)

$$\bar{\mathbf{p}} = (\sin(\theta) \cos(\varphi), \sin(\theta) \sin(\varphi), \cos(\theta)) \quad (2.1.17)$$

Note that same results can be achieved by assuming a constant propagating vector, a fixed spatial coordinate and rotating the material, transforming the elastic tensor.

## 2.1. 2. Piezoelectric Material

Constitutive equations with piezo electric coupling are presented in eqs. (2.1.18) and (2.1.19)

$$\mathbb{T}_{ij} = C_{ijkl} \mathbb{u}_{k,l} + e_{mij} \phi_{,m} \quad (2.1.18)$$

$$\mathbb{D}_i = e_{ilk} \mathbb{u}_{k,l} - \epsilon_{ij} \phi_{,j} \quad (2.1.19)$$

The field equations with electrostatic assumption are written as eqs. (2.1.20) and (2.1.21)

$$\rho_0 \left( \frac{\partial^2 \mathbb{u}_i}{\partial t^2} \right) = \mathbb{T}_{j,i,j} \quad (2.1.20)$$

$$\mathbb{D}_{i,i} = 0 \quad (2.1.21)$$

In these equations,  $\bar{\mathbb{T}}$ ,  $\bar{\mathbb{D}}$ ,  $\bar{\mathbb{u}}$  and  $\phi$  are stress, electric displacement field, mechanical displacement field and electric potential, respectively.  $C_{ijkl}$ ,  $e_{mij}$ ,  $\epsilon_{ij}$  are the stiffness components, piezoelectric

coupling coefficients and electric permittivity constants of the material, respectively. Free charge density within the material is assumed to be zero. Substituting eqs (2.1.18) and (2.1.19) in eqs. (2.1.20) and (2.1.21), gives the equation of motion for electric displacement and stress, represented in eq. (2.1.22) and eq. (2.1.22), respectively.

$$\mathbb{D}_{i,i} = e_{ilk} \mathbb{u}_{k,li} - \epsilon_{ij} \phi_{,ji} = 0 \quad (2.1.22)$$

$$\rho_0 \left( \frac{\partial^2 \mathbb{u}_i}{\partial t^2} \right) = C_{ijkl} \mathbb{u}_{k,lj} + e_{mij} \phi_{,mj} \quad (2.1.23)$$

Using the same methodology described in section 2.1.1, the field variable can be written as a summation of a complex variable plus its complex conjugate, (eq. (2.1.3)), eqs. (2.1.22) and (2.1.23) become as eqs. (2.1.24) and (2.1.25), respectively.

$$e_{ilk} u_{k,li} - \epsilon_{ij} \phi_{,ji} = 0 \quad (2.1.24)$$

$$\rho_0 \left( \frac{\partial^2 u_i}{\partial t^2} \right) = C_{ijkl} u_{k,lj} + e_{mij} \phi_{,mj} \quad (2.1.25)$$

Assuming a solution for the displacement field and the electric potential as represented in eq. (2.1.23),

$$(u_k(\bar{x}, t), \phi) = (U_k, \phi) e^{I\omega \left( \frac{\bar{p} \cdot \bar{x}}{c} - t \right)} \quad (2.1.26)$$

and substituting eq. (2.1.26) in eqs. (2.1.22) and (2.1.23), results in eqs. (2.1.27) and (2.1.28), respectively.

$$e_{ilk} p_l p_i U_k - \phi \epsilon_{ij} p_j p_i = 0 \quad (2.1.27)$$

$$\rho_0 c^2 U_i = C_{ijkl} p_l p_j U_k + e_{mij} p_m p_j \phi \quad (2.1.28)$$

Equation (2.1.24) is a scalar equation that allows to write  $\phi$  in terms of  $U_k$ , shown in eq. (2.1.26)

$$\phi = \frac{e_{ilk} p_l p_i U_k}{\epsilon_{ij} p_j p_i} \quad (2.1.29)$$

The i and j in the denominator are dummy and can be replaced by any character for convenience.

Substituting eq. (2.1.29) in eq. (2.1.28) and gives eq. (2.1.30)

$$\rho_0 c^2 U_i = C_{ijkl} p_l p_j U_k + e_{mij} p_m p_j \left( \frac{e_{nlk} p_l p_n}{\epsilon_{fg} p_f p_g} \right) U_k \text{ or}$$

$$\left( \rho_0 c^2 \delta_{ik} - C_{ijkl} p_l p_j - e_{mij} p_m p_j \left( \frac{e_{nlk} p_l p_n}{\epsilon_{f g} p_f p_g} \right) \right) U_k = 0 \quad (2.1.30)$$

Similar to the non-piezoelectric case we define

$$\hat{\Gamma}_{ik} = \left( C_{ijkl} + \left( \frac{e_{nlk} p_n e_{mij} p_m}{\epsilon_{f g} p_f p_g} \right) \right) p_l p_j \quad (2.1.31)$$

$\hat{C}_{ijkl} = C_{ijkl} + \left( \frac{e_{nlk} p_n e_{mij} p_m}{\epsilon_{f g} p_f p_g} \right)$  is called the stiffened elastic tensor. Using this definition, eq. (2.1.31) looks the same as eq. (2.1.12).

In this case the three values found for  $c$  are different than the non-piezo, however, for most crystals this difference is not significant. To compare, the phase velocities of plane waves for  $\text{LiNbO}_3$  are shown in figure 2.4, where the piezoelectric effects are considered.

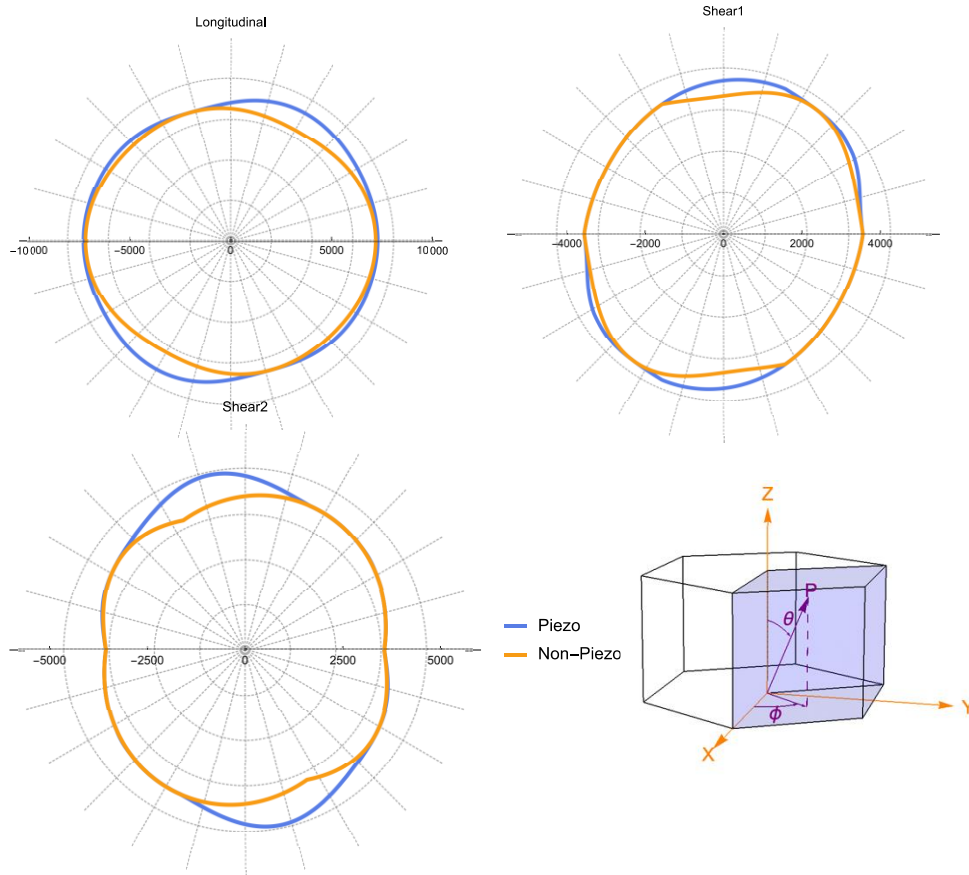


Figure 2. 4. Phase velocity for different direction of propagation in Y-Z plane -LiNbO<sub>3</sub>

The numerical code, in Mathematica, to find the above solutions is presented in Appendix A.

## 2.2. Surface Elastic Waves with General Anisotropy

Surface waves travel mainly on a very thin layer of the surface. The amplitude of the wave drops rapidly away from the free surface. This causes the most part of the wave's energy stays near the surface which makes the wave have higher Intensity in comparison to of the bulk propagation and act as a waveguide.

### 2.2.1. Surface Elastic Wave

In this section, it is assumed the wave is propagating in the  $x$  direction with no variation in the  $y$  direction. With this assumption, the wave appears as a plane wave in  $y$  direction, figure. 2.5.

The wave equation is the same as eq. (2.1.10), except in the case of surface waves, the boundary conditions are to be implemented as well. The boundary conditions are represented in eq. (2.2.1) (a) and (b). The displacement field must go to zero when  $x_3 \rightarrow \infty$  the top surface must be traction free.

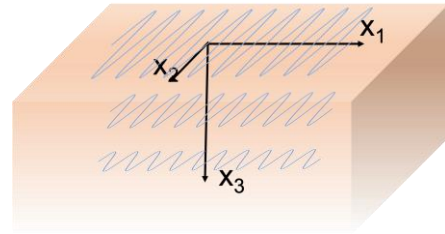


Figure 2. 5. Surface Elastic wave propagating in  $x$  direction and decay in  $x_3$

$$\lim_{x_3 \rightarrow \infty} u \rightarrow 0$$

$$(2.2.1) (a)$$

$$T_{3k}n_3 = 0$$

$$(2.2.1) (b)$$

where  $n_3$  is the normal to the free surface.

The solution to the surface wave equation is assumed to have the form represented in eq. (2.2.2) with propagation in  $x_1$  and decay in  $x_3$  directions, respectively.

$$u_i(\bar{x}, t) = a_i e^{-Isk x_3} e^{Ik x_1} e^{-I\omega t} \quad (\text{To have decay in } x_3 \text{ direction } \text{Im}(s) < 0) \quad (2.2.2)$$

Expanding the derivative indices, only for derivatives with respect to  $x_1$  and  $x_3$  (i.e. derivatives with respect  $x_2$  are zero), of the wave equation, eq. (2.1.10), results in eq. (2.2.3)

$$C_{i1k1}u_{k,11} + C_{i3k1}u_{k,13} + C_{i1k3}u_{k,31} + C_{i3k3}u_{k,33} = -\rho\omega^2 u_i \quad (2.2.3)$$

Substituting eq. (2.2.2) in eq. (2.2.3), gives an eigenvalue equation, eq. (2.2.4), with  $\rho c^2$  being the eigenvalues and  $a_k$  the eigenvectors.

$$(\Gamma_{ik} - \rho c^2 \delta_{ki}) a_k = 0 \quad (2.2.4)$$

where,

$$\Gamma_{ik} = C_{i1k1} - 2sC_{i3k1} + s^2C_{3ik3} \quad (2.2.5)$$

One major difference that makes the solution of surface waves more complicated is that the coefficient matrix,  $\Gamma_{ik}$ , contains an unknown value,  $s$ . This causes one not to be able to find an analytic solution for the surface waves. The two unknowns,  $s$ , and  $c$  are solved for iteratively using the above equation and one with the boundary condition that is discussed below.

Although the value of  $s$  cannot be found directly, the value of  $c^2$  is assumed in eq. (2.2.4), and the corresponding determinant is solved to find values of  $s$ . Given that the  $\Gamma_{ik}$  matrix is 3 by 3 and second order in  $s$ , one expects 6 solutions for  $s$  which will be conjugate pairs. Keeping the values of  $s$  which have negative imaginary magnitude satisfies the boundary condition eq. (2.2.1) (a). The displacement field can then be expanded as the summation of three eigenvectors, as shown in eq. (2.2.6),

$$u_i(\vec{x}) = \sum_{\mu=1}^3 \alpha_{\mu} a_i^{\mu} e^{-Is_{\mu}k x_3} e^{-Ik x_1} \quad (2.2.6)$$

where  $\alpha_{\mu}$  are yet undetermined weighting coefficients for the total solution and the  $a_i^{\mu}$  are the eigenvectors with assumed eigenvalue  $c^2$ . To be a solution, eq. (2.2.6) must still satisfy the other boundary condition, eq. (2.2.1) (b).

To satisfy this boundary condition, eq. (2.2.6) is substituted in eq. (2.2.1) (b) and eq. (2.2.7) is obtained after some algebraic manipulation and extraction of the exponential terms.

$$\sum_{\mu=1}^3 (C_{3ji1} + C_{3ji3} s_{\mu}) \alpha_{\mu} a_i^{\mu} = \sum_{\mu=1}^3 B_{\mu j} \alpha_{\mu} = 0 \text{ at } x_3 = 0 \quad (2.2.7)$$

after defining,  $B_{\mu j} = (C_{3ji1} + C_{3ji3} s_{(\mu)}) a_i^{(\mu)}$ . For eq. (2.2.7) to hold for non-trivial  $\alpha_{\mu}$ , eq. (2.2.8) must be fulfilled, i.e.

$$Det[B_{\mu j}] = 0. \quad (2.2.8)$$

To solve the eigen value problem above, the surface wave velocity had to be assumed, since there is no direct way of calculating it from the analytical solution, up to this point. The process followed

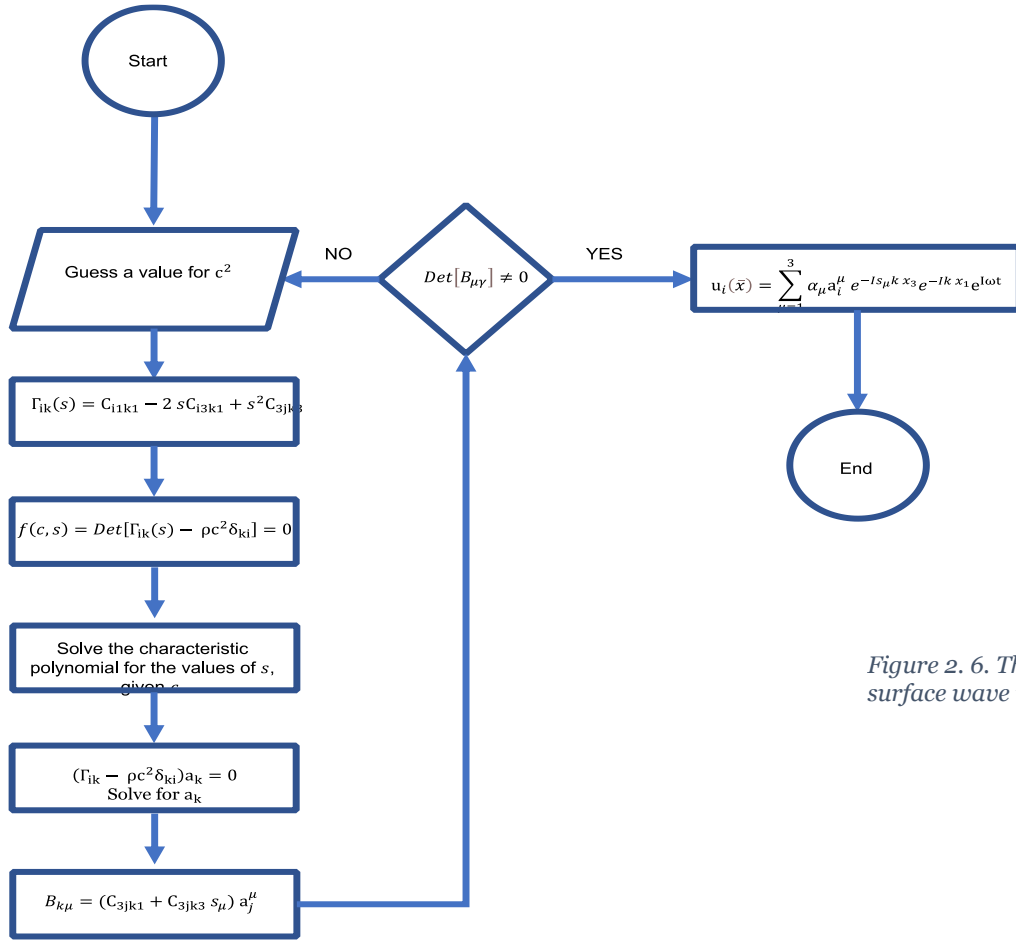


Figure 2. 6. The flowchart to solve for the surface wave velocity iteratively.

is to guess an initial value for velocity and solve the eigenvalue equation in eq. (2.24). Assembling the calculated eigenvalues and eigenvectors in eq. (2.27), the determinant of the boundary condition matrix,  $B_{\mu j}$  is calculated. A non-zero determinant  $B_{\mu j}$  represents an error term due to an incorrect value selected for  $c^2$ . By using a “Shooting Method”, this process can be iterated to find the correct surface velocity that makes the determinate of  $B_{\mu j}$  go to zero. Once the determinant of  $B_{\mu j}$  is equal to zero, the values of  $\alpha_{\mu}$  can be determined, to within an arbitrary factor of one of the components. The voltage component is usually selected as the arbitrary component. Figure 2.6 provides a general flowchart of the process used. Once values of  $\alpha_{\mu}$ ,  $c^2$  and  $s_{\mu}$  are found, eqs. (2.26) and (2.2.2) are used to assemble the solution for  $u_i(\bar{x}, t)$ . Adding the



complex conjugate  $u_i(\bar{x}, t)$  to itself provides the complete solution. The numerical code, in Mathematica, can be found in Appendix A.

### 2.2.2. Surface Waves in Piezoelectric Materials

Constitutive equations and piezo electric field equations with electrostatic assumption are represented in Section 2.1.2, eqs. (2.1.18-21).

Using the four-dimensional notation used by Taylor and Crampin[48], the piezoelectric field equations can be written as a single equation represented in eq. (2.2.9).

$$\rho_0 \eta_{\alpha\beta} \left( \frac{\partial^2 \mathbb{w}_\alpha}{\partial t^2} \right) = \mathbb{T}_{k\beta,k} \quad \alpha = 1,2,3,4 \quad (2.2.9)$$

Where,  $\eta_{\alpha\beta} = \delta_{\alpha\beta} - \delta_{\alpha 4} \delta_{\beta 4}$ ,  $\mathbb{w}_k$  is the mechanical displacement field (where  $k = 1,2,3$ ),  $\mathbb{w}_4 = \phi$  is the electric potential and  $\mathbb{T}_{k4}$  are the electric displacement field components, represented in eq. (2.2.10).

$$\mathbb{w}_\alpha = \mathbb{w}_k \quad (k = 1,2,3), \mathbb{w}_4 = \phi \quad (2.2.10)$$

$$\mathbb{D}_k = \mathbb{T}_{k4}$$

The constitutive relations can also be written in a single equation represented in eq. (2.2.11),

$$\mathbb{T}_{k\beta} = C_{\beta k \gamma n} \mathbb{w}_{\gamma,n} \quad (2.2.11)$$

where,

$$C_{\beta k \gamma n} = C_{lkmn} \quad \beta, \gamma = 1,2,3$$

$$C_{4k \gamma n} = e_{nlk} = C_{\beta k 4n} \quad (2.2.12)$$

$$C_{4k 4n} = -\epsilon_{kn}$$

Traction free and charge free<sup>1</sup> boundary conditions can be written as in eq. (2.2.13)

$$\mathbb{T}_{3\beta} n_3 = 0 \quad (2.2.13)$$

where  $n_3$  is the normal to the free surface.

---

<sup>1</sup> In vacuum, no electrodes or open circuit and negligible gradients over IDT width

Using the same methodology described in Section 2.1.1, the field variable can be written as a summation of a complex variable plus its complex conjugate. Similar to eq. (2.1.3), eq. (2.2.9) can be written as eq. (2.2.14)

$$\rho_0 \eta_{\alpha\beta} (u_\alpha(\bar{x}, t))_{,tt} = C_{\beta k \gamma n} u_{\gamma, nk}(\bar{x}, t) \quad (2.2.14)$$

and a corresponding equation for the complex conjugate term. Assuming a monochromatic wave propagation (single frequency), the displacement field can be represented as eq. (2.2.15).

$$u_\gamma(\bar{x}, t) = u_\gamma(\bar{x}) e^{-I\omega t} \quad (2.2.15)$$

Substituting eq. (2.2.15) in eq. (2.2.14), results eq. (2.2.16).

$$-\rho_0 \eta_{\alpha\beta} \omega^2 u_\alpha(\bar{x}) = C_{\beta k \gamma n} u_{\gamma, nk} \quad (2.2.16)$$

The solution to the surface wave can be assumed to have the form represented in eq. (2.2.2) with propagation in  $x_1$  and decay in  $x_3$  directions, respectively.

$$u_\gamma(\bar{x}) = a_\gamma e^{-Is kx_3} e^{Ikx_1} \quad (\text{To have decay in } x_3 \text{ direction } Im(s) < 0) \quad (2.2.17)$$

Substituting eq. (2.2.17) in eq. (2.2.16), results in eq. (2.2.18)

$$(\rho_0 \eta_{\gamma\beta} c^2 - \Gamma_{\gamma\beta}) a_\gamma = 0 \quad (2.2.18)$$

Where

$$\Gamma_{\gamma\beta} = C_{\beta 3 \gamma 3} s^2 - (C_{\beta 1 \gamma 3} + C_{\beta 3 \gamma 1}) s + C_{\beta 1 \gamma 1} \quad (2.2.19)$$

### 2.2.3. Analytic Results for Surface Waves in Piezoelectric Materials

In the same manner as the elastic surface wave formulation in Section 2.21, eq. (2.2.19) becomes an eigenvalue problem in  $s$ . In this case, there are eight roots, labelled  $s_\mu$ , that form four complex conjugate pairs. To satisfy the decay condition, only the four roots with negative imaginary magnitude will have the desired physical meaning. Similar to the previous Section 2.1, the displacement field can be expanded as the summation of four eigen vectors, i.e., modes, of the problem eigensystem as in eq. (2.2.20).

$$u_\gamma(x_3) = \sum_{\mu=1}^4 \alpha^\mu a_\gamma^\mu e^{-Is k x_3} \quad (2.2.20)$$

Substituting eq. (2.2.20) in eq. (2.2.13) to satisfy the boundary condition, eq. (2.2.21) is obtained.

$$\sum_{\mu=1}^4 B_{\mu\gamma} \alpha^\mu = 0 \quad (2.2.21)$$

where  $B_{\mu\gamma} = (C_{3\gamma\alpha 1} + C_{3\gamma\alpha 3} s_\mu) a_\alpha^\mu$ . For eq. (2.2.21) to hold true for nontrivial  $\alpha^\mu$ , eq. (2.2.22) must be fulfilled

$$\text{Det}[B_{\mu\gamma}] = 0 \quad (2.2.22)$$

The same iterative process explained in section 2.2.1 is implemented to find the surface wave velocity and the four unknowns  $s_\mu$  coefficients. Once these are obtained, eqs. (2.2.20), (2.2.17) and (2.2.15) are used to assemble the solution for  $u_\gamma(\bar{x}, t)$ . Adding the complex conjugate of  $u_\gamma(\bar{x}, t)$  to itself provides the total solution  $\mathbb{u}_\gamma$  which can be decomposed into its displacement and voltage components (i.e.  $\mathbb{u}_k (k = 1,2,3), \mathbb{u}_4 = \phi$ ).

Solutions were obtained, using the numerical code in Appendix A, for 128 Y-Cut, X propagating  $\text{LiNbO}_3$ . The surface wave velocity obtained for this cut is 3986.5 [m/s]. Figure 2.7. shows the stress values on the top surface. The values for  $T_{3\beta}$  are zero as expected. Figures 2.8. and 2.9 show

displacement field components and the voltage along the  $x_3 = Z$  direction, respectively. As the results show in figures 2.8 and 2.9, the amplitude of the wave approaches to zero very rapidly into the depth of the bulk material. These three figures show that the boundary

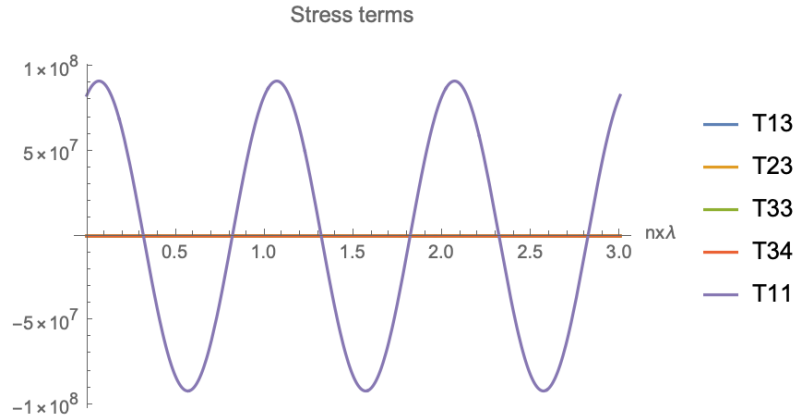


Figure 2. 7. The stress value son the top surface verses the direction of propagation. The values for  $T_{i3}$  are zero, which shows the boundary conditions are satisfied

conditions are satisfied, and the waves have the expected surface propagation characteristics.

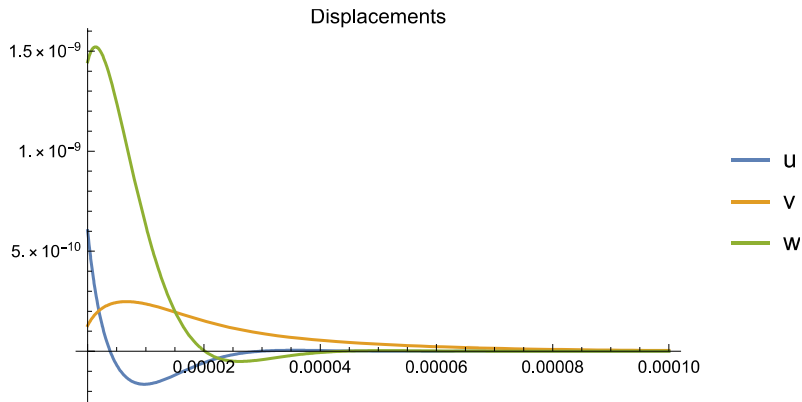


Figure 2. 8. Displacement field in the z direction

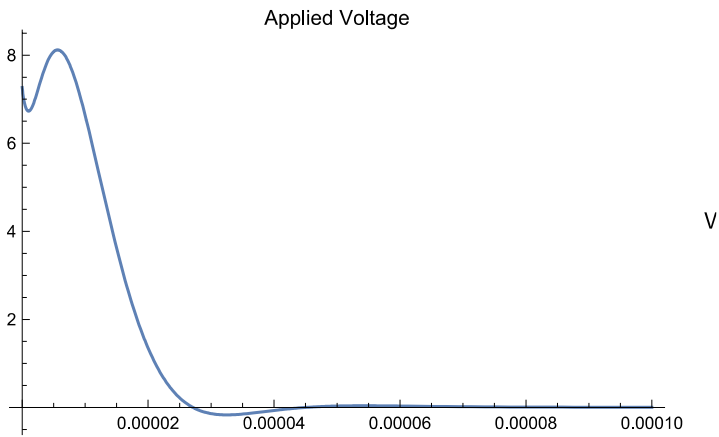


Figure 2. 9. Voltage in the z direction

### 2.2.2. Finite Element Analysis Results

To further investigate surface elastic waves, a finite element simulation, using COMSOL Multiphysics platform for implementation was developed and is presented in this section. The model has a 3D geometry with Interdigital Transducer (IDT) on the top surface that creates a surface wave as shown in figure 2.10.

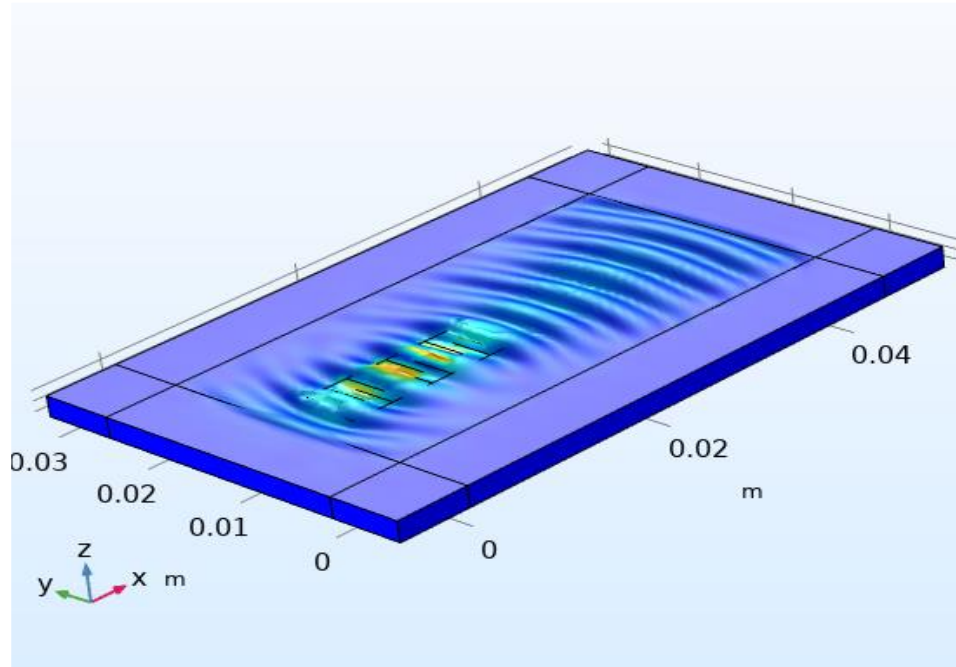


Figure 2. 10. Surface elastic wave generated on 128 Y-Cut LiNbO<sub>3</sub>

Since it is assumed that there is no variation in the y direction, it is computationally economical to have only one element in the y direction as shown in figure 2.11.

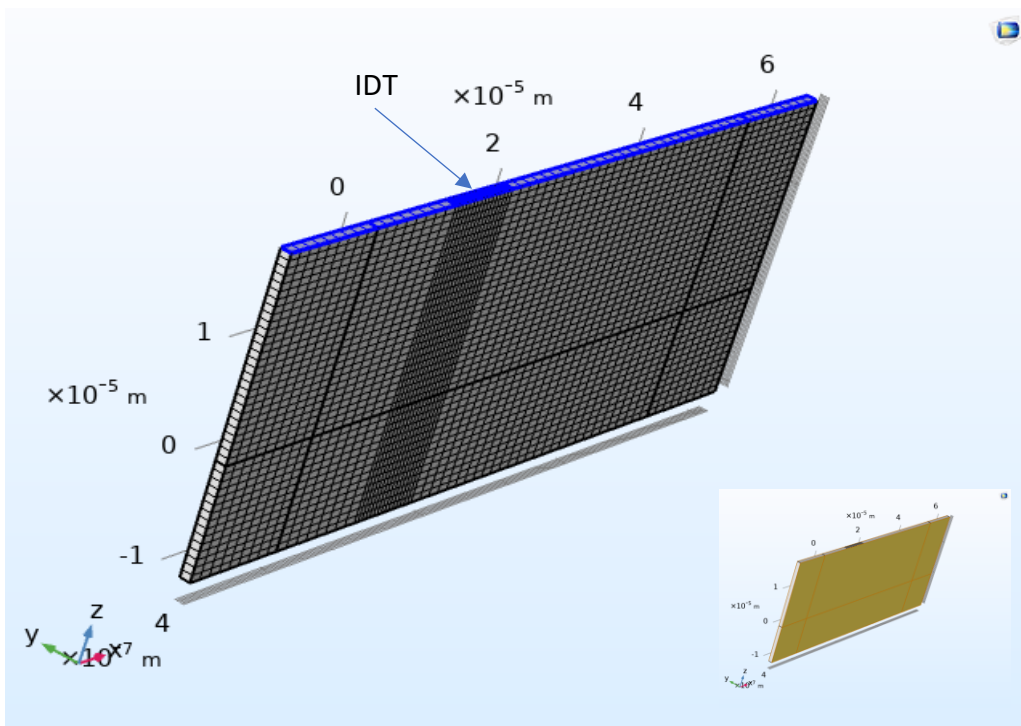


Figure 2. 11. One element in the y direction with continuity condition on the sides.

Table 1- The properties used in COMSOL simulation

EXPRESSION	VALUE
SIGNAL FREQUENCY	2 [GHz]
SURFACE WAVE VELOCITY	3986.5[m/s]
WAVELENGTH OF SIGNAL WAVE ( $\lambda$ )	1.9 E-6 m
LENGTH	19* $\lambda$
WIDTH	Mesh size
HIGHT	8* $\lambda$
MESH SIZE	$\lambda/32$

The material constants for 128 Y-Cut LiNbO<sub>3</sub> are calculated using the code developed for coordinate rotation, discussed in chapter 1. Figures 2.12 and 2.13 show the results obtained for electric potential and the displacement, respectively, with propagation in the x direction. It is evident in this figures that most of the wave's energy is confined to the top surface and the amplitude of the waves decrease in the z direction, which validates the obtained results.

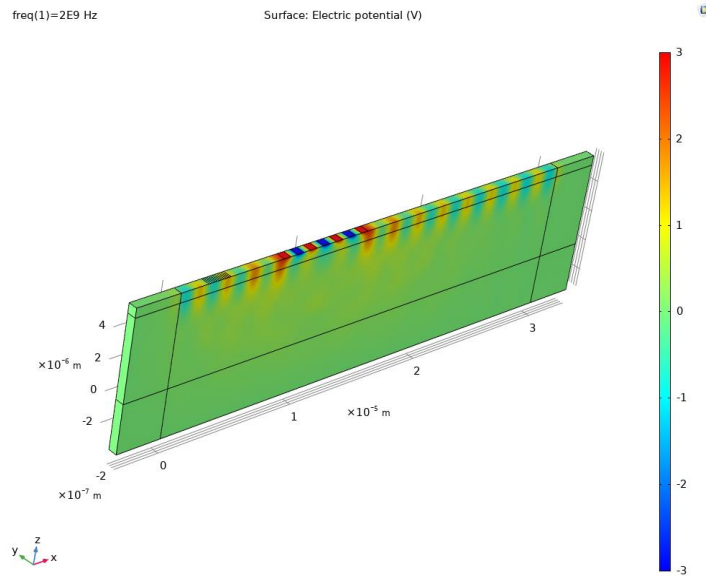


Figure 2. 12. The electric potential,  $u_4$  in eq. 2.2.10, propagating in the x direction and decaying in the z direction

The finite element results are compared with the quasi-analytical solution obtained in the

Mathematica code. Figure 2.14 (a) and (b) show the stress component in the x direction,  $T_{11}$ , obtained from COMSOL model and the Mathematica code. The difference of amplitudes in the

propagating region between the two methods is approximately 6%, showing very good agreement between the two.

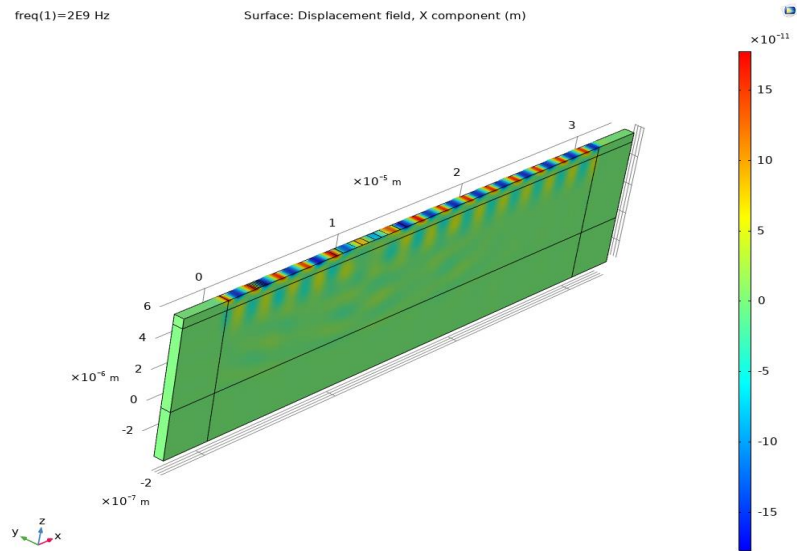


Figure 2.13. Displacement in the x direction,  $u_1$  in eq. 2.2.10, propagating in propagating on the x direction and decaying in the z direction

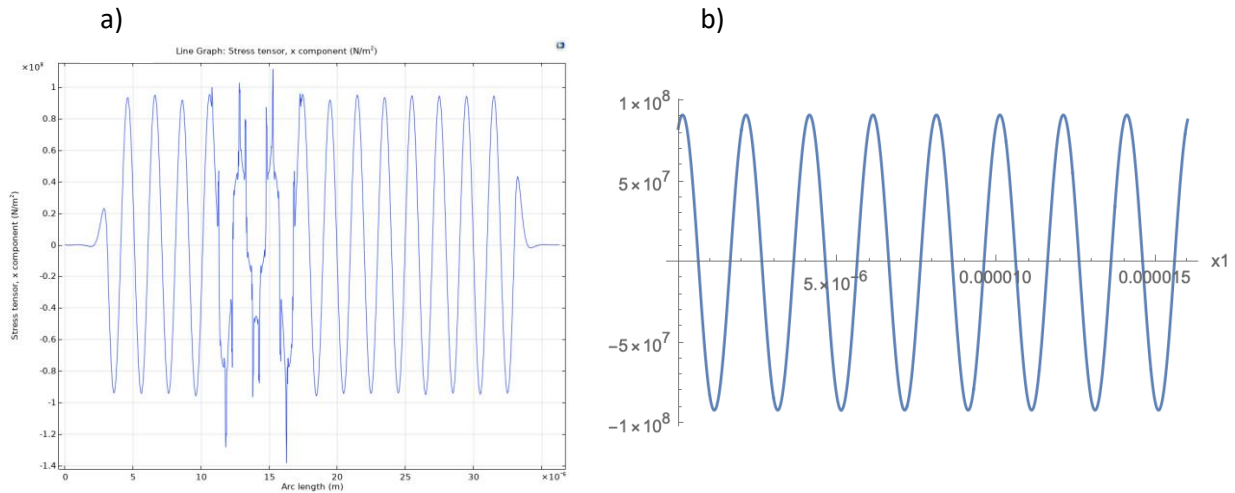


Figure 2.14. The stress component in the x direction,  $\mathbb{T}_{11}$ , obtained from a) COMSOL model and b) the Mathematica code

## Chapter 3 Propagation of Nonlinear Elastic Waves

In this chapter, the study of waves is extended to nonlinear materials with finite strain. This is utilized to model waving mixing effects that will be used to produce parametric amplification.

### 3.1. Coupled Wave Equations for Plane Elastic Waves

Nonlinear terms are the result of either material nonlinearities, i.e., higher order terms in the constitutive equations, or geometric nonlinearity which appears when small strain approximations are exceeded. Starting with the nonlinear constitutive equations, the second Piola-Kirchoff stress tensor is approximated as a series expansion of the strain energy with respect to the Lagrangian strain,  $\mathbb{S}_{ij}$ , in eq. (3.1.1), which is the same as eq. (1.1) without the piezoelectric effect.

$$\mathbb{T}_{ij} = \frac{\partial \Phi}{\partial \mathbb{S}_{ij}} = C_{ijkl} \mathbb{S}_{kl} + \frac{1}{2} C_{ijklmn} \mathbb{S}_{kl} \mathbb{S}_{mn} + \dots \quad (3.1.1)$$

where  $\Phi$  is the elastic energy function,  $C_{ijkl}$  is the rank four stiffness tensor, that is associated with linear behavior,  $C_{ijklmn}$  is the rank six stiffness tensor that represents quadratic nonlinearity and the Lagrangian strain,  $\mathbb{S}_{ij}$ , which is given in eq. (3.1.2)

$$\mathbb{S}_{ij} = \frac{1}{2} (\mathbb{w}_{i,j} + \mathbb{w}_{j,i} + \mathbb{w}_{k,i} \mathbb{w}_{k,j}) \quad (3.1.2)$$

Where  $\mathbb{w}(\bar{X}, t) = \bar{X} - \bar{x}(\bar{X}, t)$ , is the displacement field, the vectors  $\bar{x}$  and  $\bar{X}$  describe the material position in the deformed and undeformed states, respectively, while  $\mathbb{w}_{i,j} = \frac{\partial \mathbb{w}_i}{\partial X_j}$ , is the derivative of the displacement with respect to the *undeformed coordinate*.

Lagrangian strain can be divided into linear and geometrically nonlinear terms as in eq. (3.1.3)

$$\mathbb{S}_{ij} = \mathbb{S}_{ij}^L + \mathbb{S}_{ij}^{NL} \quad (3.1.3)$$

Substituting eq. (3.1.3) in eq. (3.1.1), results in eq. (3.1.4).



$$\mathbb{T}_{ij} = C_{ijkl}(\mathbb{S}_{kl}^L + \mathbb{S}_{kl}^{NL}) + \frac{1}{2}C_{ijklmn}(\mathbb{S}_{kl}^L\mathbb{S}_{mn}^L + \mathbb{S}_{kl}^L\mathbb{S}_{mn}^{NL} + \mathbb{S}_{kl}^{NL}\mathbb{S}_{mn}^L + \mathbb{S}_{kl}^{NL}\mathbb{S}_{mn}^{NL}) \quad (3.1.4)$$

keeping the terms up to the second order in displacement gradients, the nonlinear constitutive equations is written in eq. (3.1.5).

$$\mathbb{T}_{ij} = C_{ijkl}(\mathbb{S}_{kl}^L + \mathbb{S}_{kl}^{NL}) + \frac{1}{2}C_{ijklmn}(\mathbb{S}_{kl}^L\mathbb{S}_{mn}^L) \quad (3.1.5)$$

Substituting for  $\mathbb{S}_{ij}^L$  and  $\mathbb{S}_{ij}^{NL}$  from eq. (3.1.2), eq. (3.1.5) becomes

$$\mathbb{T}_{ij} = \frac{1}{2}C_{ijkl}(\mathbb{w}_{k,l} + \mathbb{w}_{l,k}) + \frac{1}{2}C_{ijkl}\mathbb{w}_{p,k}\mathbb{w}_{p,l} + \frac{1}{2}C_{ijklmn}\mathbb{w}_{k,l}\mathbb{w}_{m,n} \quad (3.1.6)$$

The equation of motion is written in terms of first Piola-Kirchoff stress as shown in eq. (3.1.7)

$$\frac{\partial \bar{\sigma}_{ji}}{\partial X_j} = \rho_0 \frac{\partial^2 \mathbb{w}_i}{\partial t^2} \quad (3.1.7)$$

Here  $\rho_0$  is the density of the material represented in the undeformed coordinate system.

The first Piola-Kirchoff stress is related to the second Piola-Kirchoff stress by eq. (3.1.8),

$$\bar{\sigma}_{ji} = \mathbb{T}_{jl} \frac{\partial x_i}{\partial X_l} = \mathbb{T}_{jl} \left( \delta_{il} + \frac{\partial \mathbb{w}_i}{\partial X_l} \right) = \mathbb{T}_{ji} + \mathbb{T}_{jl} \frac{\partial \mathbb{w}_i}{\partial X_l} \quad (3.1.8)$$

Substituting for  $\mathbb{T}_{ij}$  from eq (3.1.6), and, keeping the terms up to the second order in displacement gradients, the term  $\mathbb{T}_{jl} \frac{\partial \mathbb{w}_i}{\partial X_l}$  in eq. (3.1.8) is found in eq. (3.1.9)

$$\mathbb{T}_{jl} \frac{\partial \mathbb{w}_i}{\partial X_l} = C_{jnkl}\mathbb{w}_{k,l}\mathbb{w}_{i,n} = C_{jnkl}\delta_{im}\mathbb{w}_{k,l}\mathbb{w}_{m,n}. \quad (3.1.9)$$

Considering symmetry properties of the rank four and six tensors, and by substituting from eqs. (3.1.6) and (3.1.9), into eq. (3.1.8), the first Piola-Kirchoff stress can be found in terms of displacement gradients in eq. (3.1.10).

$$\bar{\sigma}_{ji} = C_{ijkl}\mathbb{w}_{k,l} + \frac{1}{2}C_{ijklmn}^{(e)}\mathbb{w}_{k,l}\mathbb{w}_{m,n} \quad (3.1.10)$$

where

$$C_{ijklmn}^{(e)} = C_{jiklmn} + 2C_{jnkl}\delta_{im} + C_{jinl}\delta_{km} \quad (3.1.11)$$

is the effective rank six tensor. Substituting for  $\bar{\sigma}_{ji}$  from eq. (3.1.10) into the equation of motion, eq. (3.1.7), eq. (3.1.12) is derived.

$$(C_{ijkl} \mathbb{u}_{k,l} + \frac{1}{2} C_{ijklmn}^{(e)} \mathbb{u}_{k,l} \mathbb{u}_{m,n} )_{,j} = \rho_0 \frac{\partial^2 \mathbb{u}_i}{\partial t^2}. \quad (3.1.12)$$

As in Chapter 2 the definition of eq. (2.1.3) is used to introduce the complex displacement field  $\bar{u}(\bar{x}, t)$  which transforms eq. (3.1.12) into eq. (3.1.13).

$$(C_{ijkl} (u_{k,l} + u_{k,l}^*) + \frac{1}{4} C_{ijklmn}^{(e)} (u_{k,l} u_{m,n} + u_{k,l} u_{m,n}^* + u_{k,l}^* u_{m,n} + u_{k,l}^* u_{m,n}^*))_{,j} = \rho_0 \left( \frac{\partial^2 (u_i + u_i^*)}{\partial t^2} \right) \quad (3.1.13)$$

The previous expression contains product terms of  $\bar{u}(\bar{x}, t)$  and  $\bar{u}^*(\bar{x}, t)$  in addition to those of  $\bar{u}(\bar{x}, t)$  making the expression more complicated than the linear equation.

The nonlinear effects are approximated as a perturbation of the linear system when the nonlinear terms are small. This is shown in eq. (3.1.14), where each  $\bar{u}^q$  term is at frequency  $\omega_q$ .

$$u_j(\bar{x}, t) = \sum_q u_j^q(\bar{x}) e^{-I\omega_q t} \quad (3.1.14)$$

Substituting eq. (3.1.14) in eq. (3.1.13) and using the notational convention described in eq. 3.1.15

(a) and 3.1.15 (b)

$$u_i^q(\bar{x}) = u_i(\omega_q) \quad 3.1.15 \text{ (a)}$$

$$u_i^{*q}(\bar{x}) = u_i^*(\omega_q) = u_i(-\omega_q) \quad 3.1.15 \text{ (b)}$$

leads to eq. (3.1.16).

$$\begin{aligned} & \left[ C_{ijkl} \sum_q (u_{k,l}(\omega_q) e^{-I\omega_q t} + u_{k,l}(-\omega_q) e^{I\omega_q t}) = \frac{1}{4} \sum_{r,s} C_{ijklmn}^{(e)} (u_{k,l}(\omega_r) u_{m,n}(\omega_s) e^{-I(\omega_r + \omega_s)t} + \right. \\ & u_{k,l}(\omega_r) u_{m,n}(-\omega_s) e^{-I(\omega_r - \omega_s)t} + u_{k,l}(-\omega_r) u_{m,n}(\omega_s) e^{-I(-\omega_r + \omega_s)t} + \\ & \left. u_{k,l}(-\omega_r) u_{m,n}(-\omega_s) e^{-I(-\omega_r - \omega_s)t} \right]_{,j} = -\rho_0 \sum_q \omega_q^2 (u_i(\omega_q) e^{-I\omega_q t} + u_i(-\omega_q) e^{I\omega_q t}) \quad (3.1.16) \end{aligned}$$

The exponential terms are collected so that the same frequency exists in each summand. This requires  $\omega_q = \omega_r + \omega_s$  where  $r$ ,  $q$ , and  $s$  can take on negative values as appropriate to satisfy the conjugate frequency notation of eq. 3.1.15 (b). This implies:

$$(C_{ijkl} u_{k,l}(\omega_q) + \frac{1}{2} \sum_{(r,s)} C_{ijklmn}^{(e)} u_{k,l}(\omega_r) u_{m,n}(\omega_s))_{,j} = -\rho_0 \omega_q^2 u_i(\omega_q) \quad (3.1.17)$$

The summation in eq. (3.1.17) is over all frequency combinations that satisfy the constraint  $\omega_q = \omega_r + \omega_s$  for each  $\omega_q$  independently. The notation  $(r, s)$  here is used to represent pairs that satisfies

this constraint  $\omega_q = \omega_r + \omega_s$  for  $r$ ,  $s$ , and  $q$ ; hence, they are not independent of each other.

Distributing the derivatives in eq. (3.1.17) leads to eq. (3.1.18).

$$C_{ijkl}u_{k,lj}(\omega_q) + \frac{1}{2}\sum_{(r,s)} C_{ijklmn}^{(e)}(u_{k,lj}(\omega_r)u_{m,n}(\omega_s) + u_{k,l}(\omega_r)u_{m,nj}(\omega_s)) = -\rho_0\omega_q^2 u_i(\omega_q) \quad (3.1.18)$$

If waves at different frequencies have the same propagation direction, i.e.,  $u_j^q(\bar{x})$  are collinear, the eigen basis of eq. (2.1.15) can be used to expand all of them. Projecting these displacement fields on the eigen basis results in eq. (3.1.19)

$$u_i(\omega_q) = \sum_{\alpha} u^{\alpha}(\omega_q) l_i^{\alpha} \quad (3.1.19)$$

In this equation, the component  $u^{\alpha}$  is the amplitude of the  $\alpha$  mode and defines the component of “particle” displacement (for example quasi-longitudinal, shear, etc.) in the  $\bar{l}^{\alpha}$  direction. If we assume the displacement field at frequency  $\omega_q$  is composed of only one mode, i.e., its particle displacements are aligned with only one of the eigen basis vectors, we can simplify eq. (3.1.19) to eq. (3.1.20)

$$u_i(\omega_q) = u^{(\alpha)}(\omega_q) l_i^{(\alpha)}. \quad (3.1.20)$$

This is referred to as a mono-mode assumption.

The scalar quantity  $\xi$  is defined to be the inner product of the  $\bar{p}$  and  $\bar{x}$  vectors as shown in eq. (3.1.21)

$$\xi = \bar{p} \cdot \bar{x} \quad (3.1.21)$$

Where  $\bar{p}$  in this equation is the unit vector representing the direction of propagation. The derivative of  $\xi$  with respect to  $\bar{x}$  is represented in eq. (3.1.22).

$$\frac{\partial \xi}{\partial x_i} = p_i. \quad (3.1.22)$$

If the variation of the amplitude of a wave over its wavelength is small, the slowly varying amplitude assumption (SVA) applies. The SVA assumes the spatial dependence of the amplitude function for a wave can be decomposed into the product of a slowly varying envelope term, or amplitude, and a harmonic function capturing its oscillations. Under the SVA assumption the

wave components at different frequencies,  $u^\alpha(\omega_q)$ , propagating in direction  $\bar{p}$ , i.e. along  $\xi$ , have the form of eq. (3.1.23),

$$u^{(\alpha)}(\omega_q) = u^{(\alpha)}(\bar{x}) e^{Ik_q^{(\alpha)}\xi} = u^{(\alpha)}(\omega_q) e^{Ik_q^{(\alpha)}\xi} \quad (3.1.23)$$

where  $u^{(\alpha)}$  is the slowly varying amplitude term and  $k_q^{(\alpha)}$  is the magnitude of the wave vector for the wave component at frequency  $\omega_q$  in mode  $\alpha$ .

Taking the first and the second derivatives of displacement in eq. (3.1.20) with respect to  $x$ , in addition to use of the chain rule results in eqs. (3.1.24) and (3.1.25), respectively.

$$u_{k,l}(\omega_q) = u_{,\xi}^{(\alpha)}(\omega_q) p_l l_k^\alpha, \quad (3.1.24)$$

and

$$u_{k,lj}(\omega_q) = u_{,\xi\xi}^{(\alpha)}(\omega_q) p_l p_j l_k^\alpha \quad (3.1.25)$$

Substituting eqs. (3.1.24) and (3.1.25) into eq. (3.1.18) gives eq. (3.1.26).

$$C_{ijkl} p_l p_j l_k^\alpha u_{,\xi\xi}^{(\alpha)}(\omega_q) + \frac{1}{2} \sum_{(r,s)} C_{ijklmn} p_j p_l p_n l_k^{(\beta)} l_m^{(\gamma)} (u_{,\xi\xi}^{(\beta)}(\omega_r) u_{,\xi}^{(\gamma)}(\omega_s) + u_{,\xi}^{(\beta)}(\omega_r) u_{,\xi\xi}^{(\gamma)}(\omega_s)) = -\rho_0 \omega_q^2 l_i^\alpha u^{(\alpha)}(\omega_q) \quad (3.1.26)$$

Using the definition of  $\Gamma_{ik} = C_{ijkl} p_j p_l$  in eq. (2.1.13) also defining  $\Lambda_{ikm}$  in eq. (3.1.27)

$$\Lambda_{ikm} = C_{ijklmn} p_j p_l p_n \quad (3.1.27)$$

eq. (3.1.26) is rewritten as eq. (3.1.28).

$$\Gamma_{ik} l_k^\alpha u_{,\xi\xi}^{(\alpha)}(\omega_q) + \frac{1}{2} \sum_{(r,s)} \Lambda_{ikm} l_k^{(\beta)} l_m^{(\gamma)} (u_{,\xi\xi}^{(\beta)}(\omega_r) u_{,\xi}^{(\gamma)}(\omega_s) + u_{,\xi}^{(\beta)}(\omega_r) u_{,\xi\xi}^{(\gamma)}(\omega_s)) = -\rho_0 \omega_q^2 l_i^\alpha u^{(\alpha)}(\omega_q) \quad (3.1.28)$$

With eq. (3.1.23), the first and second derivatives of  $u^{(\alpha)}(\omega_q)$  with respect to  $\xi$  are presented in eq. (3.1.29) and (3.1.30), respectively.

$$u_{,\xi}^{(\alpha)}(\omega_q) = [u_{,\xi}^{(\alpha)}(\omega_q) + Ik_q^{(\alpha)} u^{(\alpha)}(\omega_q)] e^{Ik_q^{(\alpha)}\xi} \quad (3.1.29)$$

$$u_{,\xi\xi}^{(\alpha)}(\omega_q) = [u_{,\xi\xi}^{(\alpha)}(\omega_q) + 2Ik_q^{(\alpha)} u_{,\xi}^{(\alpha)}(\omega_q) - (k_q^{(\alpha)})^2 u^{(\alpha)}(\omega_q)] e^{Ik_q^{(\alpha)}\xi} \quad (3.1.30)$$

With the assumption of SVA, the inequalities in (3.1.31) hold

$$u_{,\xi\xi}^{(\alpha)}(\omega_q) \ll k_q^{(\alpha)} u_{,\xi}^{(\alpha)}(\omega_q) \ll (k_q^{(\alpha)})^2 u^{(\alpha)}(\omega_q) \quad (3.1.31)$$

and eq. (3.1.30) simplifies to

$$u_{,\xi\xi}^{(\alpha)}(\omega_q) = \left[ 2Ik_q^{(\alpha)} u_{,\xi}^{(\alpha)}(\omega_q) - (k_q^{(\alpha)})^2 u^{(\alpha)}(\omega_q) \right] e^{Ik_q^{(\alpha)}\xi} \quad (3.1.32)$$

Substituting eqs. (3.1.29) and (3.1.30) into eq. (3.1.26) and discarding the low order terms in inequalities (3.1.31), eq. (3.1.33) is obtained.

$$\begin{aligned} & \left[ \Gamma_{ik} 2Ik_q^{(\alpha)} l_k^{(\alpha)} u_{,\xi}^{(\alpha)}(\omega_q) - \left( \Gamma_{ik} (k_q^{(\alpha)})^2 l_k^{(\alpha)} - \rho_0 \omega_q^2 l_i^{(\alpha)} \right) u^{(\alpha)}(\omega_q) \right] e^{Ik_q^{(\alpha)}\xi} - \\ & \frac{1}{2} \sum_{(r,s)} \Lambda_{ikm} \sum_{\beta,\gamma} \left[ Ik_r^{(\beta)} k_s^{(\gamma)} \left( k_r^{(\beta)} + k_s^{(\gamma)} \right) l_k^{(\beta)} l_m^{(\gamma)} u^{(\beta)}(\omega_r) u^{(\gamma)}(\omega_s) \right] e^{I(k_r^{(\beta)} + k_s^{(\gamma)})\xi} = 0 \end{aligned} \quad (3.1.33)$$

In chapter 2.1 it is shown,  $\sum_{\alpha} \left( \Gamma_{ik} (k_q^{(\alpha)})^2 l_k^{\alpha} - \rho_0 \omega_q^2 l_i^{\alpha} \right) u^{\alpha}(\omega_q) = 0$ , and eq. (3.1.33) simplifies to eq. (3.1.34).

$$\begin{aligned} & \left[ \Gamma_{ik} k_q^{(\alpha)} l_k^{(\alpha)} u_{,\xi}^{(\alpha)}(\omega_q) \right] e^{Ik_q^{(\alpha)}\xi} - \frac{1}{4} \sum_{(r,s)} \Lambda_{ikm} \sum_{\beta,\gamma} \left[ k_r^{(\beta)} k_s^{(\gamma)} \left( k_r^{(\beta)} + \right. \right. \\ & \left. \left. k_s^{(\gamma)} \right) l_k^{(\beta)} l_m^{(\gamma)} u^{(\beta)}(\omega_r) u^{(\gamma)}(\omega_s) \right] e^{I(k_r^{(\beta)} + k_s^{(\gamma)})\xi} = 0 \end{aligned} \quad (3.1.34)$$

Multiplying both sides of eq. (3.1.34) by  $l_i^{(\alpha)}$ ,

$$\begin{aligned} & \left[ \Gamma_{ik} k_q^{(\alpha)} l_k^{(\alpha)} u_{,\xi}^{(\alpha)}(\omega_q) \right] e^{Ik_q^{(\alpha)}\xi} = \frac{1}{4} \sum_{(r,s)} \Lambda_{ikm} l_i^{(\alpha)} l_k^{(\beta)} l_m^{(\gamma)} \left[ k_r^{(\beta)} k_s^{(\gamma)} \left( k_r^{(\beta)} + \right. \right. \\ & \left. \left. k_s^{(\gamma)} \right) u^{(\beta)}(\omega_r) u^{(\gamma)}(\omega_s) \right] e^{I(k_r^{(\beta)} + k_s^{(\gamma)})\xi} \end{aligned} \quad (3.1.35)$$

With the definitions,  $G^{\alpha\alpha} = \Gamma_{ik} l_i^{(\alpha)} l_k^{\alpha}$  and  $H^{\alpha\beta\gamma} = \Lambda_{ikm} l_i^{\alpha} l_k^{\beta} l_m^{\gamma}$ , and  $K_{rs}^{\beta\gamma} = k_r^{(\beta)} k_s^{(\gamma)} \left( k_r^{(\beta)} + k_s^{(\gamma)} \right)$  eq.

(3.1.35) can be rewritten as eq. (3.1.36)

$$\left[ G^{\alpha\alpha} k_q^{(\alpha)} u_{,\xi}^{(\alpha)}(\omega_q) \right] = \frac{1}{4} \sum_{(r,s)} H^{\alpha\beta\gamma} \left[ K_{rs}^{\beta\gamma} u^{(\beta)}(\omega_r) u^{(\gamma)}(\omega_s) \right] e^{I(k_r^{(\beta)} + k_s^{(\gamma)} - k_q^{(\alpha)})\xi} \quad (3.1.36)$$

In a second order process involving two distinct frequencies  $\omega_r$  and  $\omega_s$  that satisfy  $\omega_q = \omega_r + \omega_s$ ,

$\omega_q = \omega_s + \omega_r$  also needs to be considered. Equation (3.1.36) for a pair of  $\omega_r$  and  $\omega_s$  becomes,

$$G^{\alpha\alpha} k_q^{(\alpha)} u_{,\xi}^{(\alpha)}(\omega_q) = \frac{1}{4} (H^{\alpha\beta\gamma} + H^{\alpha\beta\gamma}) \left[ K_{rs}^{\beta\gamma} u^{(\beta)}(\omega_r) u^{(\gamma)}(\omega_s) \right] e^{I(k_r^{(\beta)} + k_s^{(\gamma)} - k_q^{(\alpha)})\xi} \quad (3.1.37)$$

Further simplifying

$$\mathbf{u}_{,\xi}^{(\alpha)}(\omega_q) = \frac{1}{4} \frac{(H^{\delta\beta\gamma} + H^{\delta\beta\gamma})}{G^{\alpha\alpha}} \left[ \frac{k_{rs}^{\beta\gamma}}{k_q^{(\alpha)}} \mathbf{u}^{(\beta)}(\omega_r) \mathbf{u}^{(\gamma)}(\omega_s) \right] e^{I(\Delta k_{rsq})\xi} \quad (3.1.38)$$

$$\text{where } \Delta k_{rsq} = k_r^\beta + k_s^\gamma - k_q^\alpha \quad (3.1.39)$$

Equation (3.1.38) is the most general form of the coupled wave equations for a frequency mixing process in a nonlinear elastic material under the mono-mode and slowly varying amplitude assumptions, regardless of the number of frequencies involved. In general, analytic solutions of eq. (3.1.38) do not exist and numerical methods must be applied for a specific frequency mixing process. In Section 4.3 analytic solutions of eq. (3.1.38) for the process of Difference Frequency Generation (DFG) involving three frequency components is given and its application to parametric amplification process is discussed.

## 3.2. Coupled Wave Equations for Piezoelectric Surface Elastic Waves

To design an electromechanical device, the piezoelectric characteristic of the material must be considered to transfer electrical energy into strain energy.

Going back to eq. (1.1), the volume energy is expanded approximately as

$$\begin{aligned} \Phi = & \frac{1}{2} C_{ijkl} \mathbb{S}_{ij} \mathbb{S}_{kl} + \frac{1}{6} C_{ijklmn} \mathbb{S}_{ij} \mathbb{S}_{kl} \mathbb{S}_{mn} - e_{mij} \mathbb{E}_m \mathbb{S}_{ij} - \frac{1}{2} e_{mijkl} \mathbb{E}_m \mathbb{S}_{ij} \mathbb{S}_{kl} - \frac{1}{2} \varepsilon_{mn} \mathbb{E}_m \mathbb{E}_n - \\ & \frac{1}{6} \varepsilon_{mnp} \mathbb{E}_m \mathbb{E}_n \mathbb{E}_p - \frac{1}{2} l_{mnij} \mathbb{E}_m \mathbb{E}_n \mathbb{S}_{ij} + h. o. t. \end{aligned} \quad (1.1)$$

And the stress term is derived in eq. (3.2.1).

$$\mathbb{T}_{ij} = C_{ijkl} \mathbb{S}_{kl} + \frac{1}{2} C_{ijklmn} \mathbb{S}_{kl} \mathbb{S}_{mn} - e_{mij} \mathbb{E}_m - e_{mijkl} \mathbb{E}_m \mathbb{S}_{kl} - \frac{1}{2} l_{mnij} \mathbb{E}_m \mathbb{E}_n \quad (3.2.1)$$

In comparison to eq. (3.1.1), two more nonlinear terms are present. The electroelastic term is  $e_{mijkl} \mathbb{E}_m \mathbb{S}_{kl}$  and electrostriction is represented by  $l_{mnij} \mathbb{E}_m \mathbb{E}_n$ . In addition, eq. (3.2.2)

$$\mathbb{D}_i = \varepsilon_{ij} \mathbb{E}_j + \frac{1}{2} \varepsilon_{inp} \mathbb{E}_n \mathbb{E}_p + e_{ipq} \mathbb{S}_{pq} + \frac{1}{2} e_{imnpq} \mathbb{S}_{mn} \mathbb{S}_{pq} + l_{ijpq} \mathbb{E}_j \mathbb{S}_{pq} \quad (3.2.2)$$

represents the electric displacement field in the presence of higher order terms.

As discussed in section 3.1, the equations of motion are written for the first Piola-Kirchoff stress terms. The stress terms obtained from the volume energy are the symmetric second Piola-Kirchoff stresses. To convert the stress terms in eq (3.2.3) to the first Piola-Kirchoff stress terms, the same equation as in eq (3.1.8), is utilized

$$\bar{\sigma}_{ji} = \mathbb{T}_{jl} \frac{\partial x_i}{\partial X_l} = \mathbb{T}_{jl} \left( \delta_{il} + \frac{\partial \mathbb{w}_i}{\partial X_l} \right) = \mathbb{T}_{ji} + \mathbb{T}_{jl} \frac{\partial \mathbb{w}_i}{\partial X_l} \quad (3.1.8)$$

Substituting eq. (3.1.2) in eqs. (3.2.1) and (3.2.2) for the strain terms and with electrostatic assumption,  $\mathbb{E}_j = \phi_{,j}$ , eqs. (3.2.3) and (3.2.4) are derived.

$$\bar{\sigma}_{ji} = C_{ijkl} \mathbb{w}_{k,l} + \frac{1}{2} C_{ijklmn}^{(e)} \mathbb{w}_{k,l} \mathbb{w}_{m,n} + e_{mij} \phi_{,m} + e_{mjikl}^{(e)} \phi_{,m} \mathbb{w}_{k,l} - \frac{1}{2} l_{mnji}^{(e)} \phi_{,m} \phi_{,n} \quad (3.2.3)$$

$$\mathbb{D}_i = -\varepsilon_{ij} \phi_{,j} + \frac{1}{2} \varepsilon_{inp} \phi_{,n} \phi_{,p} + e_{ipq} \mathbb{w}_{p,q} + \frac{1}{2} e_{imnpq}^{-(e)} \mathbb{w}_{m,n} \mathbb{w}_{p,q} - \frac{1}{2} l_{inpq}^{(e)} \phi_{,n} \mathbb{w}_{p,q} \quad (3.2.4)$$

where, from previous section, eq. (3.1.11) we have

$$C_{ijklmn}^{(e)} = C_{jiklmn} + 2C_{jnkl} \delta_{im} + C_{jinl} \delta_{km} \quad (3.1.11)$$

$$e_{mjikl}^{(e)} = e_{mijkl} + e_{mj} \delta_{ki} \quad (3.2.5)$$

$$l_{mnji}^{(e)} = l_{mnji} + \delta_{mn} \delta_{ji} - \delta_{jm} \delta_{in} - \delta_{jn} \delta_{im} \quad (3.2.6)$$

Using the four-dimensional notation of Taylor and Crampin[48], the piezoelectric field equations can be written as a single equation represented in eq. (3.2.7). Definition of the field variables,  $\mathbb{w}_\alpha$  and  $\mathbb{D}_k$  are the same as section 2.2. eq. (2.2.10).

$$\mathbb{w}_\alpha = (\mathbb{w}_k, \mathbb{w}_4 = \phi) \quad \alpha = 1,2,3,4$$

$$\mathbb{D}_k = \mathbb{T}_{k4}$$

$$\eta_{\alpha\beta} = \delta_{\alpha\beta} - \delta_{\alpha 4} \delta_{\beta 4} \quad (2.2.10)$$

$$\rho_0 \eta_{\alpha\beta} \left( \frac{\partial^2 \mathbb{w}_\alpha}{\partial t^2} \right) = (\mathbb{T}_{k\beta})_{,k} \quad (3.2.7)$$

$$\mathbb{T}_{k\beta} = C_{\beta k \gamma n} \mathbb{w}_{\gamma,n} + \gamma_{\beta k \gamma l \delta n} \mathbb{w}_{\gamma,l} \mathbb{w}_{\delta,n} \quad (3.2.8)$$

In eq. (3.2.8),  $C_{\beta k \gamma n}$  are the same as eq. (2.2.12) and the nonlinear constants are defined in eq. 3.2.9 (a-d).

$$\gamma_{ijklmn} = \frac{1}{2} C_{ijklmn}^{(e)} \quad (3.2.9) \text{ (a)}$$

$$\gamma_{ikjl4n} = \gamma_{ik4njl} = e_{mikjl}^{(e)} \quad (3.2.9) \text{ (b)}$$

$$\gamma_{ik4l4n} = -\frac{1}{2} l_{lnik}^{(e)} \quad (3.2.9) \text{ (c)}$$

$$\gamma_{4k4l4n} = \frac{1}{2} \epsilon_{kln} \quad (3.2.9) \text{ (d)}$$

In the case of a nonlinear surface wave, the nonlinear boundary condition, given in eq. (3.2.10) must be satisfied.

$$\mathbb{T}_{3\alpha} n_3 = C_{\beta 3 \gamma n} \mathbb{u}_{\gamma, n} + \gamma_{\beta 3 \gamma l \delta n} \mathbb{u}_{\gamma, l} \mathbb{u}_{\delta, n} = 0 \quad \text{at } x_3 = 0 \quad (3.2.10)$$

where,  $n_3$  is the normal to the free surface.

Integrating from both sides of the eq. (3.2.7) with respect to  $x_3$ , leads to eq. 3.2.11 (a).

$$\int_0^\infty \rho_0 \eta_{\alpha\beta} \left( \frac{\partial^2 \mathbb{u}_\alpha}{\partial t^2} \right) dx_3 = \int_0^\infty (\mathbb{T}_{k\beta})_{,k} dx_3 \quad 3.2.11 \text{ (a)}$$

Expanding the right-hand side of eq. (3.2.10), gives eq. (3.2.11 b).

$$\int_0^\infty (\mathbb{T}_{k\beta})_{,k} dx_3 = \int_0^\infty (\mathbb{T}_{1\beta})_{,1} dx_3 + \int_0^\infty (\mathbb{T}_{3\beta})_{,3} dx_3 \quad (3.2.11) \text{ (b)}$$

The last term in eq. (3.2.11) can be integrated to produce eq. (3.2.12).

$$\int_0^\infty (\mathbb{T}_{3\beta})_{,3} dx_3 = \mathbb{T}_{3\beta}(x_3 \rightarrow \infty) - \mathbb{T}_{3\beta}(x_3 \rightarrow 0) \quad (3.2.12)$$

Stress terms go to zero as  $x_3$  goes to infinity, and the stress-free boundary condition on  $x_3 = 0$ , makes the second term of eq. (3.2.12) go to zero, equation (3.2.10) simplifies to eq. (3.2.13).

$$\int_0^\infty \rho_0 \eta_{\alpha\beta} \left( \frac{\partial^2 \mathbb{u}_\alpha}{\partial t^2} \right) dx_3 = \int_0^\infty ((\mathbb{T}_{1\beta})_{,1}) dx_3 \quad (3.2.13)$$

Using the same methodology described in the chapter 2, the definition of eq. (2.1.3) that introduces the complex displacement field  $\bar{u}(\bar{x}, t)$  eq. (3.2.13) is transformed into eq. (3.2.14).

$$\begin{aligned} \int_0^\infty \rho_0 \eta_{\alpha\beta} (u_\alpha(\bar{x}, t) + u_\alpha^*(\bar{x}, t))_{,tt} dx_3 = \int_0^\infty \left[ C_{\beta 1 \gamma n} (u_{\gamma, n}(\bar{x}, t) + u_{\gamma, n}^*(\bar{x}, t)) + \right. \\ \left. \frac{1}{2} \gamma_{\beta 1 \gamma l \delta n} (u_{\gamma, l}(\bar{x}, t) u_{\delta, n}(\bar{x}, t) + u_{\gamma, l}(\bar{x}, t) u_{\delta, n}^*(\bar{x}, t) + u_{\gamma, l}^*(\bar{x}, t) u_{\delta, n}(\bar{x}, t) + u_{\gamma, l}^*(\bar{x}, t) u_{\delta, n}^*(\bar{x}, t)) \right]_{,1} dx_3 \end{aligned} \quad (3.2.14)$$

Assuming  $u_\gamma$  is superposition of monochromatic harmonic waves, it can be written as eq. (3.2.15)



$$u_\gamma(\bar{x}, t) = \sum_q u_\gamma^q(\bar{x}) e^{-l\omega_q t} \quad (3.2.15)$$

Substituting eq. (3.2.15) in eq. (3.2.14), for every pair of  $(r, s)$  that satisfies  $\omega_q = \omega_r + \omega_s$ , eq. (3.2.16) is obtained.

$$\int_0^\infty -\rho_0 \omega_q^2 \eta_{\alpha\beta} u_\alpha^q(\bar{x}) dx_3 = \int_0^\infty [C_{\beta 1 \gamma n} u_{\gamma, n1}^q(\bar{x}) + \frac{1}{2} \gamma_{\beta 1 \gamma l \delta n} (u_{\gamma, l1}^r(\bar{x}) u_{\delta, n}^s(\bar{x}) + u_{\gamma, l}^r(\bar{x}) u_{\delta, n1}^s(\bar{x}) + u_{\gamma, l1}^s(\bar{x}) u_{\delta, n}^r(\bar{x}) + u_{\gamma, l}^s(\bar{x}) u_{\delta, n1}^r(\bar{x}))] dx_3 \quad (3.2.16)$$

Due to symmetry of  $\gamma_{\beta 1 \gamma l \delta n}$  for  $(n, l)$  and  $(\delta, \gamma)$  in above equation, and as explained in chapter 2, eq. (3.2.16) can be written as eq. (3.2.17).

$$\int_0^\infty -\rho_0 \omega_q^2 \eta_{\alpha\beta} u_\alpha^q(\bar{x}) dx_3 = \int_0^\infty C_{\beta 1 \gamma n} u_{\gamma, n1}^q(\bar{x}) + \gamma_{\beta 1 \gamma l \delta n} (u_{\gamma, l1}^r(\bar{x}) u_{\delta, n}^s(\bar{x}) + u_{\gamma, l}^r(\bar{x}) u_{\delta, n1}^s(\bar{x})) dx_3 \quad (3.2.17)$$

With the slowly varying amplitude assumption, explained in section, 3.1, the solution to the nonlinear surface wave is expanded in the basis of the linear problem, with the envelope of each mode being the function of  $x_1$ .

$$u_\gamma^q(\bar{x}) = \sum_\mu \alpha^{q\mu}(x_1) a_\gamma^\mu e^{-Is_\mu k_q x_3} e^{Ik_q x_1} \quad (3.2.18)$$

Taking the derivatives of the  $u_\gamma^q(\bar{x})$  terms in eq. (3.2.18),

$$u_{\gamma, 1}^q(\bar{x}) = \sum_\mu (\alpha_{, 1}^{q\mu}(x_1) + Ik_q \alpha^{q\mu}(x_1)) a_\gamma^\mu e^{-Is_\mu k_q x_3} e^{Ik_q x_1} \quad (3.2.19) (a)$$

$$u_{\gamma, 11}^q(\bar{x}) = \sum_\mu (\alpha_{, 11}^{q\mu}(x_1) + 2Ik_q \alpha_{, 1}^{q\mu}(x_1) - k_q^2 \alpha^{q\mu}(x_1)) a_\gamma^\mu e^{-Is_\mu k_q x_3} e^{Ik_q x_1} \quad (3.2.19) (b)$$

$$u_{\gamma, 13}^q(\bar{x}) = \sum_\mu (-Is_\mu k_q \alpha_{, 1}^{q\mu}(x_1) + (s_\mu k_q^2) \alpha^{q\mu}(x_1)) a_\gamma^\mu e^{-Is_\mu k_q x_3} e^{Ik_q x_1} \quad (3.2.19) (c)$$

$$u_{\gamma, 3}^q(\bar{x}) = \sum_\mu -Is_\mu k_q \alpha^{q\mu}(x_1) a_\gamma^\mu e^{-Is_\mu k_q x_3} e^{Ik_q x_1} \quad (3.2.19) (d)$$

$$u_{\gamma, 33}^q(\bar{x}) = \sum_\mu -s_\mu^2 k_q^2 \alpha^{q\mu}(x_1) a_\gamma^\mu e^{-Is_\mu k_q x_3} e^{Ik_q x_1} \quad (3.2.19) (e)$$

Expanding the terms inside the integral in eq. (3.2.17), leads to eq. (3.2.20)

$$C_{\beta 1 \gamma n} u_{\gamma, n1}^q(\bar{x}) + \gamma_{\beta 1 \gamma l \delta n} (u_{\gamma, l1}^r(\bar{x}) u_{\delta, n}^s(\bar{x}) + u_{\gamma, l}^r(\bar{x}) u_{\delta, n1}^s(\bar{x})) = C_{\beta 1 \gamma 1} u_{\gamma, 11}^q(\bar{x}) + C_{\beta 1 \gamma 3} u_{\gamma, 13}^q(\bar{x}) + [\gamma_{\beta 1 \gamma 1 \delta 1} (u_{\gamma, 11}^r(\bar{x}) u_{\delta, 1}^s(\bar{x}) + u_{\gamma, 1}^r(\bar{x}) u_{\delta, 11}^s(\bar{x})) + \gamma_{\beta 1 \gamma 1 \delta 3} (u_{\gamma, 11}^r(\bar{x}) u_{\delta, 3}^s(\bar{x}) + u_{\gamma, 1}^r(\bar{x}) u_{\delta, 13}^s(\bar{x})) + u_{\gamma, 13}^r(\bar{x}) u_{\delta, 1}^s(\bar{x}) + u_{\gamma, 3}^r(\bar{x}) u_{\delta, 11}^s(\bar{x}) + \gamma_{\beta 1 \gamma 3 \delta 3} (u_{\gamma, 13}^r(\bar{x}) u_{\delta, 3}^s(\bar{x}) + u_{\gamma, 3}^r(\bar{x}) u_{\delta, 13}^s(\bar{x}))] \quad (3.2.20)$$

Substituting the derivatives calculated in eqs. (3.2.19 a-e) in eq. (3.2.20) and with the inequalities that are the results of SVA from eq. (3.1.21) (a), eq. (3.2.21) (b) is obtained.

$$u_{,\xi\xi}^{(\alpha)}(\omega_q) \ll k_q^{(\alpha)} u_{,\xi}^{(\alpha)}(\omega_q) \ll (k_q^{(\alpha)})^2 u^{(\alpha)}(\omega_q) \quad (3.1.21) \text{ (a)}$$

$$\begin{aligned} \int_0^\infty \rho_0 \omega_q^2 \eta_{\alpha\beta} \sum_\mu \alpha^{q\mu} a_\alpha^\mu e^{-Is_\mu k_q x_3} e^{Ik_q x_1} dx_3 &= \int_0^\infty \sum_\mu (C_{\beta 1\gamma 1} (2 Ik_q \alpha_{,1}^{q\mu} - k_q^2 \alpha^{q\mu}) + \\ (C_{\beta 1\gamma 3}) (-Is_\mu k_q \alpha_{,1}^{q\mu} + (s_\mu k_q^2) \alpha^{q\mu})) a_\gamma^\mu e^{-Is_\mu k_q x_3} e^{Ik_q x_1} &+ \sum_{\eta,\theta=1}^4 [\gamma_{\beta 1\gamma 1\delta 1} (-k_r^2 Ik_s - k_s^2 Ik_r) + \\ \gamma_{\beta 1\gamma 1\delta 3} (k_r^2 (Is_\theta k_s) + k_s^2 (Is_\eta k_r) + (s_\eta k_r^2) Ik_s + (s_\theta k_s^2) Ik_r) - \gamma_{\beta 1\gamma 3\delta 3} ((s_\eta k_r^2) Is_\theta k_s + \\ (s_\theta k_s^2) Is_\eta k_r)] a_\gamma^\eta a_\delta^\theta \alpha^{s\theta} \alpha^{r\eta} e^{-I(s_\eta k_r + s_\theta k_s) x_3} e^{I(k_r + k_s) x_1} dx_3 & \quad (3.2.21) \text{ (b)} \end{aligned}$$

In the above equations, for conciseness,  $\alpha^{q\mu}(x_1)$  is substituted with  $\alpha^{q\mu}$ , but it is still a function of  $x_1$ .

Recalling the linear propagation of the surface wave, eq. (2.2.9)

$$\rho_0 \eta_{\alpha\beta} \left( \frac{\partial^2 \mathbb{w}_i}{\partial t^2} \right) = \mathbb{T}_{k\beta,k} \quad (2.2.9)$$

the  $\mathbb{T}_{k\beta,k}$  term is expanded and taking the integral with respect to  $x_3$  gives eq. (3.2.22)

$$\int_0^\infty \rho_0 \eta_{\alpha\beta} \left( \frac{\partial^2 \mathbb{w}_i}{\partial t^2} \right) dx_3 = \int_0^\infty \mathbb{T}_{k\beta,k} dx_3 = \int_0^\infty \mathbb{T}_{1\beta,1} dx_3 + \int_0^\infty \mathbb{T}_{3\beta,3} dx_3 \quad (3.2.22)$$

The  $\int_0^\infty \mathbb{T}_{3\beta,3} dx_3$  term vanishes as in eq. (3.2.12), and eq. (3.2.22) becomes eq. (3.2.23).

$$\int_0^\infty \rho_0 \eta_{\alpha\beta} \left( \frac{\partial^2 \mathbb{w}_i}{\partial t^2} \right) dx_3 = \int_0^\infty \mathbb{T}_{1\beta,1} dx_3 \quad (3.2.23)$$

Substituting the linear surface wave solution eq. (2.2.20), in eq. (3.2.23), eq. (3.2.24) is obtained.

$$\begin{aligned} \int_0^\infty -\rho_0 \omega_q^2 \eta_{\alpha\beta} \sum_\mu \alpha^{q\mu} a_\alpha^\mu e^{-Is_\mu k_q x_3} e^{Ik_q x_1} dx_3 &= \int_0^\infty \sum_\mu (-C_{\beta 1\gamma 1} k_q^2 \alpha^{q\mu} - \\ C_{\beta 1\gamma 3} (s_\mu k_q^2) \alpha^{q\mu}) a_\gamma^\mu e^{-Is_\mu k_q x_3} e^{Ik_q x_1} dx_3 & \quad (3.2.24) \end{aligned}$$

Based on this equation, eq. (3.2.21), simplifies to eq. (3.2.25).

$$\begin{aligned} \int_0^\infty \sum_\mu (C_{\beta 1\gamma 1} (2 k_q \alpha_{,1}^{q\mu}) - (C_{\beta 1\gamma 3}) (s_\mu k_q \alpha_{,1}^{q\mu})) a_\gamma^\mu e^{-Is_\mu k_q x_3} e^{Ik_q x_1} &+ \sum_{\eta,\theta=1}^4 [\gamma_{\beta 1\gamma 1\delta 1} (k_r^2 k_s + k_s^2 k_r) - \\ \gamma_{\beta 1\gamma 1\delta 3} (k_r^2 (s_\theta k_s) + k_s^2 (s_\eta k_r) + (s_\eta k_r^2) k_s + (s_\theta k_s^2) k_r) + \gamma_{\beta 1\gamma 3\delta 3} ((s_\eta k_r^2) s_\theta k_s + \\ (s_\theta k_s^2) s_\eta k_r)] a_\gamma^\eta a_\delta^\theta \alpha^{s\theta} \alpha^{r\eta} e^{-I(s_\eta k_r + s_\theta k_s) x_3} e^{I(k_r + k_s) x_1} dx_3 &= 0 \quad (3.2.25) \end{aligned}$$

Since  $k_q = k_r + k_s$ , and after some algebraic simplifications, eq. (3.2.25) can be further reduced to eq. (3.2.25).

$$\int_0^\infty \sum_\mu (2 C_{\beta 1 \gamma 1} - C_{\beta 1 \gamma 3} s_\mu) k_q \alpha_{,1}^{q\mu} a_\gamma^\mu e^{-I s_\mu k_q x_3} + k_s k_r \sum_{\eta, \theta=1}^4 [\gamma_{\beta 1 \gamma 1 \delta 1} (k_r + k_s) - \gamma_{\beta 1 \gamma 1 \delta 3} (k_r s_\theta + k_s s_\eta + k_r s_\eta + k_s s_\theta) + s_\eta s_\theta \gamma_{\beta 1 \gamma 3 \delta 3} (k_r + k_s)] a_\gamma^\eta a_\delta^\theta \alpha^{s\theta} \alpha^{r\eta} e^{-I (s_\eta k_r + s_\theta k_s) x_3} dx_3 = 0 \quad (3.2.26)$$

Evaluating the integral of eq. (3.2.26) yields eq. (3.2.27)

$$\sum_\mu \frac{1}{s_\mu} (2 C_{\beta 1 \gamma 1} - C_{\beta 1 \gamma 3} s_\mu) \alpha_{,1}^{q\mu} a_\gamma^\mu + k_s k_r \sum_{\eta, \theta=1}^4 \frac{1}{(s_\eta k_r + s_\theta k_s)} [\gamma_{\beta 1 \gamma 1 \delta 1} (k_r + k_s) - \gamma_{\beta 1 \gamma 1 \delta 3} (k_r s_\theta + k_s s_\eta + k_r s_\eta + k_s s_\theta) + s_\eta s_\theta \gamma_{\beta 1 \gamma 3 \delta 3} (k_r + k_s)] a_\gamma^\eta a_\delta^\theta \alpha^{s\theta} \alpha^{r\eta} = 0 \quad (3.2.27)$$

Define,

$$H_{\mu\beta} = \frac{1}{s_\mu} (2 C_{\beta 1 \gamma 1} - C_{\beta 1 \gamma 3} s_\mu) a_\gamma^\mu \quad (3.2.28)$$

$$E_{\eta\theta\beta} = \frac{k_s k_r}{(s_\eta k_r + s_\theta k_s)} [\gamma_{\beta 1 \gamma 1 \delta 1} (k_r + k_s) - \gamma_{\beta 1 \gamma 1 \delta 3} (k_r s_\theta + k_s s_\eta + k_r s_\eta + k_s s_\theta) + s_\eta s_\theta \gamma_{\beta 1 \gamma 3 \delta 3} (k_r + k_s)] a_\gamma^\eta a_\delta^\theta \quad (3.2.29)$$

Eq. (3.2.27) becomes

$$\sum_\mu H_{\mu\beta} \alpha_{,1}^{q\mu} = - \sum_{\eta, \theta=1}^4 E_{\eta\theta\beta} \alpha_\gamma^{r\eta} \alpha_\delta^{s\theta} \quad (3.2.30)$$

The above relation represents 4 equations. For each frequency triplet, i.e. q,r,s combination, this set of 4 equations will be written 3 times. This results in 12 nonlinear equations for the 12 unknown values of  $\alpha$ .

To evaluate the magnitude of the nonlinear terms and their significant verses the linear terms, the linear and nonlinear stress terms are calculated by substituting the values of linear displacement field and electric potential achieved by solving the linear problem, eqs. (3.2.31) and (3.2.32).

$$e_{ilk} u_{k,li} - \epsilon_{ij} \phi_{,ji} = 0 \quad (3.2.31)$$

$$\rho_0 \left( \frac{\partial^2 u_i}{\partial t^2} \right) = C_{ijkl} u_{k,lj} + e_{mij} \phi_{,mj} \quad (3.2.32)$$

In this example, it is assumed that the wave is propagating along the  $z$  axis in  $\text{LiNbO}_3$  and there is an applied voltage,  $V = 4.9$  [V]. Using the Mathematica code developed for the linear case, the displacement components are obtained and plotted in figure. 3.1.

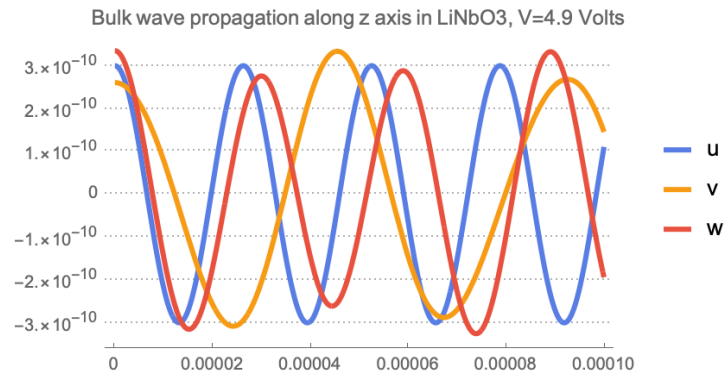


Figure 3. 1. Bulk wave propagation of linear elastic wave

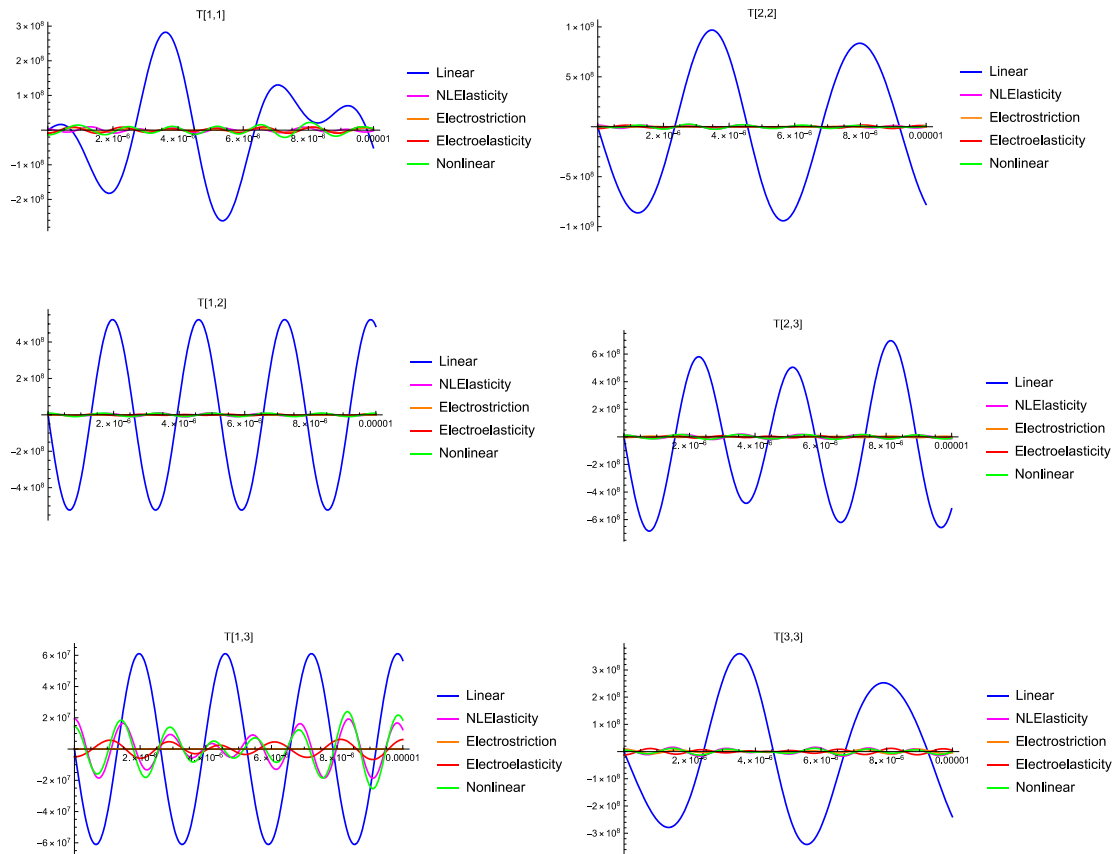


Figure 3. 2. Linear and nonlinear stress terms

Figure 3.2. shows the six components of the stress. The three nonlinear stress terms,  $\frac{1}{2}C_{ijklmn}\phi_{k,l}\phi_{m,n}$ ,  $e_{mijkl}\phi_{m}\phi_{k,l}$ ,  $l_{mnij}\phi_{,m}\phi_{,n}$ , are shown separately to show the significance of each of them. The nonlinear term seems very small and appears to have no effect. However, figure 3.3 and 3.4 show by increasing the frequency of the propagating wave, from 1.5 [GHz] to 3.5 [GHz], the amplitude of the nonlinear terms increase to where they can have impact.

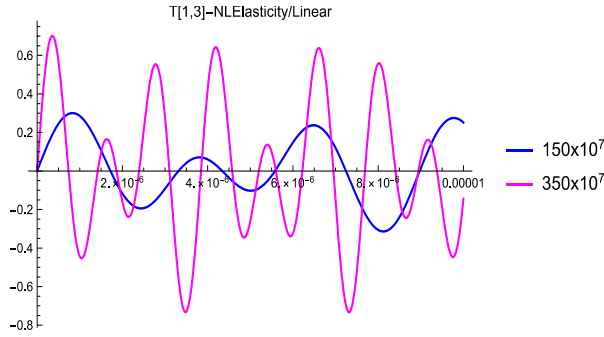


Figure 3. 4.  $T_{13}$  calculated at two frequencies

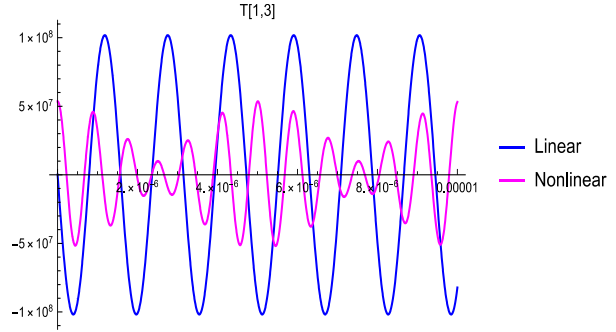


Figure 3. 3. linear and nonlinear stress terms at frequency 3.5 [GHz]

This section indicates that a requirement to see a tangible effect from nonlinear terms is to operate at higher frequencies, e.g., 3 [GHz] in case of  $\text{LiNbO}_3$

## Chapter 4 Parametric Amplification of Bulk Elastic Waves

Parametric frequency mixing or frequency conversion, in a second order nonlinear process involving three frequencies can be classified into three categories. Sum frequency generation (SFG) or up conversion, second harmonic generation (SHG), and difference frequency generation (DFG) or down conversion. In SFG, two input waves, say  $\omega_1$  and  $\omega_2$ , generate a third higher frequency wave  $\omega_{\text{SFG}} = \omega_1 + \omega_2$ . In SHG, the input waves are at the same frequency  $\omega_1 = \omega_2$  and generate an output at  $\omega_{\text{SHG}} = 2\omega_1$ . With DFG, the inputs interact to generate a wave at  $\omega_{\text{DFG}} = \omega_3 - \omega_2$ , the difference frequency.

Parametric amplification uses the process of DFG to amplify the input signal and generates a byproduct wave component at frequency  $\omega_{\text{DFG}}$ , i.e.,  $\omega_{\text{DFG}}$  is not the target of the amplification process. In the process of parametric amplification, it is common to refer to the three interacting frequency components as the idler, pump, and signal such that  $\omega_i = \omega_p - \omega_{\text{sig}}$ . The higher frequency component is the pump wave which gets its name from the fact it supplies energy, pumping up the amplitude of the lower frequency signal wave,  $\omega_{\text{sig}}$  and  $\omega_i$ .

### 4.1. Phase Matching Condition and Intensity of the Involving Waves

In general, when signal  $\omega_{\text{sig}}$  and pump  $\omega_p$  waves are supplied to the medium, conservation of elastic energy, with  $\omega_{\text{SFG}} = \omega_p + \omega_{\text{sig}}$ , implies that with SFG, one phonon at signal frequency and another at pump frequency must annihilate simultaneously (combine) to generate a phonon at SFG. In difference frequency generation,  $\omega_{\text{sig}} = \omega_p - \omega_i$ , a phonon at signal and idler frequencies are generated when a phonon at pump frequency annihilates. Both these processes can happen simultaneously when the pump and signal waves are input at the boundary. When parametric

amplification of the signal wave is of interest, generation of a sum frequency wave reduces the intensity of both pump and signal waves, which results in an overall reduction in the intensity of the signal wave instead of amplifying it. Therefore, it is significant to know what are the conditions that allow a frequency mixing process to happen. This section provides an investigation of these effects.

In a process involving only three wave components such that  $\omega_q = \omega_r + \omega_s$ , the change in intensity of a wave at frequency  $\omega_q$  with respect to  $\xi$ , has the form of eq. (4.1.1),

$$\frac{dI_q}{d\xi} = \mathcal{A}_{(r,s)} \text{Cos}(\psi_{rsq}) \quad (4.1.1)$$

where  $\mathcal{A}_{(r,s)}$  is a positive quantity that depends on the material properties, the wave intensities.

$$\psi_{rsq} = \Delta k_{rsq} \xi + \phi_c + \phi_r + \phi_s - \phi_q. \quad (4.1.2)$$

In this equation,  $\phi_c$  is a function of the effective material properties and is either 0 or  $\pi$ .  $\Delta k_{rsq}$  is the phase mismatch in eq. (3.1.39), and  $\phi_r$ ,  $\phi_s$  and  $\phi_q$  are the phases of the wave envelopes at frequencies  $\omega_r$ ,  $\omega_s$  and  $\omega_q$ , respectively. The phasor of the wave envelope is represented by  $u(\omega) = |u(\omega)| e^{i\phi}$ .

Equation (4.1.1) shows that the derivative of the intensity with respect to the propagation distance  $\xi$  changes sign periodically, with periodicity  $\frac{\pi}{\psi}$ . While  $\text{Cos}(\psi) > 0$ , the frequency mixing process transfers energy from the wave components at frequencies  $\omega_r$  and  $\omega_s$  to the  $\omega_q$  wave and reverses energy flow when  $\text{Cos}(\psi)$  changes sign. Hence, elastic energy flows back and forth among different frequency components over a distance  $\frac{\pi}{\psi}$ . The interaction distance before the frequency conversion process is reversed is called the coherence length.

$$l_{\text{coh}} = \frac{\pi}{\psi} \quad (4.1.3)$$

In general, to maximize the coherence length,  $\psi$  should be minimized.  $\psi$  is composed of two parts, the sum of the wave envelope phases and the phase mismatch factor  $\Delta k_{rsq}$ . For the first part,  $\phi_c + \phi_r + \phi_s - \phi_q$  is determined by the material properties and the relative phases of the two input

waves at frequency  $\omega_r$  and  $\omega_s$ . In practice, these can be adjusted at the boundary,  $\xi = 0$ , such that  $\phi_c + \phi_r + \phi_s - \phi_q = 0$ . Consequently, the more significant factor to consider is  $\Delta k_{rsq}$ .

From eqs. (4.1.2) and (4.1.3), it is seen that with a smaller phase mismatch, larger coherence length is achieved. The ideal situation happens when the  $\Delta k_{rsq}$  term goes to zero; this is called the phase matching condition.

In a second order, nonlinear frequency conversion process involving three frequencies such that  $\omega_q = \omega_r + \omega_s$ , the phase matching condition is written as eq. (4.1.4).

$$\bar{k}_q = \bar{k}_r + \bar{k}_s \quad (4.1.4)$$

Under the assumption that all three waves are collinear, the phase matching condition, eq. (4.1.4), turns into a scalar relation among the magnitude of the wave vectors as eq. (4.1.5) (a),

$$|\bar{k}_q| = |\bar{k}_r| + |\bar{k}_s| \quad (4.1.5) \text{ (a)}$$

or in terms of phase velocities,  $c = \frac{\omega}{k}$ , with mono-mode assumption, as eq. (4.1.5) (b).

$$\frac{\omega_q}{c_q} = \frac{\omega_r}{c_r} + \frac{\omega_s}{c_s} \quad (4.1.5) \text{ (b)}$$

Once the pump and signal waves are launched in a nonlinear media, both SFG and DFG occur simultaneously. Considering  $\omega_q$  to be the signal wave at frequency  $\omega_{sig}$ , such that  $\omega_{sig} = \omega_p - \omega_i$  and  $\omega_{sig} = \omega_{SFG} - \omega_p$ , eq. (C.21a) gives the general form in eq. (4.1.6),

$$\frac{dI_{sig}}{d\xi} = \mathcal{A}_{DFG} \text{COS}(\psi_{DFG}) + \mathcal{A}_{SFG} \text{COS}(\psi_{SFG}) \quad (4.1.6)$$

where  $\mathcal{A}_{DFG}$  and  $\mathcal{A}_{SFG}$  are two positive numbers that can be obtained from eq. (C.22) in Appendix C. Initially, at  $\xi = 0$ , the energy transfer from the signal to the sum frequency wave, reduces the intensity of the signal wave until  $\text{COS}(\psi_{SFG})$  changes sign and the process is reversed. However, if the phase mismatch term is large for the process of SFG, the coherence length of this process will be small, and its effect can be negligible on the propagation of the signal wave.

If we assume the effect of SFG is negligible, eq. (4.1.6) reduces to eq. (4.1.7).

$$\frac{dI_{sig}}{d\xi} = \mathcal{A}_{DFG} \text{COS}(\psi_{DFG}) \quad (4.1.7)$$



For  $\psi_{DFG} \rightarrow 0$  at input  $\xi = 0$ , the signal wave can be supplied such that  $\phi_{sig} = \phi_p + \phi_c - \phi_i$ . A smaller value for  $\Delta k_{DFG}$  is desired so that the  $\frac{dI_{sig}}{d\xi}$  term changes sign at a larger distance from the origin, i.e. the amplification process has larger coherence length.

From the above discussion, it is concluded that parametric amplification is feasible when the associated phase matching condition is satisfied and the input waves have the appropriate initial phases.

## 4.2. Parametric Amplification

Unlike electromagnetic waves, SAW and BAW are relatively non-dispersive over the typical frequency ranges of interest and, for purposes here, the wave velocity  $c$  is not a function of the frequency of the propagating wave. In an anisotropic material where the three waves have the same mode, i.e. all displacements are along the same  $\bar{l}^\alpha$  vector, or in an isotropic material when the waves are all shear or all longitudinal mode, the velocities of the three traveling waves are equal,  $c_s = c_r = c_q$ , and Eq. (4.1.4) is always satisfied. When this happens, both the DFG and SFG wave components are phase matched which leads to poor amplification or decay of the signal wave.

One way to overcome this obstacle is to utilize the birefringent property of anisotropic materials. In this case two waves propagating in the same direction but having different displacement modes can have different phase velocities. This way by choosing the proper direction of propagation and exciting the pump and signal waves in the desired modes, the phase mismatch term can be maximized for SFG and minimized for DFG. Consequently, the SFG wave has small coherence length and does not interfere significantly with the desired DFG process.

To find the best propagation direction and modal orientation for the pump and signal waves, we start with DFG. Substituting  $\omega_i = \omega_p - \omega_{sig}$  in eq. (4.1.5 b) for the process of DFG, eq. (4.2.1) is obtained.

$$\omega_p = \left( \frac{c_i - c_{sig}}{c_i - c_p} \right) \frac{c_p}{c_{sig}} \omega_{sig} \quad (4.2.1)$$

Examining eq. (4.2.1), for  $\omega_p$  to be greater than  $\omega_{sig}$ , the phase speeds either must satisfy inequality (4.2.2) (a) or (4.2.2) (b)

$$c_{sig} > c_p > c_i \quad (4.2.2) \text{ (a)}$$

or

$$c_i > c_p > c_{sig}. \quad (4.2.2) \text{ (b)}$$

Going through the same procedure for SFG, inequalities (4.2.3) (a) and (4.2.3) (b) are achieved.

$$\omega_{SFG} = \left( \frac{c_p - c_{sig}}{c_p - c_{SFG}} \right) \frac{c_{SFG}}{c_{sig}} \omega_{sig}$$

$$c_{sig} > c_{SFG} > c_p \quad (4.2.3) \text{ (a)}$$

or

$$c_p > c_{SFG} > c_{sig} \quad (4.2.3) \text{ (b)}$$

Considering both inequalities (4.2.2) and inequalities (4.2.3), implies

$$c_{sig} > c_p > c_i \quad \text{and} \quad c_{sig} > c_{SFG} > c_p \quad (4.2.4) \text{ (a)}$$

or

$$c_i > c_p > c_{sig} \quad \text{and} \quad c_p > c_{SFG} > c_{sig} \quad (4.2.4) \text{ (b)}$$

The set of inequalities in (4.2.4 a) always have smaller phase mismatch for the process of DFG.

Therefore, solutions satisfying this set of inequalities are the ones sought here.

Assuming the eigen modes are ranked in order of decreasing phase velocity, the first pair of inequalities require the signal and pump waves to be in modes  $\bar{l}^1$  and  $\bar{l}^2$  respectively.

While the idler wave generates in all modes, for simplicity, under the mono-mode assumption, only the mode with largest coherence length is tracked and the other two are neglected. The largest coherence for this process occurs when the idler wave is in the  $\bar{l}^3$  mode. For the process of SFG, the smallest  $\Delta k_{SFG}$ , occurs for its  $\bar{l}^2$  mode, therefore, this mode has the largest coherence length

and greatest effect on the system. The other modes are assumed to be negligible. With this, the phase mismatch term for the two processes is represented in eqs. (4.2.5) and (4.2.6)

$$\Delta k_{DFG} = \frac{\omega_p}{c_2} - \frac{\omega_{sig}}{c_1} - \frac{\omega_i}{c_3} \quad (4.2.5)$$

$$\Delta k_{SFG} = \frac{\omega_p}{c_2} + \frac{\omega_{sig}}{c_1} - \frac{\omega_{SFG}}{c_2} \quad (4.2.6)$$

For situations when  $\Delta k_{SFG}$  is large and  $\Delta k_{DFG}$  is small, the sum frequency generation has negligible effect on the difference frequency generation and parametric amplification is significant. The accuracy of this assumption is further studied in the finite element simulation section. In these cases, eq. (3.1.38) can be simplified to account only for signal ( $\omega_{sig}$ ), pump ( $\omega_p$ ) and idler ( $\omega_i$ ) frequencies resulting in eqs. (4.2.7) -(4.2.9),

$$u_{,\xi}^1(\omega_{sig}) = \frac{-1(H^{123}+H^{132})}{8G^{11}} [k_p^2 k_i^3 u^2(\omega_p) u^{3*}(\omega_i)] \quad (4.2.7)$$

$$u_{,\xi}^2(\omega_p) = \frac{1(H^{213}+H^{231})}{8G^{22}} [k_s^1 k_i^3 u^1(\omega_{sig}) u^3(\omega_i)] \quad (4.2.8)$$

$$u_{,\xi}^3(\omega_i) = \frac{-1(H^{321}+H^{312})}{8G^{33}} [k_p^2 k_s^1 u^2(\omega_p) u^{1*}(\omega_s)] \quad (4.2.9)$$

where all the terms in eqs. (4.2.7) -(4.2.9) are as defined in eq. (4.1.22).

The above system of coupled equations represents three non-linear equations with three unknowns. The amplitude of the pump wave is generally much greater than the amplitude of the signal wave in envisioned applications; consequently, we assume the magnitude of the pump wave to be almost constant throughout the interaction. This will allow us to treat  $u^2(\omega_p)$  as a known function that factors out of the equations for  $u_{,\xi}^1(\omega_{sig})$  and  $u_{,\xi}^3(\omega_i)$ . The accuracy of this assumption is also discussed further in the finite element simulation results section. Under this assumption, eqs. (4.2.7) and (4.2.9) can be written as eqs. (4.2.10) and (4.2.11), respectively.

$$u_{,\xi}^1(\omega_{sig}) = \kappa_{si} u^{3*}(\omega_i) \quad (4.2.10)$$

$$u_{,\xi}^{3*}(\omega_i) = \kappa_{is} u^1(\omega_{sig}) \quad (4.2.11)$$

with

$$\kappa_{si} = \frac{-1(H^{123}+H^{132})}{8G^{11}} k_p^2 k_i^3 u^2(\omega_p) \quad (4.2.12)$$

$$\kappa_{is} = \left( \frac{-1(H^{321}+H^{312})}{8G^{33}} k_p^2 k_s^1 u^2(\omega_p) \right)^* \quad (4.2.13)$$

By introducing

$$\kappa = \sqrt{\kappa_{si}\kappa_{is}} \quad (4.2.14)$$

eqs. (4.2.10) and (4.2.11) have the solutions of the form eqs. (4.2.15) and (4.2.16), respectively,

$$u^1(\omega_s) = u_0^\alpha \frac{(e^{k\xi} + e^{-k\xi})}{2} = u_0^1 \text{Cosh}(k\xi) \quad (4.2.15)$$

$$u^{3*}(\omega_2) = \sqrt{\frac{\kappa_{is}}{\kappa_{si}}} u_0^1 \frac{(e^{k\xi} - e^{-k\xi})}{2} = \sqrt{\frac{\kappa_{is}}{\kappa_{si}}} u_0^1 \text{Sinh}(k\xi) \quad (4.2.16)$$

where  $u_0^1$  is the amplitude of the signal wave at  $\xi = 0$ .

The intensity of the acoustic wave at frequency  $\omega_q$  in the direction of  $\xi$  is calculated as eq. (4.2.17),

(See Appendix C).

$$I_q = \rho \frac{\omega_q^3}{k_q} |u(\omega_q)|^2 \quad (4.2.17)$$

Equation (4.2.17) for intensity, combined with equations (4.2.15) and (4.2.16), result in the gain for signal intensity of

$$\text{Gain} = \frac{I_s(l)}{I_s(0)} = \text{Cosh}^2(\kappa l). \quad (4.2.18)$$

These equations will be used in the results section for different orientations of LiNbO<sub>3</sub> to find directions of propagation such that  $\Delta k_{DFG}$  is much smaller than  $\Delta k_{SFG}$  as needed for parametric amplification. After determining the most promising directions, quantitative values for the gain in LiNbO<sub>3</sub> are provided from Eq. (4.2.18).

Here, linear, and nonlinear material properties of LiNbO<sub>3</sub> (Appendix D), are used as an example to show how the concepts and equations discussed can be applied. In the first section, propagation directions with small phase mismatch for DFG and large mismatch for SFG are determined.

Directions with a ratio of  $\frac{\Delta k_{DFG}}{\Delta k_{SFG}} < 0.2$ , are assumed as plausible candidates for parametric

amplification where the effect of SFG is negligible. The gains in directions of propagation with  $\frac{\Delta k_{DFG}}{\Delta k_{SFG}} < 0.2$  are calculated considering only the process of DFG. The directions of propagation with largest gain are indicated.

Next, the nonlinear elastic wave equations are solved numerically with Finite Element Method (FEM) simulations. In these simulations, the equations are solved considering both DFG and SFG processes (i.e., four frequency interaction). Further, in the numerical simulations, the SVA and mono-mode assumptions are not used.

These results are compared with the

analytical solutions, validating previous simplifications and assumptions.

Figure 4.1. refers the direction of the wave propagation vector  $\bar{p}$  to the crystal axes in LiNbO<sub>3</sub>, with each propagation direction determined by two angles  $\theta$  and  $\phi$  with respect to the positive Z and X axes, respectively.

An optimum direction of propagation is the one with 1) minimum phase mismatch for the process of DFG, 2) maximum phase mismatch for the process of SFG and 3) maximum gain of amplification. Based on the discussion in section IV, the phase mismatch term for the process of

DFG and SFG are,  $\Delta k_{DFG} = \frac{\omega_p}{c_2} - \frac{\omega_s}{c_1} - \frac{\omega_i}{c_3}$  and  $\Delta k_{SFG} = \frac{\omega_p}{c_2} + \frac{\omega_s}{c_1} - \frac{\omega_{SFG}}{c_2}$ , respectively. As seen in the

plots of figure 2, in an anisotropic material such as LiNbO<sub>3</sub>, the wave speeds are a function of direction of propagation. In figure 3, the optimum direction of propagation for parametric amplification is investigated. To find the direction of propagation with minimum  $\Delta k_{DFG}$  and

maximum  $\Delta k_{SFG}$ , the ratio,  $r = \frac{\Delta k_{DFG}}{\Delta k_{SFG}} = \frac{l_{coh}(SFG)}{l_{coh}(DFG)}$  is defined and calculated as a function of direction

in space with the results shown in figure 4.1 (a) for X-Y plane, i.e. propagation with  $\theta = 90^\circ$  and

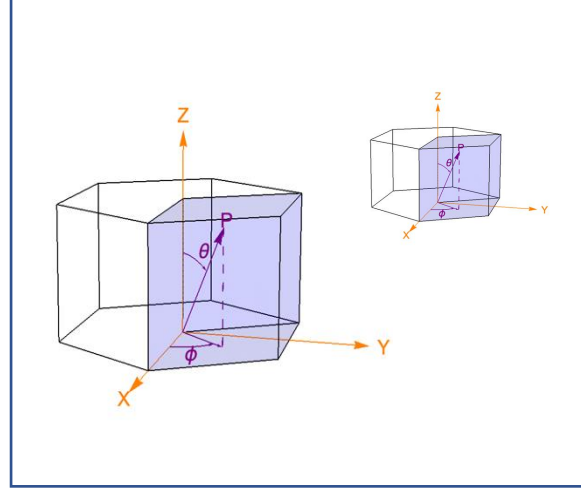


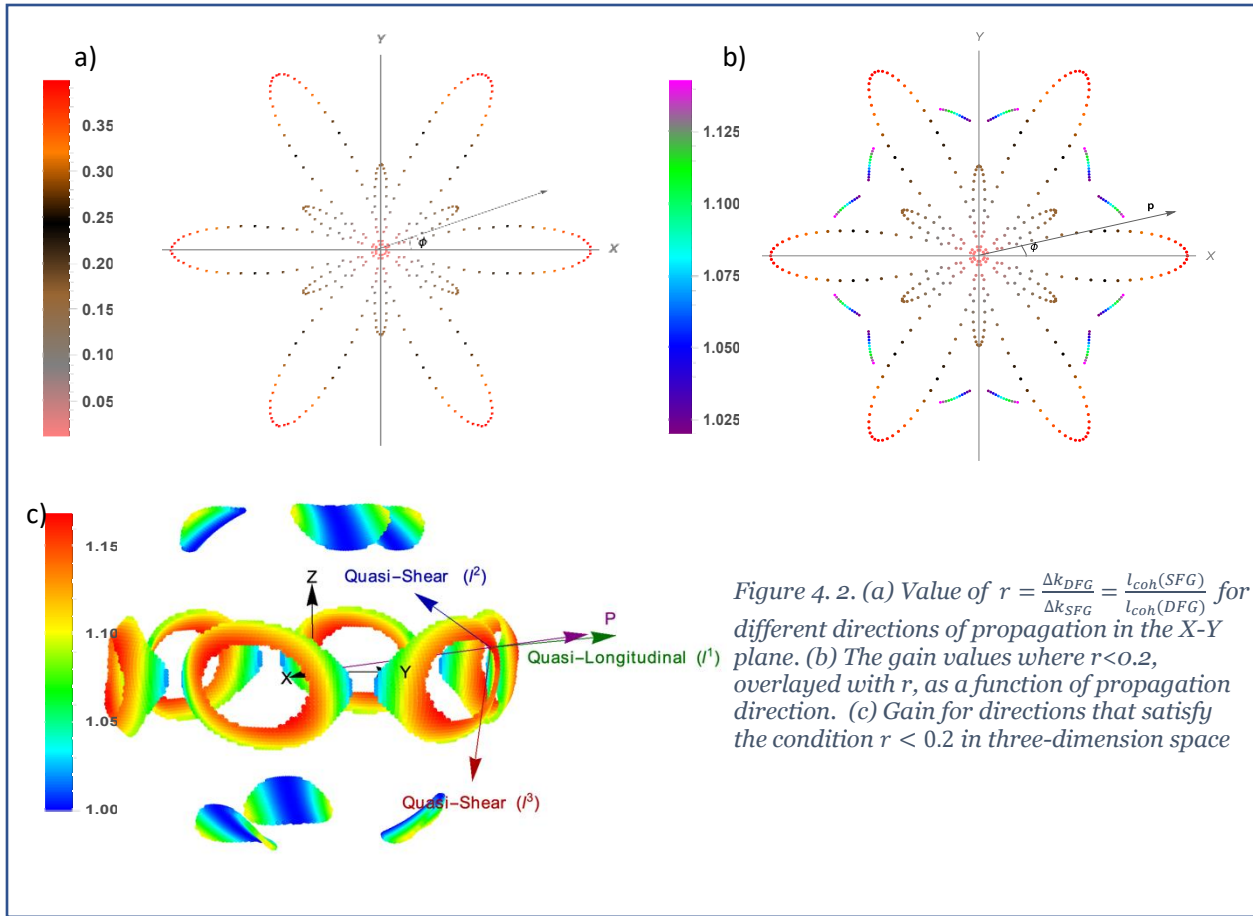
Figure 4. 1. Definition of the propagation vector with respect to the crystal axes in LiNbO<sub>3</sub>

$0 < \varphi < 360$  , as an example. The magnitude of  $r$  for each direction is proportional to the distance of the point to the origin. The color of each point indicates the value of  $r$  based on the bar-legend. An “optimum” value for  $r$  is not shown here since the  $r$  value does not determine gain. Our analytic gain results, being based on three frequency interaction, do not consider the effects of SFG. Consequently, higher values of gain can be found in certain directions, but the assumptions needed for validity of the three frequency results are violated. By choosing low  $r$  values, we are considering the gain only in regions where the 3 frequency assumptions reasonably apply. Here we have considered the points with  $r < 0.2$  as a valid metric for when SFG is negligible. This value is verified by the FEM results which show close agreement within this region. For the directions with  $r < 0.2$ , the signal gain for a DFG process, neglecting SFG, is plotted in figure 4.2 (b) for the X-Y plane, and figure 4.3 (c) for the entire space. The signal and pump waves have the frequencies,  $\omega_s = 200 \text{ MHz}$  and  $\omega_p = 800 \text{ MHz}$ , respectively and the initial amplitude of  $u_0^1 = 10 \text{ nm}$ ,  $u_0^2 = 50 \text{ nm}$ . The sparse spaces in the gain graph represent the directions that do not satisfy the condition for  $r$  and have been eliminated.

*Table 2 - Direction of propagation with maximum gain*

$\theta^\circ$	$\varphi^\circ$
82	70,190,310,110,230,350
98	10,130,250,50,170,290

The maximum signal gain over one wavelength is seen to be 16%. This response is observed in twelve directions of propagation, see table1, reflecting the crystal symmetry of  $\text{LiNbO}_3$ . The eigenvectors for the direction of propagation with  $(\theta = 82^\circ, \varphi = 70^\circ)$ , are plotted in figure 4.2. (c) as  $\vec{l}^1, \vec{l}^2$  and  $\vec{l}^3$ .



COMSOL Multiphysics finite element software was used to simulate the frequency conversion processes. Eq. (4.1.5) is implemented to solve for the four-wave, (pump, signal, idler, and sum frequency) interactions. The simulations are done in frequency domain inputting the nonlinear terms as an external stress to the linear elastic node of the structural mechanics interface in COMSOL. Enabling the geometric nonlinearity in the solution node, nonlinear strains are considered. The equations for external stresses are given in Table 4.2.

Since the spatial gradients are considered to be only in the direction of propagation, the problem can be viewed as one dimensional with the other two dimensions being constrained with periodic boundary conditions. The geometry of the model consists of a three-dimensional bar that is several signal wavelengths long and meshed with a single element across the width in the transverse directions. This is implemented by applying a coordinate transformation so that the

desired propagation direction  $\hat{p}$  aligns with the  $\hat{Z}'$  axis in the FEM coordinate system. The vectors  $\hat{p} \times \hat{Z}$  and  $\hat{p} \times \hat{Z} \times \hat{p}$  are chosen to form the  $\hat{Y}'$  and  $\hat{X}'$  axes of the FEM coordinate system, respectively. The propagation directions given throughout the results section are referenced to the original material axes, not the coordinate system used in the FEM model. As explained in chapter 1, The material constants in the transformed coordinate system are obtained using the Mathematica code in Appendix A.

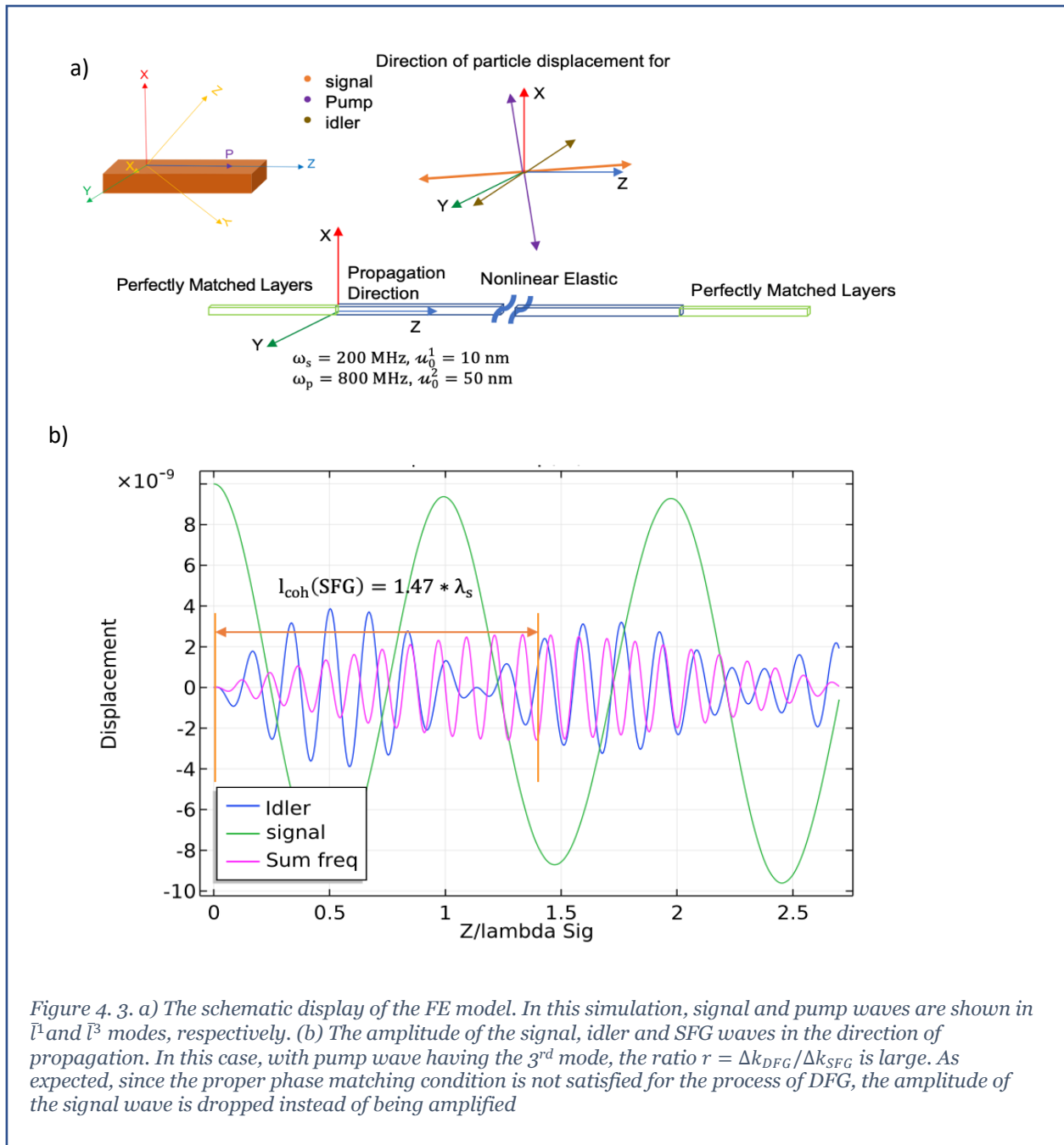
To make sure the results are not influenced by reflection from boundaries, Perfectly Matched Layers (PML) are used on both ends and simulate continuous propagation. The signal and pump waves are excited as prescribed displacements at the boundary with initial amplitudes  $u_0^1 = 10 \text{ nm}$ ,  $u_0^2 = 50 \text{ nm}$ , and frequencies of,  $\omega_s = 200 \text{ MHz}$ ,  $\omega_p = 800 \text{ MHz}$ , respectively.

Table 3-The external stress terms for the FEM simulations are given by the following where,  $C_{ijklmn}^{(e)} = \frac{1}{2}C_{ijklmn} + \frac{1}{2}C_{ijnl}\delta_{km} + C_{njkl}\delta_{im} + C_{inkl}\delta_{jm} - C_{ijkl}\delta_{mn}$  and  $C_{ijkl}$ ,  $C_{ijklmn}$  are the second- and third-order elastic constants

$T^{ext}(\omega_s)$	$C_{ijklmn}^{(e)}(u_{k,l}(\omega_p)u_{m,n}(-\omega_i) + u_{k,l}(\omega_{sum})u_{m,n}(-\omega_p))$
$T^{ext}(\omega_p)$	$C_{ijklmn}^{(e)}(u_{k,l}(\omega_s)u_{m,n}(\omega_i) + u_{k,l}(\omega_{sum})u_{m,n}(-\omega_s))$
$T^{ext}(\omega_i)$	$C_{ijklmn}^{(e)}u_{k,l}(\omega_p)u_{m,n}(-\omega_s)$
$T^{ext}(\omega_{sum})$	$C_{ijklmn}^{(e)}u_{k,l}(\omega_p)u_{m,n}(\omega_s)$

Three simulations are presented to show the effect of different parameters on the system. In the first simulations, the importance of exciting the pump and signal waves in the directions suggested by eq. (4.3.4a) are emphasized. In this simulation, pump and signal waves are sent in  $\bar{l}^1$  and  $\bar{l}^3$  directions, respectively, in contrast to what eq. (4.3.4a) would suggest. It is shown with this excitation, the phase matching condition is not favorable for DFG and parametric amplification of the signal wave does not occur. In the second simulation, pump and signal waves are applied in the  $\bar{l}^1$  and  $\bar{l}^2$  directions, in agreement with eq. (4.3.4a) and parametric amplification





of the signal wave is demonstrated. The third simulation shows non-reciprocal propagation of the signal. In the third simulation, this is accomplished by taking the model from the second simulation and reversing the propagation direction of the signal wave. The resultant magnitude of the signal wave is then seen to be quite different from the second simulation.

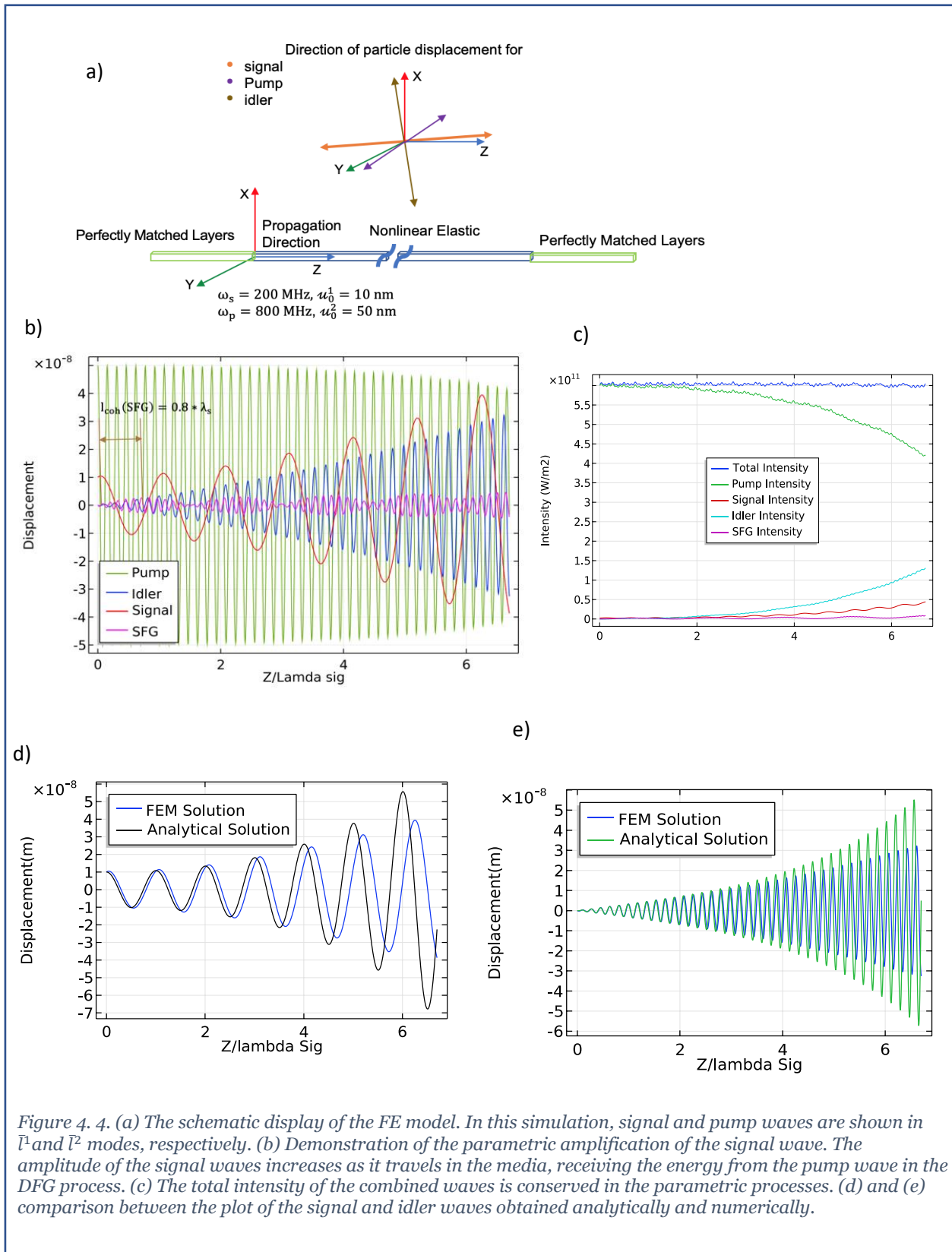
In the first simulation, the waves propagate in the direction  $\theta = 82^\circ$  and  $\varphi = 70^\circ$  and signal and pump waves are exited in  $\bar{l}^1$  and  $\bar{l}^3$  directions, respectively, which are not optimum directions to eliminate the generation of a sum frequency wave. Figure 4.3. (b) shows in this case the signal wave does not amplify, and its displacement magnitude reduces as it propagates over the first wavelength. This agrees with the results predicted in the analytical discussion.

The analytical coherence lengths, calculated from eq. (4.2.3), for the two processes are  $l_{coh}(DFG) = 0.3 * \lambda_s$  and  $l_{coh}(SFG) = 1.47 * \lambda_s$  with  $r = \frac{\Delta k_{DFG}}{\Delta k_{SFG}} = 4.64$ . The coherence length estimated from the graph of figure 4.3. (b) matches calculated values to within the resolution of the plot. As expected, the plot shows that coherence length of the SFG is larger than the DFG since  $\Delta k_{DFG} > \Delta k_{SFG}$ .

In the second simulation, the same geometry and material properties are used, however, a more favorable phase matching condition for DFG is applied. Graphical representation of the pump and signal waves in figure 4.4. (a) shows the signal and pump waves are launched in the medium with modal displacements in  $\bar{l}^1$  and  $\bar{l}^2$  directions, respectively. This choice was made based on the inequalities (4.3.4a), derived in section 4.3. The waves propagate in the direction with  $\theta = 82^\circ$  and  $\varphi = 70^\circ$ , which is the direction of propagation with maximum gain, obtained from the analytical results, figure 4.2. (c). Based on the analytical results, eq. (4.2.3), the coherence length calculated for SFG is  $l_{coh}(SFG) = 0.81 * \lambda_s$ . This is in reasonable agreement with the estimate of  $0.8 * \lambda_s$  shown on the graph of the figure 4.4. (b). The larger phase mismatch for the SFG,  $r = \frac{\Delta k_{DFG}}{\Delta k_{SFG}} = 0.16$ , eliminates its adverse effect on signal amplification and the red plot in figure 4.4. (b) shows the increasing signal amplitude as the wave travels. This demonstrates the parametric amplification of the wave as the result of energy transfer from the pump wave. It is also seen that the amplitude of the pump wave is constant, indicating the approximate, but reasonable, assumption of constant amplitude for the pump. Figure 4.4. (c) plots the total intensity of the combined waves along with the intensity of each wave component as a function of position in the

direction of propagation. It is seen that the total intensity of the waves is conserved, and the intensity of the pump wave decreases while the intensity of the signal and idler waves increases.

The conservation of the total intensity of the involved waves is due to nature of the problem being



parametric. Figure 4.4. (d) and (e) compare the plot of the signal and idler waves obtained analytically and numerically over a distance of four signal wavelengths in the material. This figure shows close agreement between analytic and numerical results for about three signal wavelengths, demonstrating the approximate range of validity for the slowly varying amplitude assumption.

### 4.3. Breaking Reciprocity

In this section, it is shown in a parametric amplification process when the required phase matching condition is satisfied for pump and signal waves traveling in the same direction, the signal wave is amplified and when the signal wave travels in a direction opposite the pump wave, the required phase matching condition cannot be satisfied. Therefore, the magnitude of the signal wave at the destination is different depending on its direction of propagation. This results in directional dependency of the propagation of the

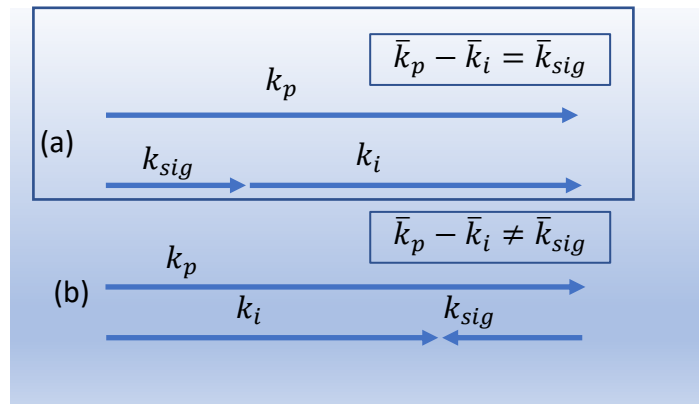


Figure 4.5. propagation of two elastic waves (a) in the same direction, (b) in the opposite direction. Non-reciprocal propagation of the elastic wave can be realized through the phase matching condition.

signal wave. It is concluded that in a nonlinear media with a traveling pump wave in one direction, non-reciprocal propagation of an elastic wave can be achieved.

The phase matching condition for the process of DFG for pump, signal, and idler waves when,  $\omega_p - \omega_i = \omega_{sig}$ , is written as eq. (4.3.1).

$$\bar{k}_p - \bar{k}_i = \bar{k}_{sig} \quad (4.3.1)$$

When the pump and signal waves travel in the same direction, figure 4.5. (a), eq. (4.3.1) is satisfied. However, when the pump and signal waves travel in opposite direction, figure 4.5. (b), the relationship among their wave vectors cannot satisfy the required phase matching condition and the frequency conversion process cannot take place in this situation. Therefore, without

energy transfer between the pump and signal waves, the amplitude of the signal wave remains constant. This directional bias in amplitude of the signal wave is interpreted as non-reciprocity in its propagation. In addition, when the DFG does not happen, the idler frequency does not generate. That means comparing the Fourier spectrum of the elastic wave in the forward direction, figure 4.5. (a), versus the backward direction, 4.5. (b), the idler frequency is only observed for the forward direction and is absent in the backward direction.

Another simulation with the objective of investigating non-reciprocity in propagation of the signal wave is performed. The same model setup as the second simulation was used, except, the signal wave was sent in the opposite direction of the pump wave. The results plotted in figure 4.6. (b) and (c) show that by reversing the direction of propagation of the signal wave, the pump and signal waves do not couple; consequently, the idler wave is not generated. Also seen, there is no energy transfer from or to the pump and signal waves.

Comparing the second and third simulations shows that the amplitude of the signal wave is quite different over equivalent distances of travel. For the nonlinear elastic media, the pump wave creates a symmetry breaking field, and the signal wave propagation becomes non-reciprocal.

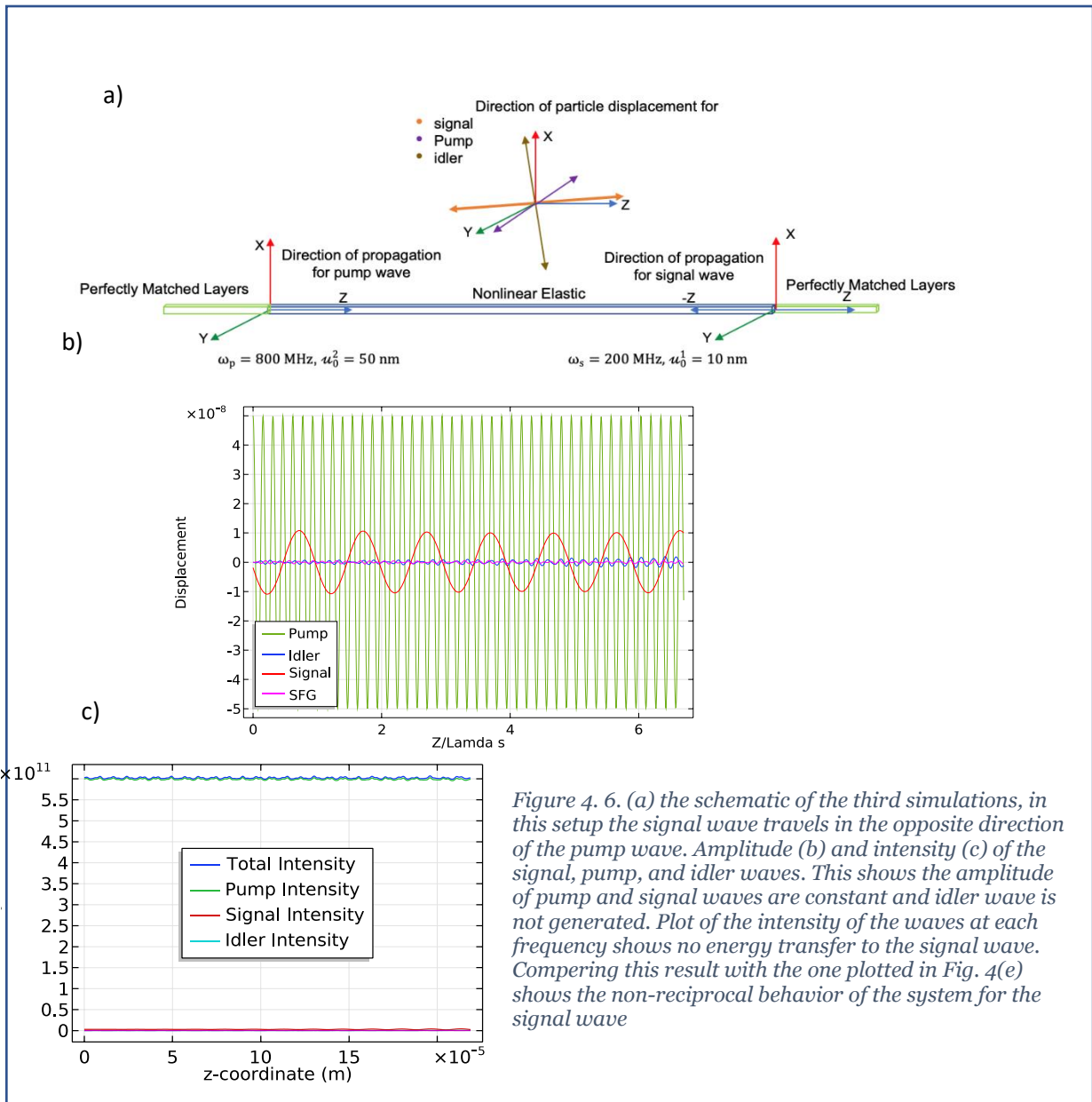


Figure 4. 6. (a) the schematic of the third simulations, in this setup the signal wave travels in the opposite direction of the pump wave. Amplitude (b) and intensity (c) of the signal, pump, and idler waves. This shows the amplitude of pump and signal waves are constant and idler wave is not generated. Plot of the intensity of the waves at each frequency shows no energy transfer to the signal wave. Comparing this result with the one plotted in Fig. 4(e) shows the non-reciprocal behavior of the system for the signal wave

# Chapter 5 Frequency Mixing in Piezoelectric Surface Elastic Waves

In chapter 3, the theoretical framework for coupled wave solutions was derived. In this chapter, that framework is applied into a physical model using the Finite Element Method (FEM). The model demonstrated uses two sets of Interdigitated Electrodes (IDT)s to excite a nonlinear substrate to produce a pump and signal wave. The interaction of the pump with signal creates an intermediate idler wave as discussed in chapter 4. This creates an amplification of the signal wave and demonstrates the potential to use this parametric amplification for real devices, such as RF front ends.

To implement the nonlinear propagation model for piezoelectric surface waves, a 3D finite element model is set up in COMSOL Multiphysics to take advantage of element generation and solvers provided. The equations derived in chapter 3 were programmed directly into COMSOL. Like most commercial packages, COMSOL does provide nonlinear capability but can be only used for limited materials with specific energy functions i.e., Ramberg-Osgood, Hardin-Drnevich, etc. For anisotropic materials in the presence of electromechanical coupling, the nonlinear terms were implemented as a piezoelectric material node with external stress terms. eq. (5.1) shows the nonlinear wave equation derived, where the nonlinear stress terms are highlighted in eq. (5.2).

$$-\rho_0 \omega_q^2 \eta_{\alpha\beta} u_\alpha^q(\bar{x}) = \left[ C_{\beta k \gamma n} (u_{\gamma,n}^q(\bar{x})) + \frac{1}{2} \gamma_{\beta k \gamma l \delta n} \sum_{(r,s)} u_{\gamma,l}^r(\bar{x}) u_{\delta,n}^s(\bar{x}) \right]_{,k} \quad (5.1)$$

$$T_{k\beta}^{NL} = \frac{1}{2} \gamma_{\beta k \gamma l \delta n} \sum_{(r,s)} u_{\gamma,l}^r(\bar{x}) u_{\delta,n}^s(\bar{x}) \quad (5.2)$$

The equations are solved for a three-wave frequency mixing application. This requires a pump, signal, and idler wave at specific frequencies. The problem, modeled in frequency domain, for the first time in the literature, which reduces the computational cost a lot in comparison to time domain. Three Multiphysics systems of equations are coupled through the external stress terms that are added to each of the piezoelectric modules used.



The surface waves from the signal and pump frequencies are excited on the piezoelectric material using IDTs. Linear and nonlinear material constants of 128 Y-cut LiNbO<sub>3</sub> are used in the simulations.

There is no input wave at the Idler frequency. The wave at this frequency is generated through the process of difference frequency generation in the nonlinear medium in the presence of the Pump and Signal waves. Figure 5.1 shows the voltage decay into the depth of the substrate for both the pump and signal waves, indicating the

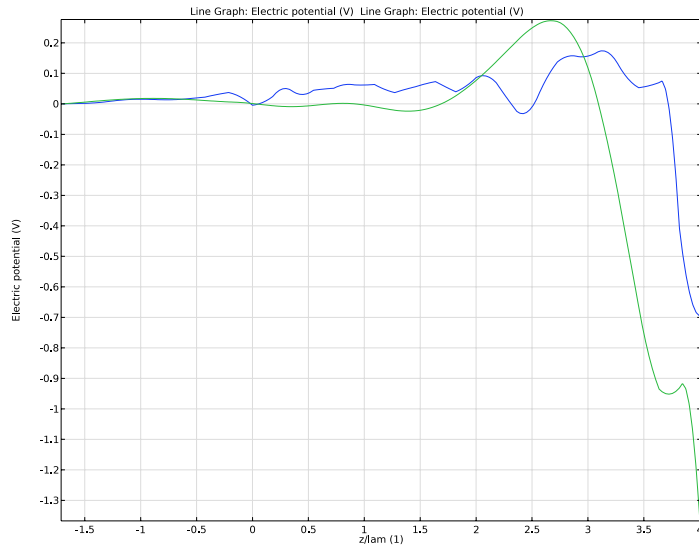


Figure 5. 1. Decaying Pump and Signal wave in the material's depth

expected SAW characteristics. Figure 5.2 shows the mechanical displacement of the traveling waves propagating across the substrate as generated from the IDTs.

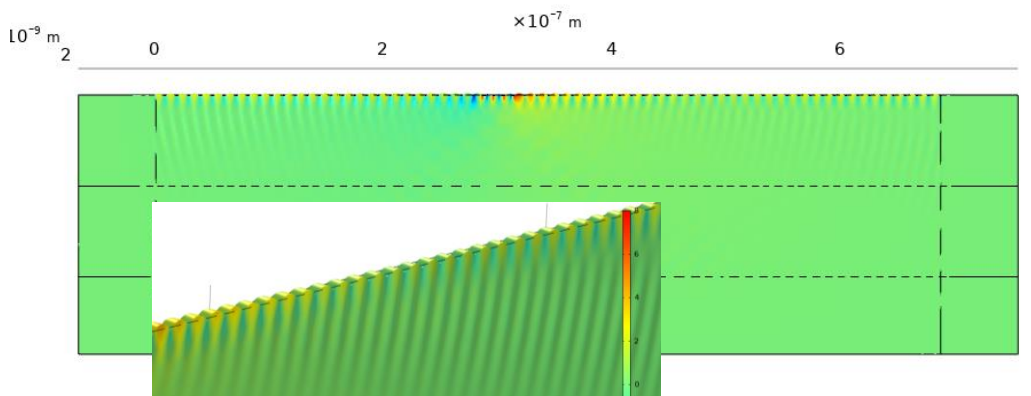


Figure 5. 2. Propagation of the Pump wave generated by sets of IDTs

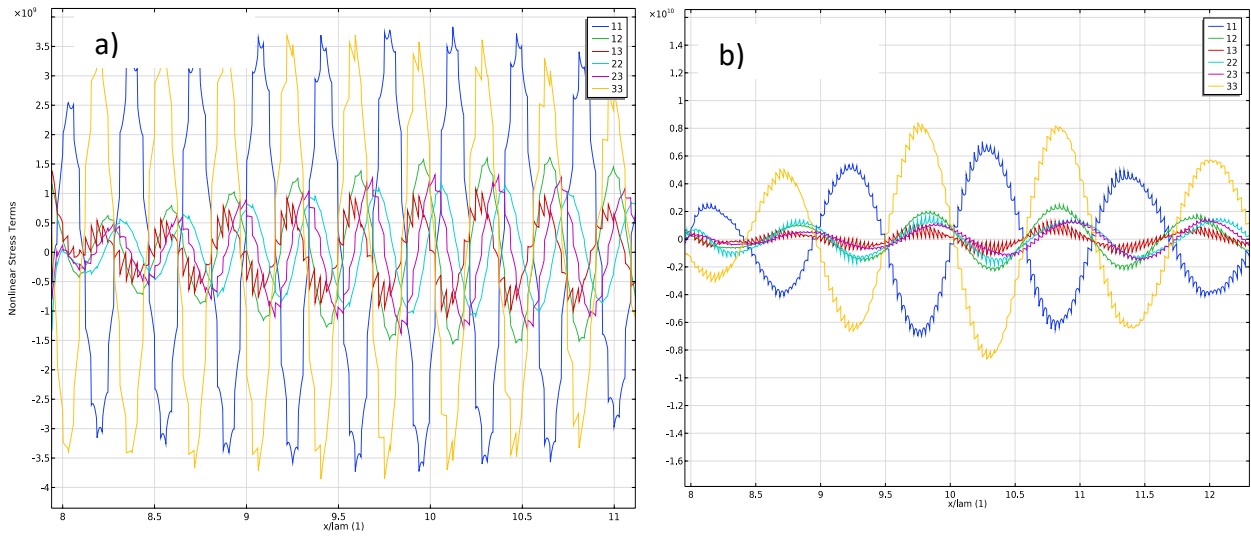


Figure 5. 3. The nonlinear stress terms that are input as external stress for a) Idler and b) Signal

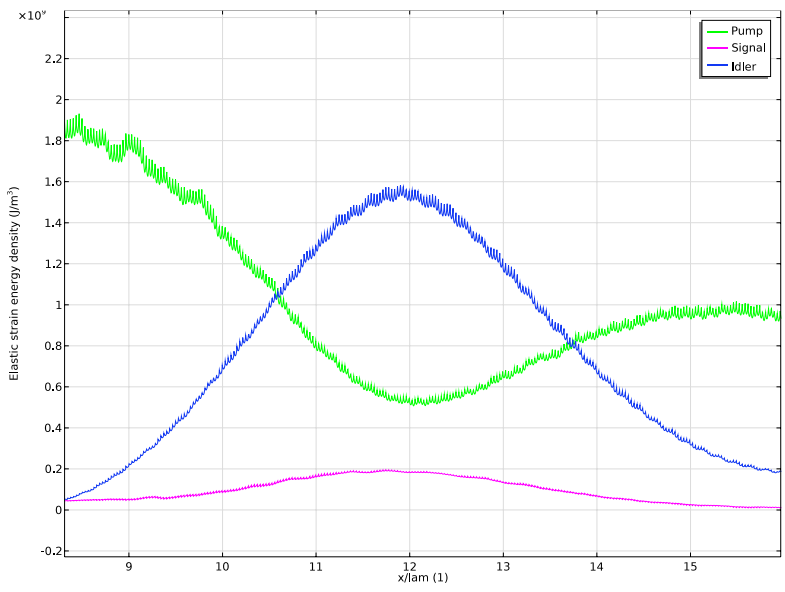


Figure 5. 4. The Strain Energy for each frequency shows the transfer of energy from the pump wave to signal and idler waves

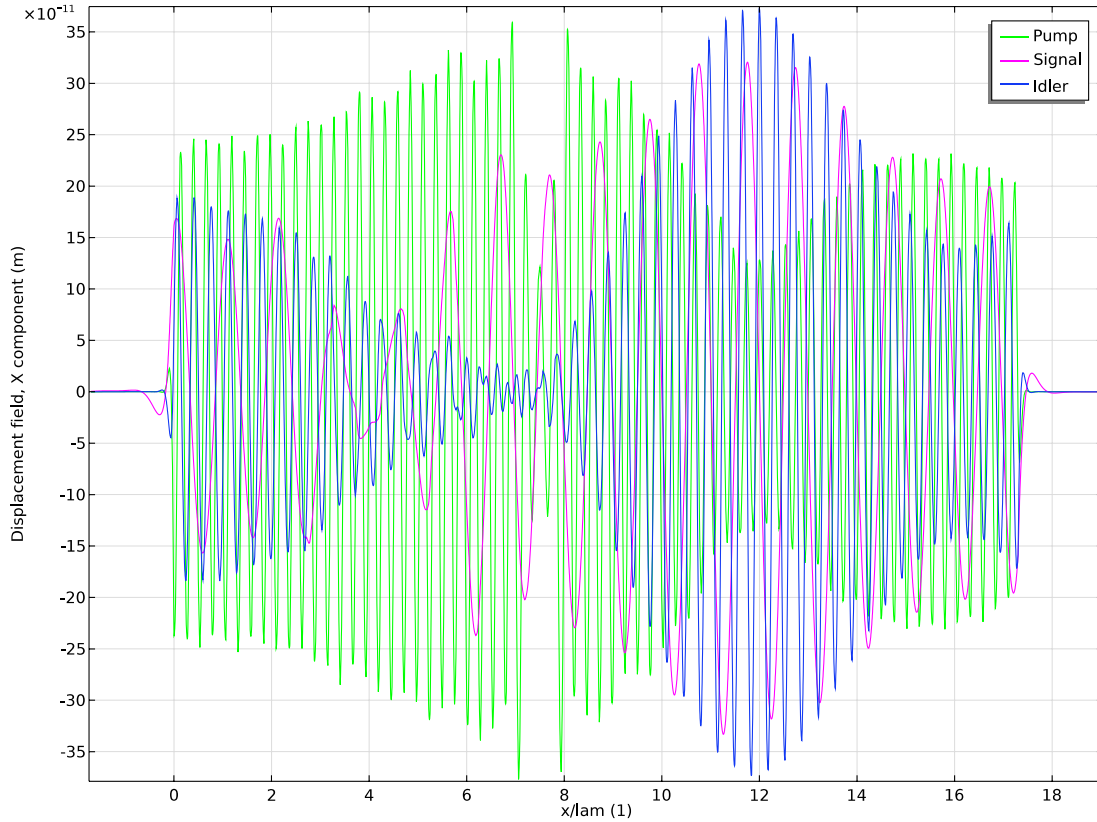


Figure 5.5. The x component of the displacement field. It shows that Signal and Idler waves are amplified, and the direction of the energy flow changes

Figure 5.3 shows the stresses generated along the top surface of the substrate. All the components of stress are plotted in each graph, with Figure 5.3 (a) showing the signal and (b) the idler. As can be seen in graph (b), the idler frequency generated by the wave mixing occurs at the frequency  $\omega_p - \omega_s$ . The horizontal axes of the graphs are scaled to the signal wavelength. Of particular note is the increase in the signal amplitude between 5 and 13 wavelengths across the top surface. This is the parametric amplification desired. After 13 wavelengths, the signal again decreases due to coherence length effects discussed in chapter 4. With better tuning of the model, the coherence length could be dramatically increased with a corresponding improvement in signal amplification performance.

## Chapter 6 Parametric Amplification using Lamb Waves

As discussed in detail in chapter 4, the process of parametric amplification is hampered by sum frequency generation. This is due to transfer of the energy from signal wave to the sum frequency wave, which in turn leads to smaller distance where the signal is being amplified. In the case of surface wave propagation, the phase velocity is not a function of the propagating wave's frequency.

In a nonlinear medium with excitation of signal and pump frequencies, both sum and difference frequencies are phase matched and are generated. Lamb waves, on the other hand, have a dispersion curve with phase velocity that varies with frequency. This makes them a better option for parametric amplification application since this can provide a means to increase the coherence length of the difference frequency

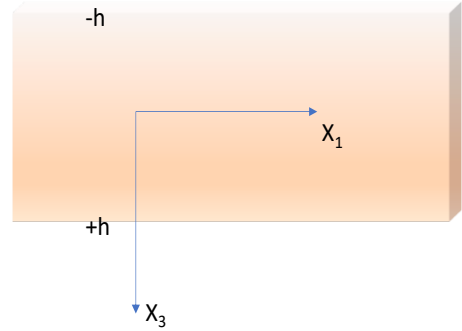


Figure 6. 1. Direction of propagation and geometry of Lamb wave

while decreasing the sum frequency. In this chapter, it is

shown by taking the advantage of dispersive characteristic of Lamb waves, parametric amplification of elastic waves is possible.

As shown in figure 6.1, it is assumed the wave is propagating in the  $x_1$  direction and there is no variation in the  $x_2$  direction. The dispersion relation for Lamb waves is shown in eq. (6.1)[49]

$$\frac{\omega^2}{V_T^4} = 4k^2 q^2 \left[ 1 - \frac{p \tan (ph + \alpha)}{q \tan (qh + \alpha)} \right] \quad (6.1)$$

where

$p^2 = \omega^2 \left( \frac{1}{V_L^2} - \frac{1}{v^2} \right)$ ,  $q^2 = \omega^2 \left( \frac{1}{V_T^2} - \frac{1}{v^2} \right)$ ,  $V_L^2 = \frac{c_{11}}{\rho}$  and  $V_T^2 = \frac{c_{66}}{\rho}$ .  $V_L$  and  $V_T$  are the phase velocities of the *bulk* longitudinal and shear waves, respectively.  $2h$  is the thickness of the material and  $\alpha = 0$  or  $\frac{\pi}{2}$ , which represents the symmetric and antisymmetric modes of the Lamb wave.

The material properties of Aluminum, Appendix D, are used to plot the dispersion curve in eq. (6.1) using a code in Mathematica. Figure 6.2 shows the phase velocity of the Lamb wave as a

function of frequency. The figure shows wave at frequencies 4 and 8 [MHz] have almost the same wave speed, 5489 [m/s], whereas the wave at frequency equal to sum of the two, 12 [MHz] has different velocity, 4308 [m/s]. Based on eq. (4.1.5) (a),

$$|\bar{k}_q| = |\bar{k}_r| + |\bar{k}_s| \quad (4.1.5) (a)$$

the difference frequency generation is phased matched, but the sum frequency generation is quasi phased matched. Hence, the process of the DFG has longer coherence length and the signal wave can be amplified before losing its energy to the wave at the sum frequency.

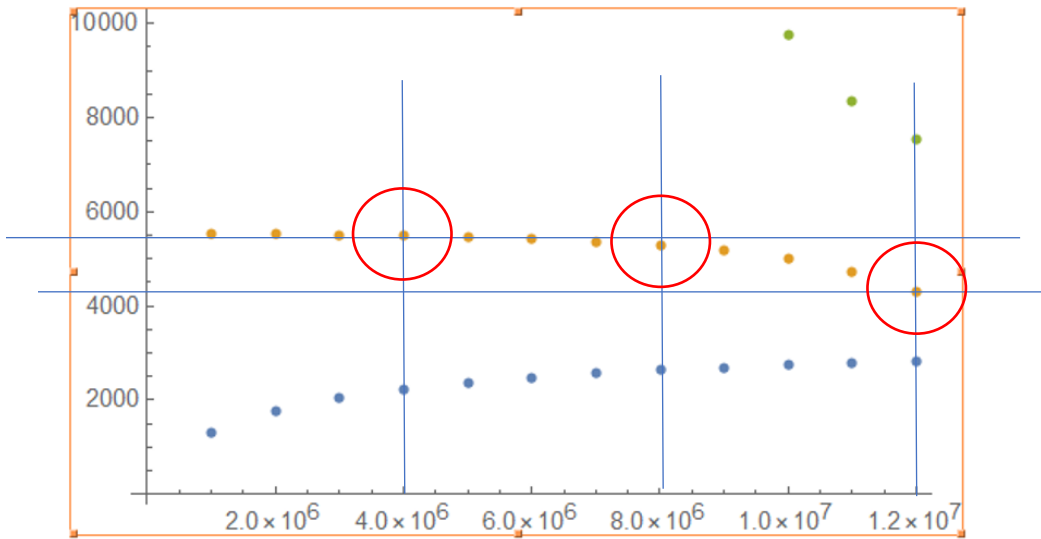


Figure 6. 2. Dispersion curve of the Lamb wave and selected frequencies

To further investigate the possibility of the parametric amplification, a numerical model was developed using COMSOL Multiphysics. Two input Lamb waves, pump and signal are generated using prescribed boundary displacement in the  $x_2$  direction, figure 6.3.

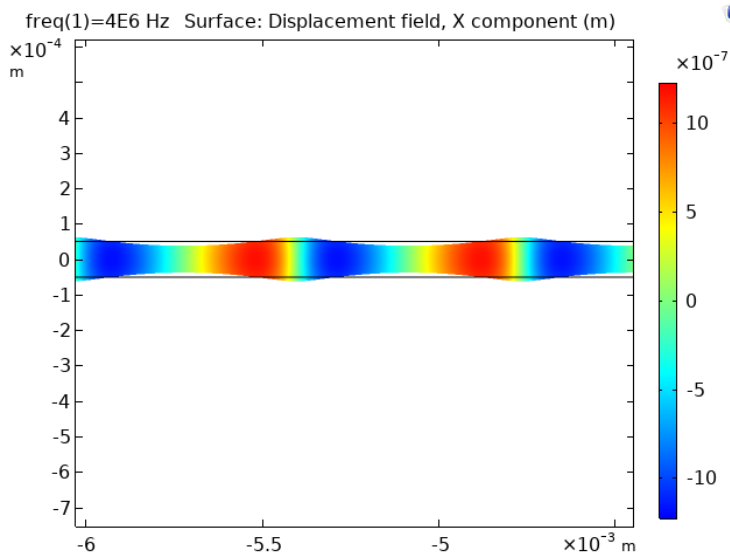


Figure 6. 3. Excitation of the so mode of Lamb wave

Figure 6.3 shows the result of numerical simulation. In this figure, as expected from theory, the coherence length of the SFG is shorter than the DFG and parametric amplification of the signal wave is achieved.

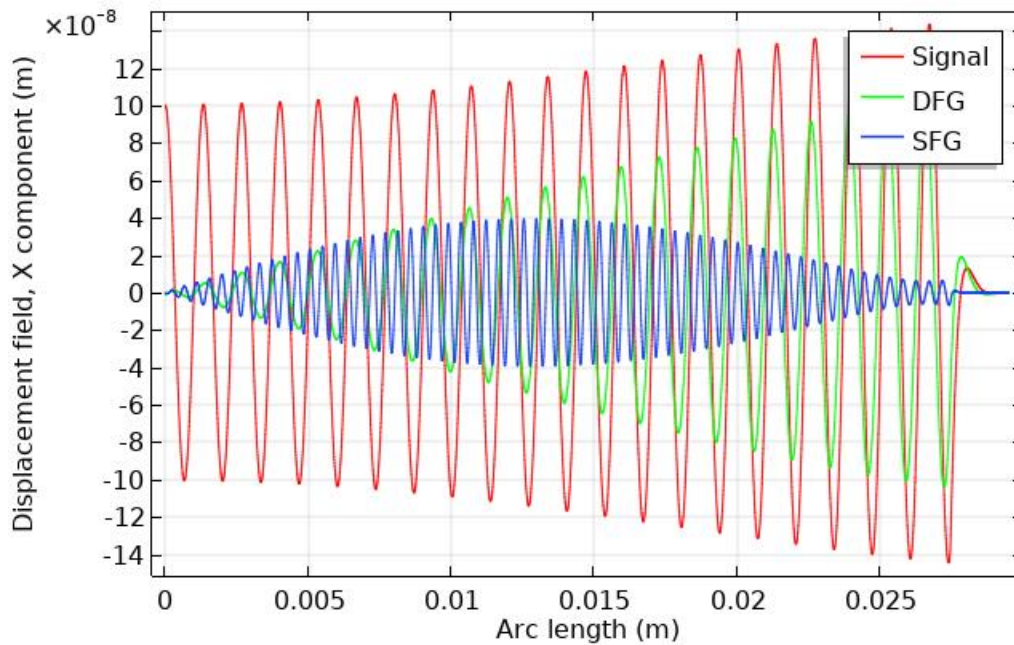


Figure 6. 4. Parametric Amplification of the signal wave

## Conclusions

This work has shown the derivation and verification of a system of equations that can be used for determining amplification effects due to difference frequency generation associated with bulk and surface waves. A simplified version of these equations was solved quasi-analytically for the “three wave” problem. These idealized equations indicate promising modes of operation for the non-degenerate eigenvalue case where amplification of the signal wave is achieved. This was verified numerically using a FEM model. Without the analytic equations to guide selection of the required system characteristics, i.e., which mode to operate the pump, signal, and idler as well as frequency determination, it would be very difficult to create an amplifier due the large number of choices available in the parameter space and the relatively limited number of combinations that can produce parametric amplification. Lamb waves were also analyzed and shown to have characteristics that could be favorable to the realization of actual amplifier devices due to the ability of controlling coherence length separately for difference and sum frequency generation.

# Appendix A Mathematica Code Used for Solution of Wave Problems



## Material Properties

```

Clear[matLiNb03dens, matLiNb03C4, matLiNb03C6]
matLiNb03dens = 4.7 * 103;
matLiNb03C4 = {c[1, 1] → 203 * 109, c[2, 2] → 203 * 109, c[3, 3] → 242.4 * 109,
  c[1, 2] → 57.3 * 109, c[1, 3] → 75.2 * 109, c[1, 4] → 8.5 * 109, c[2, 3] → c[1, 3],
  c[4, 4] → 59.5 * 109, c[5, 5] → c[4, 4], c[6, 6] →  $\frac{1}{2}$  (c[1, 1] - c[1, 2]),
  c[2, 4] → -c[1, 4], c[5, 6] → c[1, 4], c[1, 5] → 0, c[1, 6] → 0, c[2, 5] → 0,
  c[2, 6] → 0, c[3, 4] → 0, c[3, 5] → 0, c[3, 6] → 0, c[4, 5] → 0, c[4, 6] → 0};
matLiNb03C6 = {c[1, 1, 1] → -512 * 109, c[1, 1, 2] → 454 * 109, c[1, 1, 3] → 728 * 109,
  c[1, 1, 4] → -410 * 109, c[1, 2, 3] → 719 * 109, c[1, 2, 4] → 55 * 109,
  c[1, 3, 3] → -34 * 109, c[1, 3, 4] → -1 * 109, c[1, 4, 4] → -37 * 109, c[1, 5, 5] → -599 * 109,
  c[2, 2, 2] → -478 * 109, c[3, 3, 3] → -363 * 109, c[3, 4, 4] → -540 * 109,
  c[4, 4, 4] → -41 * 109, c[1, 2, 2] → c[1, 1, 1] + c[1, 1, 2] - c[2, 2, 2],
  c[2, 5, 6] →  $\frac{1}{2}$  (c[1, 1, 4] - c[1, 2, 4]), c[1, 5, 6] →  $\frac{1}{2}$  (c[1, 1, 4] + 3 c[1, 2, 4]),
  c[1, 6, 6] →  $\frac{1}{2}$  (-2 c[1, 1, 1] - c[1, 1, 2] + 3 c[2, 2, 2]), c[2, 2, 3] → c[1, 1, 3],
  c[2, 2, 4] → -c[1, 1, 4] - 2 c[1, 2, 4], c[2, 3, 3] → c[1, 1, 3],
  c[2, 3, 4] → -c[1, 3, 4], c[2, 4, 4] → c[1, 5, 5], c[2, 5, 5] → c[1, 4, 4],
  c[4, 6, 6] → c[1, 2, 4], c[4, 5, 5] → -c[4, 4, 4], c[3, 5, 6] → c[1, 3, 4],
  c[3, 5, 5] → c[3, 4, 4], c[2, 6, 6] →  $\frac{1}{2}$  (2 c[1, 1, 1] - c[1, 1, 2] - c[2, 2, 2]),
  c[3, 6, 6] →  $\frac{1}{2}$  (c[1, 1, 3] - c[1, 2, 3]), c[4, 5, 6] →  $\frac{1}{2}$  (-c[1, 1, 4] + c[1, 5, 5])};

```

## Mapping functions for converting tensor formats

```

pretty[s_] := {s[lst_] => Subscript[s, FromDigits@{lst}]};

```

```

Clear[m2to1V, m1to2V, f2to1V, f4to2V, f6to3V,
      ord, mL2to1V, mL1to2V, fL2to1V, fL6to2V, fL2to6V]
m2to1V = Thread[Rule[
  {{1, 1}, {2, 2}, {3, 3}, {2, 3}, {1, 3}, {1, 2}, {3, 2}, {3, 1}, {2, 1}}, Range[9]]];
m1to2V = Thread[Rule[Range[9],
  {{1, 1}, {2, 2}, {3, 3}, {2, 3}, {1, 3}, {1, 2}, {3, 2}, {3, 1}, {2, 1}}]];
f2to1V[{i_, j_}] := Sort[{i, j}] /. m2to1V
f2to1V[i_, j_] := f2to1V[{i, j}];

f4to2V[{i_, j_, k_, l_}] := Sort[{f2to1V[i, j], f2to1V[k, l]}];
f4to2V[i_, j_, k_, l_] := f4to2V[{i, j, k, l}]
f6to3V[{i_, j_, k_, l_, m_, n_}] := Sort[{f2to1V[i, j], f2to1V[k, l], f2to1V[m, n]}];
f6to3V[i_, j_, k_, l_, m_, n_] := f6to3V[{i, j, k, l, m, n}]

ord = Flatten[IntegerDigits /@ #, 1] & /@
  {{1111}, {2222}, {3333}, {2323}, {1313}, {1212}, {1312}, {2312}, {3312}, {2212}, {1112},
  {1113}, {1123}, {1133}, {1122}, {2233}, {3323}, {2313}, {3313}, {2213}, {2223}};
mL2to1V = Thread[Rule[f4to2V /@ ord, Range[21]]];
mL1to2V = Thread[Rule[Range[21], f4to2V /@ ord]];
fL2to1V[b_List] /; Length[b] == 2 := b /. mL2to1V
fL2to1V[i_, j_] := fL2to1V[{i, j}]
fL6to2V[{i_, j_, k_, l_, m_, n_}] := {f2to1V[i, j], fL2to1V@f4to2V[k, l, m, n]}
fL6to2V[i_, j_, k_, l_, m_, n_] := fL6to2V[{i, j, k, l, m, n}]

fL2to6V[{i_, j_}] := {i /. m1to2V, j /. mL1to2V /. m1to2V} // Flatten
fL2to6V[i_, j_] := fL2to6V[{i, j}]

```

## The cprime matrix functions

```

Clear[gamma, cPrime, c4, c6, n]
gamma[i_, j_, k_, l_, m_, n_] := c4 @@ f4to2V[i, m, k, l] KroneckerDelta[j, m]
gamma[i_, j_, {k_, l_, m_, n_}] := gamma[i, j, k, l, m, n]
cPrime[i_, j_, k_, l_, m_, n_] :=
  c6 @@ f6to3V[j, i, k, l, m, n] + 2 gamma[i, j, k, l, m, n] + gamma[i, m, n, l, j, k]

```

## Setup

```

Clear[Gamma, Delta, G, L]
Gamma[p_][i_, k_] := Sum[c4 @@ f4to2V[i, j, k, l] p[[j]] p[[l]], {j, 1, 3}, {l, 1, 3}]
Delta[p_][i_, k_, m_] := Sum[cPrime[j, i, k, l, m, n] p[[j]] p[[l]] p[[n]], {j, 3}, {l, 3}, {n, 3}]
G[p_, l_] := Sum[Gamma[p][i, k] l[[i]] l[[k]], {i, 3}, {k, 3}];
L[p_, l_] := Sum[Delta[p][i, k, m] l[[i]] l[[k]] l[[m]], {i, 3}, {k, 3}, {m, 3}];

```

## Plots w $\Theta$

```

Clear[p, mat, ans, vel]
Clear[l, u3, f1, fi, v, k1, k2, k3, fp]
Clear[k12, k21]
deg = 60;
theta = 70;
makeFunc[theta_, deg_] := Module[{ $\theta$ ,  $\phi$ , p, r1, r2, mat, ans,
  vel, f1, fp1, fp2, fp, fi, u3, u0, l, v, k1, k2, k3, k12, k21, A1, A},
  p = {Sin[ $\theta$ ] Cos[ $\phi$ ], Sin[ $\theta$ ] Sin[ $\phi$ ], Cos[ $\theta$ ]} /. { $\theta \rightarrow$  theta  $\frac{\pi}{180}$ ,  $\phi \rightarrow$  deg  $\frac{\pi}{180}$ };
  p = p / Norm[p] // N;
  r1 = {c4[i_, j_]  $\rightarrow$  c[i, j], c6[i_, j_, k_]  $\rightarrow$  c[i, j, k]};
  r2 = {c[i_, j_]  $\rightarrow$  0, c[i_, j_, k_]  $\rightarrow$  0};
  mat = Table[ $\Gamma$ [p][i, j], {i, 1, 3}, {j, 1, 3}] /. r1 //. matLinB03C4;
  ans = Eigensystem[mat];
  vel = Sqrt@{ans[[1]] / matLinB03dens};
  f1 = 100  $\times$  106;
  (*fp1[{c2_, c3_, c1_}] :=  $\frac{c2-c1}{c2-c3} \frac{c3}{c1}$ ; c1=signal vel, c2=pump vel, c3=idler vel *)
  fp2[{c1_, c3_, c2_}] := If[c2 == c3, 0,  $\frac{c2 - c1}{c2 - c3} \frac{c3}{c1}$ ];
  fp = fp2[vel] f1;
  fi = fp - f1;
  u3 = 5  $\times$  10-8;
  u0 = 1  $\times$  10-8;
  l = ans[[2, 1]];
  v = vel[[1]];
  k1 = 2  $\pi$  f1 / v; k2 = 2  $\pi$  fi / v; k3 = 2  $\pi$  fp / v;

  k12 :=  $\frac{-1}{4} \frac{L[p, l]}{G[p, l]} u3 k3 k2$ ;
  k21 :=  $\frac{-k3 k1}{4} \frac{L[p, l]}{G[p, l]} u3^*$ ;
  A1 = u0 Cosh[Sqrt[k12 k21] z];
  Return[If[fp == 0, 0, A = A1 /. r1 //. matLinB03C4 //. matLinB03C6 /. r2 // Simplify]]
]

```

```

maxThetaPhi[theta_, deg_] := Module[{theta, phi, p, r1, r2, mat, ans,
  vel, f1, fp1, fp2, fp, fi, u3, u0, l, v, k1, k2, k3, k12, k21, A1, A},
  p = {Sin[theta] Cos[phi], Sin[theta] Sin[phi], Cos[theta]} /. {theta -> theta  $\frac{\pi}{180}$ , phi -> deg  $\frac{\pi}{180}$ };
  p = p / Norm[p] // N;
  r1 = {c4[i_, j_] -> c[i, j], c6[i_, j_, k_] -> c[i, j, k]};
  r2 = {c[i_, j_] -> 0, c[i_, j_, k_] -> 0};
  mat = Table[Gamma[p][i, j], {i, 1, 3}, {j, 1, 3}] /. r1 /. matLinNb03C4;
  ans = Eigensystem[mat];
  vel = Sqrt@ (ans[[1]] / matLinNb03dens);
  f1 = 100 * 10^6;
  (*fp1[{c2_, c3_, c1_}] :=  $\frac{c2-c1}{c2-c3} \frac{c3}{c1}$ ; *)
  fp2[{c1_, c3_, c2_}] := If[c2 == c3, 0,  $\frac{c2 - c1}{c2 - c3} \frac{c3}{c1}$ ];
  fp = fp2[vel] f1;
  fi = fp - f1;

  u3 = 5 * 10^-8;
  u0 = 1 * 10^-8;
  l = ans[[2, 1]];
  v = vel[[1]];
  k1 = 2 * pi * f1 / v; k2 = 2 * pi * fi / v; k3 = 2 * pi * fp / v;

  k12 :=  $\frac{-1}{4} \frac{L[p, l]}{G[p, l]} u3 k3 k2$ ;
  k21 :=  $\frac{-k3 k1}{4} \frac{L[p, l]}{G[p, l]} u3^*$ ;
  Return[If[fp == 0, 0, k12 * k21 /. r1 /. matLinNb03C4 /. matLinNb03C6 /. r2 // Simplify]]
]

Maximize[{maxThetaPhi[th, phi], 0 <= th <= 180, 0 <= phi <= 360}, {th, phi}]

v[theta_, deg_] := Module[{p, r1, mat, ans, theta, phi},
  p = {Sin[theta] Cos[phi], Sin[theta] Sin[phi], Cos[theta]} /. {theta -> theta  $\frac{\pi}{180}$ , phi -> deg  $\frac{\pi}{180}$ };
  p = p / Norm[p] // N;
  r1 = {c4[i_, j_] -> c[i, j]};
  mat = Table[Gamma[p][i, j], {i, 1, 3}, {j, 1, 3}] /. r1 /. matLinNb03C4;
  Return[Sqrt@ (Eigensystem[mat] [[1]] / matLinNb03dens)];
]

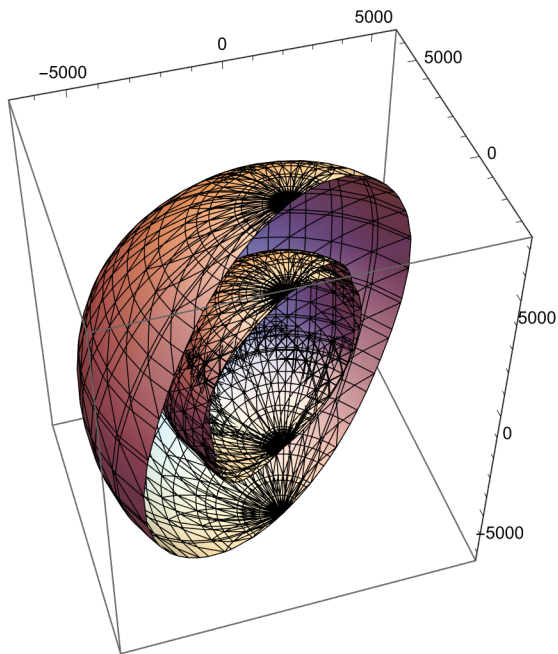
```

```
(mat1 = Array[c, {6, 6}] /. {c[i_, j_] /; i > j -> c[j, i]} // . matLinb03C4) // MatrixForm
```

$$\begin{pmatrix} 203000000000 & 5.73 \times 10^{10} & 7.52 \times 10^{10} & 8.5 \times 10^9 & 0 & 0 \\ 5.73 \times 10^{10} & 203000000000 & 7.52 \times 10^{10} & -8.5 \times 10^9 & 0 & 0 \\ 7.52 \times 10^{10} & 7.52 \times 10^{10} & 2.424 \times 10^{11} & 0 & 0 & 0 \\ 8.5 \times 10^9 & -8.5 \times 10^9 & 0 & 5.95 \times 10^{10} & 0 & 0 \\ 0 & 0 & 0 & 0 & 5.95 \times 10^{10} & 8.5 \times 10^9 \\ 0 & 0 & 0 & 0 & 8.5 \times 10^9 & 7.285 \times 10^{10} \end{pmatrix}$$

```
p1 =
```

```
SphericalPlot3D[Evaluate[{{v[ $\frac{\theta}{\pi}$  180,  $\frac{\phi}{\pi}$  180] [[1]], v[ $\frac{\theta}{\pi}$  180,  $\frac{\phi}{\pi}$  180] [[2]], v[ $\frac{\theta}{\pi}$  180,  $\frac{\phi}{\pi}$  180] [[3]]}],  
{ $\theta$ , 0,  $\pi$ }, { $\phi$ ,  $32 \frac{\pi}{180}$ ,  $32 \frac{\pi}{180} + \pi$ }]
```



```
FindMaximum[{Evaluate[maxThetaPhi[th, phi]], 0 ≤ th ≤ 180, 0 ≤ phi ≤ 360}, {th, 53}, {phi, 32}]  
{5.64015 × 1012, {th → 54.006, phi → 34.1846}}
```

## Linear Waves (Lin\_Piezo.nb)

```
In[ ]:= { $\alpha$ ,  $\beta$ ,  $\gamma$ } = {3 × 10-9, 3 × 10-9, 3 × 10-9};
```

```
torin[ $\theta$ _, fri_] :=
```

```
Module[{b,  $\epsilon$ Sum, ebSum,  $\Gamma$ piez, ev, eV, matSaw, matM, matK, cra, sol, S, ss11, eb, eb,  
 $\phi$ 1,  $\phi$ 2,  $\phi$ 3, kp1, kp2, kp3, upiez, dupiez, phi, dphi, a11, amat1, ar1, b22, amat2,  
ar2, c33, amat3, ar3, A1, A2, A3, A2n, tlinear, tlinearnel, tnonlin,  
tnonlinee, tnonlineel, dlin, dnel, dnonlinee, dnonlin, dnonlineel,  $\sigma$ ,  $\lambda$ 1,  
 $\lambda$ 2,  $\lambda$ 3, tlineartot, tNlineartot, LElasticity, Piezoelectricity, Ltot,  
NLElasticity, Electrostriction, Electroelasticity, Nltot, u1, u2, u3},
```

```

b = {0, Sin[θ], Cos[θ]};
eSum =
  Sum[ep[f, g] × b[[f]] × b[[g]], {f, 3}, {g, 3}] /. r3[e] /. r4[c] /. r2[ep] //. matLiNb03e4 //.
  matLiNb03e4 //. matLiNb03C4;
ebSum[k_] := Sum[(e[m, n, k] × b[[m]] × b[[n]]), {n, 3}, {m, 3}] /. r3[e] /. r4[c] /. r2[ep] //.
  matLiNb03e4 //. matLiNb03e4 //. matLiNb03C4;
Γpiez[i_, k_] := (Sum[(c[i, j, k, 1] × b[[1]] × b[[j]]), {j, 3}, {1, 3}]) +  $\frac{ebSum[i] \times ebSum[k]}{eSum}$ ;

{matM, matK} =
  {Table[KroneckerDelta[β, γ] matLiNb03dens, {β, 1, 3}, {γ, 1, 3}], Table[Γpiez[β, γ],
    {β, 1, 3}, {γ, 1, 3}]} /. r3[e] /. r4[c] /.
  r2[ep] //. matLiNb03e4 //. matLiNb03e4 //. matLiNb03C4;
{ev, eV} = Eigensystem[{matK, matM}];
eV = (eV / Norm /@ eV);
S = Sqrt[eV];

{A1, A2, A3} = eV;
ss11 = Select[S, # > 0 &];
{kp1, kp2, kp3} = 2 π fri / ss11;
eb = ebSum[#] & /@ Range@3;

{λ1, λ2, λ3} = ss11 / fri;

 $\phi_1 = \frac{eb.A1}{eSum}$ ;
 $\phi_2 = \frac{eb.A2}{eSum}$ ;
 $\phi_3 = \frac{eb.A3}{eSum}$ ;

u1[ξ_] := upiez[1][ξ] × A1[[1]] + upiez[2][ξ] × A1[[2]] + upiez[3][ξ] × A1[[3]];

upiez[i_][ξ_] := α A1[[i]] Exp[I kp1 ξ] + β A2[[i]] Exp[I kp2 ξ] + γ A3[[i]] Exp[I kp3 ξ];
dupiez[i_][k_][ξ_] :=
  I b[[k]] (α kp1 A1[[i]] Exp[I kp1 ξ] + β kp2 A2[[i]] Exp[I kp2 ξ] + γ kp3 A3[[i]] Exp[I kp3 ξ]);
phi[ξ_] := α φ1 Exp[I kp1 ξ] + β φ2 Exp[I kp2 ξ] + γ φ3 Exp[I kp3 ξ];
dphi[m_][ξ_] :=
  I b[[m]] (α kp1 φ1 Exp[I kp1 ξ] + β kp2 φ2 Exp[I kp2 ξ] + γ kp3 φ3 Exp[I kp3 ξ]);
(*Return[dupiez[1][3][x]];
Return[dphi[3][x]];*)
u1[ξ_] := upiez[1][ξ] × A1[[1]] + upiez[2][ξ] × A1[[2]] + upiez[3][ξ] × A1[[3]];
u2[ξ_] := upiez[1][ξ] × A2[[1]] + upiez[2][ξ] × A2[[2]] + upiez[3][ξ] × A2[[3]];
u3[ξ_] := upiez[1][ξ] × A3[[1]] + upiez[2][ξ] × A3[[2]] + upiez[3][ξ] × A3[[3]];
LElasticity[i_, j_][x_] :=

```

```

Sum[c[i, j, k, l] × dupiez[k][l][x], {k, 3}, {l, 3}] /. r3[e] /. r4[c] /. r2[ep] //.
  matLiNb03e4 //. matLiNb03e4 //. matLiNb03C4;
(*Return[tlinear[1,3][x]];*)

Piezoelectricity[i_, j_][x_] :=
  Sum[e[m, i, j] × dphi[m][x], {m, 3}] /. r3[e] /. r4[c] /. r2[ep] //. matLiNb03e4 //.
  matLiNb03e4 //. matLiNb03C4;
(*Return[tlinearnel[2,3][x]];*)
Ltot[i_, j_][x_] := LElasticity[i, j][x] + Piezoelectricity[i, j][x];

(*Return[tnonlin[1,3][x]];*)

dlin[m_][x_] :=
  (Sum[e[m, i, j] × dupiez[i][j][x], {i, 3}, {j, 3}] /. r3[e] /. r4[c] /. r2[ep] //.
  matLiNb03e4 //. matLiNb03e4 //. matLiNb03C4);
(*Return[dlin[3][x]];*)

dnel[m_][x_] :=
  -Sum[ep[m, n] × dphi[n][x], {n, 3}] /. r3[e] /. r4[c] /. r2[ep] //. matLiNb03e4 //.
  matLiNb03e4 //. matLiNb03C4;
(*Return[dnel[3][x]];*)

NLElasticity[i_, j_][x_] :=
  
$$\left( \frac{1}{2} (\text{Sum}[c[i, j, k, l, m, n] \times \text{dupiez}[k][l][x] \times \text{dupiez}[m][n][x], \right.$$

  
$$\left. \{k, 3\}, \{l, 3\}, \{m, 3\}, \{n, 3\}] /. r6[c] //. \text{matc6} \right);$$


Electrostriction[i_, j_][x_] :=
  
$$\left( -\frac{1}{2} \text{Sum}[q[m, n, j, i] \times \text{dphi}[m][x] \times \text{dphi}[n][x], \{m, 3\}, \{n, 3\}] /. r3[\text{epn}] /. r4\text{NS}[q] /. \right.$$

  
$$\left. r5[\text{en}] /. r6[c] //. \text{matc6} //. \text{matq6} //. \text{mate4} //. \text{mate6} //. \text{mate6} \right);$$

(*Return[tnonlinee[1,3][x]];*)
Electroelasticity[i_, j_][x_] :=
  Sum[en[m, j, i, k, l] × dphi[m][x] × dupiez[k][l][x], {m, 3}, {k, 3}, {l, 3}] /. r5[en] /.
  r3[epn] /. r4NS[q] /. r5[en] /.
  r6[c] //. matc6 //. matq6 //. mate4 //. mate6 //. mate6;

NLtot[i_, j_][x_] :=
  NLElasticity[i, j][x] + Electrostriction[i, j][x] + Electroelasticity[i, j][x];

(*Return[tnonlineel[1,3][x]];*)
dnonlinee[m_][x_] :=
  Sum
$$\left[ \frac{1}{2} \text{epn}[m, n, p] \times \text{dphi}[n][x] \times \text{dphi}[p][x], \{n, 3\}, \{p, 3\} \right] /. r3[\text{epn}] /. r4\text{NS}[q] /.$$

  r5[en] /. r6[c] //. matc6 //. matq6 //. mate4 //. mate6 //. mate6;
(*Return[dnonlinee[3][x1,x2,x3]];*)

```

```

dnonlin[m_][x_] :=
  Sum[ $\frac{1}{2}$  en[m, i, j, k, l] × dupiez[i][j][x] × dupiez[k][l][x], {i, 3}, {j, 3},
    {k, 3}, {l, 3}] /. r3[epn] /. r4NS[q] /. r5[en] /.
    r6[c] //. matc6 //. matq6 //. mate4 //. mate6 //. mate6;
(*Return[dnonlin[3][x]];*)
dnonlineel[m_][x_] :=
  Sum[-q[m, n, i, j] × dphi[n][x] × dupiez[i][j][x], {n, 3}, {i, 3}, {j, 3}] /. r3[e] /.
    r4[c] /. r2[ep] /. r3[epn] /. r4NS[q] /. r5[en] /.
    r6[c] //. matc6 //. matq6 //. mate4 //. mate6 //. mate6;

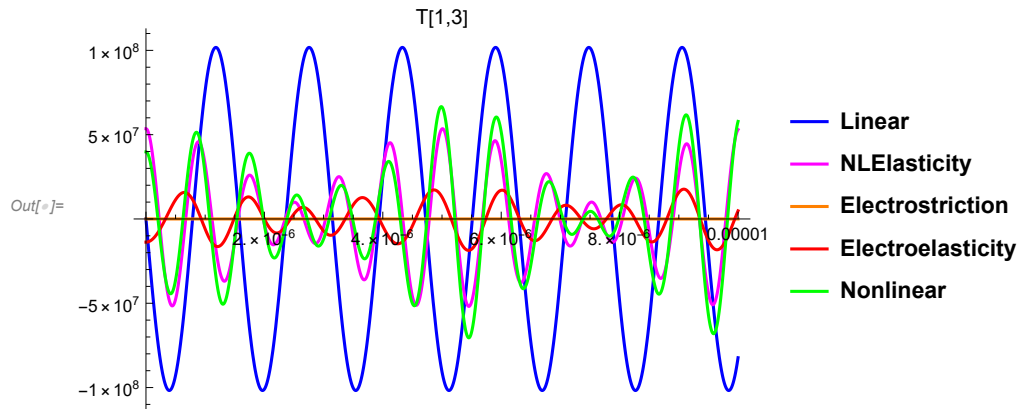
Return[NLElasticity[1, 3][x] / Ltot[1, 3][x]]
]

```

```

In[ ]:= Plot[Evaluate@Re[torin[Pi/2, 250*10^7]], {x, 0, 10^-5},
  PlotStyle → {Blue, Magenta, Orange, Red, Green}, PlotLegends →
  {"Linear", "NLElasticity", "Electrostriction", "Electroelasticity", "Nonlinear"},
  PlotLabel → "T[1,3]", PlotRange → All]

```



## Material Coefficients (NL\_Saw.nb)

```

In[ ]:= Clear[matLiNb03C6, matLiNb03q6, matLiNb03C4, matLiNb03e4, matLiNb03e4, matLiNb03e6]
$MaxExtraPrecision = 100;
Clear[prec, setPrec, x]
prec = 90;
setPrec = {Rule[x_, y_] /; Precision@y < prec ⇒ Rule[x, SetPrecision[y, prec] ]};
matLiNb03dens = SetPrecision[4.7*10^3, prec];

matLiNb03e4 =
  {e[1, 1] → 0, e[2, 1] → -2.53764, e[3, 1] → 0.193644, e[1, 2] → 0, e[2, 2] → 2.53764,
  e[3, 2] → 0.193644, e[1, 3] → 0, e[2, 3] → 0, e[3, 3] → 1.30863, e[2, 4] → 3.69594,
  e[1, 4] → 0, e[3, 4] → 0, e[1, 5] → 3.69594, e[2, 5] → 0, e[3, 5] → 0,
  e[1, 6] → -2.53384, e[2, 6] → 0, e[3, 6] → 0} /. setPrec;

(matLiNb03e4 = {ep[1, 1] → er*43.6, ep[2, 2] → er*43.6,
  ep[3, 3] → er*29.16, ep[1, 2] → 0, ep[1, 3] → 0, ep[2, 1] → 0, ep[2, 3] → 0,

```



$ep[3, 1] \rightarrow 0, ep[3, 2] \rightarrow 0 \} /. \{er \rightarrow 8.8542 * 10^{-12}\} /. setPrec);$

matLiNb03C4 =

$\{c[1, 1] \rightarrow 203 * 10^9, c[2, 2] \rightarrow 203 * 10^9, c[3, 3] \rightarrow 242.4 * 10^9, c[1, 2] \rightarrow 57.3 * 10^9,$   
 $c[1, 3] \rightarrow 75.2 * 10^9, c[1, 4] \rightarrow 8.5 * 10^9, c[2, 3] \rightarrow c[1, 3], c[4, 4] \rightarrow 59.5 * 10^9,$   
 $c[5, 5] \rightarrow c[4, 4], c[6, 6] \rightarrow \frac{1}{2} (c[1, 1] - c[1, 2]), c[2, 4] \rightarrow -c[1, 4],$   
 $c[5, 6] \rightarrow c[1, 4], c[1, 5] \rightarrow 0, c[1, 6] \rightarrow 0, c[2, 5] \rightarrow 0, c[2, 6] \rightarrow 0,$   
 $c[3, 4] \rightarrow 0, c[3, 5] \rightarrow 0, c[3, 6] \rightarrow 0, c[4, 5] \rightarrow 0, c[4, 6] \rightarrow 0 \} /. setPrec;$

matLiNb03C6 =  $\{c[1, 1, 1] \rightarrow -512 * 10^9, c[1, 1, 2] \rightarrow 454 * 10^9, c[1, 1, 3] \rightarrow 728 * 10^9,$

$c[1, 1, 4] \rightarrow -410 * 10^9, c[1, 2, 3] \rightarrow 719 * 10^9, c[1, 2, 4] \rightarrow 55 * 10^9,$   
 $c[1, 3, 3] \rightarrow -34 * 10^9, c[1, 3, 4] \rightarrow -1 * 10^9, c[1, 4, 4] \rightarrow -37 * 10^9, c[1, 5, 5] \rightarrow -599 * 10^9,$   
 $c[2, 2, 2] \rightarrow -478 * 10^9, c[3, 3, 3] \rightarrow -363 * 10^9, c[3, 4, 4] \rightarrow -540 * 10^9,$   
 $c[4, 4, 4] \rightarrow -41 * 10^9, c[1, 2, 2] \rightarrow c[1, 1, 1] + c[1, 1, 2] - c[2, 2, 2],$   
 $c[2, 5, 6] \rightarrow \frac{1}{2} (c[1, 1, 4] - c[1, 2, 4]), c[1, 5, 6] \rightarrow \frac{1}{2} (c[1, 1, 4] + 3 c[1, 2, 4]),$   
 $c[1, 6, 6] \rightarrow \frac{1}{4} (-2 c[1, 1, 1] - c[1, 1, 2] + 3 c[2, 2, 2]), c[2, 2, 3] \rightarrow c[1, 1, 3],$   
 $c[2, 2, 4] \rightarrow -c[1, 1, 4] - 2 c[1, 2, 4], c[2, 3, 3] \rightarrow c[1, 3, 3],$   
 $c[2, 3, 4] \rightarrow -c[1, 3, 4], c[2, 4, 4] \rightarrow c[1, 5, 5], c[2, 5, 5] \rightarrow c[1, 4, 4],$   
 $c[4, 6, 6] \rightarrow c[1, 2, 4], c[4, 5, 5] \rightarrow -c[4, 4, 4], c[3, 5, 6] \rightarrow c[1, 3, 4],$   
 $c[3, 5, 5] \rightarrow c[3, 4, 4], c[2, 6, 6] \rightarrow \frac{1}{4} (2 c[1, 1, 1] - c[1, 1, 2] - c[2, 2, 2]),$   
 $c[3, 6, 6] \rightarrow \frac{1}{2} (c[1, 1, 3] - c[1, 2, 3]), c[4, 5, 6] \rightarrow \frac{1}{2} (-c[1, 4, 4] + c[1, 5, 5]),$   
 $c[1, 1, 5] \rightarrow 0, c[1, 1, 6] \rightarrow 0, c[1, 2, 5] \rightarrow 0, c[1, 3, 5] \rightarrow 0, c[1, 4, 5] \rightarrow 0,$   
 $c[1, 4, 6] \rightarrow 0, c[2, 2, 5] \rightarrow 0, c[2, 2, 6] \rightarrow 0, c[2, 3, 5] \rightarrow 0, c[2, 3, 6] \rightarrow 0,$   
 $c[1, 3, 6] \rightarrow 0, c[2, 4, 5] \rightarrow 0, c[2, 4, 6] \rightarrow 0, c[3, 3, 4] \rightarrow 0, c[3, 3, 5] \rightarrow 0,$   
 $c[3, 3, 6] \rightarrow 0, c[3, 4, 5] \rightarrow 0, c[3, 4, 6] \rightarrow 0, c[4, 4, 5] \rightarrow 0, c[4, 4, 6] \rightarrow 0,$   
 $c[5, 5, 5] \rightarrow 0, c[5, 5, 6] \rightarrow 0, c[5, 6, 6] \rightarrow 0, c[6, 6, 6] \rightarrow 0, c[1, 2, 6] \rightarrow 0 \} /. setPrec;$

matLiNb03q6 =

$\{q[1, 1] \rightarrow 1.11 * 10^{-9}, q[1, 2] \rightarrow -2.1 * 10^{-9}, q[1, 3] \rightarrow 2.32 * 10^{-9}, q[1, 4] \rightarrow 1.51 * 10^{-9},$   
 $q[3, 1] \rightarrow 0.19 * 10^{-9}, q[3, 3] \rightarrow -2.76 * 10^{-9}, q[4, 1] \rightarrow 1.85 * 10^{-9}, q[4, 4] \rightarrow -1.83 * 10^{-9},$   
 $q[1, 2] \rightarrow q[2, 1], q[2, 2] \rightarrow q[1, 1], q[2, 3] \rightarrow q[1, 3], q[2, 4] \rightarrow -q[1, 4],$   
 $q[6, 5] \rightarrow q[1, 4], q[3, 2] \rightarrow q[3, 1], q[6, 6] \rightarrow \frac{1}{2} (q[1, 1] - q[1, 2]),$   
 $q[4, 2] \rightarrow -q[4, 1], q[5, 3] \rightarrow q[4, 4], q[5, 6] \rightarrow q[4, 1] \} /. setPrec;$

matLiNb03e6 =  $\{en[1, 1, 5] \rightarrow 17.1, en[1, 1, 6] \rightarrow -4.7, en[1, 2, 5] \rightarrow 19.9, en[1, 2, 6] \rightarrow 15.9,$

$en[1, 3, 5] \rightarrow 19.6, en[1, 3, 6] \rightarrow -0.9, en[1, 3, 5] \rightarrow 19.6, en[1, 4, 5] \rightarrow 20.3,$   
 $en[3, 1, 1] \rightarrow 14.7, en[3, 1, 2] \rightarrow 13, en[3, 1, 3] \rightarrow -10, en[3, 1, 4] \rightarrow 11,$   
 $en[3, 3, 3] \rightarrow -17.3, en[3, 4, 4] \rightarrow -10.2, en[1, 4, 6] \rightarrow \frac{1}{2} (en[1, 1, 5] - en[1, 2, 5]),$

```

en[2, 1, 1] →  $\frac{1}{2}$  (en[1, 1, 6] - 3 en[1, 2, 6]),
en[2, 1, 2] →  $\frac{1}{2}$  (en[1, 1, 6] - en[1, 2, 6]), en[2, 1, 3] → en[1, 3, 6],
en[2, 1, 4] → en[1, 2, 5], en[2, 2, 2] → -(en[2, 1, 1] + 2 en[1, 2, 2]),
en[2, 2, 3] → -en[1, 3, 6], en[2, 2, 5] → en[1, 4, 5],
en[2, 5, 6] →  $\frac{1}{2}$  (en[1, 1, 5] - en[1, 2, 5]), en[2, 6, 6] → en[2, 1, 2],
en[3, 2, 2] → en[3, 1, 1], en[3, 2, 3] → en[3, 1, 3], en[3, 2, 4] → -en[3, 1, 4],
en[3, 5, 5] → en[3, 4, 4], en[2, 2, 4] → en[1, 1, 5], en[2, 3, 4] → en[1, 3, 5],
en[2, 4, 4] → -en[1, 4, 5], en[3, 5, 6] → -en[3, 2, 4],
en[3, 6, 6] →  $\frac{1}{2}$  (en[3, 2, 2] - en[3, 1, 2]) } /. setPrec;
matLiNb03e6 = {epn[1, 1] → (-2.81*10^-19), epn[2, 2] → (-2.×4*10^-19),
epn[3, 3] → (-2.91*10^-19), epn[2, 4] → (4.6*10^-19)} /. setPrec;

```

## Voigt Notation Conversion and Coordinate Transforms

Convert To/From Voigt notation

In[ ]:=

```
Clear[V, v]
V[{i_ : Integer}] := V[i]
V[i_ : Integer] :=
  i /. {1 -> {1, 1}, 2 -> {2, 2}, 3 -> {3, 3}, 4 -> {2, 3}, 5 -> {1, 3}, 6 -> {1, 2}}
V[i_ : Integer, j_ : Integer] :=
  Sort[{i, j}] /. {{1, 1} -> 1, {2, 2} -> 2, {3, 3} -> 3, {2, 3} -> 4, {1, 3} -> 5, {1, 2} -> 6}
V[{i_ : Integer, j_ : Integer}] := V[i, j]
v[lst_] := Flatten[V/@lst]
vr[lst_] := Reverse[V /@ Sort /@ Partition[Reverse[lst], 2]]

r44 = {c[4, j_, 4, l_] => -ep[j, l],
  c[i_, j_, 4, l_] => e[l, i, j], c[4, j_, k_, l_] => e[j, k, l]};

rn1 = {c[4, k_, 4, l_, 4, n_] => 0.5`90*epn[k, l, n],

  c[i_, k_, 4, l_, 4, n_] => -0.5`90*q[l, n, i, k], c[4, k_, 4, i_, l_, n_] =>
  -0.5`90*q[k, i, l, n], c[4, k_, i_, l_, 4, n_] => -0.5`90*q[k, n, i, l],

  c[4, n_, i_, k_, j_, l_] => en[n, i, k, j, l],

  c[i_, k_, j_, l_, 4, n_] => en[n, i, k, j, l],
  c[i_, k_, 4, n_, j_, l_] => en[n, i, k, j, l],

  c[i_, k_, m_, n_, j_, l_] => 0.5`90*c[i, k, m, n, j, l]};
```

## Coordinate Transforms

In[ ]:=

```
Clear[XForm, XForm2, XForm3, XForm4, XForm4NS, XForm5, XForm6]
XForm[mat_, L_, rank_] := Module[{nmat, iLst, jLst},
  iLst = Symbol /@ ("i" <> ToString[#] &) /@ Range[rank];
  jLst = Symbol /@ ("j" <> ToString[#] &) /@ Range[rank];
  Return[nmat];
]

XForm2[mat_, L_] := Module[{pLst, eLst, f, nm, m},
  nm = Head@mat[[1, 1]];
  pLst = Union[Sort /@ Tuples[Range[3], {2}]];
  f[{i1_, i2_}] := Sum[L[[i1, j1]] L[[i2, j2]] nm[j1, j2], {j1, 3}, {j2, 3}] /. mat;
  Return[Append[Thread[Rule[Apply[nm, pLst, {1}], f /@ pLst]], Rule[ρ, ρ /. mat]]];
]

XForm3[mat_, L_] := Module[{pLst, eLst, f, nm, m},
  nm = Head@mat[[1, 1]];
  pLst = Flatten[Table[{i, j}, {i, 3}, {j, 6}], 1];
  eLst = Flatten@{#1, V[#2]} & @@@ pLst;
```

```

f[{i1_, i2_, i3_}] :=
  Sum[L[[i1, j1]] L[[i2, j2]] L[[i3, j3]] nm[j1, j2, j3], {j1, 3}, {j2, 3}, {j3, 3}] /.
    {nm[i_, j_, k_] => nm@@ {i, V@Sort[{j, k}]}} //. mat;
Return[Append[Thread[Rule[Apply[nm, pLst, {1}], f /@ eLst]], Rule[ρ, ρ /. mat]]];
]
XForm4[mat_, L_] := Module[{pLst, eLst, f, nm, m},
  nm = Head@mat[[1, 1]];
  pLst = Union[Sort /@ Tuples[Range[6], {2}]];
  eLst = v /@ pLst;
  f[{i1_, i2_, i3_, i4_}] :=
    Sum[L[[i1, j1]] L[[i2, j2]] L[[i3, j3]] L[[i4, j4]] nm[j1, j2, j3, j4],
      {j1, 3}, {j2, 3}, {j3, 3}, {j4, 3}]
    /. {nm[i_, j_, k_, l_] => nm@@ Sort@vr[{i, j, k, l}]} //. mat;
  Return[Append[Thread[Rule[Apply[nm, pLst, {1}], f /@ eLst]], Rule[ρ, ρ /. mat]]];
]
XForm4NS[mat_, L_] := Module[{pLst, eLst, f, nm, m},
  nm = Head@mat[[1, 1]];
  pLst = Union[Tuples[Range[6], {2}]];
  eLst = v /@ pLst;
  f[{i1_, i2_, i3_, i4_}] :=
    Sum[L[[i1, j1]] L[[i2, j2]] L[[i3, j3]] L[[i4, j4]] nm[j1, j2, j3, j4],
      {j1, 3}, {j2, 3}, {j3, 3}, {j4, 3}]
    /. {nm[i_, j_, k_, l_] => nm@@ Sort@vr[{i, j, k, l}]} //. mat;
  Return[Append[Thread[Rule[Apply[nm, pLst, {1}], f /@ eLst]], Rule[ρ, ρ /. mat]]];
]
XForm5[mat_, L_] := Module[{pLst, eLst, f, nm, m},
  nm = Head@mat[[1, 1]];
  pLst = Flatten[Table[{i, j, k}, {i, 3}, {j, 6}, {k, j, 6}], 2];
  eLst = Flatten@{#1, V[#2], V[#3]} &@@@ pLst;
  f[{i1_, i2_, i3_, i4_, i5_}] :=
    Sum[L[[i1, j1]] L[[i2, j2]] L[[i3, j3]] L[[i4, j4]] L[[i5, j5]] nm[j1, j2, j3, j4, j5],
      {j1, 3}, {j2, 3}, {j3, 3}, {j4, 3}, {j5, 3}] /.
    {nm[i_, j_, k_, m_, n_] => nm@@ Flatten@{i, Sort@{V[j, k], V[m, n]}}} //. mat;
  Return[Append[Thread[Rule[Apply[nm, pLst, {1}], f /@ eLst]], Rule[ρ, ρ /. mat]]];
]
XForm6[mat_, L_] := Module[{pLst, eLst, f, nm, m},
  nm = Head@mat[[1, 1]];
  pLst = Union[Sort /@ Tuples[Range[6], {3}]];
  eLst = v /@ pLst;
  f[{i1_, i2_, i3_, i4_, i5_, i6_}] :=
    Sum[L[[i1, j1]] L[[i2, j2]] L[[i3, j3]] L[[i4, j4]] L[[i5, j5]] L[[i6, j6]]
      nm[j1, j2, j3, j4, j5, j6], {j1, 3}, {j2, 3}, {j3, 3}, {j4, 3}, {j5, 3}, {j6, 3}]
    /. {nm[i_, j_, k_, l_, m_, n_] => nm@@ Sort@vr[{i, j, k, l, m, n}]} //. mat;
  Return[Append[Thread[Rule[Apply[nm, pLst, {1}], f /@ eLst]], Rule[ρ, ρ /. mat]]];
]

```

## Rotated Material Properties

In[ ]:=

```
matc4 = Chop@XForm4[matLiNb03C4,  
  {{1, 0, 0}, {0, Cos[(38/180)*Pi] // N[#, prec] &, Sin[(38/180)*Pi] // N[#, prec] &},  
  {0, -Sin[(38/180)*Pi] // N[#, prec] &, Cos[(38/180)*Pi] // N[#, prec] &}}];  
  
mate4 = XForm3[matLiNb03e4,  
  {{1, 0, 0}, {0, Cos[(38/180)*Pi] // N[#, prec] &, Sin[(38/180)*Pi] // N[#, prec] &},  
  {0, -Sin[(38/180)*Pi] // N[#, prec] &, Cos[(38/180)*Pi] // N[#, prec] &}}];  
  
(*mate4i = (XForm2[mate4, IdentityMatrix[3]] /. {(x_ -> x_) => (x -> 0)}) *)  
mate4 = (XForm2[matLiNb03e4,  
  {{1, 0, 0}, {0, Cos[(38/180)*Pi] // N[#, prec] &, Sin[(38/180)*Pi] // N[#, prec] &},  
  {0, -Sin[(38/180)*Pi] // N[#, prec] &, Cos[(38/180)*Pi] // N[#, prec] &}}]);  
  
matc6 = Chop@XForm6[matLiNb03C6,  
  {{1, 0, 0}, {0, Cos[(38/180)*Pi] // N[#, prec] &, Sin[(38/180)*Pi] // N[#, prec] &},  
  {0, -Sin[(38/180)*Pi] // N[#, prec] &, Cos[(38/180)*Pi] // N[#, prec] &}}];  
  
mate6i = (XForm5[matLiNb03e6, IdentityMatrix[3]] /. {(x_ -> x_) => (x -> 0)});  
mate6 = (XForm5[mate6i,  
  {{1, 0, 0}, {0, Cos[(38/180)*Pi] // N[#, prec] &, Sin[(38/180)*Pi] // N[#, prec] &},  
  {0, -Sin[(38/180)*Pi] // N[#, prec] &, Cos[(38/180)*Pi] // N[#, prec] &}}]);  
  
mate6i = (XForm3[matLiNb03e6, IdentityMatrix[3]] /. {(x_ -> x_) => (x -> 0)});  
mate6 = (XForm3[mate6i,  
  {{1, 0, 0}, {0, Cos[(38/180)*Pi] // N[#, prec] &, Sin[(38/180)*Pi] // N[#, prec] &},  
  {0, -Sin[(38/180)*Pi] // N[#, prec] &, Cos[(38/180)*Pi] // N[#, prec] &}}]);  
  
matq6i = (XForm4NS[matLiNb03q6, IdentityMatrix[3]] /. {(x_ -> x_) => (x -> 0)});  
matq6 = (XForm4NS[matq6i,  
  {{1, 0, 0}, {0, Cos[(38/180)*Pi] // N[#, prec] &, Sin[(38/180)*Pi] // N[#, prec] &},  
  {0, -Sin[(38/180)*Pi] // N[#, prec] &, Cos[(38/180)*Pi] // N[#, prec] &}}]);  
  
trans =  
  {{1, 0, 0}, {0, Cos[(38/180)*Pi] // N[#, prec] &, Sin[(38/180)*Pi] // N[#, prec] &},  
  {0, -Sin[(38/180)*Pi] // N[#, prec] &, Cos[(38/180)*Pi] // N[#, prec] &}}];
```

## Utility Functions for Conversion of Full Tensor Indices to Voigt

```

In[ ]:= Clear[r3, r4, r4NS, r5, r6, voigt]
r2[sym_] := sym[i_, j_] => sym@@Sort@{i, j}
r3[sym_] := sym[i_, j_, k_] => sym@@Flatten@{i, voigt[j, k]}
r4[sym_] := sym[i_, j_, k_, l_] => sym@@Sort@vr[{i, j, k, l}]
r4NS[sym_] := sym[i_, j_, k_, l_] => sym@@{V[i, j], V[k, l]}
r5[sym_] := sym[i_, j_, k_, l_, m_] => sym@@Flatten@{i, Sort[{V[j, k], V[l, m]}]}
r6[sym_] :=
  sym[i_, j_, k_, l_, m_, n_] => c@@Sort@{voigt[i, j], voigt[k, l], voigt[m, n]}
voigt[i_, j_] := Block[{pair},
  pair = Sort[{i, j}];
  Return[pair /. {{1, 1} -> 1, {2, 2} -> 2, {3, 3} -> 3, {2, 3} -> 4, {1, 3} -> 5, {1, 2} -> 6}];
]
voigt[{i_, j_}] := voigt[i, j]

```

```

In[ ]:= Clear[ct, et, le, lt, x]
ct[j_, i_, k_, r_, m_, n_] := c[j, i, k, r, m, n] +
  2 * c[j, n, k, r] KroneckerDelta[i, m] + c[j, i, n, r] KroneckerDelta[k, m];

et[m_, j_, i_, k_, r_] := en[m, j, i, k, r] + e[m, j, r] KroneckerDelta[k, i];

lT[m_, n_, i_, j_] := q[m, n, i, j];

```

```

In[ ]:= Clear[nonlicapt, nonlid]
nonlicapt[k_, r_] := Sum[
  0.5 * ((c[k, r, m, n, p, z] * u1[m][n] * u2[p][z]) - (en[z, k, r, m, n] * es1[z] * u2[m][n]) -
    (en[z, k, r, m, n] * es2[z] * u1[m][n])), {m, 3}, {n, 3}, {p, 3}, {z, 3}]

(*nonlicapt[pr_, rp_] := Sum[nonlicapt[k, r] trans[[pr, k]] trans[[rp, r]], {k, 3}, {r, 3}])

nonlid[r_] :=
  Sum[-0.5 * ((en[r, m, n, p, z] * u1[m][n] * u2[p][z]) + (lT[r, z, m, n] * es1[z] * u2[m][n]) +
    (lT[r, z, m, n] * es2[z] * u1[m][n])), {n, 3}, {p, 3}, {k, 3}, {m, 3}, {z, 3}]

nonlidf2[r_] := Sum[-0.5 * ((en[r, m, n, p, z] * u1[m][n] * u2[p][z])),
  {n, 3}, {p, 3}, {k, 3}, {m, 3}, {z, 3}]

```

## Wave Equations

```

Clear[torin, k1, fsig, fpump, γ]
fsig = 2 * 109; fpump = 4 * fsig; fid = 3 * fsig;
k1[f_] := (2 * Pi * f) / 3986.590;
lam = 2 * Pi / k1[fsig];
torin[cra_] :=
  Module[{tmp, S, ms, matsaw2, H, B, Γpsaw, matsaw1, sol, ss, as1, as11, as22, as33, as44,
    d5, a, err1, vec, matsawtest, ss11, u, u2, ut, α1, tor, ermat, err2, up1, nonlicapt3,

```

```

nonlicapt32, nonlicaptt, up2, up2t, up1t, α2, nonlicapt3p2, nonlicapt3g,
nonlicapt3p1, tlinear, upg, umag, matsaw28, mag, t33, t11, t, n1, ssmid,
cofh2, cofh, nt4h, k1, f, tnonlinear, u2mx1, u2mx3, nonlinearelastic,
nonlinearcoupling, electroelasticity, electrostriction, tabi, p, eq, uθ,
uη, eqcon, eqs, god, nt4hp, u2p, u2m, uap, pm1, pm4, pm2, pm3, wtp, u2ms, Bnon,
Bno, now, s, aa, eqs1, eqs2, eqs3, eqsT, cr, bc1, bc2, bc3, bcT, res, ans},

k1[f_] := (2*Pi*f)/3986.5`90;

H[α_, β_] := KroneckerDelta[α, β] - KroneckerDelta[α, 4] KroneckerDelta[β, 4];
Γpsaw[s_][β_, γ_] := (c[β, 3, γ, 3] s^2 - (c[β, 1, γ, 3] + c[β, 3, γ, 1]) s + c[β, 1, γ, 1]);
matsaw1 = Table[ ((matLinB03dens*cra^2*H[β, γ]) - Γpsaw[s][β, γ]), {β, 1, 4}, {γ, 1, 4}];
matsaw1 = (matsaw1 /. r44 /. r3[e] /. r4[c] /. r2[ep] //. matc4 //. mate4 //. mate4);

sol = Solve[Det[matsaw1] == 0, s];

ss = {s /. sol[[1]], s /. sol[[2]], s /. sol[[3]],
      s /. sol[[4]], s /. sol[[5]], s /. sol[[6]], s /. sol[[7]], s /. sol[[8]]};
(*Print[ss];*)
ss11 = Select[ss, Im[#] < 0 &];

B[β_, μ_] :=
  ((c[β, 3, 1, 1] - c[β, 3, 1, 3] ss11[[μ]]) a[[μ, 1]]) + ((c[β, 3, 2, 1] - c[β, 3, 2, 3]
    ss11[[μ]]) a[[μ, 2]]) + ((c[β, 3, 3, 1] - c[β, 3, 3, 3] ss11[[μ]]) a[[μ, 3]]) +
  ((c[β, 3, 4, 1] - c[β, 3, 4, 3] ss11[[μ]]) a[[μ, 4]]) /. r44 /.
  r3[e] /. r4[c] /. r2[ep] //. matc4 //. mate4 //. mate4;

as11 = NullSpace[matsaw1 /. {s -> ss11[[1]]}];
as22 = NullSpace[matsaw1 /. {s -> ss11[[2]]}];
as33 = NullSpace[matsaw1 /. {s -> ss11[[3]]}];
as44 = NullSpace[matsaw1 /. {s -> ss11[[4]]}];

a = {as11 // Flatten, as22 // Flatten, as33 // Flatten, as44 // Flatten};

matsawtest = Table[B[β, μ],
  {β, 1, 4}, {μ, 1, 4}];

err1 = Det[matsawtest];

s[s_, f_] := If[f < 0, Conjugate[s], s];
aa[a_, f_] := If[f < 0, Conjugate[a], a];

(* H term from nonlinear equation final form SAW w Piezo *)
Bnon[β_, μ_][f_] :=
  (Sum[
    (1 / s[ss11[[μ], f]) ((2 c[β, 1, γ, 1] - c[β, 1, γ, 3]) s[ss11[[μ], f]) aa[a[[μ, γ], f]),
    {γ, 4}])
  ] /. r44 /. r3[e] /. r4[c] /. r2[ep] //. matc4 //. mate4 //. mate4);

```

```

(* E term from nonlinear equation final form SAW w Piezo *)
Bno[η_, θ_, β_][f1_, f2_] :=
  
$$\frac{k1[f1] \times k1[f2]}{(s[ss11[\eta]], f1) \times k1[f1] + s[ss11[\theta]], f2) \times k1[f2]} \text{Sum}[(c[\beta, 1, \gamma, 1, \delta, 1] (k1[f1] +$$

  
$$k1[f2]) - c[\beta, 1, \gamma, 1, \delta, 3] ((s[ss11[\theta]], f2) + s[ss11[\eta]], f1))$$

  
$$k1[f1] + (s[ss11[\theta]], f2) + s[ss11[\eta]], f1)) k1[f2] +$$

  
$$s[ss11[\theta]], f2) \times s[ss11[\eta]], f1) (k1[f1] + k1[f2])) aa[a[\eta, \gamma], f1] \times$$

  
$$aa[a[\theta, \delta], f2]), \{\gamma, 4\}, \{\delta, 4\}] /. rn1 /. r3[epn] /. r4NS[q] /.$$

  r5[en] /. r6[c] //. matc6 //. matq6 //. mate4 //. mate6 //. mate6;

cr = {α[f_ /; f < 0][μ_][x_] => Conjugate[α[-f][μ][x]]};
eqs1[β_] := Sum[Bnon[μ, β][q] × D[α[q][μ][x], x], {q, {fsig}}, {μ, 4}] ==
  Sum[Bno[η, θ, β][r, sss] α[r][η][x] α[sss][θ][x],
    {r, {-fid}}, {sss, {fpump}}, {η, 4}, {θ, 4}];
eqs2[β_] := Sum[Bnon[μ, β][q] × D[α[q][μ][x], x], {q, {fid}}, {μ, 4}] ==
  Sum[Bno[η, θ, β][r, sss] α[r][η][x] α[sss][θ][x],
    {r, {-fsig}}, {sss, {fpump}}, {η, 4}, {θ, 4}];
eqs3[β_] := Sum[Bnon[μ, β][q] × D[α[q][μ][x], x], {q, {fpump}}, {μ, 4}] ==
  Sum[Bno[η, θ, β][r, sss] α[r][η][x] α[sss][θ][x],
    {r, {fid}}, {sss, {fsig}}, {η, 4}, {θ, 4}];
eqsT = Table[{eqs1[β], eqs2[β], eqs3[β]}, {β, 4}] // Flatten;
eqsT = eqsT /. cr;

cofh = (matsawtest) . {A1, A2, A3, A4};
cofh2 = (NSolve[{cofh[[2]] == 0, cofh[[3]] == 0, cofh[[4]] == 0}, {A1, A2, A3}] /. setPrec);
(*Print[cofh2];
*)
nt4h = ({A1, A2, A3, A4} /. cofh2 // Flatten) /. {A4 → 1.5`90};
nt4hp = ({A1, A2, A3, A4} /. cofh2 // Flatten) /. {A4 → .0000000004`90};

bc1 = Table[α[q][μ][0] == nt4h[[μ]], {q, {fsig}}, {μ, 4}] // Flatten;
bc2 = Table[α[q][μ][0] == 0, {q, {fid}}, {μ, 4}] // Flatten;
bc3 = Table[α[q][μ][0] == nt4hp[[μ]], {q, {fpump}}, {μ, 4}] // Flatten;
bcT = Join[{bc1, bc2, bc3}] // Flatten;

res = Table[α[q][μ], {q, {fsig, fpump, fid}}, {μ, 4}] // Flatten;

ans = NDSolve[{eqsT, bcT} // Flatten, res, {x, 0`90, 5 lam}, WorkingPrecision → 20];
Return[ans]
]

```

## Output

```

In[ ]:= ansSAWNL = torin[3986.5`90]

```

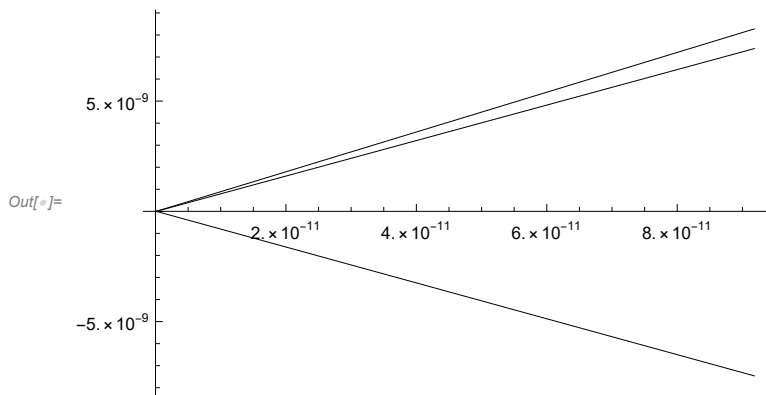
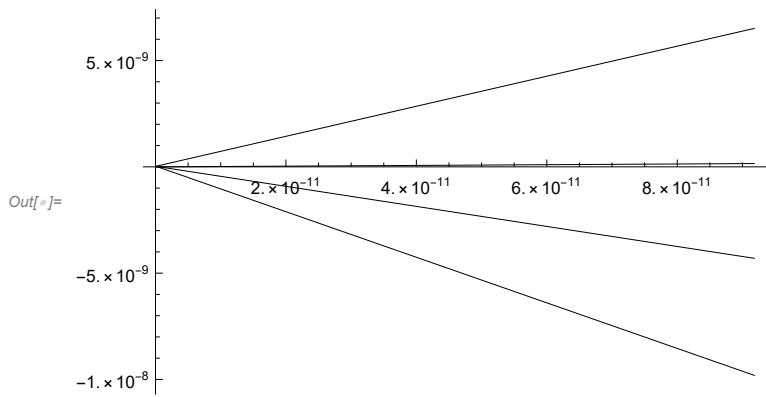
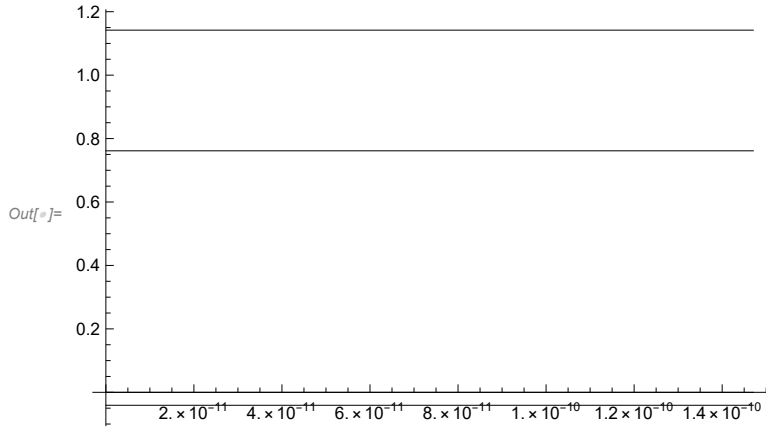




```

In[ ]:= Plot[{Im@α[2 000 000 000][1][x], Im@α[2 000 000 000][2][x], Im@α[2 000 000 000][3][x],
             Im@α[2 000 000 000][4][x]} /. ansSAWNL[[1]], {x, 0., .0001 lam}, PlotRange → All]
Plot[{Im@α[8 000 000 000][1][x], Im@α[8 000 000 000][2][x], Im@α[8 000 000 000][3][x],
      Im@α[8 000 000 000][4][x]} /. ansSAWNL[[1]], {x, 0., 3 lam}, PlotRange → All]
Plot[{Im@α[6 000 000 000][1][x], Im@α[6 000 000 000][2][x], Im@α[6 000 000 000][3][x],
      Im@α[6 000 000 000][4][x]} /. ansSAWNL[[1]], {x, 0., 3 lam}, PlotRange → All]

```



```

In[*]:= Export[{"stresses.png"}, Plot[{Evaluate[Re[torin[3986.5`90][[1]]],
    Evaluate[Re[torin[3986.5`90][[2]]], Evaluate[Re[torin[3986.5`90][[3]]],
    Evaluate[Re[torin[3986.5`90][[4]]], Evaluate[Re[torin[3986.5`90][[5]]]}],
{x1, 0, 3}, PlotRange -> All, PlotLegends -> {"T13", "T23", "T33", "T34", "T11"},
PlotLabel -> "Stress terms", AxesLabel -> {"nxλ", ""}]]

```

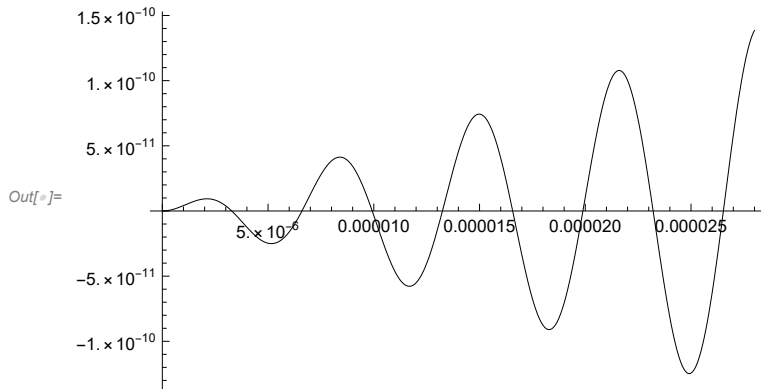
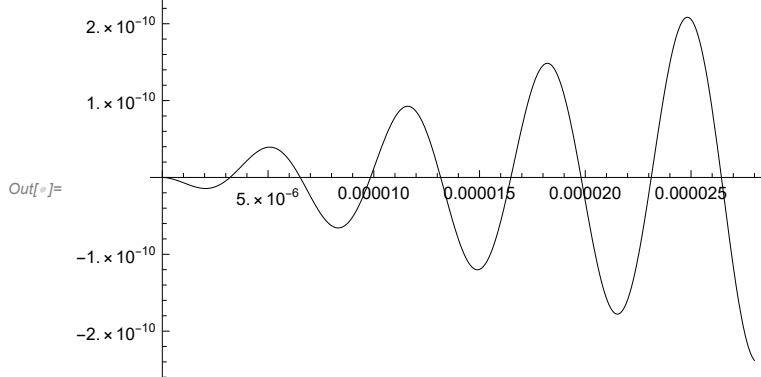
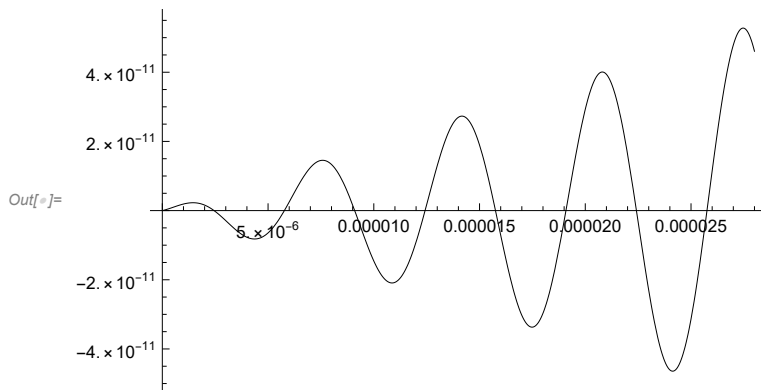
Out[\*]= {stresses.png}

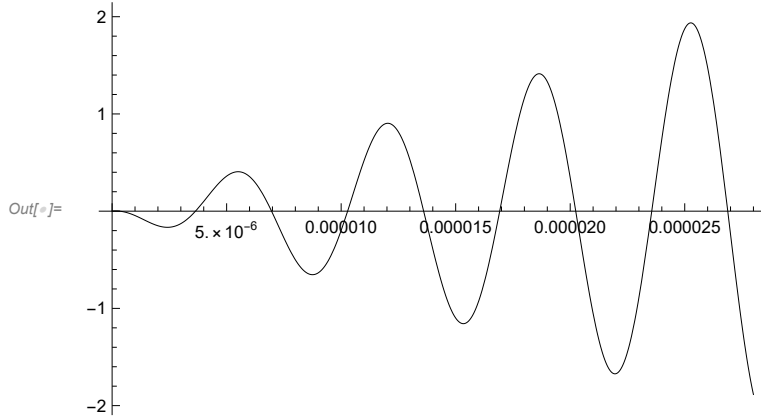
```

In[*]:= Export[{"stresses.png"}, Plot[Evaluate[Re[torin[3986.5`90][[5]]],
{x1, 0, 16 * 10^-6}, PlotRange -> All, PlotLegends -> {"T11"}, AxesLabel -> {"x1", ""}]]

```

Out[\*]= {stresses.png}

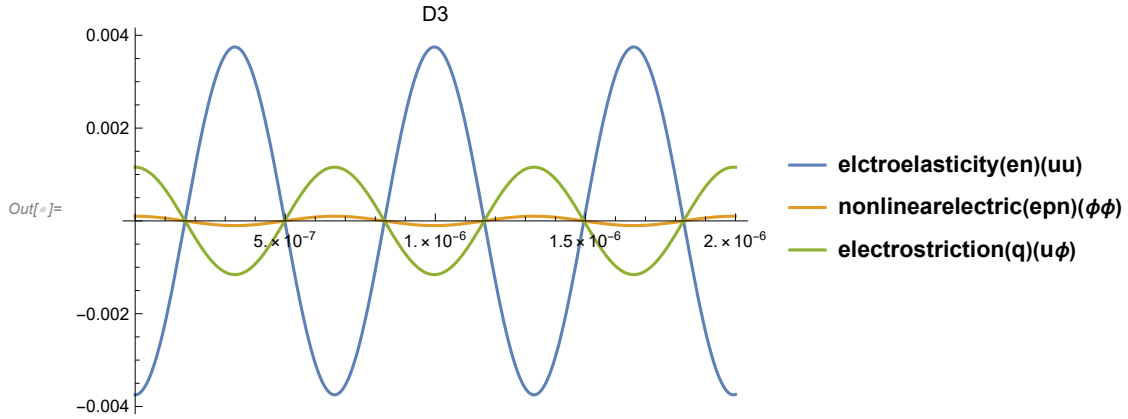




```

In[*]:= new = Plot[{Evaluate[Re[torin[3986.5`90][[1]]], Evaluate[Re[torin[3986.5`90][[2]]],
  Evaluate[Re[torin[3986.5`90][[3]]]}, {x1, 0, 0.000002},
  PlotLegends -> {"electroelasticity(en)(uu)", "nonlinearelectric(epn)(φφ)",
    "electrostriction(q)(uφ)", "e"}, PlotLabel -> "D3", PlotRange -> All]

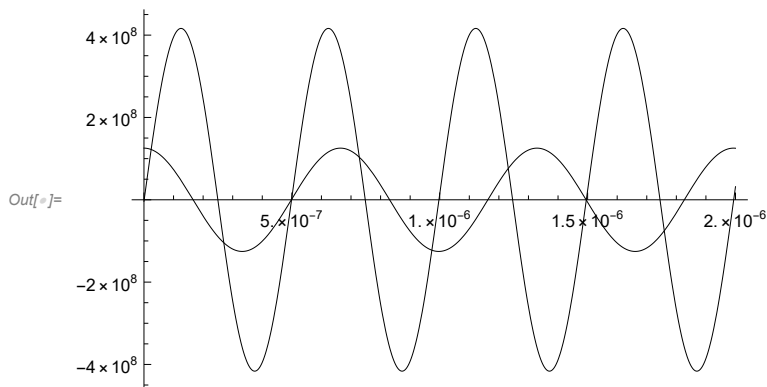
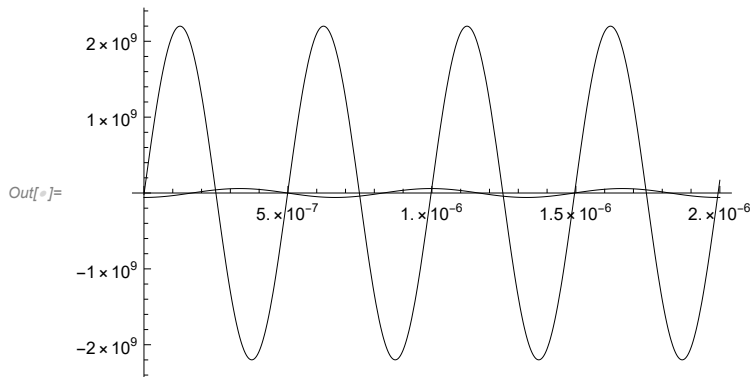
```

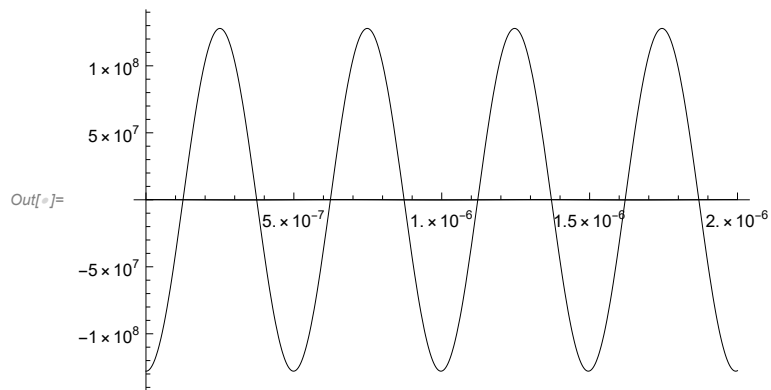
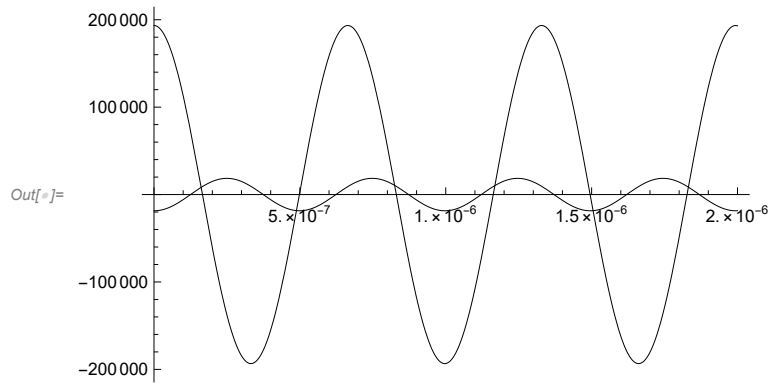
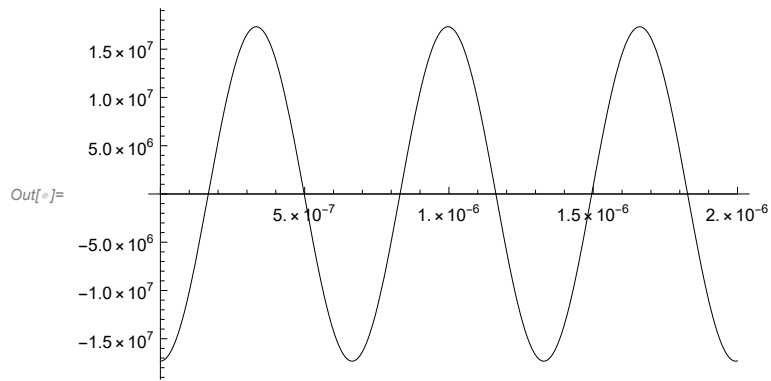
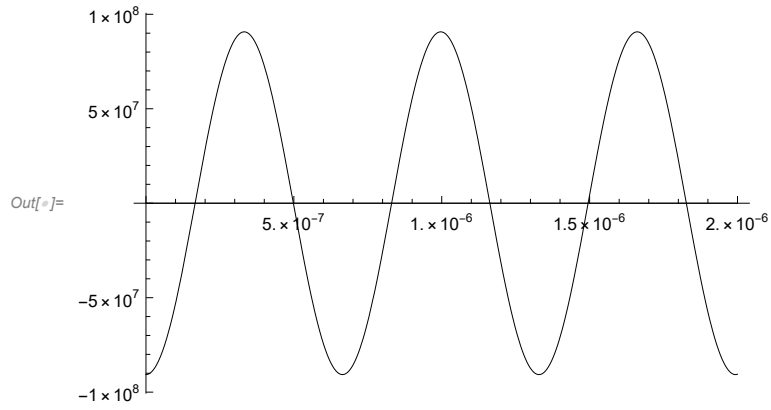


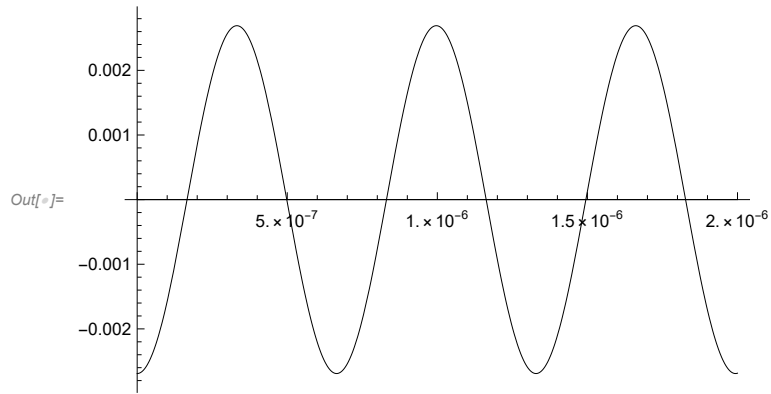
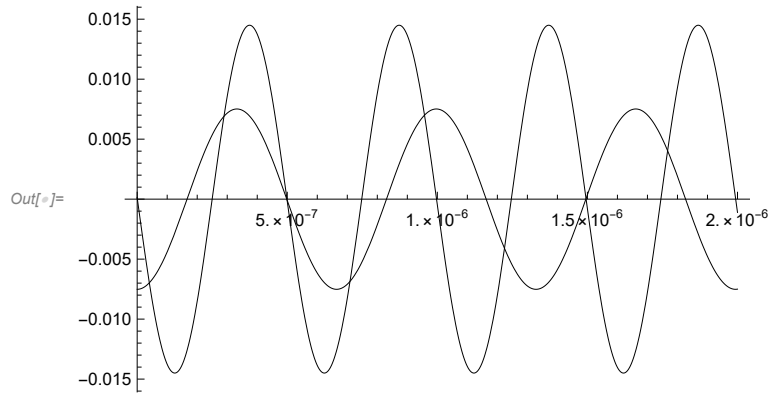
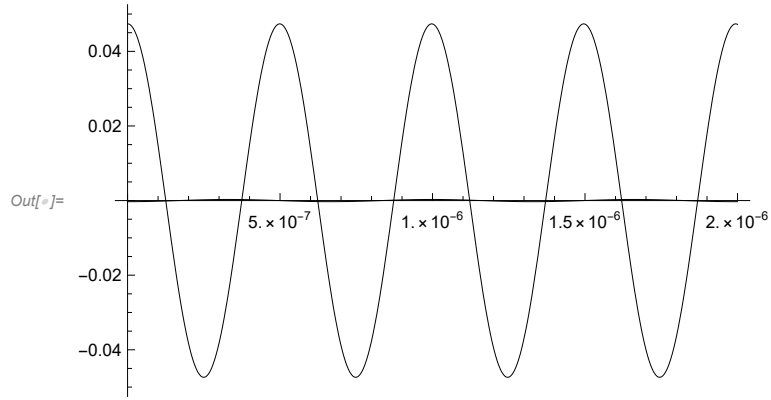
```

In[ ]:= li11 = Plot[{Evaluate[Re[torin[3986.5`90][[1]]],
  Evaluate[Re[torin[3986.5`90][[2]]]}], {x1, 0, 0.000002}]
li22 = Plot[{Evaluate[Re[torin[3986.5`90][[3]]],
  Evaluate[Re[torin[3986.5`90][[4]]]}], {x1, 0, 0.000002}]
li33 = Plot[{Evaluate[Re[torin[3986.5`90][[5]]],
  Evaluate[Re[torin[3986.5`90][[6]]]}], {x1, 0, 0.000002}]
li13 = Plot[{Evaluate[Re[torin[3986.5`90][[7]]],
  Evaluate[Re[torin[3986.5`90][[8]]]}], {x1, 0, 0.000002}]
li23 = Plot[{Evaluate[Re[torin[3986.5`90][[9]]],
  Evaluate[Re[torin[3986.5`90][[10]]]}], {x1, 0, 0.000002}]
li12 = Plot[{Evaluate[Re[torin[3986.5`90][[11]]],
  Evaluate[Re[torin[3986.5`90][[12]]]}], {x1, 0, 0.000002}]
li41 = Plot[{Evaluate[Re[torin[3986.5`90][[13]]],
  Evaluate[Re[torin[3986.5`90][[14]]]}], {x1, 0, 0.000002}]
li42 = Plot[{Evaluate[Re[torin[3986.5`90][[15]]],
  Evaluate[Re[torin[3986.5`90][[16]]]}], {x1, 0, 0.000002}]
li43 = Plot[{Evaluate[Re[torin[3986.5`90][[17]]],
  Evaluate[Re[torin[3986.5`90][[18]]]}], {x1, 0, 0.000002}]

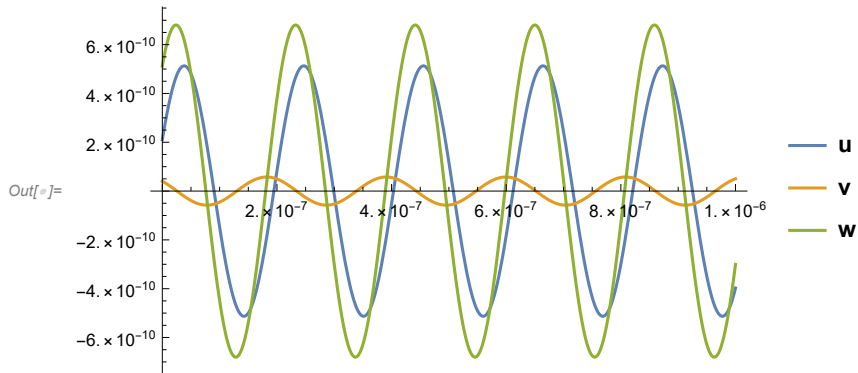
```



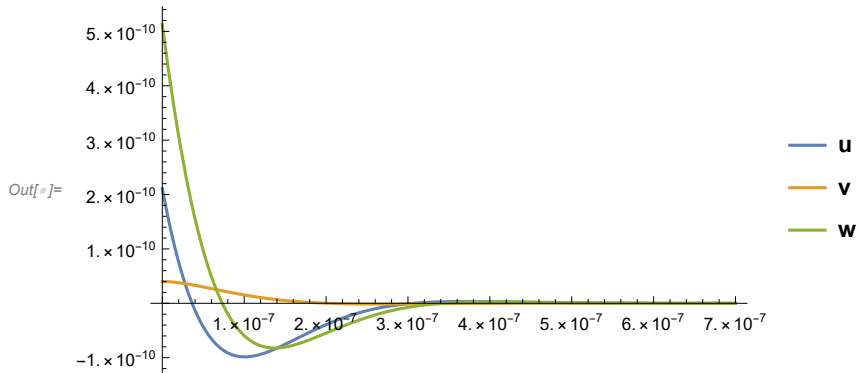




```
In[ ]:= Plot[{Evaluate[torin[3986`90][[1]], Evaluate[torin[3986`90][[2]],  
Evaluate[torin[3986`90][[3]]}], {X1, 0, 10-6}, PlotLegends -> {"u", "v", "w"}]
```



```
In[ ]:= Plot[{Evaluate[torin[3986`90][[4]],  
Evaluate[torin[3986`90][[5]], Evaluate[torin[3986`90][[6]]}],  
{X3, 0, 7 * 10-7}, PlotLegends -> {"u", "v", "w"}, PlotRange -> All]
```




---

### Comsol Code (COMSOL\_Code\_Generator.nb)

```
In[ ]:= Clear [tpump, tsig, tidler, tsum, tpumpdif, tpumpsum, tsigdif, tsigsum]
```



In[6]:=

```
tpumpdif[β_, k_] :=  
  Sum[c[β, k, γ, l, δ, n] × ur[γ, l] × us[δ, n], {γ, 4}, {l, 3}, {δ, 4}, {n, 3}] /.  
    {ur[1, 2] → 0, ur[2, 2] → 0, ur[3, 2] → 0, us[1, 2] → 0, us[2, 2] → 0, us[3, 2] →  
      0, ur[4, 2] → 0, us[4, 2] → 0} /. {ur[1, 1] → "d(u,x)", ur[1, 3] → "d(u,z)",  
      ur[2, 1] → "d(v,x)", ur[2, 3] → "d(v,z)", ur[3, 1] → "d(w,x)",  
      ur[3, 3] → "d(w,z)", ur[4, 1] → "d(V,x)", ur[4, 3] → "d(V,z)"} /.  
    {us[1, 1] → "d(u3,x)", us[1, 3] → "d(u3,z)", us[2, 1] → "d(v3,x)",  
      us[2, 3] → "d(v3,z)", us[3, 1] → "d(w3,x)", us[3, 3] → "d(w3,z)",  
      us[4, 1] → "d(V3,x)", us[4, 3] → "d(V3,z)"} /. rn1 /. r3[epn] /. r4NS[q] /.  
    r5[en] /. r6[c] //. matc6 //. matq6 //. mate4 //. mate6 //. mate6  
tpumpsum[β_, k_] :=  
  Sum[c[β, k, γ, l, δ, n] × ur[γ, l] × us[δ, n], {γ, 4}, {l, 3}, {δ, 4}, {n, 3}] /. {ur[1, 2] → 0,  
    ur[2, 2] → 0, ur[3, 2] → 0, us[1, 2] → 0, us[2, 2] → 0, us[3, 2] → 0, ur[4, 2] →  
      0, us[4, 2] → 0} /. {ur[1, 1] → "d(u4,x)", ur[1, 3] → "d(u4,z)",  
      ur[2, 1] → "d(v4,x)", ur[2, 3] → "d(v4,z)", ur[3, 1] → "d(w4,x)",  
      ur[3, 3] → "d(w4,z)", ur[4, 1] → "d(V4,x)", ur[4, 3] → "d(V4,z)"} /.  
    {us[1, 1] → "conj(d(u,x))", us[1, 3] → "conj(d(u,z))", us[2, 1] →  
      "conj(d(v,x))", us[2, 3] → "conj(d(v,z))", us[3, 1] → "conj(d(w,x))",  
      us[3, 3] → "conj(d(w,z))", us[4, 1] → "conj(d(V,x))",  
      us[4, 3] → "conj(d(V,z))"} /. rn1 /. r3[epn] /. r4NS[q] /.  
    r5[en] /. r6[c] //. matc6 //. matq6 //. mate4 //. mate6 //. mate6  
tpump[β_, k_] := tpumpsum[β, k] + tpumpdif[β, k]
```

In[7]:=

```
tsigdif[β_, k_] :=  
  Sum[c[β, k, γ, l, δ, n] × ur[γ, l] × us[δ, n], {γ, 4}, {l, 3}, {δ, 4}, {n, 3}] /. {ur[1, 2] → 0,  
    ur[2, 2] → 0, ur[3, 2] → 0, us[1, 2] → 0, us[2, 2] → 0, us[3, 2] → 0, ur[4, 2] →  
      0, us[4, 2] → 0} /. {ur[1, 1] → "d(u2,x)", ur[1, 3] → "d(u2,z)",  
      ur[2, 1] → "d(v2,x)", ur[2, 3] → "d(v2,z)", ur[3, 1] → "d(w2,x)",  
      ur[3, 3] → "d(w2,z)", ur[4, 1] → "d(V2,x)", ur[4, 3] → "d(V2,z)"} /.  
    {us[1, 1] → "conj(d(u3,x))", us[1, 3] → "conj(d(u3,z))", us[2, 1] →  
      "conj(d(v3,x))", us[2, 3] → "conj(d(v3,z))", us[3, 1] → "conj(d(w3,x))",  
      us[3, 3] → "conj(d(w3,z))", us[4, 1] → "conj(d(V3,x))",  
      us[4, 3] → "conj(d(V3,z))"} /. rn1 /. r3[epn] /. r4NS[q] /.  
    r5[en] /. r6[c] //. matc6 //. matq6 //. mate4 //. mate6 //. mate6  
tsigsum[β_, k_] :=  
  Sum[c[β, k, γ, l, δ, n] × ur[γ, l] × us[δ, n], {γ, 4}, {l, 3}, {δ, 4}, {n, 3}] /. {ur[1, 2] → 0,  
    ur[2, 2] → 0, ur[3, 2] → 0, us[1, 2] → 0, us[2, 2] → 0, us[3, 2] → 0, ur[4, 2] →  
      0, us[4, 2] → 0} /. {ur[1, 1] → "d(u4,x)", ur[1, 3] → "d(u4,z)",  
      ur[2, 1] → "d(v4,x)", ur[2, 3] → "d(v4,z)", ur[3, 1] → "d(w4,x)",  
      ur[3, 3] → "d(w4,z)", ur[4, 1] → "d(V4,x)", ur[4, 3] → "d(V4,z)"} /.  
    {us[1, 1] → "conj(d(u2,x))", us[1, 3] → "conj(d(u2,z))", us[2, 1] →  
      "conj(d(v2,x))", us[2, 3] → "conj(d(v2,z))", us[3, 1] → "conj(d(w2,x))",  
      us[3, 3] → "conj(d(w2,z))", us[4, 1] → "conj(d(V2,x))",  
      us[4, 3] → "conj(d(V2,z))"} /. rn1 /. r3[epn] /. r4NS[q] /.  
    r5[en] /. r6[c] //. matc6 //. matq6 //. mate4 //. mate6 //. mate6  
tsig[β_, k_] := tsigsum[β, k] + tsigdif[β, k]
```

```

In[*]:= tidler[β_, k_] :=
  Sum[c[β, k, γ, l, δ, n] × ur[γ, l] × us[δ, n], {γ, 4}, {l, 3}, {δ, 4}, {n, 3}] /. {ur[1, 2] → 0,
    ur[2, 2] → 0, ur[3, 2] → 0, us[1, 2] → 0, us[2, 2] → 0, us[3, 2] → 0, ur[4, 2] →
    0, us[4, 2] → 0} /. {ur[1, 1] → "d(u2,x)", ur[1, 3] → "d(u2,z)",
    ur[2, 1] → "d(v2,x)", ur[2, 3] → "d(v2,z)", ur[3, 1] → "d(w2,x)",
    ur[3, 3] → "d(w2,z)", ur[4, 1] → "d(V2,x)", ur[4, 3] → "d(V2,z)"} /.
  {us[1, 1] → "conj(d(u,x))", us[1, 3] → "conj(d(u,z))", us[2, 1] →
  "conj(d(v,x))", us[2, 3] → "conj(d(v,z))", us[3, 1] → "conj(d(w,x))",
  us[3, 3] → "conj(d(w,z))", us[4, 1] → "conj(d(V,x))",
  us[4, 3] → "conj(d(V,z))"} /. rn1 /. r3[epn] /. r4NS[q] /.
  r5[en] /. r6[c] //. matc6 //. matq6 //. mate4 //. mate6 //. mate6

```

```

In[*]:= tsum[β_, k_] :=
  Sum[c[β, k, γ, l, δ, n] × ur[γ, l] × us[δ, n], {γ, 4}, {l, 3}, {δ, 4}, {n, 3}] /. {ur[1, 2] → 0,
    ur[2, 2] → 0, ur[3, 2] → 0, us[1, 2] → 0, us[2, 2] → 0, us[3, 2] → 0, ur[4, 2] →
    0, us[4, 2] → 0} /. {ur[1, 1] → "d(u2,x)", ur[1, 3] → "d(u2,z)",
    ur[2, 1] → "d(v2,x)", ur[2, 3] → "d(v2,z)", ur[3, 1] → "d(w2,x)",
    ur[3, 3] → "d(w2,z)", ur[4, 1] → "d(V2,x)", ur[4, 3] → "d(V2,z)"} /.
  {us[1, 1] → "d(u,x)", us[1, 3] → "d(u,z)", us[2, 1] → "d(v,x)",
  us[2, 3] → "d(v,z)", us[3, 1] → "d(w,x)", us[3, 3] → "d(w,z)",
  us[4, 1] → "d(V,x)", us[4, 3] → "d(V,z)"} /. rn1 /. r3[epn] /. r4NS[q] /.
  r5[en] /. r6[c] //. matc6 //. matq6 //. mate4 //. mate6 //. mate6

```

```

In[*]:= tpumpdif[1, 1] // N
tpumpdif[1, 2] // N
tpumpdif[1, 3] // N
tpumpdif[2, 2] // N
tpumpdif[2, 3] // N
tpumpdif[3, 3] // N
tpumpdif[4, 1] // N
tpumpdif[4, 2] // N
tpumpdif[4, 3] // N

```

```

Out[*]:= 0. - 2.56 × 1011 d(u3,x) d(u,x) - 1.67483 × 1011 d(u3,z) d(u,z) -
  1.07724 × 1011 d(u,z) d(v3,x) + 16.3686 d(u,z) d(V3,x) + 1.68713 × 1010 d(u,x) d(v3,z) +
  27.7141 d(u,x) d(V3,z) - 1.07724 × 1011 d(u3,z) d(v,x) - 2.40017 × 1011 d(v3,x) d(v,x) +
  6.82416 d(V3,x) d(v,x) + 16.3686 d(u3,z) d(V,x) + 6.82416 d(v3,x) d(V,x) -
  5.55 × 10-10 d(V3,x) d(V,x) + 1.68713 × 1010 d(u3,x) d(v,z) - 1.31459 × 1011 d(v3,z) d(v,z) -
  12.4675 d(V3,z) d(v,z) + 27.7141 d(u3,x) d(V,z) - 12.4675 d(v3,z) d(V,z) +
  4.1025 × 10-10 d(V3,z) d(V,z) - 1.67483 × 1011 d(u,z) d(w3,x) - 1.07724 × 1011 d(v,x) d(w3,x) +
  16.3686 d(V,x) d(w3,x) + 5.10982 × 1011 d(u,x) d(w3,z) - 6.59622 × 1010 d(v,z) d(w3,z) +
  5.21447 d(V,z) d(w3,z) - 1.67483 × 1011 d(u3,z) d(w,x) - 1.07724 × 1011 d(v3,x) d(w,x) +
  16.3686 d(V3,x) d(w,x) - 1.67483 × 1011 d(w3,x) d(w,x) + 5.10982 × 1011 d(u3,x) d(w,z) -
  6.59622 × 1010 d(v3,z) d(w,z) + 5.21447 d(V3,z) d(w,z) + 1.55803 × 1011 d(w3,z) d(w,z)

```

$$\begin{aligned}
\text{Out}_{[u]=}^0 = & 0. - 1.07724 \times 10^{11} d(u_3, z) d(u, x) - 1.07724 \times 10^{11} d(u_3, x) d(u, z) - 2.40017 \times 10^{11} d(u, x) d(v_3, x) + \\
& 6.82416 d(u, x) d(V_3, x) - 8.4605 \times 10^{10} d(u, z) d(v_3, z) - 4.99538 d(u, z) d(V_3, z) - \\
& 2.40017 \times 10^{11} d(u_3, x) d(v, x) + 1.96051 \times 10^{10} d(v_3, z) d(v, x) + 10.554 d(V_3, z) d(v, x) + \\
& 6.82416 d(u_3, x) d(V, x) - 3.75564 d(v_3, z) d(V, x) + 1.65553 \times 10^{-10} d(V_3, z) d(V, x) - \\
& 8.4605 \times 10^{10} d(u_3, z) d(v, z) + 1.96051 \times 10^{10} d(v_3, x) d(v, z) - 3.75564 d(V_3, x) d(v, z) + \\
& 3.73297 d(V_3, z) d(v, z) - 4.99538 d(u_3, z) d(V, z) + 10.554 d(v_3, x) d(V, z) + \\
& 1.65553 \times 10^{-10} d(V_3, x) d(V, z) + 3.73297 d(v_3, z) d(V, z) - 1.07724 \times 10^{11} d(u, x) d(w_3, x) - \\
& 8.4605 \times 10^{10} d(v, z) d(w_3, x) - 4.99538 d(V, z) d(w_3, x) - 3.68926 \times 10^{10} d(u, z) d(w_3, z) - \\
& 2.96481 \times 10^{10} d(v, x) d(w_3, z) + 5.38946 d(V, x) d(w_3, z) - 2.91651 d(V, z) d(w_3, z) - \\
& 1.07724 \times 10^{11} d(u_3, x) d(w, x) - 8.4605 \times 10^{10} d(v_3, z) d(w, x) - 4.99538 d(V_3, z) d(w, x) - \\
& 3.68926 \times 10^{10} d(w_3, z) d(w, x) - 3.68926 \times 10^{10} d(u_3, z) d(w, z) - 2.96481 \times 10^{10} d(v_3, x) d(w, z) + \\
& 5.38946 d(V_3, x) d(w, z) - 2.91651 d(V_3, z) d(w, z) - 3.68926 \times 10^{10} d(w_3, x) d(w, z)
\end{aligned}$$

$$\begin{aligned}
\text{Out}_{[v]=}^0 = & 0. - 1.67483 \times 10^{11} d(u_3, z) d(u, x) - 1.67483 \times 10^{11} d(u_3, x) d(u, z) - 1.07724 \times 10^{11} d(u, x) d(v_3, x) + \\
& 16.3686 d(u, x) d(V_3, x) - 6.82725 \times 10^{10} d(u, z) d(v_3, z) - 11.5806 d(u, z) d(V_3, z) - \\
& 1.07724 \times 10^{11} d(u_3, x) d(v, x) - 8.4605 \times 10^{10} d(v_3, z) d(v, x) - 4.99538 d(V_3, z) d(v, x) + \\
& 16.3686 d(u_3, x) d(V, x) + 8.9817 d(v_3, z) d(V, x) + 5.93345 \times 10^{-10} d(V_3, z) d(V, x) - \\
& 6.82725 \times 10^{10} d(u_3, z) d(v, z) - 8.4605 \times 10^{10} d(v_3, x) d(v, z) + 8.9817 d(V_3, x) d(v, z) + \\
& 4.77798 d(V_3, z) d(v, z) - 11.5806 d(u_3, z) d(V, z) - 4.99538 d(v_3, x) d(V, z) + \\
& 5.93345 \times 10^{-10} d(V_3, x) d(V, z) + 4.77798 d(v_3, z) d(V, z) - 1.67483 \times 10^{11} d(u, x) d(w_3, x) - \\
& 6.82725 \times 10^{10} d(v, z) d(w_3, x) - 11.5806 d(V, z) d(w_3, x) - 2.3758 \times 10^{11} d(u, z) d(w_3, z) - \\
& 3.68926 \times 10^{10} d(v, x) d(w_3, z) - 4.18951 d(V, x) d(w_3, z) - 3.73297 d(V, z) d(w_3, z) - \\
& 1.67483 \times 10^{11} d(u_3, x) d(w, x) - 6.82725 \times 10^{10} d(v_3, z) d(w, x) - 11.5806 d(V_3, z) d(w, x) - \\
& 2.3758 \times 10^{11} d(w_3, z) d(w, x) - 2.3758 \times 10^{11} d(u_3, z) d(w, z) - 3.68926 \times 10^{10} d(v_3, x) d(w, z) - \\
& 4.18951 d(V_3, x) d(w, z) - 3.73297 d(V_3, z) d(w, z) - 2.3758 \times 10^{11} d(w_3, x) d(w, z)
\end{aligned}$$

$$\begin{aligned}
\text{Out}_{[w]=}^0 = & 0. + 8.00177 \times 10^{10} d(u_3, x) d(u, x) + 1.25188 \times 10^{11} d(u_3, z) d(u, z) - \\
& 7.1765 \times 10^{10} d(u, z) d(v_3, x) + 26.081 d(u, z) d(V_3, x) - 3.76345 \times 10^{10} d(u, x) d(v_3, z) + \\
& 4.04498 d(u, x) d(V_3, z) - 6.11553 d(u, z) d(V_3, z) - 7.1765 \times 10^{10} d(u_3, z) d(v, x) - \\
& 2.6921 \times 10^{11} d(v_3, x) d(v, x) + 30.7493 d(V_3, x) d(v, x) - 4.77798 d(V_3, z) d(v, x) + \\
& 26.081 d(u_3, z) d(V, x) + 30.7493 d(v_3, x) d(V, x) - 5.2025 \times 10^{-10} d(V_3, x) d(V, x) - \\
& 3.76345 \times 10^{10} d(u_3, x) d(v, z) - 1.23628 \times 10^{11} d(v_3, z) d(v, z) - 1.71448 d(V_3, z) d(v, z) + \\
& 4.04498 d(u_3, x) d(V, z) - 6.11553 d(u_3, z) d(V, z) - 4.77798 d(v_3, x) d(V, z) - \\
& 1.71448 d(v_3, z) d(V, z) - 1.45844 \times 10^{-9} d(V_3, z) d(V, z) + 1.25188 \times 10^{11} d(u, z) d(w_3, x) - \\
& 7.1765 \times 10^{10} d(v, x) d(w_3, x) + 26.081 d(V, x) d(w_3, x) - 6.11553 d(V, z) d(w_3, x) + \\
& 2.46541 \times 10^{11} d(u, x) d(w_3, z) - 2.93144 \times 10^{10} d(v, z) d(w_3, z) - 11.2685 d(V, z) d(w_3, z) + \\
& 1.25188 \times 10^{11} d(u_3, z) d(w, x) - 7.1765 \times 10^{10} d(v_3, x) d(w, x) + 26.081 d(V_3, x) d(w, x) - \\
& 6.11553 d(V_3, z) d(w, x) + 1.25188 \times 10^{11} d(w_3, x) d(w, x) + 2.46541 \times 10^{11} d(u_3, x) d(w, z) - \\
& 2.93144 \times 10^{10} d(v_3, z) d(w, z) - 11.2685 d(V_3, z) d(w, z) + 2.62661 \times 10^{11} d(w_3, z) d(w, z)
\end{aligned}$$

$$\begin{aligned}
\text{Out[=]} = & 0. + 1.68713 \times 10^{10} d(u3,x) d(u,x) - 6.82725 \times 10^{10} d(u3,z) d(u,z) - \\
& 8.4605 \times 10^{10} d(u,z) d(v3,x) + 8.9817 d(u,z) d(V3,x) - 1.31459 \times 10^{11} d(u,x) d(v3,z) - \\
& 12.4675 d(u,x) d(V3,z) + 4.77798 d(u,z) d(V3,z) - 8.4605 \times 10^{10} d(u3,z) d(v,x) + \\
& 1.96051 \times 10^{10} d(v3,x) d(v,x) - 3.75564 d(V3,x) d(v,x) + 3.73297 d(V3,z) d(v,x) + \\
& 8.9817 d(u3,z) d(V,x) - 3.75564 d(v3,x) d(V,x) - 1.25483 \times 10^{-9} d(V3,x) d(V,x) - \\
& 1.31459 \times 10^{11} d(u3,x) d(v,z) + 1.64758 \times 10^{11} d(v3,z) d(v,z) + 1.62595 d(V3,z) d(v,z) - \\
& 12.4675 d(u3,x) d(V,z) + 4.77798 d(u3,z) d(V,z) + 3.73297 d(v3,x) d(V,z) + \\
& 1.62595 d(v3,z) d(V,z) + 8.63797 \times 10^{-10} d(V3,z) d(V,z) - 6.82725 \times 10^{10} d(u,z) d(w3,x) - \\
& 8.4605 \times 10^{10} d(v,x) d(w3,x) + 8.9817 d(V,x) d(w3,x) + 4.77798 d(V,z) d(w3,x) - \\
& 6.59622 \times 10^{10} d(u,x) d(w3,z) - 1.25558 \times 10^{11} d(v,z) d(w3,z) - 10.2568 d(V,z) d(w3,z) - \\
& 6.82725 \times 10^{10} d(u3,z) d(w,x) - 8.4605 \times 10^{10} d(v3,x) d(w,x) + 8.9817 d(V3,x) d(w,x) + \\
& 4.77798 d(V3,z) d(w,x) - 6.82725 \times 10^{10} d(w3,x) d(w,x) - 6.59622 \times 10^{10} d(u3,x) d(w,z) - \\
& 1.25558 \times 10^{11} d(v3,z) d(w,z) - 10.2568 d(V3,z) d(w,z) + 1.2397 \times 10^{11} d(w3,z) d(w,z)
\end{aligned}$$

$$\begin{aligned}
\text{Out[=]} = & 0. + 5.10982 \times 10^{11} d(u3,x) d(u,x) - 2.3758 \times 10^{11} d(u3,z) d(u,z) - \\
& 3.68926 \times 10^{10} d(u,z) d(v3,x) - 4.18951 d(u,z) d(V3,x) - 6.59622 \times 10^{10} d(u,x) d(v3,z) + \\
& 5.21447 d(u,x) d(V3,z) - 3.73297 d(u,z) d(V3,z) - 3.68926 \times 10^{10} d(u3,z) d(v,x) - \\
& 2.96481 \times 10^{10} d(v3,x) d(v,x) + 5.38946 d(V3,x) d(v,x) - 2.91651 d(V3,z) d(v,x) - \\
& 4.18951 d(u3,z) d(V,x) + 5.38946 d(v3,x) d(V,x) + 4.1025 \times 10^{-10} d(V3,x) d(V,x) - \\
& 6.59622 \times 10^{10} d(u3,x) d(v,z) - 1.25558 \times 10^{11} d(v3,z) d(v,z) - 10.2568 d(V3,z) d(v,z) + \\
& 5.21447 d(u3,x) d(V,z) - 3.73297 d(u3,z) d(V,z) - 2.91651 d(v3,x) d(V,z) - \\
& 10.2568 d(v3,z) d(V,z) + 2.12426 \times 10^{-10} d(V3,z) d(V,z) - 2.3758 \times 10^{11} d(u,z) d(w3,x) - \\
& 3.68926 \times 10^{10} d(v,x) d(w3,x) - 4.18951 d(V,x) d(w3,x) - 3.73297 d(V,z) d(w3,x) + \\
& 1.55803 \times 10^{11} d(u,x) d(w3,z) + 1.2397 \times 10^{11} d(v,z) d(w3,z) + 22.9799 d(V,z) d(w3,z) - \\
& 2.3758 \times 10^{11} d(u3,z) d(w,x) - 3.68926 \times 10^{10} d(v3,x) d(w,x) - 4.18951 d(V3,x) d(w,x) - \\
& 3.73297 d(V3,z) d(w,x) - 2.3758 \times 10^{11} d(w3,x) d(w,x) + 1.55803 \times 10^{11} d(u3,x) d(w,z) + \\
& 1.2397 \times 10^{11} d(v3,z) d(w,z) + 22.9799 d(V3,z) d(w,z) - 8.05371 \times 10^{11} d(w3,z) d(w,z)
\end{aligned}$$

$$\begin{aligned}
\text{Out[=]} = & 0. + 16.3686 d(u3,z) d(u,x) + 16.3686 d(u3,x) d(u,z) + \\
& 6.82416 d(u,x) d(v3,x) - 5.55 \times 10^{-10} d(u,x) d(V3,x) + 8.9817 d(u,z) d(v3,z) + \\
& 5.93345 \times 10^{-10} d(u,z) d(V3,z) + 6.82416 d(u3,x) d(v,x) - 3.75564 d(v3,z) d(v,x) + \\
& 1.65553 \times 10^{-10} d(V3,z) d(v,x) - 5.55 \times 10^{-10} d(u3,x) d(V,x) - 1.405 \times 10^{-19} d(V3,x) d(V,x) - \\
& 1.25483 \times 10^{-9} d(v3,z) d(V,x) + 8.9817 d(u3,z) d(v,z) - 3.75564 d(v3,x) d(v,z) - \\
& 1.25483 \times 10^{-9} d(V3,x) d(v,z) + 5.93345 \times 10^{-10} d(u3,z) d(V,z) + \\
& 1.65553 \times 10^{-10} d(v3,x) d(V,z) + 16.3686 d(u,x) d(w3,x) + 8.9817 d(v,z) d(w3,x) + \\
& 5.93345 \times 10^{-10} d(V,z) d(w3,x) - 4.18951 d(u,z) d(w3,z) + 5.38946 d(v,x) d(w3,z) + \\
& 4.1025 \times 10^{-10} d(V,x) d(w3,z) + 16.3686 d(u3,x) d(w,x) + 8.9817 d(v3,z) d(w,x) + \\
& 5.93345 \times 10^{-10} d(V3,z) d(w,x) - 4.18951 d(w3,z) d(w,x) - 4.18951 d(u3,z) d(w,z) + \\
& 5.38946 d(v3,x) d(w,z) + 4.1025 \times 10^{-10} d(V3,x) d(w,z) - 4.18951 d(w3,x) d(w,z)
\end{aligned}$$

$$\begin{aligned}
\text{Out[*]} = & 0. - 11.5957 d(u3,x) d(u,x) - 12.2783 d(u3,z) d(u,z) + \\
& 2.00869 d(u,z) d(v3,x) + 1.65553 \times 10^{-10} d(u,z) d(V3,x) + 2.15588 d(u,x) d(v3,z) - \\
& 6.11553 d(u,z) d(v3,z) - 1.25483 \times 10^{-9} d(u,x) d(V3,z) + 2.00869 d(u3,z) d(v,x) - \\
& 1.59468 d(v3,x) d(v,x) - 1.39584 \times 10^{-9} d(V3,x) d(v,x) - 4.77798 d(v3,z) d(v,x) + \\
& 1.65553 \times 10^{-10} d(u3,z) d(V,x) - 1.39584 \times 10^{-9} d(v3,x) d(V,x) + \\
& 2.15588 d(u3,x) d(v,z) - 6.11553 d(u3,z) d(v,z) - 4.77798 d(v3,x) d(v,z) + \\
& 7.79531 d(v3,z) d(v,z) + 6.1656 \times 10^{-10} d(V3,z) d(v,z) - 1.25483 \times 10^{-9} d(u3,x) d(V,z) + \\
& 6.1656 \times 10^{-10} d(v3,z) d(V,z) - 3.50958 \times 10^{-19} d(V3,z) d(V,z) - 12.2783 d(u,z) d(w3,x) + \\
& 2.00869 d(v,x) d(w3,x) + 1.65553 \times 10^{-10} d(V,x) d(w3,x) - 6.11553 d(v,z) d(w3,x) - \\
& 26.0929 d(u,x) d(w3,z) + 4.77798 d(u,z) d(w3,z) + 3.73297 d(v,x) d(w3,z) - \\
& 3.98158 d(v,z) d(w3,z) + 8.63797 \times 10^{-10} d(V,z) d(w3,z) - 12.2783 d(u3,z) d(w,x) + \\
& 2.00869 d(v3,x) d(w,x) + 1.65553 \times 10^{-10} d(V3,x) d(w,x) - 6.11553 d(v3,z) d(w,x) - \\
& 12.2783 d(w3,x) d(w,x) + 4.77798 d(w3,z) d(w,x) - 26.0929 d(u3,x) d(w,z) + \\
& 4.77798 d(u3,z) d(w,z) + 3.73297 d(v3,x) d(w,z) - 3.98158 d(v3,z) d(w,z) + \\
& 8.63797 \times 10^{-10} d(V3,z) d(w,z) + 4.77798 d(w3,x) d(w,z) - 46.9193 d(w3,z) d(w,z)
\end{aligned}$$

$$\begin{aligned}
\text{Out[*]} = & 0. + 27.7141 d(u3,x) d(u,x) - 11.5806 d(u3,z) d(u,z) - \\
& 4.99538 d(u,z) d(v3,x) + 5.93345 \times 10^{-10} d(u,z) d(V3,x) - 12.4675 d(u,x) d(v3,z) + \\
& 4.77798 d(u,z) d(v3,z) + 4.1025 \times 10^{-10} d(u,x) d(V3,z) - 4.99538 d(u3,z) d(v,x) + \\
& 10.554 d(v3,x) d(v,x) + 1.65553 \times 10^{-10} d(V3,x) d(v,x) + 3.73297 d(v3,z) d(v,x) + \\
& 5.93345 \times 10^{-10} d(u3,z) d(V,x) + 1.65553 \times 10^{-10} d(v3,x) d(V,x) - \\
& 12.4675 d(u3,x) d(v,z) + 4.77798 d(u3,z) d(v,z) + 3.73297 d(v3,x) d(v,z) + \\
& 1.62595 d(v3,z) d(v,z) + 8.63797 \times 10^{-10} d(V3,z) d(v,z) + 4.1025 \times 10^{-10} d(u3,x) d(V,z) + \\
& 8.63797 \times 10^{-10} d(v3,z) d(V,z) + 1.59543 \times 10^{-19} d(V3,z) d(V,z) - 11.5806 d(u,z) d(w3,x) - \\
& 4.99538 d(v,x) d(w3,x) + 5.93345 \times 10^{-10} d(V,x) d(w3,x) + 4.77798 d(v,z) d(w3,x) + \\
& 5.21447 d(u,x) d(w3,z) - 3.73297 d(u,z) d(w3,z) - 2.91651 d(v,x) d(w3,z) - \\
& 10.2568 d(v,z) d(w3,z) + 2.12426 \times 10^{-10} d(V,z) d(w3,z) - 11.5806 d(u3,z) d(w,x) - \\
& 4.99538 d(v3,x) d(w,x) + 5.93345 \times 10^{-10} d(V3,x) d(w,x) + 4.77798 d(v3,z) d(w,x) - \\
& 11.5806 d(w3,x) d(w,x) - 3.73297 d(w3,z) d(w,x) + 5.21447 d(u3,x) d(w,z) - \\
& 3.73297 d(u3,z) d(w,z) - 2.91651 d(v3,x) d(w,z) - 10.2568 d(v3,z) d(w,z) + \\
& 2.12426 \times 10^{-10} d(V3,z) d(w,z) - 3.73297 d(w3,x) d(w,z) + 22.9799 d(w3,z) d(w,z)
\end{aligned}$$

```

In[*]= tsigdif[1, 1] // N
        tsigdif[1, 2] // N
        tsigdif[1, 3] // N
        tsigdif[2, 2] // N
        tsigdif[2, 3] // N
        tsigdif[3, 3] // N
        tsigdif[4, 1] // N
        tsigdif[4, 2] // N
        tsigdif[4, 3] // N

```

$$\begin{aligned}
\text{Out}[*]= & 0. - 2.56 \times 10^{11} \text{ conj}(d(u3, x)) d(u2, x) + 1.68713 \times 10^{10} \text{ conj}(d(v3, z)) d(u2, x) + \\
& 27.7141 \text{ conj}(d(V3, z)) d(u2, x) + 5.10982 \times 10^{11} \text{ conj}(d(w3, z)) d(u2, x) - \\
& 1.67483 \times 10^{11} \text{ conj}(d(u3, z)) d(u2, z) - 1.07724 \times 10^{11} \text{ conj}(d(v3, x)) d(u2, z) + \\
& 16.3686 \text{ conj}(d(V3, x)) d(u2, z) - 1.67483 \times 10^{11} \text{ conj}(d(w3, x)) d(u2, z) - \\
& 1.07724 \times 10^{11} \text{ conj}(d(u3, z)) d(v2, x) - 2.40017 \times 10^{11} \text{ conj}(d(v3, x)) d(v2, x) + \\
& 6.82416 \text{ conj}(d(V3, x)) d(v2, x) - 1.07724 \times 10^{11} \text{ conj}(d(w3, x)) d(v2, x) + \\
& 16.3686 \text{ conj}(d(u3, z)) d(V2, x) + 6.82416 \text{ conj}(d(v3, x)) d(V2, x) - \\
& 5.55 \times 10^{-10} \text{ conj}(d(V3, x)) d(V2, x) + 16.3686 \text{ conj}(d(w3, x)) d(V2, x) + \\
& 1.68713 \times 10^{10} \text{ conj}(d(u3, x)) d(v2, z) - 1.31459 \times 10^{11} \text{ conj}(d(v3, z)) d(v2, z) - \\
& 12.4675 \text{ conj}(d(V3, z)) d(v2, z) - 6.59622 \times 10^{10} \text{ conj}(d(w3, z)) d(v2, z) + \\
& 27.7141 \text{ conj}(d(u3, x)) d(V2, z) - 12.4675 \text{ conj}(d(v3, z)) d(V2, z) + \\
& 4.1025 \times 10^{-10} \text{ conj}(d(V3, z)) d(V2, z) + 5.21447 \text{ conj}(d(w3, z)) d(V2, z) - \\
& 1.67483 \times 10^{11} \text{ conj}(d(u3, z)) d(w2, x) - 1.07724 \times 10^{11} \text{ conj}(d(v3, x)) d(w2, x) + \\
& 16.3686 \text{ conj}(d(V3, x)) d(w2, x) - 1.67483 \times 10^{11} \text{ conj}(d(w3, x)) d(w2, x) + \\
& 5.10982 \times 10^{11} \text{ conj}(d(u3, x)) d(w2, z) - 6.59622 \times 10^{10} \text{ conj}(d(v3, z)) d(w2, z) + \\
& 5.21447 \text{ conj}(d(V3, z)) d(w2, z) + 1.55803 \times 10^{11} \text{ conj}(d(w3, z)) d(w2, z)
\end{aligned}$$

$$\begin{aligned}
\text{Out}[*]= & 0. - 1.07724 \times 10^{11} \text{ conj}(d(u3, z)) d(u2, x) - 2.40017 \times 10^{11} \text{ conj}(d(v3, x)) d(u2, x) + \\
& 6.82416 \text{ conj}(d(V3, x)) d(u2, x) - 1.07724 \times 10^{11} \text{ conj}(d(w3, x)) d(u2, x) - \\
& 1.07724 \times 10^{11} \text{ conj}(d(u3, x)) d(u2, z) - 8.4605 \times 10^{10} \text{ conj}(d(v3, z)) d(u2, z) - \\
& 4.99538 \text{ conj}(d(V3, z)) d(u2, z) - 3.68926 \times 10^{10} \text{ conj}(d(w3, z)) d(u2, z) - \\
& 2.40017 \times 10^{11} \text{ conj}(d(u3, x)) d(v2, x) + 1.96051 \times 10^{10} \text{ conj}(d(v3, z)) d(v2, x) + \\
& 10.554 \text{ conj}(d(V3, z)) d(v2, x) - 2.96481 \times 10^{10} \text{ conj}(d(w3, z)) d(v2, x) + \\
& 6.82416 \text{ conj}(d(u3, x)) d(V2, x) - 3.75564 \text{ conj}(d(v3, z)) d(V2, x) + \\
& 1.65553 \times 10^{-10} \text{ conj}(d(V3, z)) d(V2, x) + 5.38946 \text{ conj}(d(w3, z)) d(V2, x) - \\
& 8.4605 \times 10^{10} \text{ conj}(d(u3, z)) d(v2, z) + 1.96051 \times 10^{10} \text{ conj}(d(v3, x)) d(v2, z) - \\
& 3.75564 \text{ conj}(d(V3, x)) d(v2, z) + 3.73297 \text{ conj}(d(V3, z)) d(v2, z) - \\
& 8.4605 \times 10^{10} \text{ conj}(d(w3, x)) d(v2, z) - 4.99538 \text{ conj}(d(u3, z)) d(V2, z) + \\
& 10.554 \text{ conj}(d(v3, x)) d(V2, z) + 1.65553 \times 10^{-10} \text{ conj}(d(V3, x)) d(V2, z) + \\
& 3.73297 \text{ conj}(d(v3, z)) d(V2, z) - 4.99538 \text{ conj}(d(w3, x)) d(V2, z) - \\
& 2.91651 \text{ conj}(d(w3, z)) d(V2, z) - 1.07724 \times 10^{11} \text{ conj}(d(u3, x)) d(w2, x) - \\
& 8.4605 \times 10^{10} \text{ conj}(d(v3, z)) d(w2, x) - 4.99538 \text{ conj}(d(V3, z)) d(w2, x) - \\
& 3.68926 \times 10^{10} \text{ conj}(d(w3, z)) d(w2, x) - 3.68926 \times 10^{10} \text{ conj}(d(u3, z)) d(w2, z) - \\
& 2.96481 \times 10^{10} \text{ conj}(d(v3, x)) d(w2, z) + 5.38946 \text{ conj}(d(V3, x)) d(w2, z) - \\
& 2.91651 \text{ conj}(d(V3, z)) d(w2, z) - 3.68926 \times 10^{10} \text{ conj}(d(w3, x)) d(w2, z)
\end{aligned}$$

$$\begin{aligned}
\text{Out}_{[=]}^j = & 0. - 1.67483 \times 10^{11} \text{ conj}(d(u3, z)) d(u2, x) - 1.07724 \times 10^{11} \text{ conj}(d(v3, x)) d(u2, x) + \\
& 16.3686 \text{ conj}(d(V3, x)) d(u2, x) - 1.67483 \times 10^{11} \text{ conj}(d(w3, x)) d(u2, x) - \\
& 1.67483 \times 10^{11} \text{ conj}(d(u3, x)) d(u2, z) - 6.82725 \times 10^{10} \text{ conj}(d(v3, z)) d(u2, z) - \\
& 11.5806 \text{ conj}(d(V3, z)) d(u2, z) - 2.3758 \times 10^{11} \text{ conj}(d(w3, z)) d(u2, z) - \\
& 1.07724 \times 10^{11} \text{ conj}(d(u3, x)) d(v2, x) - 8.4605 \times 10^{10} \text{ conj}(d(v3, z)) d(v2, x) - \\
& 4.99538 \text{ conj}(d(V3, z)) d(v2, x) - 3.68926 \times 10^{10} \text{ conj}(d(w3, z)) d(v2, x) + \\
& 16.3686 \text{ conj}(d(u3, x)) d(V2, x) + 8.9817 \text{ conj}(d(v3, z)) d(V2, x) + \\
& 5.93345 \times 10^{-10} \text{ conj}(d(V3, z)) d(V2, x) - 4.18951 \text{ conj}(d(w3, z)) d(V2, x) - \\
& 6.82725 \times 10^{10} \text{ conj}(d(u3, z)) d(v2, z) - 8.4605 \times 10^{10} \text{ conj}(d(v3, x)) d(v2, z) + \\
& 8.9817 \text{ conj}(d(V3, x)) d(v2, z) + 4.77798 \text{ conj}(d(V3, z)) d(v2, z) - \\
& 6.82725 \times 10^{10} \text{ conj}(d(w3, x)) d(v2, z) - 11.5806 \text{ conj}(d(u3, z)) d(V2, z) - \\
& 4.99538 \text{ conj}(d(v3, x)) d(V2, z) + 5.93345 \times 10^{-10} \text{ conj}(d(V3, x)) d(V2, z) + \\
& 4.77798 \text{ conj}(d(v3, z)) d(V2, z) - 11.5806 \text{ conj}(d(w3, x)) d(V2, z) - \\
& 3.73297 \text{ conj}(d(w3, z)) d(V2, z) - 1.67483 \times 10^{11} \text{ conj}(d(u3, x)) d(w2, x) - \\
& 6.82725 \times 10^{10} \text{ conj}(d(v3, z)) d(w2, x) - 11.5806 \text{ conj}(d(V3, z)) d(w2, x) - \\
& 2.3758 \times 10^{11} \text{ conj}(d(w3, z)) d(w2, x) - 2.3758 \times 10^{11} \text{ conj}(d(u3, z)) d(w2, z) - \\
& 3.68926 \times 10^{10} \text{ conj}(d(v3, x)) d(w2, z) - 4.18951 \text{ conj}(d(V3, x)) d(w2, z) - \\
& 3.73297 \text{ conj}(d(V3, z)) d(w2, z) - 2.3758 \times 10^{11} \text{ conj}(d(w3, x)) d(w2, z)
\end{aligned}$$

$$\begin{aligned}
\text{Out}_{[=]}^j = & 0. + 8.00177 \times 10^{10} \text{ conj}(d(u3, x)) d(u2, x) - 3.76345 \times 10^{10} \text{ conj}(d(v3, z)) d(u2, x) + \\
& 4.04498 \text{ conj}(d(V3, z)) d(u2, x) + 2.46541 \times 10^{11} \text{ conj}(d(w3, z)) d(u2, x) + \\
& 1.25188 \times 10^{11} \text{ conj}(d(u3, z)) d(u2, z) - 7.1765 \times 10^{10} \text{ conj}(d(v3, x)) d(u2, z) + \\
& 26.081 \text{ conj}(d(V3, x)) d(u2, z) - 6.11553 \text{ conj}(d(V3, z)) d(u2, z) + \\
& 1.25188 \times 10^{11} \text{ conj}(d(w3, x)) d(u2, z) - 7.1765 \times 10^{10} \text{ conj}(d(u3, z)) d(v2, x) - \\
& 2.6921 \times 10^{11} \text{ conj}(d(v3, x)) d(v2, x) + 30.7493 \text{ conj}(d(V3, x)) d(v2, x) - \\
& 4.77798 \text{ conj}(d(V3, z)) d(v2, x) - 7.1765 \times 10^{10} \text{ conj}(d(w3, x)) d(v2, x) + \\
& 26.081 \text{ conj}(d(u3, z)) d(V2, x) + 30.7493 \text{ conj}(d(v3, x)) d(V2, x) - \\
& 5.2025 \times 10^{-10} \text{ conj}(d(V3, x)) d(V2, x) + 26.081 \text{ conj}(d(w3, x)) d(V2, x) - \\
& 3.76345 \times 10^{10} \text{ conj}(d(u3, x)) d(v2, z) - 1.23628 \times 10^{11} \text{ conj}(d(v3, z)) d(v2, z) - \\
& 1.71448 \text{ conj}(d(V3, z)) d(v2, z) - 2.93144 \times 10^{10} \text{ conj}(d(w3, z)) d(v2, z) + \\
& 4.04498 \text{ conj}(d(u3, x)) d(V2, z) - 6.11553 \text{ conj}(d(u3, z)) d(V2, z) - \\
& 4.77798 \text{ conj}(d(v3, x)) d(V2, z) - 1.71448 \text{ conj}(d(v3, z)) d(V2, z) - \\
& 1.45844 \times 10^{-9} \text{ conj}(d(V3, z)) d(V2, z) - 6.11553 \text{ conj}(d(w3, x)) d(V2, z) - \\
& 11.2685 \text{ conj}(d(w3, z)) d(V2, z) + 1.25188 \times 10^{11} \text{ conj}(d(u3, z)) d(w2, x) - \\
& 7.1765 \times 10^{10} \text{ conj}(d(v3, x)) d(w2, x) + 26.081 \text{ conj}(d(V3, x)) d(w2, x) - \\
& 6.11553 \text{ conj}(d(V3, z)) d(w2, x) + 1.25188 \times 10^{11} \text{ conj}(d(w3, x)) d(w2, x) + \\
& 2.46541 \times 10^{11} \text{ conj}(d(u3, x)) d(w2, z) - 2.93144 \times 10^{10} \text{ conj}(d(v3, z)) d(w2, z) - \\
& 11.2685 \text{ conj}(d(V3, z)) d(w2, z) + 2.62661 \times 10^{11} \text{ conj}(d(w3, z)) d(w2, z)
\end{aligned}$$

$$\begin{aligned}
\text{Out}_{[n]} = & 0. + 1.68713 \times 10^{10} \text{ conj}(d(u3,x)) d(u2,x) - 1.31459 \times 10^{11} \text{ conj}(d(v3,z)) d(u2,x) - \\
& 12.4675 \text{ conj}(d(V3,z)) d(u2,x) - 6.59622 \times 10^{10} \text{ conj}(d(w3,z)) d(u2,x) - \\
& 6.82725 \times 10^{10} \text{ conj}(d(u3,z)) d(u2,z) - 8.4605 \times 10^{10} \text{ conj}(d(v3,x)) d(u2,z) + \\
& 8.9817 \text{ conj}(d(V3,x)) d(u2,z) + 4.77798 \text{ conj}(d(V3,z)) d(u2,z) - \\
& 6.82725 \times 10^{10} \text{ conj}(d(w3,x)) d(u2,z) - 8.4605 \times 10^{10} \text{ conj}(d(u3,z)) d(v2,x) + \\
& 1.96051 \times 10^{10} \text{ conj}(d(v3,x)) d(v2,x) - 3.75564 \text{ conj}(d(V3,x)) d(v2,x) + \\
& 3.73297 \text{ conj}(d(V3,z)) d(v2,x) - 8.4605 \times 10^{10} \text{ conj}(d(w3,x)) d(v2,x) + \\
& 8.9817 \text{ conj}(d(u3,z)) d(V2,x) - 3.75564 \text{ conj}(d(v3,x)) d(V2,x) - \\
& 1.25483 \times 10^{-9} \text{ conj}(d(V3,x)) d(V2,x) + 8.9817 \text{ conj}(d(w3,x)) d(V2,x) - \\
& 1.31459 \times 10^{11} \text{ conj}(d(u3,x)) d(v2,z) + 1.64758 \times 10^{11} \text{ conj}(d(v3,z)) d(v2,z) + \\
& 1.62595 \text{ conj}(d(V3,z)) d(v2,z) - 1.25558 \times 10^{11} \text{ conj}(d(w3,z)) d(v2,z) - \\
& 12.4675 \text{ conj}(d(u3,x)) d(V2,z) + 4.77798 \text{ conj}(d(u3,z)) d(V2,z) + \\
& 3.73297 \text{ conj}(d(v3,x)) d(V2,z) + 1.62595 \text{ conj}(d(v3,z)) d(V2,z) + \\
& 8.63797 \times 10^{-10} \text{ conj}(d(V3,z)) d(V2,z) + 4.77798 \text{ conj}(d(w3,x)) d(V2,z) - \\
& 10.2568 \text{ conj}(d(w3,z)) d(V2,z) - 6.82725 \times 10^{10} \text{ conj}(d(u3,z)) d(w2,x) - \\
& 8.4605 \times 10^{10} \text{ conj}(d(v3,x)) d(w2,x) + 8.9817 \text{ conj}(d(V3,x)) d(w2,x) + \\
& 4.77798 \text{ conj}(d(V3,z)) d(w2,x) - 6.82725 \times 10^{10} \text{ conj}(d(w3,x)) d(w2,x) - \\
& 6.59622 \times 10^{10} \text{ conj}(d(u3,x)) d(w2,z) - 1.25558 \times 10^{11} \text{ conj}(d(v3,z)) d(w2,z) - \\
& 10.2568 \text{ conj}(d(V3,z)) d(w2,z) + 1.2397 \times 10^{11} \text{ conj}(d(w3,z)) d(w2,z)
\end{aligned}$$

$$\begin{aligned}
\text{Out}_{[n]} = & 0. + 5.10982 \times 10^{11} \text{ conj}(d(u3,x)) d(u2,x) - 6.59622 \times 10^{10} \text{ conj}(d(v3,z)) d(u2,x) + \\
& 5.21447 \text{ conj}(d(V3,z)) d(u2,x) + 1.55803 \times 10^{11} \text{ conj}(d(w3,z)) d(u2,x) - \\
& 2.3758 \times 10^{11} \text{ conj}(d(u3,z)) d(u2,z) - 3.68926 \times 10^{10} \text{ conj}(d(v3,x)) d(u2,z) - \\
& 4.18951 \text{ conj}(d(V3,x)) d(u2,z) - 3.73297 \text{ conj}(d(V3,z)) d(u2,z) - \\
& 2.3758 \times 10^{11} \text{ conj}(d(w3,x)) d(u2,z) - 3.68926 \times 10^{10} \text{ conj}(d(u3,z)) d(v2,x) - \\
& 2.96481 \times 10^{10} \text{ conj}(d(v3,x)) d(v2,x) + 5.38946 \text{ conj}(d(V3,x)) d(v2,x) - \\
& 2.91651 \text{ conj}(d(V3,z)) d(v2,x) - 3.68926 \times 10^{10} \text{ conj}(d(w3,x)) d(v2,x) - \\
& 4.18951 \text{ conj}(d(u3,z)) d(V2,x) + 5.38946 \text{ conj}(d(v3,x)) d(V2,x) + \\
& 4.1025 \times 10^{-10} \text{ conj}(d(V3,x)) d(V2,x) - 4.18951 \text{ conj}(d(w3,x)) d(V2,x) - \\
& 6.59622 \times 10^{10} \text{ conj}(d(u3,x)) d(v2,z) - 1.25558 \times 10^{11} \text{ conj}(d(v3,z)) d(v2,z) - \\
& 10.2568 \text{ conj}(d(V3,z)) d(v2,z) + 1.2397 \times 10^{11} \text{ conj}(d(w3,z)) d(v2,z) + \\
& 5.21447 \text{ conj}(d(u3,x)) d(V2,z) - 3.73297 \text{ conj}(d(u3,z)) d(V2,z) - \\
& 2.91651 \text{ conj}(d(v3,x)) d(V2,z) - 10.2568 \text{ conj}(d(v3,z)) d(V2,z) + \\
& 2.12426 \times 10^{-10} \text{ conj}(d(V3,z)) d(V2,z) - 3.73297 \text{ conj}(d(w3,x)) d(V2,z) + \\
& 22.9799 \text{ conj}(d(w3,z)) d(V2,z) - 2.3758 \times 10^{11} \text{ conj}(d(u3,z)) d(w2,x) - \\
& 3.68926 \times 10^{10} \text{ conj}(d(v3,x)) d(w2,x) - 4.18951 \text{ conj}(d(V3,x)) d(w2,x) - \\
& 3.73297 \text{ conj}(d(V3,z)) d(w2,x) - 2.3758 \times 10^{11} \text{ conj}(d(w3,x)) d(w2,x) + \\
& 1.55803 \times 10^{11} \text{ conj}(d(u3,x)) d(w2,z) + 1.2397 \times 10^{11} \text{ conj}(d(v3,z)) d(w2,z) + \\
& 22.9799 \text{ conj}(d(V3,z)) d(w2,z) - 8.05371 \times 10^{11} \text{ conj}(d(w3,z)) d(w2,z)
\end{aligned}$$



$$\begin{aligned}
\text{Out}[*]= & 0. + 16.3686 \operatorname{conj}(d(u3, z)) d(u2, x) + \\
& 6.82416 \operatorname{conj}(d(v3, x)) d(u2, x) - 5.55 \times 10^{-10} \operatorname{conj}(d(V3, x)) d(u2, x) + \\
& 16.3686 \operatorname{conj}(d(w3, x)) d(u2, x) + 16.3686 \operatorname{conj}(d(u3, x)) d(u2, z) + \\
& 8.9817 \operatorname{conj}(d(v3, z)) d(u2, z) + 5.93345 \times 10^{-10} \operatorname{conj}(d(V3, z)) d(u2, z) - \\
& 4.18951 \operatorname{conj}(d(w3, z)) d(u2, z) + 6.82416 \operatorname{conj}(d(u3, x)) d(v2, x) - \\
& 3.75564 \operatorname{conj}(d(v3, z)) d(v2, x) + 1.65553 \times 10^{-10} \operatorname{conj}(d(V3, z)) d(v2, x) + \\
& 5.38946 \operatorname{conj}(d(w3, z)) d(v2, x) - 5.55 \times 10^{-10} \operatorname{conj}(d(u3, x)) d(V2, x) - \\
& 1.405 \times 10^{-19} \operatorname{conj}(d(V3, x)) d(V2, x) - 1.25483 \times 10^{-9} \operatorname{conj}(d(v3, z)) d(V2, x) + \\
& 4.1025 \times 10^{-10} \operatorname{conj}(d(w3, z)) d(V2, x) + 8.9817 \operatorname{conj}(d(u3, z)) d(v2, z) - \\
& 3.75564 \operatorname{conj}(d(v3, x)) d(v2, z) - 1.25483 \times 10^{-9} \operatorname{conj}(d(V3, x)) d(v2, z) + \\
& 8.9817 \operatorname{conj}(d(w3, x)) d(v2, z) + 5.93345 \times 10^{-10} \operatorname{conj}(d(u3, z)) d(V2, z) + \\
& 1.65553 \times 10^{-10} \operatorname{conj}(d(v3, x)) d(V2, z) + 5.93345 \times 10^{-10} \operatorname{conj}(d(w3, x)) d(V2, z) + \\
& 16.3686 \operatorname{conj}(d(u3, x)) d(w2, x) + 8.9817 \operatorname{conj}(d(v3, z)) d(w2, x) + \\
& 5.93345 \times 10^{-10} \operatorname{conj}(d(V3, z)) d(w2, x) - 4.18951 \operatorname{conj}(d(w3, z)) d(w2, x) - \\
& 4.18951 \operatorname{conj}(d(u3, z)) d(w2, z) + 5.38946 \operatorname{conj}(d(v3, x)) d(w2, z) + \\
& 4.1025 \times 10^{-10} \operatorname{conj}(d(V3, x)) d(w2, z) - 4.18951 \operatorname{conj}(d(w3, x)) d(w2, z)
\end{aligned}$$

$$\begin{aligned}
\text{Out}[*]= & 0. - 11.5957 \operatorname{conj}(d(u3, x)) d(u2, x) + \\
& 2.15588 \operatorname{conj}(d(v3, z)) d(u2, x) - 1.25483 \times 10^{-9} \operatorname{conj}(d(V3, z)) d(u2, x) - \\
& 26.0929 \operatorname{conj}(d(w3, z)) d(u2, x) - 12.2783 \operatorname{conj}(d(u3, z)) d(u2, z) + \\
& 2.00869 \operatorname{conj}(d(v3, x)) d(u2, z) + 1.65553 \times 10^{-10} \operatorname{conj}(d(V3, x)) d(u2, z) - \\
& 6.11553 \operatorname{conj}(d(v3, z)) d(u2, z) - 12.2783 \operatorname{conj}(d(w3, x)) d(u2, z) + \\
& 4.77798 \operatorname{conj}(d(w3, z)) d(u2, z) + 2.00869 \operatorname{conj}(d(u3, z)) d(v2, x) - \\
& 1.59468 \operatorname{conj}(d(v3, x)) d(v2, x) - 1.39584 \times 10^{-9} \operatorname{conj}(d(V3, x)) d(v2, x) - \\
& 4.77798 \operatorname{conj}(d(v3, z)) d(v2, x) + 2.00869 \operatorname{conj}(d(w3, x)) d(v2, x) + \\
& 3.73297 \operatorname{conj}(d(w3, z)) d(v2, x) + 1.65553 \times 10^{-10} \operatorname{conj}(d(u3, z)) d(V2, x) - \\
& 1.39584 \times 10^{-9} \operatorname{conj}(d(v3, x)) d(V2, x) + 1.65553 \times 10^{-10} \operatorname{conj}(d(w3, x)) d(V2, x) + \\
& 2.15588 \operatorname{conj}(d(u3, x)) d(v2, z) - 6.11553 \operatorname{conj}(d(u3, z)) d(v2, z) - \\
& 4.77798 \operatorname{conj}(d(v3, x)) d(v2, z) + 7.79531 \operatorname{conj}(d(v3, z)) d(v2, z) + \\
& 6.1656 \times 10^{-10} \operatorname{conj}(d(V3, z)) d(v2, z) - 6.11553 \operatorname{conj}(d(w3, x)) d(v2, z) - \\
& 3.98158 \operatorname{conj}(d(w3, z)) d(v2, z) - 1.25483 \times 10^{-9} \operatorname{conj}(d(u3, x)) d(V2, z) + \\
& 6.1656 \times 10^{-10} \operatorname{conj}(d(v3, z)) d(V2, z) - 3.50958 \times 10^{-19} \operatorname{conj}(d(V3, z)) d(V2, z) + \\
& 8.63797 \times 10^{-10} \operatorname{conj}(d(w3, z)) d(V2, z) - 12.2783 \operatorname{conj}(d(u3, z)) d(w2, x) + \\
& 2.00869 \operatorname{conj}(d(v3, x)) d(w2, x) + 1.65553 \times 10^{-10} \operatorname{conj}(d(V3, x)) d(w2, x) - \\
& 6.11553 \operatorname{conj}(d(v3, z)) d(w2, x) - 12.2783 \operatorname{conj}(d(w3, x)) d(w2, x) + \\
& 4.77798 \operatorname{conj}(d(w3, z)) d(w2, x) - 26.0929 \operatorname{conj}(d(u3, x)) d(w2, z) + \\
& 4.77798 \operatorname{conj}(d(u3, z)) d(w2, z) + 3.73297 \operatorname{conj}(d(v3, x)) d(w2, z) - \\
& 3.98158 \operatorname{conj}(d(v3, z)) d(w2, z) + 8.63797 \times 10^{-10} \operatorname{conj}(d(V3, z)) d(w2, z) + \\
& 4.77798 \operatorname{conj}(d(w3, x)) d(w2, z) - 46.9193 \operatorname{conj}(d(w3, z)) d(w2, z)
\end{aligned}$$

$Out[ ] = 0. + 27.7141 \operatorname{conj}(d(u3, x)) d(u2, x) -$   
 $12.4675 \operatorname{conj}(d(v3, z)) d(u2, x) + 4.1025 \times 10^{-10} \operatorname{conj}(d(V3, z)) d(u2, x) +$   
 $5.21447 \operatorname{conj}(d(w3, z)) d(u2, x) - 11.5806 \operatorname{conj}(d(u3, z)) d(u2, z) -$   
 $4.99538 \operatorname{conj}(d(v3, x)) d(u2, z) + 5.93345 \times 10^{-10} \operatorname{conj}(d(V3, x)) d(u2, z) +$   
 $4.77798 \operatorname{conj}(d(v3, z)) d(u2, z) - 11.5806 \operatorname{conj}(d(w3, x)) d(u2, z) -$   
 $3.73297 \operatorname{conj}(d(w3, z)) d(u2, z) - 4.99538 \operatorname{conj}(d(u3, z)) d(v2, x) +$   
 $10.554 \operatorname{conj}(d(v3, x)) d(v2, x) + 1.65553 \times 10^{-10} \operatorname{conj}(d(V3, x)) d(v2, x) +$   
 $3.73297 \operatorname{conj}(d(v3, z)) d(v2, x) - 4.99538 \operatorname{conj}(d(w3, x)) d(v2, x) -$   
 $2.91651 \operatorname{conj}(d(w3, z)) d(v2, x) + 5.93345 \times 10^{-10} \operatorname{conj}(d(u3, z)) d(V2, x) +$   
 $1.65553 \times 10^{-10} \operatorname{conj}(d(v3, x)) d(V2, x) + 5.93345 \times 10^{-10} \operatorname{conj}(d(w3, x)) d(V2, x) -$   
 $12.4675 \operatorname{conj}(d(u3, x)) d(v2, z) + 4.77798 \operatorname{conj}(d(u3, z)) d(v2, z) +$   
 $3.73297 \operatorname{conj}(d(v3, x)) d(v2, z) + 1.62595 \operatorname{conj}(d(v3, z)) d(v2, z) +$   
 $8.63797 \times 10^{-10} \operatorname{conj}(d(V3, z)) d(v2, z) + 4.77798 \operatorname{conj}(d(w3, x)) d(v2, z) -$   
 $10.2568 \operatorname{conj}(d(w3, z)) d(v2, z) + 4.1025 \times 10^{-10} \operatorname{conj}(d(u3, x)) d(V2, z) +$   
 $8.63797 \times 10^{-10} \operatorname{conj}(d(v3, z)) d(V2, z) + 1.59543 \times 10^{-19} \operatorname{conj}(d(V3, z)) d(V2, z) +$   
 $2.12426 \times 10^{-10} \operatorname{conj}(d(w3, z)) d(V2, z) - 11.5806 \operatorname{conj}(d(u3, z)) d(w2, x) -$   
 $4.99538 \operatorname{conj}(d(v3, x)) d(w2, x) + 5.93345 \times 10^{-10} \operatorname{conj}(d(V3, x)) d(w2, x) +$   
 $4.77798 \operatorname{conj}(d(v3, z)) d(w2, x) - 11.5806 \operatorname{conj}(d(w3, x)) d(w2, x) -$   
 $3.73297 \operatorname{conj}(d(w3, z)) d(w2, x) + 5.21447 \operatorname{conj}(d(u3, x)) d(w2, z) -$   
 $3.73297 \operatorname{conj}(d(u3, z)) d(w2, z) - 2.91651 \operatorname{conj}(d(v3, x)) d(w2, z) -$   
 $10.2568 \operatorname{conj}(d(v3, z)) d(w2, z) + 2.12426 \times 10^{-10} \operatorname{conj}(d(V3, z)) d(w2, z) -$   
 $3.73297 \operatorname{conj}(d(w3, x)) d(w2, z) + 22.9799 \operatorname{conj}(d(w3, z)) d(w2, z)$

$ln[ ] =$  tidler[1, 1] // N  
tidler[1, 2] // N  
tidler[1, 3] // N  
tidler[2, 2] // N  
tidler[2, 3] // N  
tidler[3, 3] // N  
tidler[4, 1] // N  
tidler[4, 2] // N  
tidler[4, 3] // N

$Out[ ] = 0. - 2.56 \times 10^{11} \operatorname{conj}(d(u, x)) d(u2, x) + 1.68713 \times 10^{10} \operatorname{conj}(d(v, z)) d(u2, x) +$   
 $27.7141 \operatorname{conj}(d(V, z)) d(u2, x) + 5.10982 \times 10^{11} \operatorname{conj}(d(w, z)) d(u2, x) -$   
 $1.67483 \times 10^{11} \operatorname{conj}(d(u, z)) d(u2, z) - 1.07724 \times 10^{11} \operatorname{conj}(d(v, x)) d(u2, z) +$   
 $16.3686 \operatorname{conj}(d(V, x)) d(u2, z) - 1.67483 \times 10^{11} \operatorname{conj}(d(w, x)) d(u2, z) -$   
 $1.07724 \times 10^{11} \operatorname{conj}(d(u, z)) d(v2, x) - 2.40017 \times 10^{11} \operatorname{conj}(d(v, x)) d(v2, x) +$   
 $6.82416 \operatorname{conj}(d(V, x)) d(v2, x) - 1.07724 \times 10^{11} \operatorname{conj}(d(w, x)) d(v2, x) +$   
 $16.3686 \operatorname{conj}(d(u, z)) d(V2, x) + 6.82416 \operatorname{conj}(d(v, x)) d(V2, x) -$   
 $5.55 \times 10^{-10} \operatorname{conj}(d(V, x)) d(V2, x) + 16.3686 \operatorname{conj}(d(w, x)) d(V2, x) +$   
 $1.68713 \times 10^{10} \operatorname{conj}(d(u, x)) d(v2, z) - 1.31459 \times 10^{11} \operatorname{conj}(d(v, z)) d(v2, z) -$   
 $12.4675 \operatorname{conj}(d(V, z)) d(v2, z) - 6.59622 \times 10^{10} \operatorname{conj}(d(w, z)) d(v2, z) +$   
 $27.7141 \operatorname{conj}(d(u, x)) d(V2, z) - 12.4675 \operatorname{conj}(d(v, z)) d(V2, z) +$   
 $4.1025 \times 10^{-10} \operatorname{conj}(d(V, z)) d(V2, z) + 5.21447 \operatorname{conj}(d(w, z)) d(V2, z) -$   
 $1.67483 \times 10^{11} \operatorname{conj}(d(u, z)) d(w2, x) - 1.07724 \times 10^{11} \operatorname{conj}(d(v, x)) d(w2, x) +$   
 $16.3686 \operatorname{conj}(d(V, x)) d(w2, x) - 1.67483 \times 10^{11} \operatorname{conj}(d(w, x)) d(w2, x) +$   
 $5.10982 \times 10^{11} \operatorname{conj}(d(u, x)) d(w2, z) - 6.59622 \times 10^{10} \operatorname{conj}(d(v, z)) d(w2, z) +$   
 $5.21447 \operatorname{conj}(d(V, z)) d(w2, z) + 1.55803 \times 10^{11} \operatorname{conj}(d(w, z)) d(w2, z)$

$$\begin{aligned}
\text{Out}_{[u]=}^0 = & 0. - 1.07724 \times 10^{11} \text{ conj}(d(u, z)) d(u_2, x) - 2.40017 \times 10^{11} \text{ conj}(d(v, x)) d(u_2, x) + \\
& 6.82416 \text{ conj}(d(V, x)) d(u_2, x) - 1.07724 \times 10^{11} \text{ conj}(d(w, x)) d(u_2, x) - \\
& 1.07724 \times 10^{11} \text{ conj}(d(u, x)) d(u_2, z) - 8.4605 \times 10^{10} \text{ conj}(d(v, z)) d(u_2, z) - \\
& 4.99538 \text{ conj}(d(V, z)) d(u_2, z) - 3.68926 \times 10^{10} \text{ conj}(d(w, z)) d(u_2, z) - \\
& 2.40017 \times 10^{11} \text{ conj}(d(u, x)) d(v_2, x) + 1.96051 \times 10^{10} \text{ conj}(d(v, z)) d(v_2, x) + \\
& 10.554 \text{ conj}(d(V, z)) d(v_2, x) - 2.96481 \times 10^{10} \text{ conj}(d(w, z)) d(v_2, x) + \\
& 6.82416 \text{ conj}(d(u, x)) d(V_2, x) - 3.75564 \text{ conj}(d(v, z)) d(V_2, x) + \\
& 1.65553 \times 10^{-10} \text{ conj}(d(V, z)) d(V_2, x) + 5.38946 \text{ conj}(d(w, z)) d(V_2, x) - \\
& 8.4605 \times 10^{10} \text{ conj}(d(u, z)) d(v_2, z) + 1.96051 \times 10^{10} \text{ conj}(d(v, x)) d(v_2, z) - \\
& 3.75564 \text{ conj}(d(V, x)) d(v_2, z) + 3.73297 \text{ conj}(d(V, z)) d(v_2, z) - \\
& 8.4605 \times 10^{10} \text{ conj}(d(w, x)) d(v_2, z) - 4.99538 \text{ conj}(d(u, z)) d(V_2, z) + \\
& 10.554 \text{ conj}(d(v, x)) d(V_2, z) + 1.65553 \times 10^{-10} \text{ conj}(d(V, x)) d(V_2, z) + \\
& 3.73297 \text{ conj}(d(v, z)) d(V_2, z) - 4.99538 \text{ conj}(d(w, x)) d(V_2, z) - \\
& 2.91651 \text{ conj}(d(w, z)) d(V_2, z) - 1.07724 \times 10^{11} \text{ conj}(d(u, x)) d(w_2, x) - \\
& 8.4605 \times 10^{10} \text{ conj}(d(v, z)) d(w_2, x) - 4.99538 \text{ conj}(d(V, z)) d(w_2, x) - \\
& 3.68926 \times 10^{10} \text{ conj}(d(w, z)) d(w_2, x) - 3.68926 \times 10^{10} \text{ conj}(d(u, z)) d(w_2, z) - \\
& 2.96481 \times 10^{10} \text{ conj}(d(v, x)) d(w_2, z) + 5.38946 \text{ conj}(d(V, x)) d(w_2, z) - \\
& 2.91651 \text{ conj}(d(V, z)) d(w_2, z) - 3.68926 \times 10^{10} \text{ conj}(d(w, x)) d(w_2, z)
\end{aligned}$$

$$\begin{aligned}
\text{Out}_{[v]=}^0 = & 0. - 1.67483 \times 10^{11} \text{ conj}(d(u, z)) d(u_2, x) - 1.07724 \times 10^{11} \text{ conj}(d(v, x)) d(u_2, x) + \\
& 16.3686 \text{ conj}(d(V, x)) d(u_2, x) - 1.67483 \times 10^{11} \text{ conj}(d(w, x)) d(u_2, x) - \\
& 1.67483 \times 10^{11} \text{ conj}(d(u, x)) d(u_2, z) - 6.82725 \times 10^{10} \text{ conj}(d(v, z)) d(u_2, z) - \\
& 11.5806 \text{ conj}(d(V, z)) d(u_2, z) - 2.3758 \times 10^{11} \text{ conj}(d(w, z)) d(u_2, z) - \\
& 1.07724 \times 10^{11} \text{ conj}(d(u, x)) d(v_2, x) - 8.4605 \times 10^{10} \text{ conj}(d(v, z)) d(v_2, x) - \\
& 4.99538 \text{ conj}(d(V, z)) d(v_2, x) - 3.68926 \times 10^{10} \text{ conj}(d(w, z)) d(v_2, x) + \\
& 16.3686 \text{ conj}(d(u, x)) d(V_2, x) + 8.9817 \text{ conj}(d(v, z)) d(V_2, x) + \\
& 5.93345 \times 10^{-10} \text{ conj}(d(V, z)) d(V_2, x) - 4.18951 \text{ conj}(d(w, z)) d(V_2, x) - \\
& 6.82725 \times 10^{10} \text{ conj}(d(u, z)) d(v_2, z) - 8.4605 \times 10^{10} \text{ conj}(d(v, x)) d(v_2, z) + \\
& 8.9817 \text{ conj}(d(V, x)) d(v_2, z) + 4.77798 \text{ conj}(d(V, z)) d(v_2, z) - \\
& 6.82725 \times 10^{10} \text{ conj}(d(w, x)) d(v_2, z) - 11.5806 \text{ conj}(d(u, z)) d(V_2, z) - \\
& 4.99538 \text{ conj}(d(v, x)) d(V_2, z) + 5.93345 \times 10^{-10} \text{ conj}(d(V, x)) d(V_2, z) + \\
& 4.77798 \text{ conj}(d(v, z)) d(V_2, z) - 11.5806 \text{ conj}(d(w, x)) d(V_2, z) - \\
& 3.73297 \text{ conj}(d(w, z)) d(V_2, z) - 1.67483 \times 10^{11} \text{ conj}(d(u, x)) d(w_2, x) - \\
& 6.82725 \times 10^{10} \text{ conj}(d(v, z)) d(w_2, x) - 11.5806 \text{ conj}(d(V, z)) d(w_2, x) - \\
& 2.3758 \times 10^{11} \text{ conj}(d(w, z)) d(w_2, x) - 2.3758 \times 10^{11} \text{ conj}(d(u, z)) d(w_2, z) - \\
& 3.68926 \times 10^{10} \text{ conj}(d(v, x)) d(w_2, z) - 4.18951 \text{ conj}(d(V, x)) d(w_2, z) - \\
& 3.73297 \text{ conj}(d(V, z)) d(w_2, z) - 2.3758 \times 10^{11} \text{ conj}(d(w, x)) d(w_2, z)
\end{aligned}$$

$$\begin{aligned}
\text{Out}_{[n]}^j = & 0. + 8.00177 \times 10^{10} \text{ conj}(d(u,x)) d(u_2,x) - 3.76345 \times 10^{10} \text{ conj}(d(v,z)) d(u_2,x) + \\
& 4.04498 \text{ conj}(d(V,z)) d(u_2,x) + 2.46541 \times 10^{11} \text{ conj}(d(w,z)) d(u_2,x) + \\
& 1.25188 \times 10^{11} \text{ conj}(d(u,z)) d(u_2,z) - 7.1765 \times 10^{10} \text{ conj}(d(v,x)) d(u_2,z) + \\
& 26.081 \text{ conj}(d(V,x)) d(u_2,z) - 6.11553 \text{ conj}(d(V,z)) d(u_2,z) + \\
& 1.25188 \times 10^{11} \text{ conj}(d(w,x)) d(u_2,z) - 7.1765 \times 10^{10} \text{ conj}(d(u,z)) d(v_2,x) - \\
& 2.6921 \times 10^{11} \text{ conj}(d(v,x)) d(v_2,x) + 30.7493 \text{ conj}(d(V,x)) d(v_2,x) - \\
& 4.77798 \text{ conj}(d(V,z)) d(v_2,x) - 7.1765 \times 10^{10} \text{ conj}(d(w,x)) d(v_2,x) + \\
& 26.081 \text{ conj}(d(u,z)) d(V_2,x) + 30.7493 \text{ conj}(d(v,x)) d(V_2,x) - \\
& 5.2025 \times 10^{-10} \text{ conj}(d(V,x)) d(V_2,x) + 26.081 \text{ conj}(d(w,x)) d(V_2,x) - \\
& 3.76345 \times 10^{10} \text{ conj}(d(u,x)) d(v_2,z) - 1.23628 \times 10^{11} \text{ conj}(d(v,z)) d(v_2,z) - \\
& 1.71448 \text{ conj}(d(V,z)) d(v_2,z) - 2.93144 \times 10^{10} \text{ conj}(d(w,z)) d(v_2,z) + \\
& 4.04498 \text{ conj}(d(u,x)) d(V_2,z) - 6.11553 \text{ conj}(d(u,z)) d(V_2,z) - \\
& 4.77798 \text{ conj}(d(v,x)) d(V_2,z) - 1.71448 \text{ conj}(d(v,z)) d(V_2,z) - \\
& 1.45844 \times 10^{-9} \text{ conj}(d(V,z)) d(V_2,z) - 6.11553 \text{ conj}(d(w,x)) d(V_2,z) - \\
& 11.2685 \text{ conj}(d(w,z)) d(V_2,z) + 1.25188 \times 10^{11} \text{ conj}(d(u,z)) d(w_2,x) - \\
& 7.1765 \times 10^{10} \text{ conj}(d(v,x)) d(w_2,x) + 26.081 \text{ conj}(d(V,x)) d(w_2,x) - \\
& 6.11553 \text{ conj}(d(V,z)) d(w_2,x) + 1.25188 \times 10^{11} \text{ conj}(d(w,x)) d(w_2,x) + \\
& 2.46541 \times 10^{11} \text{ conj}(d(u,x)) d(w_2,z) - 2.93144 \times 10^{10} \text{ conj}(d(v,z)) d(w_2,z) - \\
& 11.2685 \text{ conj}(d(V,z)) d(w_2,z) + 2.62661 \times 10^{11} \text{ conj}(d(w,z)) d(w_2,z)
\end{aligned}$$

$$\begin{aligned}
\text{Out}_{[n]}^j = & 0. + 1.68713 \times 10^{10} \text{ conj}(d(u,x)) d(u_2,x) - 1.31459 \times 10^{11} \text{ conj}(d(v,z)) d(u_2,x) - \\
& 12.4675 \text{ conj}(d(V,z)) d(u_2,x) - 6.59622 \times 10^{10} \text{ conj}(d(w,z)) d(u_2,x) - \\
& 6.82725 \times 10^{10} \text{ conj}(d(u,z)) d(u_2,z) - 8.4605 \times 10^{10} \text{ conj}(d(v,x)) d(u_2,z) + \\
& 8.9817 \text{ conj}(d(V,x)) d(u_2,z) + 4.77798 \text{ conj}(d(V,z)) d(u_2,z) - \\
& 6.82725 \times 10^{10} \text{ conj}(d(w,x)) d(u_2,z) - 8.4605 \times 10^{10} \text{ conj}(d(u,z)) d(v_2,x) + \\
& 1.96051 \times 10^{10} \text{ conj}(d(v,x)) d(v_2,x) - 3.75564 \text{ conj}(d(V,x)) d(v_2,x) + \\
& 3.73297 \text{ conj}(d(V,z)) d(v_2,x) - 8.4605 \times 10^{10} \text{ conj}(d(w,x)) d(v_2,x) + \\
& 8.9817 \text{ conj}(d(u,z)) d(V_2,x) - 3.75564 \text{ conj}(d(v,x)) d(V_2,x) - \\
& 1.25483 \times 10^{-9} \text{ conj}(d(V,x)) d(V_2,x) + 8.9817 \text{ conj}(d(w,x)) d(V_2,x) - \\
& 1.31459 \times 10^{11} \text{ conj}(d(u,x)) d(v_2,z) + 1.64758 \times 10^{11} \text{ conj}(d(v,z)) d(v_2,z) + \\
& 1.62595 \text{ conj}(d(V,z)) d(v_2,z) - 1.25558 \times 10^{11} \text{ conj}(d(w,z)) d(v_2,z) - \\
& 12.4675 \text{ conj}(d(u,x)) d(V_2,z) + 4.77798 \text{ conj}(d(u,z)) d(V_2,z) + \\
& 3.73297 \text{ conj}(d(v,x)) d(V_2,z) + 1.62595 \text{ conj}(d(v,z)) d(V_2,z) + \\
& 8.63797 \times 10^{-10} \text{ conj}(d(V,z)) d(V_2,z) + 4.77798 \text{ conj}(d(w,x)) d(V_2,z) - \\
& 10.2568 \text{ conj}(d(w,z)) d(V_2,z) - 6.82725 \times 10^{10} \text{ conj}(d(u,z)) d(w_2,x) - \\
& 8.4605 \times 10^{10} \text{ conj}(d(v,x)) d(w_2,x) + 8.9817 \text{ conj}(d(V,x)) d(w_2,x) + \\
& 4.77798 \text{ conj}(d(V,z)) d(w_2,x) - 6.82725 \times 10^{10} \text{ conj}(d(w,x)) d(w_2,x) - \\
& 6.59622 \times 10^{10} \text{ conj}(d(u,x)) d(w_2,z) - 1.25558 \times 10^{11} \text{ conj}(d(v,z)) d(w_2,z) - \\
& 10.2568 \text{ conj}(d(V,z)) d(w_2,z) + 1.2397 \times 10^{11} \text{ conj}(d(w,z)) d(w_2,z)
\end{aligned}$$

$$\begin{aligned}
\text{Out}_{[=]} = & 0. + 5.10982 \times 10^{11} \text{ conj}(d(u,x)) d(u2,x) - 6.59622 \times 10^{10} \text{ conj}(d(v,z)) d(u2,x) + \\
& 5.21447 \text{ conj}(d(V,z)) d(u2,x) + 1.55803 \times 10^{11} \text{ conj}(d(w,z)) d(u2,x) - \\
& 2.3758 \times 10^{11} \text{ conj}(d(u,z)) d(u2,z) - 3.68926 \times 10^{10} \text{ conj}(d(v,x)) d(u2,z) - \\
& 4.18951 \text{ conj}(d(V,x)) d(u2,z) - 3.73297 \text{ conj}(d(V,z)) d(u2,z) - \\
& 2.3758 \times 10^{11} \text{ conj}(d(w,x)) d(u2,z) - 3.68926 \times 10^{10} \text{ conj}(d(u,z)) d(v2,x) - \\
& 2.96481 \times 10^{10} \text{ conj}(d(v,x)) d(v2,x) + 5.38946 \text{ conj}(d(V,x)) d(v2,x) - \\
& 2.91651 \text{ conj}(d(V,z)) d(v2,x) - 3.68926 \times 10^{10} \text{ conj}(d(w,x)) d(v2,x) - \\
& 4.18951 \text{ conj}(d(u,z)) d(V2,x) + 5.38946 \text{ conj}(d(v,x)) d(V2,x) + \\
& 4.1025 \times 10^{-10} \text{ conj}(d(V,x)) d(V2,x) - 4.18951 \text{ conj}(d(w,x)) d(V2,x) - \\
& 6.59622 \times 10^{10} \text{ conj}(d(u,x)) d(v2,z) - 1.25558 \times 10^{11} \text{ conj}(d(v,z)) d(v2,z) - \\
& 10.2568 \text{ conj}(d(V,z)) d(v2,z) + 1.2397 \times 10^{11} \text{ conj}(d(w,z)) d(v2,z) + \\
& 5.21447 \text{ conj}(d(u,x)) d(V2,z) - 3.73297 \text{ conj}(d(u,z)) d(V2,z) - \\
& 2.91651 \text{ conj}(d(v,x)) d(V2,z) - 10.2568 \text{ conj}(d(v,z)) d(V2,z) + \\
& 2.12426 \times 10^{-10} \text{ conj}(d(V,z)) d(V2,z) - 3.73297 \text{ conj}(d(w,x)) d(V2,z) + \\
& 22.9799 \text{ conj}(d(w,z)) d(V2,z) - 2.3758 \times 10^{11} \text{ conj}(d(u,z)) d(w2,x) - \\
& 3.68926 \times 10^{10} \text{ conj}(d(v,x)) d(w2,x) - 4.18951 \text{ conj}(d(V,x)) d(w2,x) - \\
& 3.73297 \text{ conj}(d(V,z)) d(w2,x) - 2.3758 \times 10^{11} \text{ conj}(d(w,x)) d(w2,x) + \\
& 1.55803 \times 10^{11} \text{ conj}(d(u,x)) d(w2,z) + 1.2397 \times 10^{11} \text{ conj}(d(v,z)) d(w2,z) + \\
& 22.9799 \text{ conj}(d(V,z)) d(w2,z) - 8.05371 \times 10^{11} \text{ conj}(d(w,z)) d(w2,z)
\end{aligned}$$

$$\begin{aligned}
\text{Out}_{[=]} = & 0. + 16.3686 \text{ conj}(d(u,z)) d(u2,x) + 6.82416 \text{ conj}(d(v,x)) d(u2,x) - \\
& 5.55 \times 10^{-10} \text{ conj}(d(V,x)) d(u2,x) + 16.3686 \text{ conj}(d(w,x)) d(u2,x) + \\
& 16.3686 \text{ conj}(d(u,x)) d(u2,z) + 8.9817 \text{ conj}(d(v,z)) d(u2,z) + \\
& 5.93345 \times 10^{-10} \text{ conj}(d(V,z)) d(u2,z) - 4.18951 \text{ conj}(d(w,z)) d(u2,z) + \\
& 6.82416 \text{ conj}(d(u,x)) d(v2,x) - 3.75564 \text{ conj}(d(v,z)) d(v2,x) + \\
& 1.65553 \times 10^{-10} \text{ conj}(d(V,z)) d(v2,x) + 5.38946 \text{ conj}(d(w,z)) d(v2,x) - \\
& 5.55 \times 10^{-10} \text{ conj}(d(u,x)) d(V2,x) - 1.405 \times 10^{-19} \text{ conj}(d(V,x)) d(V2,x) - \\
& 1.25483 \times 10^{-9} \text{ conj}(d(v,z)) d(V2,x) + 4.1025 \times 10^{-10} \text{ conj}(d(w,z)) d(V2,x) + \\
& 8.9817 \text{ conj}(d(u,z)) d(v2,z) - 3.75564 \text{ conj}(d(v,x)) d(v2,z) - \\
& 1.25483 \times 10^{-9} \text{ conj}(d(V,x)) d(v2,z) + 8.9817 \text{ conj}(d(w,x)) d(v2,z) + \\
& 5.93345 \times 10^{-10} \text{ conj}(d(u,z)) d(V2,z) + 1.65553 \times 10^{-10} \text{ conj}(d(v,x)) d(V2,z) + \\
& 5.93345 \times 10^{-10} \text{ conj}(d(w,x)) d(V2,z) + 16.3686 \text{ conj}(d(u,x)) d(w2,x) + \\
& 8.9817 \text{ conj}(d(v,z)) d(w2,x) + 5.93345 \times 10^{-10} \text{ conj}(d(V,z)) d(w2,x) - \\
& 4.18951 \text{ conj}(d(w,z)) d(w2,x) - 4.18951 \text{ conj}(d(u,z)) d(w2,z) + 5.38946 \text{ conj}(d(v,x)) d(w2,z) + \\
& 4.1025 \times 10^{-10} \text{ conj}(d(V,x)) d(w2,z) - 4.18951 \text{ conj}(d(w,x)) d(w2,z)
\end{aligned}$$

$$\begin{aligned}
\text{Out}[\ast]= & 0. - 11.5957 \text{ conj}(d(u,x)) d(u2,x) + 2.15588 \text{ conj}(d(v,z)) d(u2,x) - \\
& 1.25483 \times 10^{-9} \text{ conj}(d(V,z)) d(u2,x) - 26.0929 \text{ conj}(d(w,z)) d(u2,x) - \\
& 12.2783 \text{ conj}(d(u,z)) d(u2,z) + 2.00869 \text{ conj}(d(v,x)) d(u2,z) + \\
& 1.65553 \times 10^{-10} \text{ conj}(d(V,x)) d(u2,z) - 6.11553 \text{ conj}(d(v,z)) d(u2,z) - \\
& 12.2783 \text{ conj}(d(w,x)) d(u2,z) + 4.77798 \text{ conj}(d(w,z)) d(u2,z) + 2.00869 \text{ conj}(d(u,z)) d(v2,x) - \\
& 1.59468 \text{ conj}(d(v,x)) d(v2,x) - 1.39584 \times 10^{-9} \text{ conj}(d(V,x)) d(v2,x) - \\
& 4.77798 \text{ conj}(d(v,z)) d(v2,x) + 2.00869 \text{ conj}(d(w,x)) d(v2,x) + 3.73297 \text{ conj}(d(w,z)) d(v2,x) + \\
& 1.65553 \times 10^{-10} \text{ conj}(d(u,z)) d(V2,x) - 1.39584 \times 10^{-9} \text{ conj}(d(v,x)) d(V2,x) + \\
& 1.65553 \times 10^{-10} \text{ conj}(d(w,x)) d(V2,x) + 2.15588 \text{ conj}(d(u,x)) d(v2,z) - \\
& 6.11553 \text{ conj}(d(u,z)) d(v2,z) - 4.77798 \text{ conj}(d(v,x)) d(v2,z) + 7.79531 \text{ conj}(d(v,z)) d(v2,z) + \\
& 6.1656 \times 10^{-10} \text{ conj}(d(V,z)) d(v2,z) - 6.11553 \text{ conj}(d(w,x)) d(v2,z) - \\
& 3.98158 \text{ conj}(d(w,z)) d(v2,z) - 1.25483 \times 10^{-9} \text{ conj}(d(u,x)) d(V2,z) + \\
& 6.1656 \times 10^{-10} \text{ conj}(d(v,z)) d(V2,z) - 3.50958 \times 10^{-19} \text{ conj}(d(V,z)) d(V2,z) + \\
& 8.63797 \times 10^{-10} \text{ conj}(d(w,z)) d(V2,z) - 12.2783 \text{ conj}(d(u,z)) d(w2,x) + \\
& 2.00869 \text{ conj}(d(v,x)) d(w2,x) + 1.65553 \times 10^{-10} \text{ conj}(d(V,x)) d(w2,x) - \\
& 6.11553 \text{ conj}(d(v,z)) d(w2,x) - 12.2783 \text{ conj}(d(w,x)) d(w2,x) + 4.77798 \text{ conj}(d(w,z)) d(w2,x) - \\
& 26.0929 \text{ conj}(d(u,x)) d(w2,z) + 4.77798 \text{ conj}(d(u,z)) d(w2,z) + 3.73297 \text{ conj}(d(v,x)) d(w2,z) - \\
& 3.98158 \text{ conj}(d(v,z)) d(w2,z) + 8.63797 \times 10^{-10} \text{ conj}(d(V,z)) d(w2,z) + \\
& 4.77798 \text{ conj}(d(w,x)) d(w2,z) - 46.9193 \text{ conj}(d(w,z)) d(w2,z)
\end{aligned}$$

$$\begin{aligned}
\text{Out}[\ast]= & 0. + 27.7141 \text{ conj}(d(u,x)) d(u2,x) - 12.4675 \text{ conj}(d(v,z)) d(u2,x) + \\
& 4.1025 \times 10^{-10} \text{ conj}(d(V,z)) d(u2,x) + 5.21447 \text{ conj}(d(w,z)) d(u2,x) - \\
& 11.5806 \text{ conj}(d(u,z)) d(u2,z) - 4.99538 \text{ conj}(d(v,x)) d(u2,z) + \\
& 5.93345 \times 10^{-10} \text{ conj}(d(V,x)) d(u2,z) + 4.77798 \text{ conj}(d(v,z)) d(u2,z) - \\
& 11.5806 \text{ conj}(d(w,x)) d(u2,z) - 3.73297 \text{ conj}(d(w,z)) d(u2,z) - 4.99538 \text{ conj}(d(u,z)) d(v2,x) + \\
& 10.554 \text{ conj}(d(v,x)) d(v2,x) + 1.65553 \times 10^{-10} \text{ conj}(d(V,x)) d(v2,x) + \\
& 3.73297 \text{ conj}(d(v,z)) d(v2,x) - 4.99538 \text{ conj}(d(w,x)) d(v2,x) - 2.91651 \text{ conj}(d(w,z)) d(v2,x) + \\
& 5.93345 \times 10^{-10} \text{ conj}(d(u,z)) d(V2,x) + 1.65553 \times 10^{-10} \text{ conj}(d(v,x)) d(V2,x) + \\
& 5.93345 \times 10^{-10} \text{ conj}(d(w,x)) d(V2,x) - 12.4675 \text{ conj}(d(u,x)) d(v2,z) + \\
& 4.77798 \text{ conj}(d(u,z)) d(v2,z) + 3.73297 \text{ conj}(d(v,x)) d(v2,z) + 1.62595 \text{ conj}(d(v,z)) d(v2,z) + \\
& 8.63797 \times 10^{-10} \text{ conj}(d(V,z)) d(v2,z) + 4.77798 \text{ conj}(d(w,x)) d(v2,z) - \\
& 10.2568 \text{ conj}(d(w,z)) d(v2,z) + 4.1025 \times 10^{-10} \text{ conj}(d(u,x)) d(V2,z) + \\
& 8.63797 \times 10^{-10} \text{ conj}(d(v,z)) d(V2,z) + 1.59543 \times 10^{-19} \text{ conj}(d(V,z)) d(V2,z) + \\
& 2.12426 \times 10^{-10} \text{ conj}(d(w,z)) d(V2,z) - 11.5806 \text{ conj}(d(u,z)) d(w2,x) - \\
& 4.99538 \text{ conj}(d(v,x)) d(w2,x) + 5.93345 \times 10^{-10} \text{ conj}(d(V,x)) d(w2,x) + \\
& 4.77798 \text{ conj}(d(v,z)) d(w2,x) - 11.5806 \text{ conj}(d(w,x)) d(w2,x) - 3.73297 \text{ conj}(d(w,z)) d(w2,x) + \\
& 5.21447 \text{ conj}(d(u,x)) d(w2,z) - 3.73297 \text{ conj}(d(u,z)) d(w2,z) - 2.91651 \text{ conj}(d(v,x)) d(w2,z) - \\
& 10.2568 \text{ conj}(d(v,z)) d(w2,z) + 2.12426 \times 10^{-10} \text{ conj}(d(V,z)) d(w2,z) - \\
& 3.73297 \text{ conj}(d(w,x)) d(w2,z) + 22.9799 \text{ conj}(d(w,z)) d(w2,z)
\end{aligned}$$

```

In[ ]:= tsum[1, 1] // N
tsum[1, 2] // N
tsum[1, 3] // N
tsum[2, 2] // N
tsum[2, 3] // N
tsum[3, 3] // N
tsum[4, 1] // N
tsum[4, 2] // N
tsum[4, 3] // N

```

$$\begin{aligned}
\text{Out[*=]} &= 0. - 2.56 \times 10^{11} d(u_2, x) d(u, x) - 1.67483 \times 10^{11} d(u_2, z) d(u, z) - \\
& 1.07724 \times 10^{11} d(u, z) d(v_2, x) + 16.3686 d(u, z) d(V_2, x) + 1.68713 \times 10^{10} d(u, x) d(v_2, z) + \\
& 27.7141 d(u, x) d(V_2, z) - 1.07724 \times 10^{11} d(u_2, z) d(v, x) - 2.40017 \times 10^{11} d(v_2, x) d(v, x) + \\
& 6.82416 d(V_2, x) d(v, x) + 16.3686 d(u_2, z) d(V, x) + 6.82416 d(v_2, x) d(V, x) - \\
& 5.55 \times 10^{-10} d(V_2, x) d(V, x) + 1.68713 \times 10^{10} d(u_2, x) d(v, z) - 1.31459 \times 10^{11} d(v_2, z) d(v, z) - \\
& 12.4675 d(V_2, z) d(v, z) + 27.7141 d(u_2, x) d(V, z) - 12.4675 d(v_2, z) d(V, z) + \\
& 4.1025 \times 10^{-10} d(V_2, z) d(V, z) - 1.67483 \times 10^{11} d(u, z) d(w_2, x) - 1.07724 \times 10^{11} d(v, x) d(w_2, x) + \\
& 16.3686 d(V, x) d(w_2, x) + 5.10982 \times 10^{11} d(u, x) d(w_2, z) - 6.59622 \times 10^{10} d(v, z) d(w_2, z) + \\
& 5.21447 d(V, z) d(w_2, z) - 1.67483 \times 10^{11} d(u_2, z) d(w, x) - 1.07724 \times 10^{11} d(v_2, x) d(w, x) + \\
& 16.3686 d(V_2, x) d(w, x) - 1.67483 \times 10^{11} d(w_2, x) d(w, x) + 5.10982 \times 10^{11} d(u_2, x) d(w, z) - \\
& 6.59622 \times 10^{10} d(v_2, z) d(w, z) + 5.21447 d(V_2, z) d(w, z) + 1.55803 \times 10^{11} d(w_2, z) d(w, z) \\
\\
\text{Out[*=]} &= 0. - 1.07724 \times 10^{11} d(u_2, z) d(u, x) - 1.07724 \times 10^{11} d(u_2, x) d(u, z) - 2.40017 \times 10^{11} d(u, x) d(v_2, x) + \\
& 6.82416 d(u, x) d(V_2, x) - 8.4605 \times 10^{10} d(u, z) d(v_2, z) - 4.99538 d(u, z) d(V_2, z) - \\
& 2.40017 \times 10^{11} d(u_2, x) d(v, x) + 1.96051 \times 10^{10} d(v_2, z) d(v, x) + 10.554 d(V_2, z) d(v, x) + \\
& 6.82416 d(u_2, x) d(V, x) - 3.75564 d(v_2, z) d(V, x) + 1.65553 \times 10^{-10} d(V_2, z) d(V, x) - \\
& 8.4605 \times 10^{10} d(u_2, z) d(v, z) + 1.96051 \times 10^{10} d(v_2, x) d(v, z) - 3.75564 d(V_2, x) d(v, z) + \\
& 3.73297 d(V_2, z) d(v, z) - 4.99538 d(u_2, z) d(V, z) + 10.554 d(v_2, x) d(V, z) + \\
& 1.65553 \times 10^{-10} d(V_2, x) d(V, z) + 3.73297 d(v_2, z) d(V, z) - 1.07724 \times 10^{11} d(u, x) d(w_2, x) - \\
& 8.4605 \times 10^{10} d(v, z) d(w_2, x) - 4.99538 d(V, z) d(w_2, x) - 3.68926 \times 10^{10} d(u, z) d(w_2, z) - \\
& 2.96481 \times 10^{10} d(v, x) d(w_2, z) + 5.38946 d(V, x) d(w_2, z) - 2.91651 d(V, z) d(w_2, z) - \\
& 1.07724 \times 10^{11} d(u_2, x) d(w, x) - 8.4605 \times 10^{10} d(v_2, z) d(w, x) - 4.99538 d(V_2, z) d(w, x) - \\
& 3.68926 \times 10^{10} d(w_2, z) d(w, x) - 3.68926 \times 10^{10} d(u_2, z) d(w, z) - 2.96481 \times 10^{10} d(v_2, x) d(w, z) + \\
& 5.38946 d(V_2, x) d(w, z) - 2.91651 d(V_2, z) d(w, z) - 3.68926 \times 10^{10} d(w_2, x) d(w, z) \\
\\
\text{Out[*=]} &= 0. - 1.67483 \times 10^{11} d(u_2, z) d(u, x) - 1.67483 \times 10^{11} d(u_2, x) d(u, z) - 1.07724 \times 10^{11} d(u, x) d(v_2, x) + \\
& 16.3686 d(u, x) d(V_2, x) - 6.82725 \times 10^{10} d(u, z) d(v_2, z) - 11.5806 d(u, z) d(V_2, z) - \\
& 1.07724 \times 10^{11} d(u_2, x) d(v, x) - 8.4605 \times 10^{10} d(v_2, z) d(v, x) - 4.99538 d(V_2, z) d(v, x) + \\
& 16.3686 d(u_2, x) d(V, x) + 8.9817 d(v_2, z) d(V, x) + 5.93345 \times 10^{-10} d(V_2, z) d(V, x) - \\
& 6.82725 \times 10^{10} d(u_2, z) d(v, z) - 8.4605 \times 10^{10} d(v_2, x) d(v, z) + 8.9817 d(V_2, x) d(v, z) + \\
& 4.77798 d(V_2, z) d(v, z) - 11.5806 d(u_2, z) d(V, z) - 4.99538 d(v_2, x) d(V, z) + \\
& 5.93345 \times 10^{-10} d(V_2, x) d(V, z) + 4.77798 d(v_2, z) d(V, z) - 1.67483 \times 10^{11} d(u, x) d(w_2, x) - \\
& 6.82725 \times 10^{10} d(v, z) d(w_2, x) - 11.5806 d(V, z) d(w_2, x) - 2.3758 \times 10^{11} d(u, z) d(w_2, z) - \\
& 3.68926 \times 10^{10} d(v, x) d(w_2, z) - 4.18951 d(V, x) d(w_2, z) - 3.73297 d(V, z) d(w_2, z) - \\
& 1.67483 \times 10^{11} d(u_2, x) d(w, x) - 6.82725 \times 10^{10} d(v_2, z) d(w, x) - 11.5806 d(V_2, z) d(w, x) - \\
& 2.3758 \times 10^{11} d(w_2, z) d(w, x) - 2.3758 \times 10^{11} d(u_2, z) d(w, z) - 3.68926 \times 10^{10} d(v_2, x) d(w, z) - \\
& 4.18951 d(V_2, x) d(w, z) - 3.73297 d(V_2, z) d(w, z) - 2.3758 \times 10^{11} d(w_2, x) d(w, z) \\
\\
\text{Out[*=]} &= 0. + 8.00177 \times 10^{10} d(u_2, x) d(u, x) + 1.25188 \times 10^{11} d(u_2, z) d(u, z) - \\
& 7.1765 \times 10^{10} d(u, z) d(v_2, x) + 26.081 d(u, z) d(V_2, x) - 3.76345 \times 10^{10} d(u, x) d(v_2, z) + \\
& 4.04498 d(u, x) d(V_2, z) - 6.11553 d(u, z) d(V_2, z) - 7.1765 \times 10^{10} d(u_2, z) d(v, x) - \\
& 2.6921 \times 10^{11} d(v_2, x) d(v, x) + 30.7493 d(V_2, x) d(v, x) - 4.77798 d(V_2, z) d(v, x) + \\
& 26.081 d(u_2, z) d(V, x) + 30.7493 d(v_2, x) d(V, x) - 5.2025 \times 10^{-10} d(V_2, x) d(V, x) - \\
& 3.76345 \times 10^{10} d(u_2, x) d(v, z) - 1.23628 \times 10^{11} d(v_2, z) d(v, z) - 1.71448 d(V_2, z) d(v, z) + \\
& 4.04498 d(u_2, x) d(V, z) - 6.11553 d(u_2, z) d(V, z) - 4.77798 d(v_2, x) d(V, z) - \\
& 1.71448 d(v_2, z) d(V, z) - 1.45844 \times 10^{-9} d(V_2, z) d(V, z) + 1.25188 \times 10^{11} d(u, z) d(w_2, x) - \\
& 7.1765 \times 10^{10} d(v, x) d(w_2, x) + 26.081 d(V, x) d(w_2, x) - 6.11553 d(V, z) d(w_2, x) + \\
& 2.46541 \times 10^{11} d(u, x) d(w_2, z) - 2.93144 \times 10^{10} d(v, z) d(w_2, z) - 11.2685 d(V, z) d(w_2, z) + \\
& 1.25188 \times 10^{11} d(u_2, z) d(w, x) - 7.1765 \times 10^{10} d(v_2, x) d(w, x) + 26.081 d(V_2, x) d(w, x) - \\
& 6.11553 d(V_2, z) d(w, x) + 1.25188 \times 10^{11} d(w_2, x) d(w, x) + 2.46541 \times 10^{11} d(u_2, x) d(w, z) - \\
& 2.93144 \times 10^{10} d(v_2, z) d(w, z) - 11.2685 d(V_2, z) d(w, z) + 2.62661 \times 10^{11} d(w_2, z) d(w, z)
\end{aligned}$$

$$\begin{aligned}
\text{Out[=]} = & 0. + 1.68713 \times 10^{10} d(u, x) d(u, x) - 6.82725 \times 10^{10} d(u, z) d(u, z) - \\
& 8.4605 \times 10^{10} d(u, z) d(v, x) + 8.9817 d(u, z) d(V, x) - 1.31459 \times 10^{11} d(u, x) d(v, z) - \\
& 12.4675 d(u, x) d(V, z) + 4.77798 d(u, z) d(V, z) - 8.4605 \times 10^{10} d(u, z) d(v, x) + \\
& 1.96051 \times 10^{10} d(v, x) d(v, x) - 3.75564 d(V, x) d(v, x) + 3.73297 d(V, z) d(v, x) + \\
& 8.9817 d(u, z) d(V, x) - 3.75564 d(v, x) d(V, x) - 1.25483 \times 10^{-9} d(V, x) d(V, x) - \\
& 1.31459 \times 10^{11} d(u, x) d(v, z) + 1.64758 \times 10^{11} d(v, z) d(v, z) + 1.62595 d(V, z) d(v, z) - \\
& 12.4675 d(u, x) d(V, z) + 4.77798 d(u, z) d(V, z) + 3.73297 d(v, x) d(V, z) + \\
& 1.62595 d(v, z) d(V, z) + 8.63797 \times 10^{-10} d(V, z) d(V, z) - 6.82725 \times 10^{10} d(u, z) d(w, x) - \\
& 8.4605 \times 10^{10} d(v, x) d(w, x) + 8.9817 d(V, x) d(w, x) + 4.77798 d(V, z) d(w, x) - \\
& 6.59622 \times 10^{10} d(u, x) d(w, z) - 1.25558 \times 10^{11} d(v, z) d(w, z) - 10.2568 d(V, z) d(w, z) - \\
& 6.82725 \times 10^{10} d(u, z) d(w, x) - 8.4605 \times 10^{10} d(v, x) d(w, x) + 8.9817 d(V, x) d(w, x) + \\
& 4.77798 d(V, z) d(w, x) - 6.82725 \times 10^{10} d(w, x) d(w, x) - 6.59622 \times 10^{10} d(u, x) d(w, z) - \\
& 1.25558 \times 10^{11} d(v, z) d(w, z) - 10.2568 d(V, z) d(w, z) + 1.2397 \times 10^{11} d(w, z) d(w, z)
\end{aligned}$$

$$\begin{aligned}
\text{Out[=]} = & 0. + 5.10982 \times 10^{11} d(u, x) d(u, x) - 2.3758 \times 10^{11} d(u, z) d(u, z) - \\
& 3.68926 \times 10^{10} d(u, z) d(v, x) - 4.18951 d(u, z) d(V, x) - 6.59622 \times 10^{10} d(u, x) d(v, z) + \\
& 5.21447 d(u, x) d(V, z) - 3.73297 d(u, z) d(V, z) - 3.68926 \times 10^{10} d(u, z) d(v, x) - \\
& 2.96481 \times 10^{10} d(v, x) d(v, x) + 5.38946 d(V, x) d(v, x) - 2.91651 d(V, z) d(v, x) - \\
& 4.18951 d(u, z) d(V, x) + 5.38946 d(v, x) d(V, x) + 4.1025 \times 10^{-10} d(V, x) d(V, x) - \\
& 6.59622 \times 10^{10} d(u, x) d(v, z) - 1.25558 \times 10^{11} d(v, z) d(v, z) - 10.2568 d(V, z) d(v, z) + \\
& 5.21447 d(u, x) d(V, z) - 3.73297 d(u, z) d(V, z) - 2.91651 d(v, x) d(V, z) - \\
& 10.2568 d(v, z) d(V, z) + 2.12426 \times 10^{-10} d(V, z) d(V, z) - 2.3758 \times 10^{11} d(u, z) d(w, x) - \\
& 3.68926 \times 10^{10} d(v, x) d(w, x) - 4.18951 d(V, x) d(w, x) - 3.73297 d(V, z) d(w, x) + \\
& 1.55803 \times 10^{11} d(u, x) d(w, z) + 1.2397 \times 10^{11} d(v, z) d(w, z) + 22.9799 d(V, z) d(w, z) - \\
& 2.3758 \times 10^{11} d(u, z) d(w, x) - 3.68926 \times 10^{10} d(v, x) d(w, x) - 4.18951 d(V, x) d(w, x) - \\
& 3.73297 d(V, z) d(w, x) - 2.3758 \times 10^{11} d(w, x) d(w, x) + 1.55803 \times 10^{11} d(u, x) d(w, z) + \\
& 1.2397 \times 10^{11} d(v, z) d(w, z) + 22.9799 d(V, z) d(w, z) - 8.05371 \times 10^{11} d(w, z) d(w, z)
\end{aligned}$$

$$\begin{aligned}
\text{Out[=]} = & 0. + 16.3686 d(u, z) d(u, x) + 16.3686 d(u, x) d(u, z) + \\
& 6.82416 d(u, x) d(v, x) - 5.55 \times 10^{-10} d(u, x) d(V, x) + 8.9817 d(u, z) d(v, z) + \\
& 5.93345 \times 10^{-10} d(u, z) d(V, z) + 6.82416 d(u, x) d(v, x) - 3.75564 d(v, z) d(v, x) + \\
& 1.65553 \times 10^{-10} d(V, z) d(v, x) - 5.55 \times 10^{-10} d(u, x) d(V, x) - 1.405 \times 10^{-19} d(V, x) d(V, x) - \\
& 1.25483 \times 10^{-9} d(v, z) d(V, x) + 8.9817 d(u, z) d(v, z) - 3.75564 d(v, x) d(v, z) - \\
& 1.25483 \times 10^{-9} d(V, x) d(v, z) + 5.93345 \times 10^{-10} d(u, z) d(V, z) + \\
& 1.65553 \times 10^{-10} d(v, x) d(V, z) + 16.3686 d(u, x) d(w, x) + 8.9817 d(v, z) d(w, x) + \\
& 5.93345 \times 10^{-10} d(V, z) d(w, x) - 4.18951 d(u, z) d(w, z) + 5.38946 d(v, x) d(w, z) + \\
& 4.1025 \times 10^{-10} d(V, x) d(w, z) + 16.3686 d(u, x) d(w, x) + 8.9817 d(v, z) d(w, x) + \\
& 5.93345 \times 10^{-10} d(V, z) d(w, x) - 4.18951 d(w, z) d(w, x) - 4.18951 d(u, z) d(w, z) + \\
& 5.38946 d(v, x) d(w, z) + 4.1025 \times 10^{-10} d(V, x) d(w, z) - 4.18951 d(w, x) d(w, z)
\end{aligned}$$



$$\begin{aligned}
\text{Out[*]} = & 0. - 11.5957 d(u2,x) d(u,x) - 12.2783 d(u2,z) d(u,z) + \\
& 2.00869 d(u,z) d(v2,x) + 1.65553 \times 10^{-10} d(u,z) d(V2,x) + 2.15588 d(u,x) d(v2,z) - \\
& 6.11553 d(u,z) d(v2,z) - 1.25483 \times 10^{-9} d(u,x) d(V2,z) + 2.00869 d(u2,z) d(v,x) - \\
& 1.59468 d(v2,x) d(v,x) - 1.39584 \times 10^{-9} d(V2,x) d(v,x) - 4.77798 d(v2,z) d(v,x) + \\
& 1.65553 \times 10^{-10} d(u2,z) d(V,x) - 1.39584 \times 10^{-9} d(v2,x) d(V,x) + \\
& 2.15588 d(u2,x) d(v,z) - 6.11553 d(u2,z) d(v,z) - 4.77798 d(v2,x) d(v,z) + \\
& 7.79531 d(v2,z) d(v,z) + 6.1656 \times 10^{-10} d(V2,z) d(v,z) - 1.25483 \times 10^{-9} d(u2,x) d(V,z) + \\
& 6.1656 \times 10^{-10} d(v2,z) d(V,z) - 3.50958 \times 10^{-19} d(V2,z) d(V,z) - 12.2783 d(u,z) d(w2,x) + \\
& 2.00869 d(v,x) d(w2,x) + 1.65553 \times 10^{-10} d(V,x) d(w2,x) - 6.11553 d(v,z) d(w2,x) - \\
& 26.0929 d(u,x) d(w2,z) + 4.77798 d(u,z) d(w2,z) + 3.73297 d(v,x) d(w2,z) - \\
& 3.98158 d(v,z) d(w2,z) + 8.63797 \times 10^{-10} d(V,z) d(w2,z) - 12.2783 d(u2,z) d(w,x) + \\
& 2.00869 d(v2,x) d(w,x) + 1.65553 \times 10^{-10} d(V2,x) d(w,x) - 6.11553 d(v2,z) d(w,x) - \\
& 12.2783 d(w2,x) d(w,x) + 4.77798 d(w2,z) d(w,x) - 26.0929 d(u2,x) d(w,z) + \\
& 4.77798 d(u2,z) d(w,z) + 3.73297 d(v2,x) d(w,z) - 3.98158 d(v2,z) d(w,z) + \\
& 8.63797 \times 10^{-10} d(V2,z) d(w,z) + 4.77798 d(w2,x) d(w,z) - 46.9193 d(w2,z) d(w,z)
\end{aligned}$$

$$\begin{aligned}
\text{Out[*]} = & 0. + 27.7141 d(u2,x) d(u,x) - 11.5806 d(u2,z) d(u,z) - \\
& 4.99538 d(u,z) d(v2,x) + 5.93345 \times 10^{-10} d(u,z) d(V2,x) - 12.4675 d(u,x) d(v2,z) + \\
& 4.77798 d(u,z) d(v2,z) + 4.1025 \times 10^{-10} d(u,x) d(V2,z) - 4.99538 d(u2,z) d(v,x) + \\
& 10.554 d(v2,x) d(v,x) + 1.65553 \times 10^{-10} d(V2,x) d(v,x) + 3.73297 d(v2,z) d(v,x) + \\
& 5.93345 \times 10^{-10} d(u2,z) d(V,x) + 1.65553 \times 10^{-10} d(v2,x) d(V,x) - \\
& 12.4675 d(u2,x) d(v,z) + 4.77798 d(u2,z) d(v,z) + 3.73297 d(v2,x) d(v,z) + \\
& 1.62595 d(v2,z) d(v,z) + 8.63797 \times 10^{-10} d(V2,z) d(v,z) + 4.1025 \times 10^{-10} d(u2,x) d(V,z) + \\
& 8.63797 \times 10^{-10} d(v2,z) d(V,z) + 1.59543 \times 10^{-19} d(V2,z) d(V,z) - 11.5806 d(u,z) d(w2,x) - \\
& 4.99538 d(v,x) d(w2,x) + 5.93345 \times 10^{-10} d(V,x) d(w2,x) + 4.77798 d(v,z) d(w2,x) + \\
& 5.21447 d(u,x) d(w2,z) - 3.73297 d(u,z) d(w2,z) - 2.91651 d(v,x) d(w2,z) - \\
& 10.2568 d(v,z) d(w2,z) + 2.12426 \times 10^{-10} d(V,z) d(w2,z) - 11.5806 d(u2,z) d(w,x) - \\
& 4.99538 d(v2,x) d(w,x) + 5.93345 \times 10^{-10} d(V2,x) d(w,x) + 4.77798 d(v2,z) d(w,x) - \\
& 11.5806 d(w2,x) d(w,x) - 3.73297 d(w2,z) d(w,x) + 5.21447 d(u2,x) d(w,z) - \\
& 3.73297 d(u2,z) d(w,z) - 2.91651 d(v2,x) d(w,z) - 10.2568 d(v2,z) d(w,z) + \\
& 2.12426 \times 10^{-10} d(V2,z) d(w,z) - 3.73297 d(w2,x) d(w,z) + 22.9799 d(w2,z) d(w,z)
\end{aligned}$$

## Appendix B Coupling of the modes of an oscillator

Modes of an oscillatory system are the patterns of motion that can describe the physical state of the system. In a linear system where the superposition principle holds, the total motion of the system can be described as summation of all the modes. Mathematically, modes are orthogonal to each other, meaning that they can get excited independently and they do not transfer energy among them. Depending on the system being continuous or discrete it can have different number of modes. In a discrete system, number of the total physical modes equals to the number of degrees of freedom in the system, whereas a continuous system can have infinite number of modes.

### Discrete System

As a simple case consider a spring and mass oscillator.

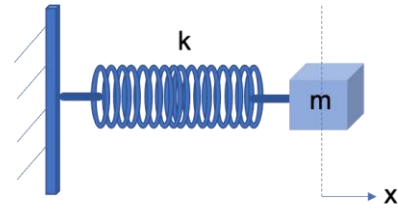


Figure B.1. Spring-Mass System

The equation of motion in  $x_1$  direction is shown in eq. (B.1).

$$m\ddot{x} = -kx \quad (\text{B.1})$$

Assuming a time harmonic solution as  $x(t) = X(t=0)e^{I\omega t}$ , where  $X$  and  $\omega$  are the amplitude and frequency of the oscillation, respectively, and  $I = \sqrt{-1}$ , eq. (B.2) becomes

$$(\omega^2 m - k)X = 0 \quad (\text{B.2})$$

The frequency of the oscillation then is

$$\omega = \pm \sqrt{\frac{k}{m}} \quad (\text{B.3})$$

The oscillation of the system can be defined as

$$x(t) = X e^{I\sqrt{\frac{k}{m}}t} + X e^{-I\sqrt{\frac{k}{m}}t} \quad (\text{B.4})$$

$X e^{I\sqrt{\frac{k}{m}}t}$  and  $X e^{-I\sqrt{\frac{k}{m}}t}$  are called the normal modes of the system. The physical motion is the real part of the solution that can be describe as

$$x(t) = \frac{X}{2} \text{Cos} \left( \sqrt{\frac{k}{m}} t \right) \quad (\text{B.5})$$

Which is a single mode equal to the number of degrees of freedom.

Now, imagine a system with two degrees of freedom,  $x_1$  and  $x_2$ . This system is consisting of two masses and three

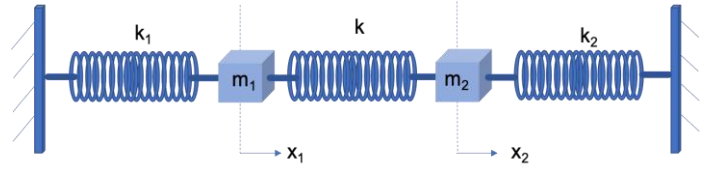


Figure B2. Two coupled Oscillators

springs and can be studied as a whole. The equation of motion is shown below

$$\ddot{x}_1 = \frac{-(k+k_1)}{m_1} x_1 + \frac{k}{m_1} x_2 \quad (\text{B.6}) \text{ (a)}$$

$$\ddot{x}_2 = \frac{-(k+k_2)}{m_2} x_2 + \frac{k}{m_2} x_1 \quad (\text{B.6}) \text{ (b)}$$

This can be viewed as a system that has two degrees of freedom, two physical modes, that are “coupled” with an intermediate spring with constant  $k$ .

Assume a solution to the above equation as

$$x_1(t) = X_1 e^{i\omega t} \quad (\text{B.7}) \text{ (a)}$$

$$x_2(t) = X_2 e^{i\omega t} \quad (\text{B.7}) \text{ (b)}$$

Substituting eq. (B.7) in eq. (B.6)

$$-\omega^2 X_1 e^{i\omega t} = \frac{-(k+k_1)}{m_1} X_1 e^{i\omega t} + \frac{k}{m_1} X_2 e^{i\omega t} \quad (\text{B.8}) \text{ (a)}$$

$$-\omega^2 X_2 e^{i\omega t} = \frac{-(k+k_2)}{m_2} X_2 e^{i\omega t} + \frac{k}{m_2} X_1 e^{i\omega t} \quad (\text{B.8}) \text{ (b)}$$

Or in a matrix form

$$\begin{bmatrix} \frac{-(k+k_1)+\omega^2 m_1}{m_1} & \frac{k}{m_1} \\ \frac{k}{m_2} & \frac{-(k+k_2)+\omega^2 m_2}{m_2} \end{bmatrix} \begin{bmatrix} X_1 \\ X_2 \end{bmatrix} = 0 \quad (\text{B.9})$$

To solve the system set  $\text{Det} \begin{bmatrix} \frac{-(k+k_1)+\omega^2 m_1}{m_1} & \frac{k}{m_1} \\ \frac{k}{m_2} & \frac{-(k+k_2)+\omega^2 m_2}{m_2} \end{bmatrix} = 0$

Which is a fourth order in terms of  $\omega$

The four solutions are

$$\omega_{c1} \rightarrow \pm \sqrt{\frac{k}{2m_1} + \frac{k_1}{2m_1} \mp \frac{1}{2} \sqrt{\left(\frac{k}{m_1} + \frac{k_1}{m_1} + \frac{k}{m_2} + \frac{k_2}{m_2}\right)^2 - 4\left(\frac{kk_1}{m_1m_2} + \frac{kk_2}{m_1m_2} + \frac{k_1k_2}{m_1m_2}\right)} + \frac{k}{2m_2} + \frac{k_2}{2m_2}} \quad (\text{B.10})$$

$$\omega_{c2} \rightarrow \pm \sqrt{\frac{k}{2m_1} + \frac{k_1}{2m_1} \pm \frac{1}{2} \sqrt{\left(\frac{k}{m_1} + \frac{k_1}{m_1} + \frac{k}{m_2} + \frac{k_2}{m_2}\right)^2 - 4\left(\frac{kk_1}{m_1m_2} + \frac{kk_2}{m_1m_2} + \frac{k_1k_2}{m_1m_2}\right)} + \frac{k}{2m_2} + \frac{k_2}{2m_2}} \quad (\text{B.11})$$

The eigenvectors are

$$[X_1, X_2] = \left[ \frac{k_2m_1 + k(m_1 - m_2) - k_1m_2 \pm \sqrt{k^2(m_1 + m_2)^2 + 2k(m_1 - m_2)(k_2m_1 - k_1m_2) + (k_2m_1 - k_1m_2)^2}}{2km_1}, 1 \right] \quad (\text{B.12})$$

The solution to the coupled system has four modes. If the coupling coefficient goes to zero,  $k \rightarrow$

0,  $\omega_{c1,c2} = \pm \sqrt{\frac{k_{1,2}}{m_{1,2}}}$ , which is the frequency of each uncoupled oscillators. This approach is called coupling of modes. Note that none of the uncoupled modes exist anymore. The system has two physical modes.

## Appendix C Calculation of the intensity of an acoustic wave

The power density or intensity of an acoustic wave, in the direction of propagation  $\bar{p}$ , can be calculated from eq. (C.1),

$$\text{Intensity} = \frac{1}{2} |\bar{p} \cdot (\bar{P} + \bar{P}^*)| \quad (\text{C.1})$$

where  $\bar{P}$  is the complex acoustic Poynting vector, represented in eq. (C.2) and  $\bar{P}^*$  denotes its complex conjugate.

$$\bar{P} = \frac{-\bar{v}^* \cdot \bar{T}}{2} \quad (\text{C.2})$$

In eq. (C.2)  $\bar{v}^*$  is the complex conjugate of the particle velocity and  $\bar{T}$  is the symmetric Cauchy Stress.

For a time-harmonic displacement field defined as  $u_k(\bar{x}, t) = u_k(\bar{x}) e^{-I\omega t}$ , where  $I = \sqrt{-1}$ , it is readily seen,

$$v_k(\bar{x}, t) = -I\omega u_k(\bar{x}, t) \quad (\text{C.3}) \text{ (a)}$$

and,

$$v_k^*(\bar{x}, t) = I\omega u_k^*(\bar{x}, t). \quad (\text{C.3}) \text{ (b)}$$

Substituting from eq. (C.3 b) for  $\bar{v}^*$  and the constitutive equations  $T_{ij}(\bar{x}, t) = C_{ijkl}u_{k,l}(\bar{x}, t)$ , for  $\bar{T}$ , into eq. (C.2), results in eq. (C.4).

$$P_j = \frac{-I\omega}{2} u_i^* C_{ijkl} u_{k,l} \quad (\text{C.4})$$

Expressed in the eigenvector basis and assuming mono-mode expansion of the displacement field, its components are represented in eq. (C.5).

$$u_i = u^{(\alpha)} l_i^{(\alpha)} \quad (\text{C.5})$$

Assuming propagation in the  $\bar{p}$  direction, and  $\xi = \bar{p} \cdot \bar{x}$ ,

$$u^{(\alpha)} = u^{(\alpha)} e^{I(k^{(\alpha)}\xi - \omega t)} \quad (\text{C.6})$$

where  $u^{(\alpha)}$  and  $k^{(\alpha)}$  are the amplitude of the displacement and wavenumber of mode  $\alpha$ , respectively. Substituting eq. (C.6) and eq. (C.5) in eq. (C.4), results in eq. (C.7).

$$P_j = \frac{\omega}{2} u^{*(\alpha)} l_i^{(\alpha)} e^{-I(k^{(\alpha)}\xi - \omega t)} C_{ijkl} u^{(\alpha)} k^{(\alpha)} l_k^{(\alpha)} p_l e^{I(k^{(\alpha)}\xi - \omega t)} \quad (\text{C.7})$$

Eq. (C.8) is obtained by multiplying both sides of eq. (C.7) by  $p_j$ .

$$p_j P_j = \frac{\omega}{2} C_{ijkl} k^{(\alpha)} u^{*(\alpha)} u^{(\alpha)} l_i^{(\alpha)} l_k^{(\alpha)} p_j p_l \quad (\text{C.8})$$

Here, with  $u^{(\alpha)} u^{*(\alpha)} = |u^{(\alpha)}|^2$ , and  $\Gamma_{ik} = C_{ijkl} p_j p_l$  eq. (C.8) reduces to eq. (C.9).

$$p_j P_j = \frac{\omega}{2} |u^{(\alpha)}|^2 \Gamma_{ik} l_i^{(\alpha)} l_k^{(\alpha)} k^{(\alpha)} \quad (\text{C.9})$$

With  $\Gamma_{mn} l_n^{(\alpha)} l_m^{(\alpha)} = \rho \frac{\omega^2}{(k^{(\alpha)})^2}$  eq. (C.9) reduces to eq. (C.10).

$$p_j P_j = \frac{\rho \omega^3}{2k^{(\alpha)}} |u^{(\alpha)}|^2 \quad (\text{C.10})$$

Substituting eq. (C.10) in eq. (C.1), the intensity of an acoustic wave can be obtained from eq.

(C.11),

$$Intensity = \frac{\rho}{2} \left| \frac{\omega^3}{k^{(\alpha)}} \right| |u^{(\alpha)}|^2 \quad (\text{C.11})$$

Or,

$$Intensity = \frac{1}{2} \rho \omega^2 c^{(\alpha)} |u^{(\alpha)}|^2, \quad (C.12)$$

where  $c^\alpha$ , is the wave speed of the mode  $\alpha$ .

From the above equation, the intensity of the wave at frequency  $\omega_q$  can be written as eq. (C.13).

$$I_q = \frac{1}{2} \rho \omega_q^2 c_q^{(\alpha)} |u^{(\alpha)}(\omega_q)|^2 \quad (C.13)$$

When the displacement is represented in its phasor notation,  $u^\alpha(\omega_q) = |u^\alpha(\omega_q)| e^{I\phi_q}$ , the magnitude of its  $\alpha$  mode can be written in terms of intensity as eq. (C.14),

$$|u^\alpha(\omega_q)| = \left( \frac{2 I_q}{\rho \omega_q^2 c_q^\alpha} \right)^{1/2} \quad (C.14)$$

and, its derivative with respect to  $\xi$  is calculated as eq. (C.15).

$$\begin{aligned} \frac{d}{d\xi} u^{(\alpha)}(\omega_q) &= \left( \frac{d}{d\xi} |u^{(\alpha)}(\omega_q)| + I |u^{(\alpha)}(\omega_q)| \frac{d\phi_q}{d\xi} \right) e^{I\phi_q} \\ &= \left( \frac{1}{2} \left( \frac{2}{\rho \omega_q^2 c_q^\alpha} \right)^{1/2} I_q^{-1/2} \frac{dI_q}{d\xi} + I |u^{(\alpha)}(\omega_q)| \frac{d\phi_q}{d\xi} \right) e^{I\phi_q} \end{aligned} \quad (C.15)$$

Solving eq. (C.15) for the derivative of the intensity with respect to  $\xi$ , eq. (C.16) is derived.

$$\frac{dI_q}{d\xi} = \left( 2\rho c_q^{(\alpha)} \right)^{1/2} I_q^{1/2} \omega_q \left( \frac{d}{d\xi} u^{(\alpha)}(\omega_q) e^{-I\phi_q} - I |u^{(\alpha)}(\omega_q)| \frac{d\phi_q}{d\xi} \right). \quad (C.16)$$

From eq. (3.1.38),  $u_\xi^{(\alpha)}$  can be written as,

$$u_\xi^{(\alpha)}(\omega_q) = \sum_{(r,s)} \left| C_{eff}^{\alpha\beta\gamma} \right| \left| \frac{k_r^{(\beta)} k_s^{(\gamma)}}{k_q^{(\alpha)}} (k_r^{(\beta)} + k_s^{(\gamma)}) \right| |u^{(\beta)}(\omega_r)| |u^{(\gamma)}(\omega_s)| e^{I(\Delta k_{rsq}\xi + \phi_c + \phi_k + \phi_r + \phi_s)} \quad (C.17)$$

where, it is assumed,

$$u^\beta(\omega_r) = |u^\beta(\omega_r)| e^{I\phi_r}, \quad u^\gamma(\omega_s) = |u^\gamma(\omega_s)| e^{I\phi_s}, \quad \frac{1}{8} \frac{(H^{\alpha\beta\gamma})}{G^{\alpha\alpha}} = \left| C_{eff}^{\alpha\beta\gamma} \right| e^{I\phi_c}$$

and

$$\left( \frac{k_r^{(\beta)} k_s^{(\gamma)}}{k_q^{(\alpha)}} (k_r^{(\beta)} + k_s^{(\gamma)}) \right) = \left| \frac{k_r^{(\beta)} k_s^{(\gamma)}}{k_q^{(\alpha)}} (k_r^{(\beta)} + k_s^{(\gamma)}) \right| e^{I\phi_k}.$$

Substituting for  $\frac{d}{d\xi} u^{(\alpha)}(\omega_q)$ , from eq. (C.17) in eq. (C.16), results in eq. (C.18),

$$\frac{dI_q}{d\xi} = \left(2\rho c_q^{(\alpha)}\right)^{1/2} I_q^{1/2} \omega_q \sum_{(r,s)} \left| C_{eff}^{\alpha\beta\gamma} \right| \left| \frac{k_r^{(\beta)} k_s^{(\gamma)}}{k_q^{(\alpha)}} (k_r^{(\beta)} + k_s^{(\gamma)}) \right| |u^{(\beta)}(\omega_r)| |u^{(\gamma)}(\omega_s)| e^{I\psi_{rsq}} - I |u^{(\alpha)}(\omega_q)| \frac{d\phi_q}{d\xi} \quad (C.18)$$

where,

$$\psi_{rsq} = \Delta k_{rsq} \xi + \phi_c + \phi_r + \phi_s - \phi_q + \phi_k \quad (C.19)$$

Substituting for  $|u^{(\beta)}(\omega_r)|$  and  $|u^{(\gamma)}(\omega_s)|$  from eq. (C.13) and using the definition of the wave

speed to substitute for  $k_q^{(\alpha)} = \frac{\omega_q}{c_q^{(\alpha)}}$ ,  $k_r^{(\beta)} = \frac{\omega_r}{c_r^{(\beta)}}$  and  $k_s^{(\gamma)} = \frac{\omega_s}{c_s^{(\gamma)}}$ , eq. (C.18), eq. (C.20) is derived

$$\frac{dI_q}{d\xi} = \sum_{(r,s)} \left( \frac{2 c_q^{(\alpha)}}{c_r^{(\beta)} c_s^{(\gamma)}} \right)^{3/2} \left( \frac{I_q I_r I_s}{\rho} \right)^{1/2} |k_r^{(\beta)} + k_s^{(\gamma)}| |C_{eff}^{\alpha\beta\gamma}| e^{I\psi_{rsq}} - 2 I I_q \frac{d\phi_q}{d\xi} \quad (C.20)$$

Dividing eq. (C.20) into real and imaginary parts results in eqs. (C.21) (a) and (C.21) (b),

respectively. Since intensity of an elastic wave is a real value eq. (C.20) represents the equation

for intensity gradient. eq. (C.21) (b) also provides the equation to solve for the change in phase

of the wave at frequency  $\omega_q$ .

$$\frac{dI_q}{d\xi} = \sum_{(r,s)} \left( \frac{2 c_q^{(\alpha)}}{c_r^{(\beta)} c_s^{(\gamma)}} \right)^{3/2} \left( \frac{I_q I_r I_s}{\rho} \right)^{1/2} |k_r^{(\beta)} + k_s^{(\gamma)}| |C_{eff}^{\alpha\beta\gamma}| \cos(\psi_{rsq}) \quad (C.21) (a)$$

$$I(2 I_q \frac{d\phi_q}{d\xi} - \sum_{(r,s)} \left( \frac{2 c_q^{(\alpha)}}{c_r^{(\beta)} c_s^{(\gamma)}} \right)^{3/2} \left( \frac{I_q I_r I_s}{\rho} \right)^{1/2} |k_r^{(\beta)} + k_s^{(\gamma)}| |C_{eff}^{\alpha\beta\gamma}| \sin(\psi_{rsq})) = 0 \quad (C.21) (b)$$

Defining

$$\mathcal{A}_{(r,s)} = \left( \frac{2 c_q^{(\alpha)}}{c_r^{(\beta)} c_s^{(\gamma)}} \right)^{3/2} \left( \frac{I_q I_r I_s}{\rho} \right)^{1/2} |k_r^{(\beta)} + k_s^{(\gamma)}| |C_{eff}^{\alpha\beta\gamma}| \quad (C.22)$$

Eq. (C.21a) is written as

$$\frac{dI_q}{d\xi} = \sum_{(r,s)} \mathcal{A}_{(r,s)} \cos(\psi_{rsq}) \quad (C.23)$$

# Appendix D Linear and Nonlinear Elastic Constants of LiNbO<sub>3</sub> and Aluminum

Table 4- Nonlinear Material Properties for Lithium Niobate (LiNbO<sub>3</sub>), ( $\times 10^9 \text{Pa}$ ) and  $C_{155} = C_{166} = C_{125} = C_{135} = C_{145} = C_{146} = C_{225} = C_{226} = C_{235} = C_{236} = C_{136} = C_{245} = C_{246} = C_{334} = C_{335} = C_{336} = C_{345} = C_{346} = C_{445} = C_{446} = C_{555} = C_{556} = C_{566} = C_{666} = C$

$C_{111}$	$C_{112}$	$C_{113}$	$C_{114}$	$C_{123}$	$C_{124}$
-512	454	728	-410	719	55
$C_{144}$	$C_{155}$	$C_{222}$	$C_{333}$	$C_{344}$	$C_{444}$
-37	-599	-478	-363	-540	-41
$C_{156}$	$C_{166}$	$C_{224}$	$C_{233}$	$C_{234}$	$C_{244}$
-122.5	-216	300	-340	1	-599
$C_{455}$	$C_{356}$	$C_{355}$	$C_{266}$	$C_{366}$	$C_{456}$
41	-1	-540	-250	4.5	-281
$C_{133}$	$C_{134}$	$C_{122}$	$C_{256}$	$C_{255}$	$C_{466}$
-34	-1	420	-232.5	-370	55
$C_{223}$					
728					



Table 5- Linear Material Properties for Lithium Niobate (LiNbO<sub>3</sub>) ( $\times 10^9 Pa$ ), density=4700 Kg/m<sup>3</sup> and  $C_{15} = C_{16} = C_{25} = C_{26} = C_{34} = C_{35} = C_{36} = C_{45} = C_{46} = 0$

C11	C12	C22	C14	C24	C13
203	57.3	203	8.5	-8.5	75.2
C23	C33	C44	C55	C56	C66
75.2	242.4	59.5	59.5	8.5	72.85

Table 6- Linear and Nonlinear Material Properties for Aluminum ( $\times 10^9 Pa$ ), density=2680 Kg/m<sup>3</sup>

<b>E</b>	<b><math>\lambda</math></b>	<b><math>\mu</math></b>	<b><i>l</i></b>	<b><i>m</i></b>	<b><i>n</i></b>
70	51	26	-250	-333	-350

## References

- [1] M. Zakeri, S. M. Keller, Y. E. Wang, and C. S. Lynch, “Nonreciprocal wave propagation and parametric amplification of bulk elastic waves in nonlinear anisotropic materials,” *New J. Phys.*, vol. 22, no. 2, p. 023009, Feb. 2020, doi: 10.1088/1367-2630/ab61d9.
- [2] J.-M. Liu, *Photonic Devices*, vol. vol 1. Cambridge University Press, 2005.
- [3] H. Suhl, “Theory of the Ferromagnetic Microwave Amplifier,” *J. Appl. Phys.*, vol. 28, no. 11, pp. 1225–1236, 1957, doi: 10.1063/1.1722623.
- [4] P. K. Tien and H. Suhl, “A Traveling-Wave Ferromagnetic Amplifier,” *Proc. IRE*, vol. 46, no. 4, pp. 700–706, 1958, doi: 10.1109/JRPROC.1958.286770.
- [5] S. M. Hanna and G. P. Murphy, “Magnetoelastic “gain” associated with saw propagation in magnetic garnet films,” *J. Appl. Phys.*, vol. 61, no. 8, pp. 4148–4150, 1987, doi: 10.1063/1.338507.
- [6] R. Fleury, D. Sounas, M. R. Haberman, and A. Alù, “Nonreciprocal acoustics,” *Acoust. Today*, vol. 11, pp. 14–21, 2015.
- [7] N. Swinck and others, “Bulk elastic waves with unidirectional backscattering-immune topological states in a time-dependent superlattice,” *J. Appl. Phys.*, vol. 118, 2015, doi: 10.1063/1.4928619.
- [8] G. Trainiti and M. Ruzzene, “Non-reciprocal elastic wave propagation in spatiotemporal periodic structures,” *New J. Phys.*, vol. 18, p. 22, 2016, doi: 10.1088/1367-2630/18/8/083047.
- [9] C. Croënne and others, “Brillouin scattering-like effect and non-reciprocal propagation of elastic waves due to spatio-temporal modulation of electrical boundary conditions in piezoelectric media,” *Appl. Phys. Lett.*, vol. 110, 2017, doi: 10.1063/1.4975680.

- [10] Y. Chen and others, “Nonreciprocal wave propagation in a continuum-based metamaterial with space-time modulated resonators,” *Phys. Rev. Appl.*, vol. 11, 2019, doi: 10.1103/PhysRevApplied.11.064052.
- [11] Y. Wang and others, “Observation of nonreciprocal wave propagation in a dynamic phononic lattice,” *Phys. Rev. Lett.*, vol. 121, 2018, doi: 10.1103/PhysRevLett.121.194301.
- [12] H. M. Jeon and others, “Propagation of non-reciprocal magnetostatic surface wave in a 20-nm-thick single crystalline yttrium iron garnet film,” *IEEE Electron Device Lett.*, vol. 38, pp. 262–265, 2017, doi: 10.1109/LED.2016.2638202.
- [13] C. Kittel, “Interaction of spin waves and ultrasonic waves in ferromagnetic crystals,” *Phys. Rev.*, vol. 110, pp. 836–841, 1958, doi: 10.1103/PhysRev.110.836.
- [14] B. B. Lax and J. Kenneth, *Microwave Ferrites and Ferrimagnetics*. McGraw-Hill, 1962.
- [15] H. S. Zhu and M. Rais-Zadeh, “Non-reciprocal acoustic transmission in a GaN delay line using the acoustoelectric effect,” *IEEE Electron Device Lett.*, vol. 38, pp. 802–805, 2017, doi: 10.1109/LED.2017.2700013.
- [16] R. Fleury, D. Sounas, and A. Alù, “Magnetless circulators for electromagnetic and acoustic waves,” in *10th European Conf. Antennas and Propagation (EuCAP, Davos)*, 2016, p. pp 1--3, doi: 10.1109/EuCAP.2016.7481951.
- [17] S. Bhuktare, A. Bose, H. Singh, and A. A. Tulapurkar, “Gyrator based on magneto-elastic coupling at a ferromagnetic/piezoelectric interface,” *Sci. Rep.*, vol. 7, p. 6, 2017, doi: 10.1038/s41598-017-00960-9.
- [18] P. Wang, L. Lu, and K. Bertoldi, “Topological phononic crystals with one-way elastic edge waves,” *Phys. Rev. Lett.*, vol. 115, 2015, doi: 10.1103/PhysRevLett.115.104302.
- [19] B. Liang, B. Yuan, and J.-C. Cheng, “Acoustic diode: rectification of acoustic energy flux in one-dimensional systems,” *Phys. Rev. Lett.*, vol. 103, 2009, doi: 10.1103/PhysRevLett.103.104301.
- [20] B. Liang, X. S. Guo, J. Tu, D. Zhang, and J. C. Cheng, “An acoustic rectifier,” *Nat. Mater.*,

- vol. 9, p. 989, 2010, doi: 10.1038/nmat2881.
- [21] A. Darabi and others, “Broadband passive nonlinear acoustic diode,” *Phys. Rev. B*, vol. 99, 2019, doi: 10.1103/PhysRevB.99.214305.
- [22] M. D. Fronk and M. J. Leamy, “Internally resonant wave energy exchange in weakly nonlinear lattices and metamaterials,” *Phys. Rev. E*, vol. 100, 2019, doi: 10.1103/PhysRevE.100.032213.
- [23] A. Mojahed, J. Bunyan, S. Tawfick, and A. F. Vakakis, “Tunable acoustic nonreciprocity in strongly nonlinear waveguides with asymmetry,” *Phys. Rev. Appl.*, vol. 12, 2019, doi: 10.1103/PhysRevApplied.12.034033.
- [24] J. G. Cui, T. Z. Yang, and L. Q. Chen, “Frequency-preserved non-reciprocal acoustic propagation in a granular chain,” *Appl. Phys. Lett.*, vol. 112, p. 4, 2018, doi: 10.1063/1.5009975.
- [25] J. Bunyan and others, “Acoustic nonreciprocity in a lattice incorporating nonlinearity, asymmetry, and internal scale hierarchy: experimental study,” *Phys. Rev. E*, vol. 97, 2018, doi: 10.1103/PhysRevE.97.052211.
- [26] K. J. Moore and others, “Nonreciprocity in the dynamics of coupled oscillators with nonlinearity, asymmetry, and scale hierarchy,” *Phys. Rev. E*, vol. 97, 2018, doi: 10.1103/PhysRevE.97.012219.
- [27] M. D. Fronk and others, “Acoustic non-reciprocity in lattices with nonlinearity, internal hierarchy, and asymmetry: computational study,” *J. Vib. Acoust.*, vol. 141, 2019, doi: 10.1115/1.4043783.
- [28] P. J. Vella, T. C. Padmore, G. I. Stegeman, and V. M. Ristic, “Nonlinear surface-wave interactions: Parametric mixing and harmonic generation,” *J. Appl. Phys.*, vol. 45, pp. 1993–2006, 1974, doi: 10.1063/1.1663536.
- [29] G. A. Maugin, *Nonlinear Electromechanical Effects and Applications*. World Scientific, 1985.

- [30] G. A. Maugin, J. P. R. Drouot, and B. Collet, *Nonlinear Electromechanical Couplings*. Wiley, 1992.
- [31] R. ~M. White and F. ~W. Voltmer, “Direct Piezoelectric Coupling to Surface Elastic Waves,” *Appl. Phys. Lett.*, vol. 7, no. 12, pp. 314–316, Dec. 1965, doi: 10.1063/1.1754276.
- [32] G. Tobolka, W. Faber, G. Albrecht, and D. Pilz, “High Volume TV-IF Filter Design, Fabrication, and Applications,” in *IEEE 1984 Ultrasonics Symposium*, 1984, pp. 1–12, doi: 10.1109/ULTSYM.1984.198253.
- [33] P. Delsing *et al.*, “The 2019 surface acoustic waves roadmap,” *J. Phys. D: Appl. Phys.*, vol. 52, no. 35, p. 353001, Aug. 2019, doi: 10.1088/1361-6463/ab1b04.
- [34] C. C. W. Ruppel, “Acoustic Wave Filter Technology—A Review,” *IEEE Trans. Ultrason. Ferroelectr. Freq. Control*, vol. 64, no. 9, pp. 1390–1400, 2017, doi: 10.1109/TUFFC.2017.2690905.
- [35] C. Campbell, *Surface Acoustic Wave Devices and Their Signal Processing Applications*. Academic, 1989.
- [36] D. Morgan, *Surface Acoustic Wave Filters: with Applications to Electronic Communications and Signal Processing*. Elsevier, 2007.
- [37] P. O. Lo/pen, “Second-Harmonic Generation in an Elastic Surface Wave in  $\alpha$ -Quartz,” *J. Appl. Phys.*, vol. 39, no. 12, pp. 5400–5404, 1968, doi: 10.1063/1.1655989.
- [38] E. G. H. Lean, C. G. Powell, and L. Kuhn, “ACOUSTIC SURFACE WAVE MIXING ON  $\alpha$ -QUARTZ,” *Appl. Phys. Lett.*, vol. 15, no. 1, pp. 10–12, 1969, doi: 10.1063/1.1652822.
- [39] N. Kalyanasundaram, “Nonlinear surface acoustic waves on an isotropic solid,” *Int. J. Eng. Sci.*, vol. 19, no. 2, pp. 279–286, 1981, doi: [https://doi.org/10.1016/0020-7225\(81\)90028-8](https://doi.org/10.1016/0020-7225(81)90028-8).
- [40] E. A. Zabolotskaya, “Nonlinear propagation of plane and circular Rayleigh waves in isotropic solids,” *J. Acoust. Soc. Am.*, vol. 91, no. 5, pp. 2569–2575, 1992, doi: 10.1121/1.402993.

- [41] M. Planat, “Multiple scale analysis of the nonlinear surface acoustic wave propagation in anisotropic crystals,” *J. Appl. Phys.*, vol. 57, no. 11, pp. 4911–4915, 1985, doi: 10.1063/1.335315.
- [42] M. F. Hamilton, Y. A. Il’inskii, and E. A. Zabolotskaya, “Nonlinear surface acoustic waves in crystals,” *J. Acoust. Soc. Am.*, vol. 105, no. 2, pp. 639–651, 1999, doi: 10.1121/1.426255.
- [43] J. H. Cantrell and W. T. Yost, “Nonlinear ultrasonic characterization of fatigue microstructures,” *Int. J. Fatigue*, vol. 23, pp. 487–490, 2001, doi: [https://doi.org/10.1016/S0142-1123\(01\)00162-1](https://doi.org/10.1016/S0142-1123(01)00162-1).
- [44] J.-Y. Kim, L. J. Jacobs, J. Qu, and J. W. Littles, “Experimental characterization of fatigue damage in a nickel-base superalloy using nonlinear ultrasonic waves,” *J. Acoust. Soc. Am.*, vol. 120, no. 3, pp. 1266–1273, 2006, doi: 10.1121/1.2221557.
- [45] A. J. Croxford, B. W. Drinkwater, and P. D. Wilcox, “NONLINEAR ULTRASONIC CHARACTERIZATION USING THE NONCOLLINEAR METHOD,” *AIP Conf. Proc.*, vol. 1335, no. 1, pp. 330–337, 2011, doi: 10.1063/1.3591872.
- [46] W. Li, Y. Xu, N. Hu, and M. Deng, “Numerical and experimental investigations on second-order combined harmonic generation of Lamb wave mixing,” *AIP Adv.*, vol. 10, no. 4, p. 45119, 2020, doi: 10.1063/1.5140588.
- [47] B. A. Auld, *Acoustic Fields and Waves in Solids*, vol. vol 1. Malabar, FL: Krieger, 1990.
- [48] D. ~B. Taylor and S. Crampin, “Surface Waves in Anisotropic Media: Propagation in a Homogeneous Piezoelectric Halfspace,” *Proc. R. Soc. London Ser. A*, vol. 364, no. 1717, pp. 161–179, Dec. 1978, doi: 10.1098/rspa.1978.0194.
- [49] J. Zou, “High Quality Factor Lamb Wave Resonators,” 博士论文, 2014, [Online]. Available: <http://www.eecs.berkeley.edu/Pubs/TechRpts/2014/EECS-2014-217.html>.